Stabilization of periodic orbits in discrete and continuous-time systems

Thiago Pereira das Chagas Perreira das Chagas

UNIVERSITE PARIS-SUD

ÉCOLE DOCTORALE : STITS

Laboratoires: Centre de recherche INRIA Paris-Rocquencourt, Équipe-projet SISYPHE
Instituto Tecnológico de Aeronáutica, São José dos Campos - Brésil

DISCIPLINE: Physique

THÈSE DE DOCTORAT EN CO-TUTELLE

soutenue le 25/06/2013

par

Thiago PEREIRA DAS CHAGAS

Stabilization of periodic orbits in discrete and continuous-time systems

Directeur de thèse :	Pierre-Alexandre BLIMAN	Directeur de recherche, INRIA
Co-directeur de thèse :	Karl HEINZ KIENITZ	Professeur, ITA
Co-directeur de thèse :	Erico Luiz REMPEL	Professeur, ITA

Composition du jury :

Présidente :	Françoise LAMNABHI-LAGARRIGUE	Directeur de recherche, SUPELEC
Rapporteurs :	Jean-Pierre BARBOT	Professeur des Universités, ENSEA
	Wilfrid PERRUQUETTI	Professeur des Universités, Ecole Centrale de Lille
Examinateurs :	Elder MOREIRA HEMERLY	Professeur, ITA
	Elbert Einstein NEHRER MACAU	Directeur de recherche, INPE

Acknowledgments

Agradeço aos meus pais pelo apoio, amor, conselhos, educação e tudo mais que utilizo para a vida e também utilizei para a realização deste trabalho.

Financial support is grateful to CAPES in Brazil and COFECUB in France. This work was also supported by the Centre de recherche Inria Paris-Rocquencourt, ITA and Université Paris-Sud, Orsay.

I am grateful to my advisors Pierre-Alexandre Bliman, Karl Heinz Kienitz and Erico Rempel by the time dedicated to this work. Special thanks to Pierre-Alexandre Bliman who was closest in recent years labor, he forced the limits of my knowledge and supported my difficulties.

I am grateful to the thesis committee by the time dedicated to review this manuscript. The suggested corrections contributed to increase the quality of the work.

Obrigado aos meus amigos que aguentaram minhas reclamações e me deram nos momentos de lazer, mesmo sem perceber, a alegria necessária para sempre continuar a trabalhar. Sem mais palavras porque os amigos sabem o quanto eu quero terminar essa tese e o ponto final está aqui, nos agradecimentos!

Abstract

The main problem evaluated in this manuscript is the stabilization of periodic orbits of non-linear dynamical systems by use of feedback control. The goal of the control methods proposed in this work is to achieve a stable periodic oscillation. These control methods are applied to systems that present unstable periodic orbits in the state space, and the latter are the orbits to be stabilized.

The methods proposed here are such that the resulting stable oscillation is obtained with low control effort, and the control signal is designed to converge to zero when the trajectory tends to the stabilized orbit. Local stability of the periodic orbits is analyzed by studying the stability of some linear time-periodic systems, using the Floquet stability theory. These linear systems are obtained by linearizing the trajectories in the vicinity of the periodic orbits.

The control methods used for stabilization of periodic orbits here are the proportional feedback control, the delayed feedback control and the prediction-based feedback control. These methods are applied to discrete and continuous-time systems with the necessary modifications. The main contributions of the thesis are related to these methods, proposing an alternative control gain design, a new control law and related results.

Keywords: **Control of chaos, Stabilization of periodic orbits, Prediction-based control, Delayed feedback control, Proportional feedback control, Floquet multipliers**

Résumé

Le problème principalement étudié dans ce manuscrit est la stabilisation d'orbites périodiques de systèmes dynamiques non linéaires à l'aide d'une commande de rétroaction (*feedback*). Le but des méthodes de contrôle proposées ici est d'obtenir une oscillation périodique stable. Ces méthodes de contrôle sont appliquées à des systèmes présentant des orbites périodiques instables dans l'espace d'état, et ces dernières sont les orbites destinées à être stabilisées.

Les méthodes proposées ici sont telles que l'oscillation stable qui en résulte est obtenue avec un effort de contrôle faible, et que la valeur de la commande tend vers zéro lorsque la trajectoire tend vers l'orbite stabilisée. La stabilité locale des orbites périodiques est analysée par l'étude de la stabilité des systèmes linéaires périodiques à l'aide de la théorie de Floquet. Ces systèmes linéaires sont obtenus par linéarisation des trajectoires au voisinage de l'orbite périodique.

Les méthodes de contrôle utilisées ici pour la stabilisation des orbites périodiques sont une loi de commande proportionnelle, une loi de commande de rétroaction retardée et une loi de commande de rétroaction basée sur une prédiction. Ces méthodes sont appliquées aux systèmes en temps discret et aux systèmes en temps continu avec les modifications nécessaires. Les contributions principales de cette thèse sont associées à ces méthodes, proposant une méthode alternative de design de gain, une nouvelle loi de commande et des résultats associés.

Mots-clés: **Contrôle du chaos, Stabilisation d'orbites périodiques, *Prediction-based control*, *Delayed feedback control*, *Proportional feedback control*, Multiplicateurs de Floquet**

Resumo

O principal problema avaliado neste manuscrito é a estabilização de órbitas periódicas em sistemas dinâmicos não-lineares utilizando controle por realimentação. O objetivo dos métodos de controle propostos neste trabalho é obter uma oscilação periódica estável. Estes métodos de controle são aplicados a sistemas que apresentam órbitas periódicas instáveis no espaço de estados, estas são as órbitas a serem estabilizadas.

Os métodos propostos aqui são tais que a oscilação periódica estável resultante é obtida utilizando um baixo esforço de controle, e o sinal de controle é projetado de forma a convergir para zero quanto a trajetória tende à órbita estabilizada. A estabilidade local de órbitas periódicas é analisada através do estudo da estabilidade de alguns sistemas lineares periódicos no tempo, utilizando a teoria de estabilidade de Floquet. Estes sistemas lineares são obtidos por linearização das trajetórias na vizinhança da órbita periódica.

Os métodos de controle utilizados aqui para estabilização de órbitas periódicas são o *proportional feedback control*, o *delayed feedback control* e o *prediction-based feedback control* (controle por realimentação baseado em predição). Estes métodos são aplicados a sistemas de tempo discreto e de tempo contínuo, com as modificações necessárias. As principais contribuições da tese são relacionadas a esses métodos, propondo um projeto de ganho de controle alternativo, uma nova lei de controle e resultados relacionados.

Palavras-chave: **Control de caos, Estabilização de órbitas periódicas, *Prediction-based control*, *Delayed feedback control*, *Proportional feedback control*, Multiplicadores de Floquet**

Contents

List of Figures

List of Tables

List of nomenclature

aPBC	approximated prediction-based control
BA	basins of attraction
BCS	band chaotic saddle
CCF	controllable canonical form
CL	control law
DAE	differential algebraic equation
DDE	delay differential equation
DFC	delayed feedback control
FP	fixed point
LTP	linear time-periodic
MC	merging crisis
ODE	ordinary differential equation
PBC	prediction-based feedback control
PDE	partial differential equation
PFC	proportional feedback control
PO	periodic orbit
SCS	surrounding chaotic saddle
SNB	saddle-node bifurcation
TUPO	target unstable periodic orbit
UPO	unstable periodic orbit
vdP	van der Pol

List of symbols

$\lvert\cdot\rvert$	absolute value
$\lvert\cdot\rvert_{max}$	largest in magnitude
$\lVert\cdot\rVert_i$	norm i
$\dot{x}$	derivative of x with respect to time
$\otimes$	Kronecker product
A'	transpose of matrix A
$A^\dagger$	Moore-Penrose pseudo-inverse of matrix A
$\mathbb{C}$	set of complex numbers
d	steady state error
∂	partial derivative
I_i	identity matrix of size $i \times i$
$Im(\cdot)$	imaginary part of a complex number
k	discrete-time index (Part I) or scalar control gain (Part II)
k_o	scalar observer/estimator control gain
K	matrix control gain
λ_i	i-th Floquet characteristic exponent
$\Lambda(A)$	set of eigenvalues of matrix A
m_j	estimated value of the state of the free system response at time $t + Ts_j$
μ_i	i-th Floquet characteristic multiplier
N	number of discretization points
$\mathbb{N}$	set of natural numbers
∇_x	gradient of a function with respect to x
p	discrete-time period of a periodic orbit
$\varphi(\cdot,\cdot,\cdot,\cdot)$	state transition map
$\Phi(\cdot,\cdot)$	sate transition matrix or matrix evolution operator
Ψ	monodromy matrix

$\mathbb{R}$	set of real numbers
$Re(\cdot)$	real part of a complex number
s_i	discretization points
t	time
t_k	the time of the k-th intersection of the Poincaré section by a trajectory
T	period in continuous-time (Part II)
u	control signal
υ	steady state control effort
x	state vector
x_k	variable x at discrete-time index k
x^*	periodic orbit
$\mathbb{Z}$	set of integer numbers

Chapter 1

Introduction

The main problem tackled in this manuscript is the stabilization of periodic orbits of nonlinear dynamical systems, using state or output feedback control. The aim of the control methods proposed in this work is a stable periodic oscillation, something which differs from the most common goal in control systems, which is a stable equilibrium point.

This thesis is motivated by the study of oscillatory systems, in particular, alternative control methods that ensure the containment of the system state within a prescribed bounded region of the state-space with low control effort. Persistent oscillations are observed in many engineering problems, for example, attitude control in aerospace engineering, flutter[1] in aeronautical engineering, shimmy[2] in automotive and aeronautics engineering, power electronics in electrical engineering and physiological oscillations (heartbeating, for example) in biomedical engineering. Oscillations are also observed in other areas, for example, ecology and economy.

The control methods considered here are applied to systems that present unstable periodic orbits (UPOs) in the state space and these UPOs are the orbits to be stabilized. The methods were proposed such that the resulting stable oscillation is obtained with low control effort, and the control signal is designed to converge to zero when the trajectory tends to the stabilized orbit. This property is achieved if the control methods only change the stability of the target orbit.

[1] Self-sustained oscillations of airplane wings and control surfaces [30]
[2] Angular self-sustained oscillations in carriage wheels [105]

The control methods used for stabilization of periodic orbits here are the *proportional feedback control* (PFC), the *delayed feedback control* (DFC) and the *prediction-based feedback control* (PBC) and the main difference between them is the reference used to form the control signal. The PFC uses as reference the target UPO itself, which is found before application. The DFC uses as reference the state delayed by the period of the target UPO and only its period is required for application. The PBC uses as reference the predicted state one period of the target orbit ahead of trajectories of the free system response and requires the system model for application.

Another motivation of the work is contributing with the literature on periodic stabilization methods, for example, reducing the dependence of previous knowledge about the target UPO, proposing alternatives to the DFC due to its limitations, proposing new methods for control gain design and contributing for the application of this type of control.

The aim of the thesis is the proposition of new methods, control laws or control gain design for stabilization of periodic orbits in discrete and continuous-time systems aiming at increasing the knowledge on the theme and solving some questions observed in the literature, in particular some limitations of the existing methods.

The stabilization of a periodic orbit of a non-linear system can be simplified to the stabilization of a linear time-periodic system. This linear system is obtained linearising the trajectories in the close vicinity of the periodic orbit and its stability analysis can be performed using the Floquet stability theory. Thus, the local stability of the periodic orbit of the non-linear system is defined by the stability of the associated linear system. Notice that the stabilized orbits shown in this manuscript are all associated to chaotic sets, but the stabilizing methods developed can be applied to any existing periodic orbit of an autonomous/non-autonomous system.

1.1 Main contributions

1.1.1 Presentation of the contributions

New control laws for the PBC applied to discrete-time systems. One contribution of the thesis is the proposition of a method to define the PBC gain on discrete-time systems resulting in a new control law (see Section 3.4 and [12]). This control law, applied to the PBC proposed by Ushio and Yamamoto [91], is based on improving stability conditions for periodic orbits using Floquet theory and results in a dead-beat controller that does not need previous information about the orbit to be stabilized.

This new control law requires an invertible input matrix, something that implies some practical limitations. Another contribution, following the results presented in [12], is the proposition of a modified control law that can be applied to systems with non-invertible input matrix. This new control law does not require previous knowledge about the orbit to be stabilized and leads to zero Floquet multipliers for the linearized system around the periodic orbit. The condition for its application is presented in Section 3.4.3.

On numerical results, the main contributions are the comparison of the proposed control law with the DFC and a brief numerical analysis on the robustness of the method subjected to a parametric uncertainty (see Section 4.3).

The theoretical results were obtained with Professors Pierre-Alexandre Bliman and Karl H. Kienitz, while the numerical essays on DFC used tools previously developed with Prof. Erico L. Rempel.

New method for numerical design of DFC constant gain. Another contribution of the thesis is the application of the method proposed in [10, 23, 51] to approximate the monodromy matrix of periodic orbits of systems with a single constant delay and modeled by delay differential equations to the numerical design of a DFC constant gain (see Section 7.4.2). The main advantage of the method is the reduction of the problem of computing the monodromy matrix of an orbit controlled by the DFC to matrix algebra only. The consequence is the reduction of the closed-loop Floquet multipliers computation time.

The computation time reduction encompassed by the method allows the numerical design of a DFC constant control gain by optimization using as cost function the largest magnitude Floquet multiplier of the orbit to be stabilized, as a function of the DFC control gain. This optimization process and a comparison with the PFC applied to the van der Pol oscillator is presented in the numerical results of Section 8.3 and in [14].

The corresponding results have been worked out with Prof. Erico L. Rempel. The results on the orthogonal collocation method used here were obtained with Prof. Pierre-Alexandre Bliman.

New control method for stabilizing periodic orbits in continuous-time systems. A new control method for stabilizing periodic orbits in continuous-time systems inspired by the PBC, originally applied for discrete-time systems, is proposed (see Section 7.3.3 and [13]). The new method uses the predicted state of the trajectory one period of the target orbit ahead, computed along trajectories of the free system using an implicit Runge-Kutta method. The PBC structure with the implicit Runge-Kutta method is solved using an estimator, resulting in an extended set of ordinary differential equations solved with any numerical integrator method. Due to the estimation of the futures states we call this new method *approximate prediction-based control* (aPBC).

Numerical results (see Section 8.4) using the aPBC on a non-autonomous system show that this method can stabilize orbits that are not stabilized by the DFC. An example of one orbit of an autonomous system stabilized by the aPBC is presented in Section 8.5. A numerical evaluation of the controller performance reducing the estimator precision is presented in Sections 8.4 and 8.5.

The corresponding results have been worked out with Professors Pierre-Alexandre Bliman and Karl H. Kienitz.

1.1.2 Chronology of the contributions and the work performed

This PhD thesis has been achieved in cooperation between Inria and ITA, through funding from the CAPES-COFECUB project Ma624/09 “Oscillatory systems in control: reduced modeling, analysis, identification and design”.

In parallel with the Master course (from February 2006 to October 2007), I began attending the Ph.D. technical disciplines in August 2007 and working with Prof. Erico L. Rempel on synchronization of chaos, characterization of chaotic attractors using periodic orbits, control of chaos on hybrid systems and improvements on control of chaos methods until August 2009. From December 2008 it was decided with Professors Karl H. Kienitz and Erico L. Rempel to work on improvements on the DFC control gain design and comparisons between DFC and PFC. It was also proposed a doctoral internship at Inria research center located at Rocquencourt, France, with Prof. Pierre-Alexandre Bliman who suggested improvements on robustness of the DFC method.

Then, in September 2009, I moved to Inria where I worked during one year with Prof. Pierre-Alexandre Bliman on improvements on the discrete-time PBC and the mathematical foundations of the new continuous-time PBC using orthogonal collocation method. Prof. Karl Heinz Kienitz visited us at Inria for one week. During this period I continued working on the improvements on DFC control gain design and comparison with the PFC for one week of January 2010 at the University of Cambridge (DAMTP) with Prof. Erico L. Rempel (the travel was funded by Inria).

In September 2010 I returned to ITA where I presented the results obtained for a board composed by two ITA professors and all my advisors as "Qualification Exam" (required by ITA). From October 2010 I finished the mathematical foundations and implemented the numerical simulations of the continuous-time PBC. In my return to ITA I used the knowledge learned on orthogonal collocation method to finish the improvements on the DFC control gain design. Finally, I obtained a position at University Estadual de Santa Cruz (UESC) in July 2011 and achieved the writing of two papers and my PhD thesis during the free time (UESC funded six months at ITA to finish the details of the thesis and initiate its writing).

1.2 Organization of the manuscript

The manuscript is divided in two parts. Part I is devoted to discrete-time systems and Part II to continuous-time systems. **Both parts can be read separately and with the**

Appendices constitute two self-contained works. Each part is divided as follows in introduction, stability analysis of periodic orbits, stabilization of linear time-periodic systems, control methods for periodic orbits, stabilization of periodic orbits, numerical results and conclusions.

Introduction. Both parts initiate with an introduction (Chapters 2 and 6) containing the mathematical description of the periodic orbit stabilization problem, review of the literature and an introduction about the control methods to be applied.

Stability analysis of periodic orbits. A review about stability analysis of periodic orbits using both Floquet and Lyapunov theories is presented (Sections 3.1 and 7.1) showing that the problem of stabilizing periodic orbit of non-linear systems can be reduced to stabilization of linear time-periodic systems.

Stabilization of linear time-periodic systems. Methods for stabilization of linear time-periodic systems are presented in Sections 3.2 and 7.2. These methods are not applied directly in this work, but, for discrete-time systems it is shown that the new control law proposed for the PBC is an special case of the deadbeat control proposed for linear time-periodic systems. These methods also indicate that some control gain design techniques, for example pole placement, can be used to improve the performance of periodic orbit stabilization methods.

Control methods for periodic orbits. The methods used to stabilize periodic orbits are presented in Sections 3.3 and 7.3. It is shown that these methods use the existence of unstable periodic orbits to achieve stable periodic orbits with ideally zero steady state control effort. The three control methods used in this manuscript are presented in details with a review of some of the literature results that are interesting to this work. The aPBC is proposed in Section 7.3.

Stabilization of periodic orbits. After the presentation of the control methods we discuss how to apply them to the stabilization of periodic orbits in Sections 3.4 and 7.4.

In the discrete-time case (Section 3.4) we focus on the PBC and develop the proposed new control law and its stability proof. The control gain design for the continuous-time controllers are presented in Section 7.4, in special, the proposed design method applied to the DFC.

Numerical results. The numerical results contained in the manuscript are presented in Chapter 4 for the discrete-time case and in Chapter 8 for the continuous-time case.

Conclusions. The partial conclusions are presented in Chapters 5 and 9. The global conclusions are in Chapter 10.

Part I

Discrete-time systems

Chapter 2

Introduction

Stabilization of periodic orbits consists in changing the stability of an *existing unstable periodic solution* of a dynamical system, in this chapter, a discrete-time dynamical system. The stabilizing methods take advantage of the existing unstable solution to obtain a stable periodic solution using low feedback control effort. The methods can be applied to oscillatory systems where one of the performance requirements is a periodic oscillation.

Consider the following discrete-time dynamical system:

$$x_{k+1} = f(k, x_k, u_k), \quad x_0 \text{ given} \tag{2.1}$$

where $x : \mathbb{N} \to \mathbb{R}^n$, $u : \mathbb{N} \to \mathbb{R}^m$, $k, m, n \in \mathbb{N}$ and $f : \mathbb{N} \times \mathbb{R}^n \times \mathbb{R}^m \to \mathbb{R}^n$ is a p-periodic function with respect to time k, that is, by definition

$$\forall k \in \mathbb{N}, \quad \forall x \in \mathbb{R}^n, \quad \forall u \in \mathbb{R}^m, \qquad f(k+p, x, u) = f(k, x, u). \tag{2.2}$$

We assume moreover the existence of a p-periodic solution x_k^* to the free system (2.1), that is, the system obtained by setting $u_k = 0$, $k \geq 0$. In other words

$$\forall k \in \mathbb{N}, \qquad x_{k+p}^* = x_k^* \tag{2.3}$$

and

$$\forall k \in \mathbb{N}, \qquad x^*_{k+1} = f(k, x^*_k, 0_m). \tag{2.4}$$

We assume that this periodic solution is unstable (the stability analysis of periodic orbits in discrete-time systems is discussed in Section 3.1). Our ultimate objective in this part is to synthesize periodic feedback laws $u_k(x_k)$ that stabilize it, that is, such that

$$\forall k \in \mathbb{N}, \quad \forall x \in \mathbb{R}^n, \qquad u_{k+p}(x) = u_k(x)$$

and such that x^* is a stable solution of the closed-loop system

$$x_{k+1} = f(k, x_k, u_k(x_k)) \tag{2.5}$$

with $u : \mathbb{N} \times \mathbb{R}^n \to \mathbb{R}^m$ defined latter. Notice that, when the open-loop system (2.1) and the feedback are periodic with respect to time k, the same is true for the closed-loop system (2.5).

The control signal u used in this work has to verify ideally,

$$u_k(x^*_k) = 0, \qquad k \geq 0. \tag{2.6}$$

That is, on the periodic orbit the control effort is zero and the unstable periodic solution x^*_k of $f(k, x_k, 0)$ is a stable periodic solution of $f(k, x_k, u_k(x_k))$.

Non-linear systems with chaotic sets in their state space are examples of dynamical systems that present unstable periodic orbits (UPO). In fact, if there is a chaotic set in the n-dimensional state space formed by x_k, it is known that the chaotic set is composed by an infinite number of UPOs [1, 24] and the number of UPOs per period p increases exponentially with p [20, 29].

Ott *et al.* [67] proposed *to stabilize the UPOs embedded in the chaotic sets* by small time-dependent parametric perturbations. Stabilizing such UPOs is known as *chaos control*. Chaos control aims at eliminating chaotic behaviour in non-linear dynamical systems by stabilizing one of the UPOs embedded in a chaotic set with low control effort. The

method proposed in [67] specifically uses chaos basic characteristics among which are the sensitive dependence on initial conditions and the infinite number of unstable periodic orbits embedded in the chaotic sets [20, 24].

Another characteristic of chaotic behaviour is that trajectories on chaotic attractors come arbitrarily close to any of the embedded UPOs due to ergodicity [24]. Specific control applications where long transient times are accepted (in return for a low control effort necessity, for example) can take advantage of this characteristics by applying the control signal only when the free system trajectory is in the vicinity of the target UPO. In the present work the ergodicity property of chaos is not used because we are interested in reducing the transient time.

The most common application of stabilization of periodic orbits by state-feedback satisfying condition (2.6) is the control method introduced by Pyragas [70]. Pyragas proposed two different feedback methods, initially for continuous-time systems, namely proportional feedback control and delayed feedback control. We present rapidly these methods in the sequel.

Proportional feedback control (PFC). This method uses the target UPO as reference signal for the control signal in order that, for the closed-loop system (2.5), x_k^* is stable and condition (2.6) is satisfied. The necessity to determine and to store the values of the solution on the entire UPO is the principal disadvantage for application of the PFC method, specially in the case of large p or for high dimensional discrete-time systems with complex dynamics.

Details about the method and a review of the literature are in Section 3.3.1.

Delayed feedback control (DFC). This method uses the state of the system delayed by the period p of the target UPO as reference for a control signal that satisfies condition (2.6). The application of the DFC depends only upon the ability of recording the past p delayed states resulting in an easily implementable control method. Note that, as will be seen in Section 3.3.2, the analytic design of the control gain depends upon the previous knowledge of the entire UPO.

The DFC has known limitations, one of them is the *odd number limitation* (see Section 3.3.2). Some modification on the original method proposed by Pyragas [70] where developed to overcome these limitations. One of these methods, proposed to overcome the odd number limitation, is the prediction-based control.

Details about the DFC, its application, control gain design, modifications on the control law and review of the literature are presented in Section 3.3.2.

We now introduce a third method, central to our contribution.

Prediction based control (PBC). This method, proposed by Ushio and Yamamoto [91], uses *the value of the state one period ahead, computed along the trajectories of the free system response* as reference for the control signal. This control signal also satisfies condition (2.6). Details about the method and review of the literature is presented in Section 3.3.3.

A first contribution of this work is the proposition of a method to define the PBC gain, more specifically, a method that does not need previous knowledge about the UPO position. The results were initially published in [12]. Details about the definition of the control gain and stabilization of periodic orbits with the PBC are presented in Section 3.4.

A comparison between the DFC and the PBC is performed in Section 4.2. These results were originally published in [11]. Other numerical analysis used to clarify the characteristics of the PBC with the proposed control laws are presented in Section 4.

Organization of Part I. Stabilization of periodic orbits using the methods presented in this chapter is performed through stabilization of the linearised time-periodic system that governs the perturbed trajectories in the close vicinity of the target UPO. We thus recall the basic notions on stability analysis of periodic orbits by its linearised dynamics using the Floquet and the Lyapunov theories in Section 3.1, the stabilization of linear time-periodic systems (LTP) in Section 3.2 and the control methods for stabilization of periodic orbits in non-linear systems in Section 3.3. We then study stabilization of periodic orbits using the PBC and present the contributions of Part I in Section 3.4. In

the latter section we provide a sufficient stability condition for periodic orbits and use this condition for the development of the proposed control laws for the PBC. Numerical examples exploring the characteristics of the PBC method using the new control laws and a comparison with the DFC are presented in Chapter 4. The conclusions of Part I are in Chapter 5.

Chapter 3

Feedback stabilization of unstable periodic orbits

3.1 Stability analysis of periodic orbits

In this section we present two methods for stability analysis of linear difference periodic systems (see Appendix A). Both methods can be used for the stability analysis of periodic orbits of non-linear system by studying the behaviour of a perturbed trajectory governed by the linearised system in the vicinity of the periodic solution.

First we introduce the Floquet stability theory, the method used in this work, and then we introduce the Lyapunov stability theory that can also be used for the same purpose.

3.1.1 Floquet stability theory

Here we present the concepts on the stability of linear periodic discrete-time dynamical systems based on the Floquet theory and these results are applied to the local stability of periodic orbits of non-linear discrete-time dynamical systems.

Linear systems

Let us consider a linear discrete-time dynamical system described by the difference equation

$$x_{k+1} = A_k x_k, \tag{3.1}$$

where $k \in \mathbb{N}$, $x : \mathbb{N} \to \mathbb{R}^n$ is a column vector and $A : \mathbb{N} \to \mathbb{R}^{n \times n}$ (see Appendix A). Assume that A_k is a p-periodic state matrix, that is

$$A_k = A_{k+p}, \quad \forall k \in \mathbb{N}. \tag{3.2}$$

The stability of linear periodic systems according to the Floquet theory [5] depends on the eigenvalues of the *monodromy matrix* (Appendix A), called the *Floquet characteristic multipliers* $\mu_i \in \mathbb{C}$, $i = 1, \ldots, n$:

Proposition 3.1 (see Proposition 3.3 in [5])**.** (*i*) *The system* (3.1) *is asymptotically stable if and only if the characteristic multipliers of* A_k *have absolute value lower than* 1*.* (*ii*) *The system* (3.1) *is stable if and only if the characteristic multipliers of* A_k *have absolute value lower than or equal to* 1 *and those characteristic multipliers with absolute value equal to* 1 *are simple roots of the minimal polynomial of the monodromy matrix* Ψ_k*.* □

See Appendix B for stability definitions.

The state transition matrix or the matrix evolution operator $\Phi(k+q, k)$, $q \in \mathbb{N}$ (see Appendix A), of (3.1) is calculated as follows

$$\Phi(k+q, k) = \prod_{l=0}^{q-1} A_{k+l} \tag{3.3}$$

where, here and in the sequel, the matrices in the product are ordered from the right to the left for increasing l.

The monodromy matrix Ψ_k is calculated as the state transition matrix over a period $[k, k+p]$ [5]:

$$\Psi_k = \Phi(k+p, k) = \prod_{l=0}^{p-1} A_{k+l} \tag{3.4}$$

and thus any solution of (3.1) also fulfils:

$$x_{k+p} = \Psi_k x_k. \tag{3.5}$$

Note that Ψ_k is a p-periodic matrix, but the characteristic multipliers are constant for all k [5].

The Floquet theory can be used to analyse the stability of periodic orbits of non-linear systems by studying the convergence/divergence of a perturbation, governed by a linear periodic difference system, in the vicinity of the periodic orbit [3, 40].

Application to non-linear systems

Consider a non-linear discrete-time dynamical system described by the difference equation (2.5) with the p-periodic solution x_k^* for $u_k(x_k) = 0$ indicated in (2.2). Here we study the behaviour of a trajectory in the vicinity of x_k^*.

Proposition 3.2 (Stability of periodic orbits of discrete-time systems)**.** *A periodic orbit x_k^* of the recursive dynamical system* (2.5) *is locally asymptotically stable if the linear dynamical system that describes the evolution of a perturbed trajectory in the close vicinity of x_k^* is asymptotically stable.* □

Proof. Consider a perturbation $\delta x_0 : \mathbb{N} \times \mathbb{R}^n \to \mathbb{R}^n$ applied to the periodic state x_0^*. The initial condition of (2.5), x_0, is defined by

$$x_0 = x_0^* + \delta x_0. \tag{3.6}$$

The discrete-time evolution δx_k of the initial perturbation δx_0 for $u_k(x_k) = 0$ is obtained substituting the perturbed trajectory (3.6) in (2.5),

$$x_{k+1}^* + \delta x_{k+1} = f(k, x_k^* + \delta x_k, 0).$$

Expanding $f(k, x_k^* + \delta x_k, 0)$ around x_k^* for δx_k sufficiently small we obtain

$$f(k, x_k^* + \delta x_k) \approx f(k, x_k^*, 0) + \nabla_x f(k, x, 0)|_{x=x_k^*} \delta x_k,$$

$$\delta x_{k+1} \approx \nabla_x f(k, x, 0)|_{x=x_k^*} \delta x_k. \tag{3.7}$$

$\nabla_x f(k, x, 0) \in \mathbb{R}^{n\times n}$ is the Jacobian matrix of the system, here a time-periodic matrix due to the periodicity of $f(k, x_k^*, 0)$. The stability of x^* is analysed according to the convergence/divergence of δx_k governed by (3.7), reducing the problem to the stability analysis of the linear periodic system (3.1).

Once obtained the equation that governs the perturbation it is possible to define a discrete-time monodromy matrix $\Psi_k \in \mathbb{R}^{n\times n}$ for the periodic orbit x_k^*:

$$\delta x_{k+p} = \Psi_k \delta x_k. \tag{3.8}$$

We calculate the monodromy matrix according to (3.3) using (3.7)

$$\Psi_k = \prod_{l=0}^{p-1} \nabla_x f(k+l, x, 0)|_{x=x_{k+l}^*}. \tag{3.9}$$

The eigenvalues of Ψ_k (Floquet multipliers) are calculated to analyse the stability of the linear system (3.7). If it is asymptotically stable, then $\delta x_k \to 0$ and $f(k, x_0, 0) \to x_k^*$ as $k \to \infty$. □ □

3.1.2 Lyapunov stability theory

The Lyapunov stability theory for linear periodic system is presented here. For more details see [5]. For simplicity this theory will not be extended to the stability analysis of periodic orbits of non-linear system, but this subject can be performed directly using the formulation of the previous subsection.

Proposition 3.3 (Periodic Lyapunov Lemma, adapted from Proposition 3.5 in [5])**.** *The system* (3.1) *with the p-periodic matrix* A_k *is asymptotically stable if and only if there exist p-periodic positive definite matrices* P_k*,* $k = 0, 1, \ldots, p-1$*, such that:*

$$A_k P_k A_k' - P_{k+1} < 0, \tag{3.10}$$

where $P : \mathbb{N} \to \mathbb{R}^{n\times n}$. □

Consider the following Lyapunov function for the system (3.1):

$$V(k, x) = x_k' P_k^{-1} x_k. \tag{3.11}$$

A Lyapunov function for system (3.1) is any function $V : \mathbb{N} \times \mathbb{R}^n \to \mathbb{R}$ such that

- $V(k, x)$ is continuous in x, $\forall x \neq 0$;
- $V(k, x) > 0$, $\forall k$, $\forall x \neq 0$;
- $V(k, 0) = 0$, $\forall k$;
- $V(k + 1, x_{k+1}) - V(k, x_k) < 0$, $\forall k$, $\forall x_k \in \mathbb{R}^n$.

From the last condition we obtain exactly (3.10) with V defined by (3.11).
By subsequent iteration of the inequality (3.10), one obtains

$$\begin{aligned} P_{k+1} &> A_k P_k A_k' \\ P_{k+2} &> A_{k+1} \left(A_k P_k A_k'\right) A_{k+1}' \\ &\cdots \\ P_{k+p} &> \Psi_k P_k \Psi_k'. \end{aligned}$$

Considering a p-periodic solution of (3.1) we have $P_{k+p} = P_k$ and

$$P_k > \Psi_k P_k \Psi_k'. \tag{3.12}$$

Condition (3.12) thus relates the Floquet theory presented in the previous subsection to the Lyapunov theory presented here resulting in Proposition 3.3. If P_k is positive definite, Ψ_k is contractive (Floquet multipliers inside the unit circle) and (3.1) is asymptotically stable.

3.2 Stabilization of linear time-periodic systems

This section follows the statements presented in [5] aiming at present basic facts about the subject. Expansions on the theme can be obtained on this reference.

Consider a linear p-periodic discrete-time dynamical system described by the following difference equation

$$x_{k+1} = A_k x_k + B_k u_k \tag{3.13}$$

with the feedback control law and output

$$u_k(x_k) = K_k x_k, \tag{3.14a}$$

$$y_k(x_k) = C_k x_k, \tag{3.14b}$$

respectively. $x : \mathbb{N} \to \mathbb{R}^n$ is the state vector, $A : \mathbb{N} \to \mathbb{R}^{n\times n}$ is the state matrix, $B : \mathbb{N} \to \mathbb{R}^{n\times m}$ is the input matrix, $u : \mathbb{N} \times \mathbb{R}^n \to \mathbb{R}^m$ is the input vector, $K : \mathbb{N} \to \mathbb{R}^{m\times n}$ is the gain matrix, $C : \mathbb{N} \to \mathbb{R}^{g\times n}$ is the output matrix and $y : \mathbb{N} \times \mathbb{R}^n \to \mathbb{R}^g$ is the output vector, $n, m, g \in \mathbb{N}$.

The periodicity is verified by $A_{k+p} = A_k$ and $B_{k+p} = B_k$, $p \in \mathbb{N}$.

Definition 3.4 (Stabilization of discrete-time linear periodic systems by state feedback)**.** *Choose the matrix K_k (possibly p-periodic) such that the system* (3.13) *with control law* (3.14a) *is asymptotically stable, that is, the monodromy matrix* (3.4) *of the closed-loop system* (3.15) *has all the eigenvalues inside the unit cycle.*

$$x_{k+1} = (A_k + B_k K_k)\, x_k \quad \square \tag{3.15}$$

The existence of a stabilizing K_k depends upon the controllability of (3.13). *Controllability is concerned with the problem of driving a state point to any other state point by feeding the system* (3.13) *with a suitable input sequence.* For the mathematical developments, it is advisable to articulate the necessary definitions in a formal way as follows [5].

Definition 3.5 (Controllability of linear systems, adapted from [85]). *(i) System* (3.13) *is controllable on the time interval* $[k_1, k_2]$ *if, for each value of* $x^1, x^2 \in \mathbb{R}^n$*, there exists an input* $u_k, k_1 \leq k < k_2$*, such that for* $x_{k_1} = x^1$*, one has* $x_{k_2} = x^2$*. (ii) For any integer* $\tau \geq 0$*, system* (3.13) *is controllable in time* τ *if, for each value of* $x^1, x^2 \in \mathbb{R}^n$*, there exist time instants* k_1, k_2*,* $k_2 = k_1 + \tau$ *and an input* $u_k, k_1 \leq k < k_2$*, such that for* $x_{k_1} = x^1$*, one has* $x_{k_2} = x^2$*. (iii) System* (3.13) *is controllable if, for each value of* $x^1, x^2 \in \mathbb{R}^n$*, there exist time instants* k_1, k_2*,* $k_2 > k_1$ *and an input* $u_k, k_1 \leq k < k_2$*, such that for* $x_{k_1} = x^1$*, one has* $x_{k_2} = x^2$*.* □

The Definition 3.5 is valid only for linear systems where the definition of controllable and reachable states are equivalent. For controllability for nonlinear system see [85].

The controllability of linear time-invariant systems is a special case of Definition 3.5 for $A_k = A$ and $B_k = B$, constant matrices in (3.13). The controllability of

$$x_{k+1} = Ax_k + Bu_k \tag{3.16}$$

can be characterized in terms of the pair (A, B).

For the linear system (3.16), or equivalently the pair $(A,\ B)$, all three properties in Definition 3.5 are verified.

Another important concept for control problems is reconstructability, associated with the possibility of distinguishing two *past measurements of the output variable* states from the observation of the corresponding output signals when the system is subject to the same input function [5].

Definition 3.6 (Reconstructability of linear systems, adapted from Definition 4.3 in [5]). *(i) The state* $x \in \mathbb{R}^n$ *of system* (3.13) *is unreconstructable over* $[k_1,\ k_2]$*, if there exists a free motion* ($u_k = 0$) *ending in* $x_k = x$ *which results in the output* $y_k(x_k) = 0$ *of* (3.14b)*,* $\forall k \in [k_1,\ k_2 - 1]$*. (ii) System* (3.13) *is reconstructable over* $[k_1,\ k_2]$ *if any non-zero state is not unreconstructable over* $[k_1,\ k_2]$*. (iii) System* (3.13) *is reconstructable at time* k_1 *if there exists a time* $k_2 > k_1$ *such that it is reconstructable on* $[k_1,\ k_2]$*. (iv) System* (3.13) *is reconstructable if it is reconstructable at any time instant.* □

See [85] for general definitions of observable and reconstructable states and observability applied to nonlinear systems.

Here are the main approaches to synthesize stabilizing gain K_k that have been explored in the literature [5]:

- Stabilization by Lyapunov method: Find a periodic feedback gain in such a way that the closed-loop system is stable (any K_k meeting such a requirement is named stabilizing gain). This problem can be solved using the Lyapunov stability theory shown in Section 3.1.2 satisfying the condition (3.10).

- Pole assignment: Find a periodic feedback gain so as to position the closed-loop characteristic multipliers in given locations in the complex plane. This problem can be solved using the Floquet stability theory shown in Section 3.1.1 finding a K_k such that the eigenvalues of the closed-loop monodromy matrix are set as required.

- Optimal control: Find a periodic feedback gain so as to minimize the quadratic performance index

$$J = \sum_{k=0}^{+\infty} z_k' z_k,$$

  where z_k is the "performance evaluation variable". A typical choice is to assume a linear dependence of z_k upon x_k and u_k:

$$z_\tau = E_\tau x_\tau + N_\tau u_\tau.$$

- Invariantization: Find a feedback control law so that the closed-loop system is time-invariant up to a periodic state space coordinate change. Note that this method does not directly lead to stabilization, it is a tool used to reduce the stabilization of linear periodic systems to the stabilization of linear time-invariant systems.

Here we focus on the pole assignment/placement problem and its relation to the invariantization problem. We also provide shortly the stabilization by Lyapunov direct method.

3.2.1 Stabilization by direct Lyapunov method

The choice of a stabilizing periodic control gain for the periodic system (3.13) with control signal (3.14a) using the direct Lyapunov method is given by

Proposition 3.7 (Direct Lyapunov method, see Proposition 13.1 in [5])**.** *All stabilizing p-periodic gains K_k are given by*

$$K_k = W_k' P_k^{-1},$$

where W_k and $P_k > 0$ are p-periodic solutions of the linear matrix inequality (3.17)*.*

$$\begin{bmatrix} -P_{k+1} & B_k W_k' + A_k P_k \\ W_k B_k' + P_k A_k' & -P_k \end{bmatrix} < 0 \tag{3.17}$$

□

Proof. The linear matrix inequality (3.17) is obtained using the result of Lemma 3.8 and the Proposition 3.3 applied to the closed loop system (3.15).

Lemma 3.8 (Schur complement Lemma, see Lemma 3.1 in [5])**.** *Consider the partitioned matrix:*

$$R = \begin{bmatrix} E & F \\ F' & H \end{bmatrix}$$

with $E = E'$ and $H = H'$. Then,

- *Matrix R is negative definite if and only if*

$$H < 0, \quad E - FH^{-1}F' < 0.$$

- *Matrix R is negative semi-definite if and only if*

$$H \leq 0, \quad E - FH^{\dagger}F' \leq 0, \quad F(I - HH^{\dagger}) = 0.$$

where $\dagger$ denotes the Moore-Penrose pseudo-inverse. □

Proposition 3.3 applied to (3.15) The closed-loop version of (3.10) is:

$$P_{k+1} > (A_k + B_k K_k)\, P_k\, (A_k + B_k K_k)'\,. \tag{3.18}$$

Using (3.18) multiplying P_k by $P_k P_k^{-1}$, on the left, and $P_k^{-1} P_k$, on the right, with the control gain defined in the statement of Proposition 3.7 we obtain

$$-P_{k+1} + (A_k P_k + B_k W_k')\, P_k^{-1}\, (A_k P_k + B_k W_k')' < 0. \tag{3.19}$$

The linear matrix inequality of Proposition 3.7 is obtained by direct application of Lemma 3.8 to (3.19). This achieves the proof of Proposition 3.7. □

3.2.2 Eigenvalue assignment by state feedback

Definition 3.9 (Periodic eigenvalue assignment problem, adapted from page 1565 in [87])**.** *Given the linear time-periodic closed-loop system* (3.15)*, let* (A_k, B_k) *be a controllable periodic pair. Find periodic* $m \times n$ *matrices* K_k *such that*

$$\Lambda(\Psi_k) = \Gamma,$$

where $\Psi_k \in \mathbb{R}^{n\times n}$ *is the monodromy matrix of* (3.15)*,* $\Lambda(\Psi_k) \in \mathbb{C}^n$ *is the set of eigenvalues of* Ψ_k *and* $\Gamma \in \mathbb{C}^n$ *is an arbitrary set of* n *complex conjugate numbers.* □

Two strategies for pole assignment in linear time-periodic systems are presented, the sampled feedback and the instantaneous feedback [5, 18, 19, 87]. A specific case of pole placement via instantaneous feedback control is the dead-beat control, where $\Lambda(\Psi_k) = 0_n$. These three cases are discussed as follows.

Eigenvalue assignment via sampled feedback

This strategy consists in applying the state feedback using only one sampled state per cycle and operate in open loop in the inter-period instants. The control signal is defined by

$$u_k(x_l) = \bar{K}_k x_l, \quad k \in \Big[l, \quad l+p-1\Big], \quad l = ip+\tau, \quad i, \tau \in \mathbb{N}, \tag{3.20}$$

where the gain $\bar{K}_k$ is a p-periodic function suitable designed and τ is a fixed lag time.

The closed-loop system with the previous control signal for one period p is

$$x_{l+p} = \left[\Phi(l+p,l) + \sum_{j=l+1}^{l+p} \Phi(l+p,j) B_{j-1} \bar{K}_{j-1}\right] x_l = (F_l + G_l M_l)\, x_l \tag{3.21}$$

where $\Phi(k_2,k_1)$, is the free system state transition matrix, $F_l = \Phi(l+p,l)$, $G_l = \Big[G_1 \quad \cdots \quad G_p\Big]$, $G_j = \Phi(l+p,l+j)B_{l+j-1}$ and $M_l = \Big[\bar{K}'_{l+0} \quad \bar{K}'_{l+1} \quad \cdots \quad \bar{K}'_{l+p-1}\Big]'$.

The equation (3.21) is named the time-invariant reformulation of (3.13) [5, 18, 19, 87].

This problem can be expressed as follows.

Definition 3.10 (Eigenvalue assignment via sampled feedback)**.** *Chose a matrix M_l of the closed-loop system* (3.21) *obtained by the time-invariant reformulation of* (3.13) *using the control signal* (3.20) *such that $\Lambda(F_l + G_l M_l) = \Gamma$.* □

The pole assignment via sampled feedback is solved in [87] using the Schur decomposition on the pair (A_k, B_k), which uses only unitary transformations and promotes numerical stability in algorithms.

Note that the existence of a solution for the problem of Definition 3.10 depends on the Lemma 3.11.

Lemma 3.11 (adapted from Lemma 1 in [18])**.** *The pair (A_k, B_k) of system* (3.13) *with control signal* (3.20) *is controllable if and only if the pair (F_l, G_l) of system* (3.21) *is controllable.* □

Eigenvalue assignment via instantaneous feedback

For the instantaneous feedback case the control signal is defined as in (3.14a) and the problem is defined as in Definition 3.4.

The closed-loop system with control signal (3.14a) for one period p is

$$x_{k+p} = \prod_{j=k}^{k+p-1} (A_j + B_j K_j) x_k. \tag{3.22}$$

The solution of the problem of Definition 3.9 is suggested in [5] by relating the instantaneous feedback case with the sampled feedback case by using

$$K_{k+i} = \bar{K}_{k+i} \left[\prod_{j=k}^{k+i-1} (A_j + B_j \bar{K}_j) \right]^{-1}, \quad i = 0, 1, \cdots, p-1. \tag{3.23}$$

The solution of the pole assignment problem is done choosing, among all possible $\bar{K}_k$ which assign the prescribed characteristic multipliers of (3.22)*, any choice for which the invertibility of $A_k + B_k \bar{K}_k$ is met for all k.* However, finding an algorithm of wide applicability which exploits the time-invariant view point is still an open question [5].

Dead-beat control via state feedback

Definition 3.12 (State dead-beat control, see page 1092 in [32])**.** *Find a (possibly dynamic) linear controller for system* (3.13) *such that the state of the closed-loop system is driven to the origin in a finite interval of time, for any initial state and any initial time.* □

According to Theorem 3.13, the dead-beat control is a specific case of the eigenvalue assignment via instantaneous feedback.

Theorem 3.13 (see Theorem 1 in [32])**.** *If $C_k = I_n$* (3.14b)*, the state dead-beat control problem admits a solution of the form* (3.14a) *if and only if system* (3.13) *is controllable. Moreover, the matrix K_k in* (3.14a) *can be chosen periodic of period p.* □

For the state dead-beat control we set $\Lambda(\Psi_k) = \Gamma = \{0\}$ [87] and the time interval to the convergence of the trajectory to the origin is limited by the following theorem:

Theorem 3.14 (see Theorem 2 in [32]). *If $C_k = I_n$ and the system* (3.13) *is controllable, then the control law* (3.14a) *can be chosen so that, for any initial time, the system is driven to the origin within an interval of time not greater than np, with K_k periodic of period p.* □

When C_k has rank $< n$, the dead-beat controller can be applied if the pair $(A_k,\ C_k)$ is reconstructable by using a state observer. In [32] it is described a state dead-beat observer and the association with the dead-beat controller for stabilization of controllable and reconstructable systems.

3.3 Control methods for periodic orbits

Here we detail the principal feedback control methods for stabilization of periodic orbits.

3.3.1 Proportional feedback control (PFC)

This method uses as reference signal the target UPO itself and the control signal is defined by

$$u_k(x_k) = K_k(x_k)\,(x_k^* - x_k)\,. \tag{3.24}$$

$K_k(x_k) \in \mathbb{N} \times \mathbb{R}^n \to \mathbb{R}^{m \times n}$ may be a time-varying control gain that depends on the system state such that x_k^* is stable and condition (2.6) is satisfied. The application of the PFC method depends on the previous knowledge of the target UPO and this is the principal disadvantage of the method. Application of PFC to discrete-time system with constant gain K is exemplified in [38].

3.3.2 Delayed feedback control (DFC)

This method uses the state of the system delayed by the period p of the target UPO as reference. The control signal for the DFC is thus defined

$$u_k(x_k) = K_k(x_k)\,(x_{k-p} - x_k)\,. \tag{3.25}$$

where $K_k(x_k) \in \mathbb{N} \times \mathbb{R}^n \to \mathbb{R}^{n\times n}$ is a (possibly time-varying and state-dependent) control gain.

Pyragas [70] initially proposed a constant scalar control gain K that could be tuned experimentally. The controlled system with a constant K appears as having dimension $n(1+p)$, once the delayed states are included as components of state for the closed loop system.

The study of the DFC for discrete-time dynamical systems with K constant is done in [15,61,62,81,90,99,100,103]. In these references, the analytical proposition of a stabilizing K depends on the previous knowledge of x_k^*. Most of the references define the problem for equilibrium states ($p = 1$).

A DFC method with a time-varying control gain dependent upon the system state ($K_k(x_k)$) received the name adaptive DFC [78]. In this method, the control gain is defined as

$$K_{k+1}(x_k) = K_k(x_{k-1}) - \frac{\varepsilon}{2}\left.\frac{\partial\|x_{k-1} - x_k\|^2}{\partial K}\right|_{K=K_k(x_{k-1})}.$$

The gain $K_{k+1}(x_k)$, defined for equilibrium states, is adjusted at each time k in such a way that the error between x_{k-1} and x_k decreases in time. The update of K is based on a gradient descent of the squared error $E_k(x_k) = \frac{1}{2}\|x_{k-1} - x_k\|^2$, where E implicitly depends on K through x. The derivative of E with respect to K increases the state of the original system by $n + d(1+2n)$ variables (see Equation (4) in [78]), d is the number of elements of the control gain.

The great advantage of this method is the non dependence on the previous knowledge of x_k^* for the calculation of $K_{k+1}(x_k)$. The choice of ε was not detailed. Its convergence rate is similar to the original DFC.

Two limitations were identified from the analysis of the initially proposed DFC: the first is the impossibility to control orbits with longer periods [103], i.e., more unstable [20]; the second is the impossibility to control orbits with an odd number of Floquet multipliers [5] real and greater than $+1$ (*odd number limitation*) [90, 99, 100, 103].

The first limitation can be overcome with the extended delayed feedback control or generalized feedback control [53, 89, 104]. This method uses not only one delayed state $(x_{k-p} - x_k)$ as in (3.25), but the sum of the, ideally infinite, terms $(x_{k-mp} - x_k)$, $m = 1, 2, \ldots, +\infty$, with each term in the sum multiplied by its own constant control gain defined by proper rule.

The second limitation (the odd number limitation) can be overcome using the dynamic delayed feedback control. This method presents the control signal, $u_k(x_k)$, as the output of a new dynamical system. Another method derived by the DFC, that satisfies the condition (2.6) and does not present the odd number limitation is the prediction-based control, described in the next section. Note that the adaptive DFC also presents the odd number limitation.

3.3.3 Prediction based control (PBC)

This method, proposed by Ushio and Yamamoto [91] with extension in [40] and later studied in [63], uses a control signal defined by

$$u_k(x_k) = K_k(x_k) \left(\varphi(k+p, k, x_k, 0) - x_k\right), \tag{3.26}$$

where $\varphi(k_1, k_0, x, 0)$ is the value at time k_1 of the state of (2.5) with $x_{k_0} = x$ and $u_k = 0$, $k_0 \leq k \leq k_1$. In other words, $\varphi(k_1, k_0, x, 0)$ is the value at time k_1 of the state along the trajectory departing from x at time k_0 of the free system ($u_k \equiv 0$).

The PBC does not extend the original system state as the DFC, but it necessitates the prediction of *the state one period ahead, computed along the trajectories of the free system response.*

A constant control gain K, defined in terms of x_k^*, for the PBC is used in [7, 63, 91]. The principal advantage with respect to the DFC is the non existence of the odd number limitation.

A time varying control gain defined for the target UPO, $K_k(x_k^*)$, was defined in [40]. In this reference the authors exemplify the application of the PBC leading all the Floquet multipliers of the controlled system to zero, something which is characteristic of the dead-beat controllers [32].

The contribution of the present work in the domain of discrete-time systems is the proposition of a method to define the PBC gain (Section 3.4). The results were initially published in [12]. The control scheme shown here is based on improved sufficient stability conditions and leads to stabilizing gains. Three control laws are proposed for p-periodic orbits:

- The first, CL 1, is based on linear time-invariant gain K, whose determination depends upon prior UPO knowledge;
- The second, CL 2, is based on time-periodic state-dependent gain $K_k(x_k^*)$, whose determination also depends on the UPO knowledge;
- The third, CL 3, is based on non-linear time-variant state dependent $K_k(x_k)$ and *does not depend on prior knowledge on the UPO position*, only its period is necessary.

The three control laws lead to different behaviours in terms of convergence rate and size of basin of attraction (Section 4.1), although, all the Floquet multipliers of the controlled orbit are fixed on the origin. The third control law (CL 3) has the clear advantage of not requiring the exact knowledge of the UPO position.

The control laws proposed here are inspired from dead-beat controllers designed for linear periodic systems [32]. They are applied to stabilization of periodic orbits of chaotic non-linear systems using the feedback control input (3.26).

A comparison between the DFC, with a gain matrix obtained by minimization of the Floquet multipliers of the controlled orbit [44], and the PBC, with the control law 3, is performed in Section 4.2. These results were originally published in [11]. The basins

of attraction and the control effort are calculated numerically for some periodic orbits controlled by both methods. These results are used to compare the stability and the convergence rate of the trajectories controlled by both methods.

The chaos control methods studied in literature consider that all the states of the controlled dynamical system are directly accessible by the controller using an input matrix equal to the identity. Here, the control method is initially applied considering this characteristic, restricting the design to invertible input matrices (Section 3.4.2). However, a subsequent design of the PBC for a non-invertible input matrix is also done (Section 3.4.3 and numerical results in Section 4.4).

We complete the analysis on the method applying the PBC subject to parameters uncertainty in Section 4.3. We consider a situation where one parameter of the prediction model is different from the application model (system). This analysis is of special interest because the control laws proposed here depend on the cancellation of the linear dynamics of a trajectory in the vicinity of the controlled orbit.

3.4 Stabilization of periodic orbits

The previous sections were a review of results presented on literature. From now on we present the new results provided by this work.

It was shown previously that the stabilization of periodic orbits of non-linear systems can be studied as stabilization of the linearised system around the periodic orbit. The stabilization processes departs from the definition of the closed-loop monodromy matrix and the calculation of a control gain that makes the system stable. The stabilization can be performed by different methods of stabilization of linear periodic systems, all of them aiming at setting all the Floquet multipliers inside the unit cycle.

The application of the methods shown in Section 3.2 in stabilizing periodic orbits of non-linear systems does not have, a priori, any restriction, although, none of them consider an ideally zero control effort when the trajectory is on the target UPO (2.6), the principal advantage of chaos control methods.

Consider the non-linear discrete-time dynamical system described by (2.5) and the existence of the hyperbolic periodic orbit x^* of period $p \in \mathbb{N}$.

The goal here is stabilizing the UPO x^* of (2.1) subjected to the control restriction (2.6). The transition from x_k to x_{k+p} of (2.5) is defined by the closed-loop state transition map

$$x_{k+p} = \varphi(k+p, k, x_k, u_k(x_k)). \tag{3.27}$$

On the periodic orbit, the condition (2.6) guarantees that any p-periodic orbit that satisfies (2.2) is also a p-periodic orbit of (3.27). Then,

$$x^*_{k+p} = x^*_k = \varphi(k+p, k, x^*_k, u_k(x^*_k)) = \varphi(k+p, k, x^*_k, 0). \tag{3.28}$$

The matrix

$$\Psi_k = \nabla_x \varphi(k+p, k, x, u_k(x))|_{x=x^*_k}$$

is the monodromy matrix associated to the orbit x^* of the closed-loop discrete-time system (2.5). The stability of the periodic orbit of system (2.5) is related to the spectrum of the monodromy matrix, being stable if all the eigenvalues (Floquet characteristic multipliers [5]) have modulus less than or equal to 1 (Proposition 3.1).

In the following we describe the calculation of the monodromy matrix and propose the control laws based on sufficient stability conditions for UPOs controlled by the PBC [12]. The PBC is the focus of this chapter and in this section we define the stabilization of periodic orbits using it. For that, we use the PBC with the control signal defined by (3.26).

3.4.1 Stabilization by the prediction-based control

A sufficient stability condition for periodic orbits of discrete-time dynamical systems controlled by the PBC is defined in this section based on the spectrum of Ψ_k. The result obtained in Theorem 3.16 (end of the section) enables the development of stabilizing control laws for UPO's using the PBC.

According to (2.5) and (3.26), the closed-loop discrete-time dynamical system controlled using the PBC is defined by

$$x_{k+1} = \varphi(k+1, k, x_k, u_k(x_k)) = f(k, x_k, K_k(x_k)(\varphi(k+p, k, x_k, 0) - x_k)). \tag{3.29}$$

In the sequel, for any $x \in \mathbb{R}^n$ and $K \in \mathbb{R}^{q\times n}$, $q \in \mathbb{N}$, we use the notation

$$\begin{aligned} \psi(k, x, K) &\doteq f(k, x, u_k(x)) \\ u_k(x) &= K(\varphi(k+p, k, x, 0) - x). \end{aligned} \tag{3.30}$$

The first step for the definition of the sufficient stability condition for periodic orbits is to obtain Ψ_k. This matrix, for the closed-loop system, is calculated according to the proposed Lemma 3.15.

Lemma 3.15. *For any p-periodic point x_k^*, $k, p \in \mathbb{N}$, of the trajectory x^* of the closed-loop system* (3.29)*, one has*

$$\Psi_k = \prod_{l=0}^{p-1} \nabla_x \psi(k+l, x, K_{k+l}(x_{k+l}^*))\big|_{x=x_{k+l}^*} \tag{3.31}$$

and the matrices in the product are ordered from right to left for increasing indices l. □

The interest of formula (3.31) *is that no derivative of $K_k(x_k)$ with respect to x_k appears in the right-hand side.* Thus, Lemma 3.15 provides a simplification in the computation of the monodromy matrix spectrum: as indicated by (3.31), the dependence of the gain with respect to the state does not modify the Jacobian $\nabla_x \psi(k, x, K_k(x))$ in the points of the periodic orbit.

Proof. Expanding the result of equation (3.9), the monodromy matrix of the closed-loop system is calculated as follows,

$$\Psi_k = \prod_{l=0}^{p-1} \nabla_x \psi(k+l, x, K_{k+l}(x))|_{x=x_{k+l}^*}.$$

Now, using the definition of $\psi(k, x, K)$, (3.30), we compute the derivative using the general chain rule [49]

$$\nabla_x \psi(k, x, K_k(x)) = \nabla_x f(k, x, u_k(x_k)) + \nabla_u f(k, x_k, u) K_k(x_k) \nabla_x (\varphi(k+p, k, x, 0) - x) + \nabla_u f(k, x_k, u) \nabla_x K_k(x) (\varphi(k+p, k, x_k, 0) - x_k)$$

and apply $x = x_k = x_k^*$, resulting in

$$\nabla_x \psi(k, x, K_k(x))|_{x=x_k^*} = \nabla_x \psi(k, x, K_k(x_k^*))|_{x=x_k^*} + \nabla_u f(k, x_k^*, u)\, \nabla_x K_k(x)|_{x=x_k^*} (\varphi(k+p, k, x_k^*, 0) - x_k^*).$$

On the periodic orbit, we have $\varphi(k+p, k, x_k^*, 0) = x_k^*$, and the term containing $\nabla_x K_k(x)$ is zero. This provides the desired result. □

Observe that, for any $k \in \mathbb{Z}$, the (i, j)-th component of the product of the tensor $\frac{\partial K_k(x)}{\partial x}\Big|_{x=x_k^*}$ by the vector $(\varphi(k+p, k, x_k^*, 0) - x_k^*)$ can be computed using the following sum

$$\sum_{j'=1}^{n} \left(\frac{\partial K_{k,ij'}(x)}{\partial x_j}\bigg|_{x=x_k^*} \cdot (\varphi(k+p, k, x_k^*, 0) - x_k^*)_{j'} \right).$$

This sum illustrates the dimensional consistence on the matrices multiplications shown in the proof of the lemma.

The simplification provided by the Lemma 3.15 is used in the Theorem 3.16 to define a sufficient stability condition for a periodic orbit of (3.29).

Theorem 3.16. *Assume the Jacobian* $\nabla_x \psi(k, x, K_k(x_k^*))\,\big|_{x=x_k^*}$ *of the system* (3.29) *is zero at least for one point of the periodic orbit* x_k^**. Then, the periodic orbit* x^* *is locally exponentially stable.* □

Proof. The proof is obtained by direct observation of the result in Lemma 3.15: under the conditions of the statement, $\Psi_k = 0_n$, which yields stability of the associated fixed point, and thus stability of the periodic cycle. □

Theorem 3.16 reduces the problem of the stabilization of periodic orbits of discrete-time dynamical system controlled by the PBC to the problem of leading the Jacobian of one point of the orbit to zero (matrix composed by zeros) with the simplification provided by Lemma 3.15. The next step is to define a gain matrix $K_k(x_k)$ that leads to the desired result.

Note that the result shown in the Theorem 3.16 sets not only the eigenvalues of the monodromy matrix equal zero, but the entire matrix is equal to zero. This results in the cancellation of the linearized dynamics around the periodic orbit. Setting all the eigenvalues of the monodromy matrix to zero is characteristic of dead-beat controllers and leads do finite-time convergence for linear dynamics. However, applying this result, as we do here, to the linearized dynamics around the periodic orbit does not ensure finite-time convergence of the trajectories of the nonlinear system towards the latter.

3.4.2 Stabilizing control laws: The invertible input matrix case

Theorem 3.17. *If $\nabla_u f(k,x,u)$ is an invertible matrix for $x = x_k^*$ and $u = u_k(x_k^*)$ and the linear map that describes the evolution of a perturbation in the close vicinity of a trajectory of system (3.29) for $u_k(x_k) = 0$ is hyperbolic, then there exists a control gain $K_k(x_k)$ that satisfies Theorem 3.16 .* □

Invertible $\nabla_u f(k,x,u)$ matrix is typically the case for systems such that

$$x_{k+1} = g(k, x_k) + u_k, \tag{3.32}$$

where x and u are vectors of the same dimension and the systems can be fully actuated.

Proof. From Lemma 3.15,

$$\nabla_x \psi(k, x, K_k(x))|_{x=x_k^*} = 0_n$$

is equivalent to

$$\nabla_x f(k, x, u_k(x_k^*))|_{x=x_k^*} + [\nabla_u f(k,x,u) K_k(x) (\nabla_x \varphi(k+p, k, x, 0) - I_n)]_{x=x_k^*, u=u_k(x_k^*)} = 0_n. \tag{3.33}$$

If $\nabla_u f(k,x,u)$ and $(\nabla_x \varphi(k+p,k,x,0) - I_n)$ are invertible for $x = x_k^*$ and $u = u_k(x_k^*)$, $K_k(x_k)$ can be isolated in the right side of (3.33). This is the case if $\nabla_x \varphi(k+p,k,x,0)$ is hyperbolic (eigenvalues different from one, see Appendix A). □ □

The values of $K_k(x_k)$ selected in the sequel will be shown to fulfill Theorem 3.17.

• **Control law CL 1.** *$K(x_0^*)$ is a constant matrix defined by:*

$$K(x_0^*) = -(\nabla_u f(0,x_0^*,u)|_{u=u_0(x_0^*)})^{-1} \nabla_x f(0,x,u_0(x_0^*))|_{x=x_0^*} (\nabla_x \varphi(p,0,x,0) - I_n)^{-1}\big|_{x=x_0^*}. \tag{3.34}$$

This results in a linear time-invariant control law whose determination also depends upon the UPO knowledge.

• **Control law CL 2.** *$K_k(x_k^*)$ is a time-varying matrix defined for each time $k \in \mathbb{Z}$ by:*

$$K_k(x_k^*) = \\ -(\nabla_u f(k,x_k^*,u)|_{u=u_k(x_k^*)})^{-1} \nabla_x f(k,x,u_k(x_k^*))|_{x=x_k^*} (\nabla_x \varphi(k+p,k,x,0) - I_n)^{-1}\big|_{x=x_k^*}, \tag{3.35}$$

This results in a linear time-periodic control law whose determination depends also upon the UPO knowledge.

Application of CL 1 or CL 2 necessitates to define which of the orbit points is the point x_0^*. A possible choice is to take x_0^* as the point of the cycle minimizing the distance from x_0.

Both control laws explicitly use the target UPO to obtain the control gain. The design of the controllers follows the same requirements of the PFC, the exact knowledge of the UPO for the definition of the control gain.

A similar control law for dimension-1 discrete-time systems is applied in [40], here the CL1 and CL2 are provided for n-dimensional systems.

• **Control law CL 3.** *$K_k(x_k)$ is given as*

$$K_k(x_k) = \\ -\left(\nabla_u f(k, x_k, u)|_{u=u_k(x_k)}\right)^{-1} \nabla_x f(k, x, u_k(x_k))|_{x=x_k} \left(\nabla_x \varphi(k+p, k, x, 0) - I_n\right)^{-1}\Big|_{x=x_k}. \tag{3.36}$$

Contrary to CL 1 and CL 2, the choice CL 3 does *not* require any knowledge on the UPO (except the period p). The calculus of $K_k(x_k)$ depends only on the actual state of the trajectory.

One advantage of CL 3 is the fact that it avoids the necessity of finding the UPO before stabilizing it. Another advantage is that, when designing the control gain for CL 1 or CL 2 (or any other control method that depends on the UPO position), errors in the UPO approximation lead to less accurate control gains. The PBC with CL 3 can be applied to find (or refine, for inaccurate approximations) UPOs when using other control methods.

Putting the term (3.36) in (3.29) reminds the Newton-Raphson method [68] applied to the iterative search for zeros of the map $(\varphi(k+p, k, x, 0) - x)$, which uses the adjustment law $x \leftarrow x + \Delta$, $\Delta = -(\nabla_x \varphi(k+p, k, x, 0) - I_n)^{-1}(\varphi(k+p, k, x, 0) - x)$. The difference here is that the adjustment is done on $f(k, x_k, u_k(x_k))$, the map that defines the state dynamics and not on the state itself. Note that the Newton-Raphson method is commonly used to find UPOs [68].

The three control laws satisfy the condition of Theorem 3.17, this implies that the control laws proposed in this work result in the suppression of the linearised dynamics (perturbation) around the periodic orbit ($\Psi_k = 0_n$). This is done cancelling the linearised dynamics at, at least, one point of the orbit ($\nabla_x \psi(k, x, K_k(x_k^*))|_{x=x_k^*} = 0_n$) and depends on the exact knowledge of $f(k, x_k, u_k(x_k))$ for the calculation of $\nabla_x f(k, x, u_k(x_k))$ and the future state. Model discrepancy with respect to the application system makes $\Psi_k \neq 0_n$. A brief robustness analysis of the control method is done by simulations in the numerical results presented in Section 4.3.

3.4.3 Stabilizing control laws: The non-invertible input matrix case

The control laws proposed in the Section 3.4.2 are limited to systems (3.29) that present an invertible input matrix $\nabla_u f(k, x_k, u)$. Here we provide alternatives for a non-invertible $\nabla_u f(k, x_k, u) : \mathbb{N} \times \mathbb{R}^n \times \mathbb{R}^m \to \mathbb{R}^{n \times m}$ with $K_k(x_k) : \mathbb{N} \times \mathbb{R}^n \to \mathbb{R}^{m \times n}$ in the special case of single input systems. We thus take

$$m = 1.$$

Notice that the condition (3.33) may be impossible to satisfy for the new $\nabla_u f(k, x_k, u)$ and the Theorem 3.16 is not applicable (Lemma 3.15 is still valid).

For the cases where the condition (3.33) can not be satisfied we provide the control law (3.39) below with a non-linear time-varying control gain $K_k(x_k)$ that may be applied making the Floquet multipliers of the controlled orbit equal to zero. The monodromy matrix is not necessarily 0_n, but this control law is equivalent to CL 3, in the sense that the Floquet multipliers are equal to 0, while no previous knowledge about the UPO is required. The main requirement to apply the result we are about to state (Theorem 3.19 below) is the existence of a given change of basis transforming, at any frozen time, the system linearised around the periodic orbit in its controllable canonical form.

Theorem 3.18 (Controllable canonical form, adapted from Theorem 5.1 in [54])**.** *Let the state equations of a linear time-invariant system be described by* (3.16) *in the scalar input case ($m = 1$). If the matrix function*

$$Q = \begin{bmatrix} B & AB & A^2B & \cdots & A^{n-1}B \end{bmatrix}$$

is nonsingular, then there exists a nonsingular transformation

$$z_k = Tx_k \qquad or \qquad x_k = T^{-1}z_k$$

which transforms (3.16) *to the controllable canonical form (CCF):*

$$z_{k+1} = A_c z_k + B_c u_k \tag{3.37}$$

where $A_c = TAT^{-1}$ *and* $B_c = TB_k$ *are*

$$A_c = \begin{bmatrix} 0 & 1 & 0 & 0 & \cdots & 0 \\ 0 & 0 & 1 & 0 & \cdots & 0 \\ 0 & 0 & 0 & 1 & \cdots & 0 \\ \vdots & \vdots & \vdots & \vdots & \ddots & \vdots \\ 0 & 0 & 0 & 0 & \cdots & 1 \\ -a_1 & -a_2 & -a_3 & -a_4 & \cdots & -a_n \end{bmatrix} \qquad B_c = \begin{bmatrix} 0 \\ 0 \\ 0 \\ \vdots \\ 0 \\ 1 \end{bmatrix}.$$

The transforming matrix T *is given by*

$$T = \begin{bmatrix} P \\ PA \\ \vdots \\ PA^{n-1} \end{bmatrix} \tag{3.38}$$

where

$$P = \begin{bmatrix} 0 & 0 & \cdots & 1 \end{bmatrix} Q^{-1}. \quad \square$$

Notice that there exist different controllable canonical representations of the system (3.16). These representations are obtained by using a transformation matrix defined differently from (3.38).

Theorem 3.19. *Assume that the unstable p-periodic orbit of system* (2.1) *is hyperbolic and that, for any* $k \geq 0$ *and for any* x_k*, the pair* $\Big(A_k(x_k), \quad B_k(x_k)\Big)$ *is controllable, where*

$$A_k(x_k) = \nabla_x f(k, x, u_k(x_k))|_{x=x_k}$$
$$B_k(x_k) = \nabla_u f(k, x_k, u)|_{u=u_k(x_k)}$$

are associated to the closed-loop system (3.30) *with scalar input signal* $u_k(x_k)$.

Assume that there exists a constant (with respect to k*) change-of-basis matrix* T *that transforms* $\Big(A_k(x_k), \quad B_k(x_k)\Big)$ *into the controllable canonical form* $\Big(TA_k(x_k)T^{-1}, \quad TB_k(x_k)\Big)$ *of Theorem 3.18. Then it is possible to set to zero all the Floquet multipliers of the closed-loop system* (3.30) *using the time-varying control gain vector* $K_k(x_k)$ *defined by*

$$K_k(x_k) = \\ \begin{bmatrix} 0_{1\times n-1} & 1 \end{bmatrix} \left(T^{-1}NT - \nabla_x f(k,x,u_k(x_k))|_{x=x_k}\right) \left(\nabla_x \varphi(k+p,k,x,0)|_{x=x_k} - I_n\right)^{-1} \quad (3.39)$$

where N *is the nilpotent matrix defined as*

$$N_{i,j} = \begin{cases} 1, & \text{if } j = i+1, \\ 0, & \text{otherwise.} \end{cases} \quad \square \quad (3.40)$$

Proof. Using Lemma 3.15 we calculate the Jacobian matrix of the closed-loop system (3.30) in the CCF of Theorem 3.18 as

$$\nabla_x \psi(k,x,k_k(x_k^*))|_{x=x_k^*} = \\ T\left[A_k(x_k^*) + B_k(x_k^*)K_k(x_k^*)\left(\nabla_x \varphi(k+p,k,x,0)|_{x=x_k^*} - I_n\right)\right]T^{-1}.$$

and for each time $k = 0, 1, \ldots, p$ we want to guarantee

$$T\left[A_k(x_k^*) + B_k(x_k^*)K_k(x_k^*)\left(\nabla_x \varphi(k+p,k,x,0)|_{x=x_k^*} - I_n\right)\right]T^{-1} = N \quad (3.41)$$

where $N \in \mathbb{R}^{n\times n}$ is the nilpotent matrix (3.40). If we manage to realize (3.41), then from (3.31) we have that

$$\Psi_k = \prod_0^{p-1} T^{-1}NT = T^{-1}N^pT \quad (3.42)$$

has all its eigenvalues equal to zero due to similarity between N and $T^{-1}NT$. For $p \geq n$, we obtain the special case $\Psi_k = 0_n$.

We attempt now to solve equation (3.41) for the gain value $K_k(x_k^*)$. From (3.41) we deduce

$$TB_k(x_k^*)K_k(x_k^*) = \left(N - TA_k(x_k^*)T^{-1}\right) T \left(\nabla_x \varphi(k+p,k,x,0)|_{x=x_k^*} - I_n\right)^{-1} \tag{3.43}$$

where, using the fact that the pair $\Big(TA_k(x_k)T^{-1},\ \ TB_k(x_k)\Big)$ is in the CCF and we are using scalar input function, one gets

$$TB_k(x_k^*)K_k(x_k^*) = \begin{bmatrix} 0_{(n-1)\times n} \\ K_k(x_k^*) \end{bmatrix}. \tag{3.44}$$

The defined N implies that $(N - TA_k(x_k^*)T^{-1})$ has the first $n-1$ lines equal to $0_{(n-1)\times n}$ guaranteeing the identity for the $(n-1)$ first lines of (3.43).

From (3.40), (3.43) and (3.44) we obtain

$$K_k(x_k^*) = \begin{bmatrix} 0_{1\times n-1} & 1 \end{bmatrix} \left(T^{-1}NT - A_k(x_k^*)\right) \left(\nabla_x \varphi(k+p,k,x,0)|_{x=x_k^*} - I_n\right)^{-1}. \tag{3.45}$$

Notice that:

- Applying (3.45) for $k \geq 0$ at any state x_k we have (3.39) and local stability of x_k^* is guaranteed by (3.41) and (3.42);
- If it is not possible to obtain a constant matrix T using (3.38) then (3.42) is not verified and zero eigenvalues are not guaranteed. However stability of x_k^* may be achieved by using others control laws. □

□

General results for multi input systems can be obtained with (3.38) defined for general input matrices. This can be done in future works.

Chapter 4

Numerical results

The numerical examples are divided in four parts. We compare the three control laws proposed for the PBC shown in the Section 3.4.2 using the Logistic map as case study in the first part (Section 4.1). We compare the PBC with the proposed CL 3 with the DFC using as case study the Hénon map in the second part (Section 4.2). The DFC gain is tuned minimizing the modulus of the Floquet multipliers of the controlled orbits. A brief numerical robustness analysis of the PBC with the CL 3, and the DFC for the system subject to parametric uncertainty is done in the third part (Section 4.3). The fourth part is dedicated to the non-invertible input matrix case (Section 4.4).

4.1 Comparison among the prediction-based control laws

The proposed control laws for the PBC are applied to the Logistic map. The proposed laws were developed for n-dimensional discrete-time systems, but a system of dimension $n = 1$ simplifies the numerical analysis and the comparison among the three control laws.

The Logistic map The closed-loop Logistic map is given by

$$x_{k+1} = g(x_k) + u_k(x_k), \tag{4.1}$$

where $x : \mathbb{N} \to \mathbb{R}$ and $u : \mathbb{N} \times \mathbb{R} \to \mathbb{R}$. The function g is given by

$$g(x) = rx(1 - x), \tag{4.2}$$

for a given parameter $r \in \mathbb{R}$. The control signal is

$$u_k(x) = K_k(x)(\varphi(k + p, k, x, 0) - x) \tag{4.3}$$

where here $\varphi(k + p, k, x, 0) = g^p(x)$ and $K : \mathbb{N} \times \mathbb{R} \to \mathbb{R}$.

4.1.1 Applying CL 3 and finding UPOs

The first step is applying the CL 3 because there is not the necessity of any knowledge about the target UPO position. We use the CL 3 to find the UPO's and the CL 1 and CL 2 gains. Note that UPOs of the Logistic map can be found apolitically, but the CL 3 simplifies the search.

The CL 3 applied to different values of the parameter r, initial condition x_0 and UPO of period p of the Logistic map is shown in Figure 4.1. In Figure 4.1(a) a 2-periodic orbit is stabilized for $r = 4$ and initial condition $x_0 = 0.48$ resulting in $K_k(x_k^*)$ shown in Table 4.1. In Figure 4.1(b) a 3-periodic orbit is stabilized for $r = 4$ and initial condition $x_0 = 0.69$ resulting in $K_k(x_k^*)$ shown in Table 4.2. In Figure 4.1(c) a 5-periodic orbit is stabilized for $r = 4$ and initial condition $x_0 = 0.57$ resulting in $K_k(x_k^*)$ shown in Table 4.3. In Figure 4.1(d) a 6-periodic orbit is stabilized for $r = 3.65$ and initial condition $x_0 = 0.52$ resulting in $K_k(x_k^*)$ shown in Table 4.4. The figure shows the evolution of the state x_k and the control effort $u_k(x_k)$.

The first characteristic observed in the proposed scheme is the fast convergence of the trajectory to the vicinity of the target UPO. We consider that the UPO is stabilized when $|u_k(x_k)| < 10^{-10}$, remaining below this threshold for the following k. The Figure 4.1(d) can be compared to [63, Fig. 5], where the convergence is achieved for k between 100 and 200 and using a larger control effort for the same conditions.

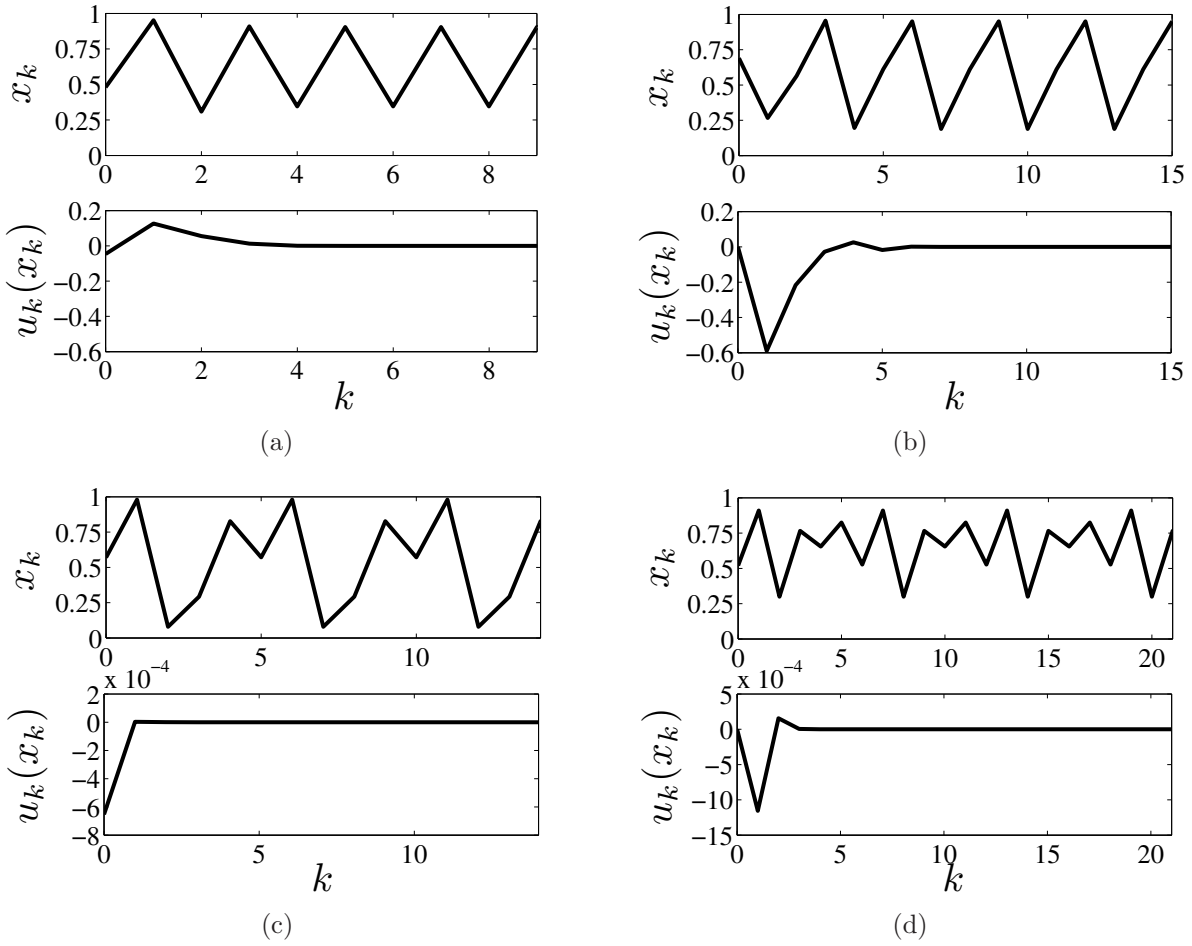

Figure 4.1: Example of the evolution of the state x_k and the control effort $u_k(x_k)$ for the Logistic map controlled using the CL 3: (a) $r = 4$, $x_0 = 0.48$ and $p = 2$; (b) $r = 4$, $x_0 = 0.69$ and $p = 3$; (c) $r = 4$, $x_0 = 0.57$ and $p = 5$; (d) $r = 3.65$, $x_0 = 0.52$ and $p = 6$.

Table 4.1: Points and respective values of the control gain for the stabilized UPO of Figure 4.1(a).

Time	k	$k+1$
x_k^*	0.90451	0.34549
$K_k(x_k^*)$	-0.64721	0.24721

Table 4.2: Points and respective values of the control gain for the stabilized UPO of Figure 4.1(b).

Time	k	$k+1$	$k+2$
x_k^*	0.18826	0.61126	0.95048
$K_k(x_k^*)$	-0.35628	0.12716	0.51484

Table 4.3: Points and respective values of the control gain for the stabilized UPO of Figure 4.1(c).

Time	k	$k+1$	$k+2$	$k+3$	$k+4$
x_k^*	0.57116	0.97975	0.79373×10^{-1}	0.29229	0.82743
$K_k(x_k^*)$	-0.17250×10^{-1}	-0.11630	0.10197	0.50353×10^{-1}	-0.79377×10^{-1}

Table 4.4: Points and respective values of the control gain for the stabilized UPO of Figure 4.1(d).

Time	k	$k+1$	$k+2$	$k+3$	$k+4$	$k+5$
x_k^*	0.90983	0.29944	0.76568	0.65486	0.82497	0.52704
$K_k(x_k^*)$	-0.54423	0.26633	-0.35281	-0.20564	-0.43154	-0.35909×10^{-1}

4.1.2 Comparing the three control laws by convergence rate and control effort

The transient of $u_k(x_k)$ for trajectories converging to the target UPOs for the three control laws are compared on Figure 4.2. The examples refer only to stabilized orbits of period p, as there are control gains that make trajectories controlled by the CL 1 and CL 2 diverge to the infinity or converge to fixed points or periodic orbits that do not correspond to a solution of the free system (4.1) (situation that also occurs for the DFC)[1]. In Figure 4.2(a) a 2-periodic orbit is stabilized for $x_0 = 0.48$, the control gain used for the CL 2 is the one obtained in the simulation of Figure 4.1(a) and the control gain used for CL 1 is $K = 0.24721$. In Figure 4.2(b) a 5-periodic orbit is stabilized for $x_0 = 0.6469$, the control gain used for the CL 2 is the one obtained in the simulation of Figure 4.1(c) and the control gain used for CL 1 is $K = -0.17250 \times 10^{-1}$.

The trajectories shown in the Figure 4.2 make explicit the fact that, if the stabilization succeeds, the convergence for the CL 3 is faster than the convergence for the other two control laws. This is better evidenced for trajectories with initial conditions farther from the target UPO.

[1]Notice that p-periodic orbits of the closed-loop system may exist that are not p-periodic orbits of the free system. However, the occurrence of this phenomena is investigated by $u_k(x_k)$ not converging to zero. This contrasts with the DFC, where p-periodic orbits of the closed-loop and the free system are exactly the same.

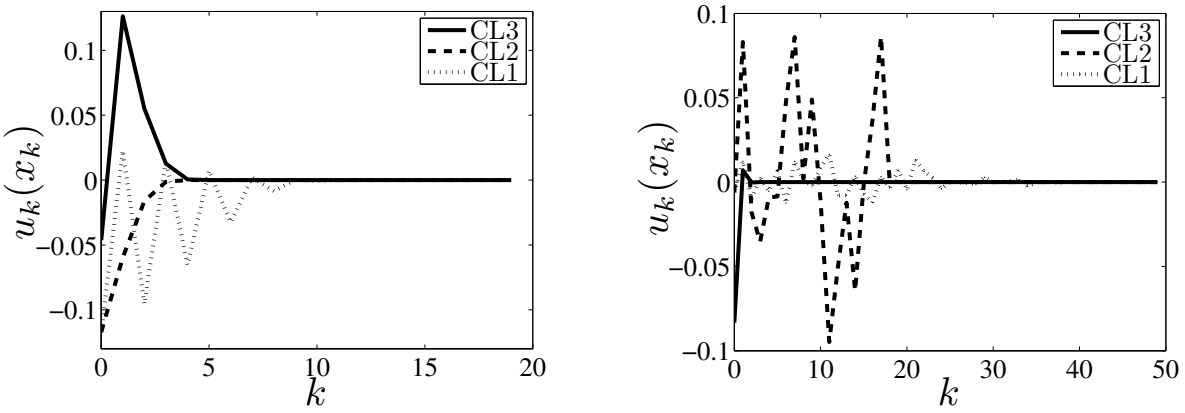

(a) (b)

Figure 4.2: Comparison among the control effort $u_k(x_k)$ transient of trajectories converging to stabilized orbits of the Logistic map using the three control laws (legend in the figure) for $r = 4$: (a) $x_0 = 0.48$ and $p = 2$; (b) $x_0 = 0.6469$ and $p = 5$.

Table 4.5: Points and respective values of the control gain for one of the stabilized UPO of Figure 4.4.

Time	k	$k+1$	$k+2$
x_k^*	0.41318	0.96985	0.11698
$K_k(x_k^*)$	0.77177 $\times 10^{-1}$	-0.41764	0.34046

4.1.3 Comparing the three control laws by basins of attraction

The comparison among the control laws is completed by the size of the basins of attraction (BA) of the stabilized orbits. The BAs here are the set of initial conditions that converge to a specific periodic orbit of the closed-loop system. The BAs of stabilized period-2 orbits are shown in the Figure 4.3 and period-3 are shown in the Figure 4.4. The different control laws are represented in the sub-figures (a), (b) or (c) of each figure. In Figures 4.3(c), 4.4(b) and 4.4(c), the BAs obtained for different control gains are divided in the vertical axis. The Logistic map has only one period-2 orbit for $r = 4$ and the control gain on the orbit was obtained in the simulation of Figure 4.1(a). This results in two different gains for the CL 1. There exists two period-3 orbits for $r = 4$ with two different values of $K_k(x_k^*)$ (two sets of control gains for the CL 2), the first is the one obtained in the simulation of Figure 4.1(b) (Table 4.2) and the other is $K_k(x_k^*)$ shown in Table 4.5. This results in six different control gains for the CL 1.

The basins of attraction of the fixed points (FP: period-1 orbits) are shown for $p = 2$ and $p = 3$ when using the CL 3, the other control laws do not stabilize fixed points when applying $p \neq 1$. The BAs of the orbit with period divisor of p decrease in length for higher values of p. Another phenomenon observed when increasing p (see Figure 4.5) is that more orbits are stabilized, decreasing their individual BAs, but increasing the length of the set of the BAs of all stabilized orbits. This occurs due to the exponential growth of the UPO quantity by period and the local stability of the orbits achieved for the orbits of the closed-loop system.

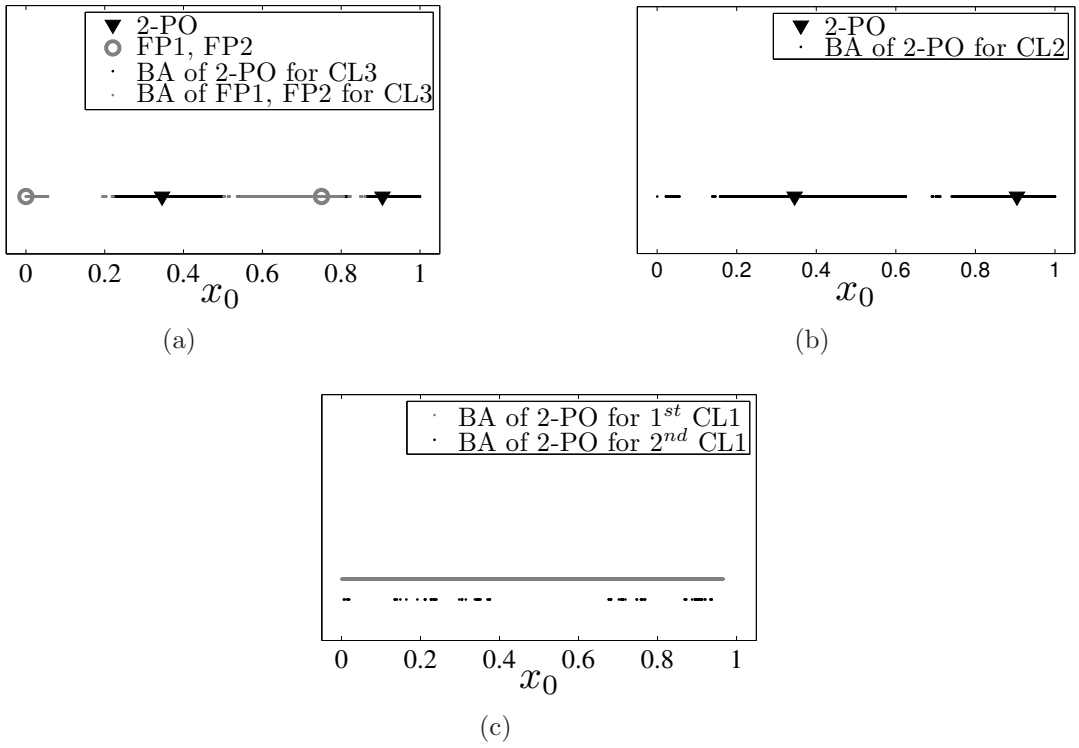

Figure 4.3: Basins of attraction (BAs) of stabilized period-2 orbits of the Logistic map controlled with the three different control laws for $r = 4$. FP1 and FP2 are fixed points and FP1, specifically, does not belong to the chaotic attractor.

The comparison of previous results shows that the CL 3 leads to faster convergence of trajectories to the target UPO while the CL 1 leads to slower convergence. The comparison of the BAs shows that the CL 3 leads to smaller BAs (when analysing a specific orbit) and different initial conditions may lead to different stabilized orbits. Specific values of the control gain for the CL 1 lead to the largest BAs. In both cases, the CL 2 leads

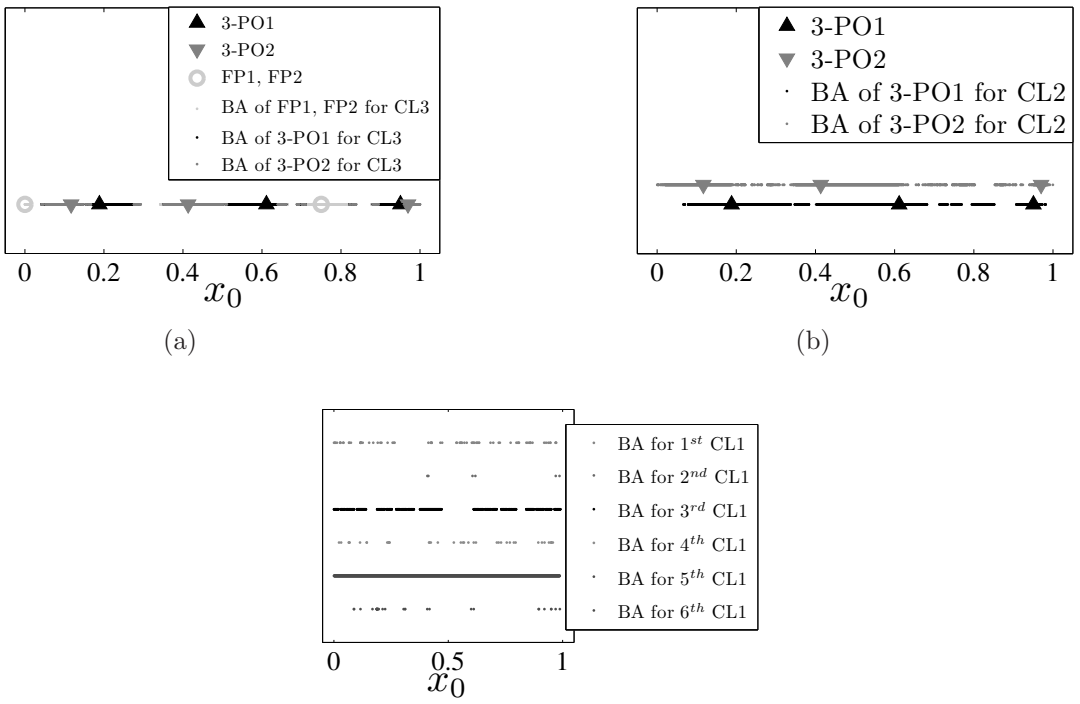

Figure 4.4: Basins of attraction (BAs) of stabilized period-3 orbits of the Logistic map controlled with the three different control laws for $r = 4$. FP1 and FP2 are fixed points and FP1, specifically, does not belong to the chaotic attractor.

to intermediate results. The greatest advantage of CL 3 is that its application is much simpler than the others, it can be also used to find the UPOs or the stabilizing gains of the other control laws.

4.2 Comparison between prediction-based and delayed feedback control

We now compare the PBC and DFC using the closed-loop Hénon map (4.4) as a case study. We chose CL 3 because only the period of the UPO is needed for tuning the controller gain. We wish to reduce the implementation complexity finding the UPOs using the CL 3.

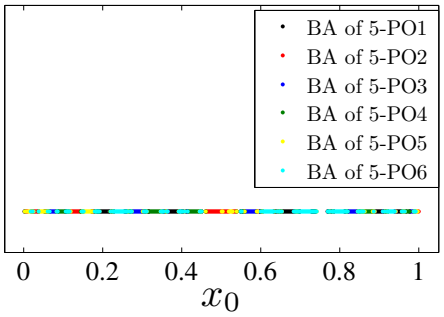

Figure 4.5: Basins of attraction (BAs) of stabilized periodic orbits of the Logistic map using the CL 3 with $p = 5$ and $r = 4$.

The Hénon map

$$x_{k+1} = g(x_k) + u_k(x_k), \tag{4.4}$$

where $x : \mathbb{N} \to \mathbb{R}^2$ and $u : \mathbb{N} \times \mathbb{R}^2 \to \mathbb{R}^2$. The function g is given by

$$g(x_k) = \begin{bmatrix} a - x_{1,k}^2 + bx_{2,k} \\ x_{1,k} \end{bmatrix}, \tag{4.5}$$

for given parameters $a, b \in \mathbb{R}$. For the PBC we have

$$u_k(x_k) = K_k(x_k)(\varphi(k + p, k, x_k, 0) - x_k), \tag{4.6}$$

where $\varphi(k + p, k, x, 0) = g^p(x)$ and $K : \mathbb{N} \times \mathbb{R}^2 \to \mathbb{R}^{2\times 2}$.

For the DFC we have

$$u(x_k) = K(x_{k-p} - x_k), \tag{4.7}$$

where $u : \mathbb{R}^2 \times \mathbb{R}^2$ and $K \in \mathbb{R}^{2\times 2}$.

We use the bifurcation digram of Figure 4.6 to identify chaos and its infinite number of UPOs. The diagram was generated plotting 500 points of $x_{1,k}$ after discarding the transient for $0 \leq k \leq 500$ using $b = 0.3$ and $0 \leq a \leq 2$. A stable solution is not found for $a > 1.428$. In the sequel $a = 1.4$ and $b = 0.3$.

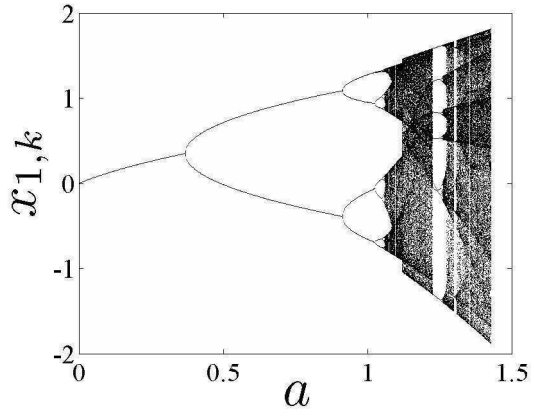

Figure 4.6: Bifurcation diagram of the Hénon map for $b = 0.3$.

Table 4.6: UPOs with period up to 6 of the Hénon map.

UPO	FP1.1	FP1.2	P2	P4	P6.1	P6.2
Period	1	1	2	4	6	6
Free system eigenvalues	[-1.9237, 0.1559]	[3.2598, -0.0920]	[-3.0101, -0.0299]	[-8.6394, -0.0009]	[-27.5147, -2×10^{-5}]	[28.1250, 2×10^{-5}]

4.2.1 Applying CL 3 and finding UPOs

The first step is finding the target UPOs. This is a simple task when studying the Hénon map and these orbits can be easily found analytically. However, the PBC with the CL 3 can be used to systematize the process for this simple example or even more complex systems. It is possible to make a grid of initial conditions on the region of the state space that contains the chaotic set, apply the CL 3 for one value of p, for a large k and for each initial condition, collect the points of the stabilized orbits and identify the period-p orbits. The points of the identified orbits are used to design the control gains for the DFC.

A list of UPOs with period up to 6 is shown in the Table 4.6 with their period and eigenvalues for the free system. There is no orbits of period 3 and 5 for the chosen a and b.

4.2.2 Designing the DFC control gain by optimization

The design of the control gain for the DFC is done by choosing a constant matrix K that minimizes the largest, in modulus, Floquet multiplier $|\mu|_{max}$ of the controlled orbit. The

Table 4.7: DFC control gain K; largest, in modulus, Floquet multipliers ($|\mu|_{max}$); Floquet multipliers (μ) of the stabilized orbits of the Hénon map.

UPO	FP1.1	P2	P4
K	$\begin{bmatrix} -0.75420 & 0.01369 \\ -0.28878 & -0.00023 \end{bmatrix}$	$\begin{bmatrix} -0.16542 & 0.00675 \\ -1.98560 & 0.31435 \end{bmatrix}$	$\begin{bmatrix} -0.62885 & -0.18505 \\ 0.19533 & -0.19424 \end{bmatrix}$
$\|\mu\|_{max}$	0.25346	0.5904	0.79702
μ	-0.2534 $\pm$0.0046i	-0.5901 $\pm$0.0190i	-0.7954 $\pm$0.0509i

minimization is performed using the MATLAB® routine *fminsearch* that implements the Nelder-Med simplex direct-search method [55]. The initial condition of the elements of the matrix K were scanned between -1 and 1. The matrix Ψ_k and its eigenvalues were computed for each K and the local minima of the largest eigenvalue in modulus were obtained (see Appendix C for the DFC monodromy matrix calculation). In Table 4.7 we summarise the best stabilizing K and the respective largest eigenvalue of the controlled orbit and its modulus.

After several tests, adjusting the convergence parameters and initial conditions, no matrix gain was found that stabilizes the period-6 orbits and the fixed point FP1.2 with the DFC. It is not proved here that these orbits can not be stabilized with the DFC, but these results are in agreement with the literature, since orbits of higher periods and orbits with an odd number of real Floquet multipliers larger than +1 (*odd-number limitation*) are not stabilized by the DFC [89,90,103,104]. Observing the Table 4.7 we see that $|\mu|_{max}$ increases when increasing the period of the controlled orbit, resulting in $|\mu|_{max} > 1$ for the orbit P6.1. The orbits FP1.2 and P6.2 have one Floquet multiplier real and larger than +1, characteristic of orbits originated from saddle-node bifurcations [1]. The other orbits are originated by period-doubling bifurcations.

4.2.3 Comparing PBC and DFC by basins of attraction

The basis of attraction of the orbits controlled by the DFC are shown in the Figure 4.7. The initial condition of the delayed states was set on the target UPO, this results in 2 and 4 simulations for each basins of attraction for the orbits P2 and P4, respectively. The initial condition was set varying the initial point of the orbit and consequently the order

of the points $x_{k-1} \dots x_{k-p}$ in these cases. The basin of attraction of the orbit P4, locally stable when controlled by the DFC, is not shown here. A scan with a step of 0.005 in $x_{1,0}$ and $x_{2,0}$ was not sufficient to find a point that converges to the orbit and we conclude that its basin of attraction is limited to a very small vicinity of the orbit. In the Figure 4.7(b), the colours blue and green were used to separate the BA of the P2 in two parts, according to the initial condition of the delayed states.

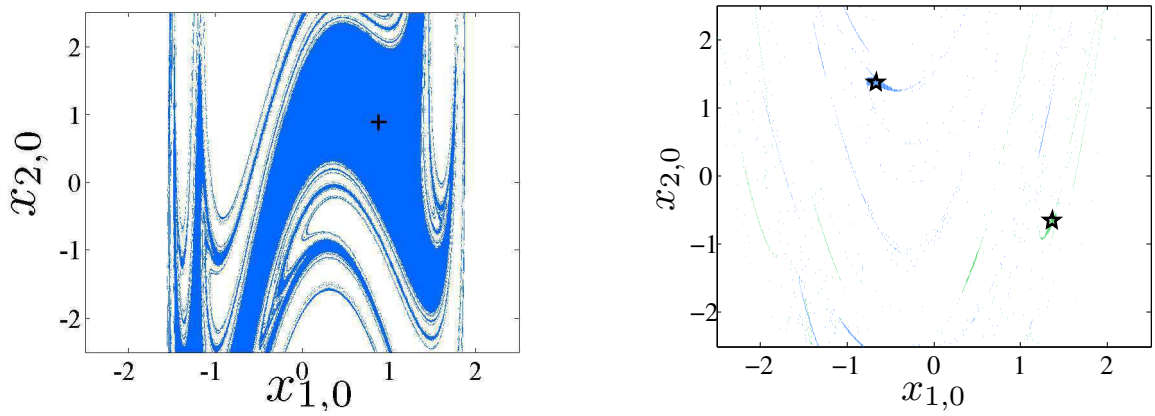

(a) (b)

Figure 4.7: Basins of attraction of the orbits controlled by the DFC for the Hénon map. (a) FP1.1 (+), (b) P2 ($\star$)

The basins of attraction of the orbits controlled by the PBC are shown in the Figure 4.8. We observe that all the orbits of period p and its divisors are controlled for the same value of p used in the control laws. This results in more than one BA represented in each figure. The basins of FP1.1 and FP1.2 are also shown in the Figures 4.8(b) and 4.8(c), this suggests that the basins of the orbits with period divisor of p reduce the size when increasing p. The basin of the orbit P2 was not included in the Figure 4.8(c), the same choice was adopted for the BAs of the orbits FP1.1, FP1.2 and P2 in the Figure 4.8(d). The orbit FP1.2 does not pertain to the chaotic attractor of the Hénon map for the chosen a and b, however it was also stabilized.

Comparing Figures 4.7 and 4.8 we observe that the PBC with the proposed control law not only stabilizes orbits that the DFC does not stabilize, but also leads to larger basins of attractions. Although, as verified for the Logistic map when applying the CL 3, different orbits are stabilized with the PBC, the orbits of period-p and its divisors.

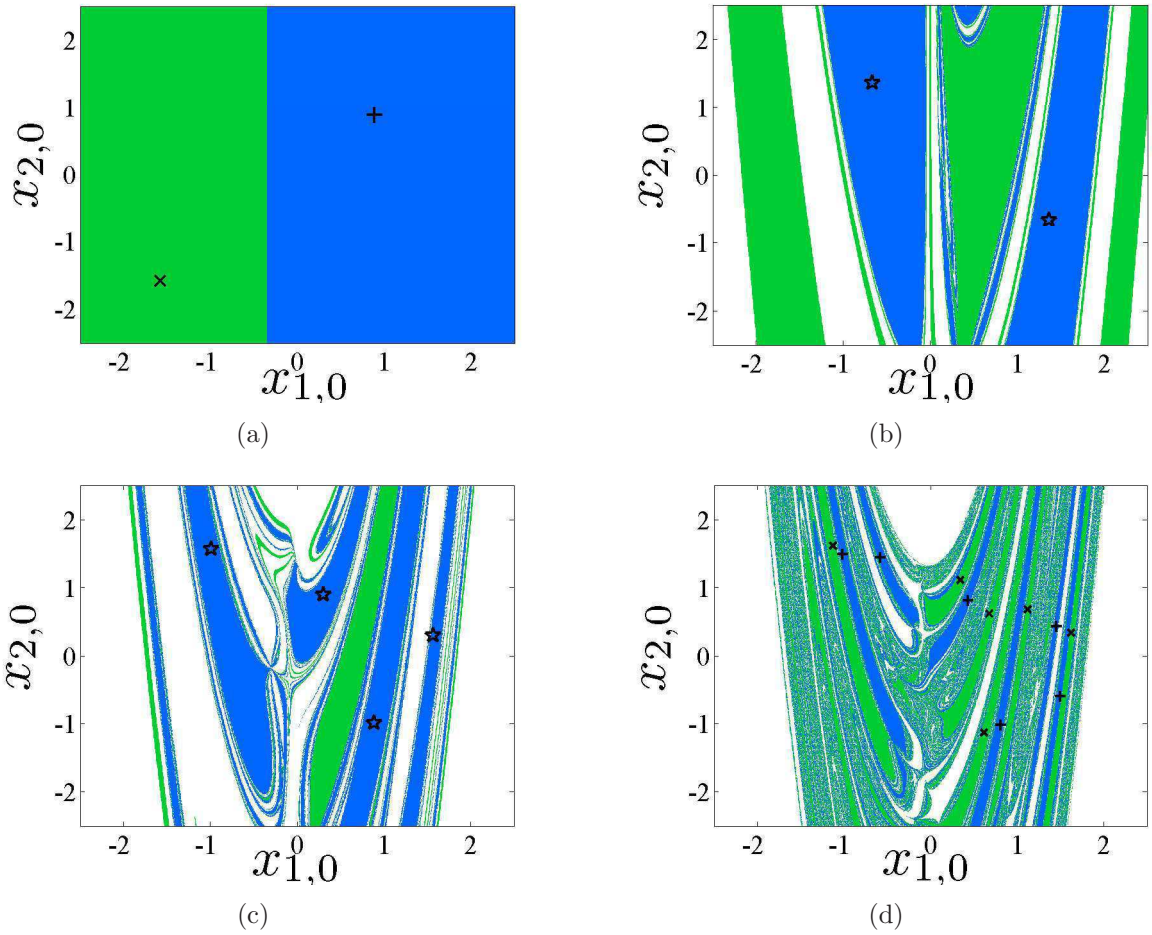

Figure 4.8: Basins of attraction of the orbits controlled by the PBC for the Hénon map. (a) $p = 1$, FP1.1 (+) and its BA blue and FP1.2 (×) and its BA in green; (b) $p = 2$, P2 ($\star$) and its BA in blue and the BAs of the fixed points in green; (c) $p = 4$, P4 ($\star$) and its BA in blue and the BAs of the fixed points in green; (d) $p = 6$, P6.1 (×) and its BA in green, P6.2(+) and its BA in blue.

A characteristic better observed in this bi-dimensional example (notably in Figures 4.8(c) and 4.8(d)) is the apparent fractal boundary between the basins [1].

4.2.4 Comparing PBC and DFC by convergence rate and control effort

Figure 4.9 shows the sum of the modulus of the control effort in both directions to control the orbits P2 and P4 using the DFC and the PBC. The vertical axis is in logarithmic scale to better compare the convergence rate to the UPO using each method, the control

effort is represented for $\|u_k(x_k)\|\|_1 > 10^{-10}$, $\|\cdot\|_1$ is the norm-1. The data corresponding to the DFC in the Figure 4.9(b) are plotted at each ten points. The convergence rate of the trajectory in both cases is faster for the PBC, this happens even with the extended states of the DFC initially set on the target UPO and using as x_{k-1} the point of x_k^* closer to x_0. The trajectory controlled with the PBC presents lower control effort amplitude compared to the DFC for the tests performed.

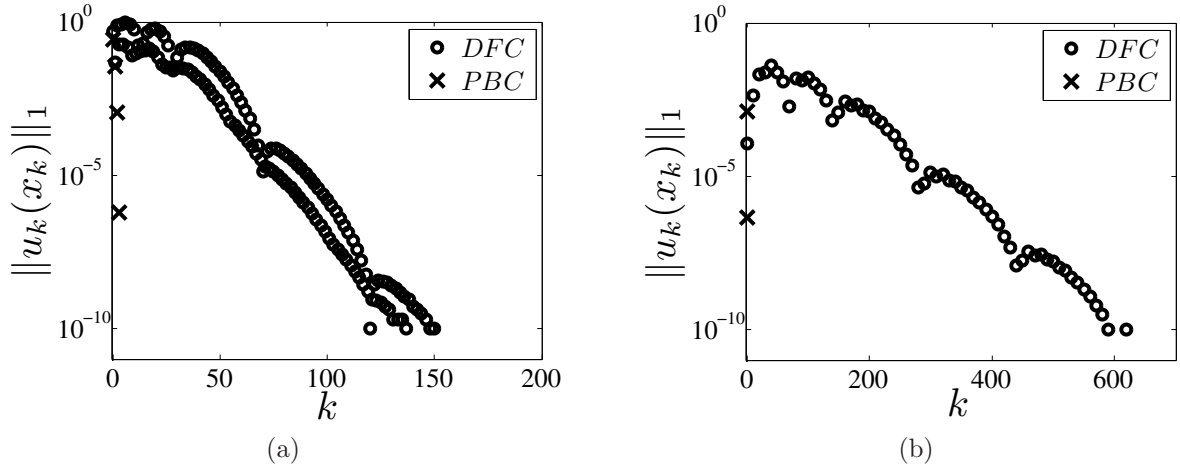

Figure 4.9: Time series of the control effort applied to stabilize periodic orbits of the Hénon map using the DFC and PBC. (a) $p = 2$, $x_0 = [-0.5;\ 1]$; (b) $p = 4$, $x_0 = [0.305;\ 0.893]$.

We verified that the PBC does not present the known limitations of the DFC related to the odd-number limitation and to high periods. The basins of attraction and the convergence rate of the trajectories of the orbits stabilized by the PBC are larger than for the DFC, with a lower control effort.

The PBC depends on a free system prediction model when applied, but the DFC can be applied without model, it is only necessary to record the delayed states. This characteristic favours the DFC, but its control gain design depends on a model and on the target UPO for an analytical or numerical tuning. The PBC with the proposed control law has the advantage of being independent of previous knowledge about the target UPO position and it is useful for applications where the orbit is unknown.

The choice of the cost function for the optimization of the DFC control gain favours the local stability of the controlled orbit, however it does not guarantee a maximum for

the basin of attraction size. The possibility of better results than the ones presented in the comparison between methods is not to be excluded.

4.3 A brief robustness analysis on the prediction-based control

Here we evaluate the robustness of the PBC using the CL 3 for a system subjected to parametric uncertainties and compare the results for the DFC under the same conditions.

4.3.1 Defining the uncertainties

The PBC case. For the PBC we consider a parametric error between the real free system $f(k, x_k, 0)$ and the free system prediction model, here named $\hat{f}(k, x_k, 0)$. In the sequel, $\hat{\cdot}$ refers to the prediction model. We apply the CL 3 (3.36) on the closed-loop system

$$\begin{aligned} \psi(k, x, K) &\doteq f(k, x, u_k(x)) \\ u_k(x) &= K(\hat{\varphi}(k+p, k, x, 0) - x), \end{aligned} \tag{4.8}$$

where $\hat{\varphi}(k+p, k, x, 0)$ is defined for $\hat{f}(k, x, 0)$.

Note that the Lemma 3.15 is not (necessarily) valid now because x_k^* is not (necessarily) a periodic orbit of $\psi(k, x_k, K_k(x_k))$ with $u_k(x_k)$ defined in (4.8), namely $\hat{x}_k^*$. The monodromy matrix of this new orbit is given by

$$\Psi_k = \prod_{l=0}^{p-1} \nabla_x \psi(k+l, x, K_{k+l}(x))|_{x=\hat{x}^*(k+l)}\,, \tag{4.9}$$

with

$$\begin{aligned} \nabla_x \psi(k, x, K_k(x)) = \nabla_x f(k, x, u_k(x_k)) + \nabla_u \hat{f}(k, x_k, u) K_k(x_k) \nabla_x (\hat{\varphi}(k+p, k, x, 0) - x) + \\ \nabla_u \hat{f}(k, x_k, u) \nabla_x K_k(x) (\hat{\varphi}(k+p, k, x_k, 0) - x_k). \end{aligned}$$

The DFC case. For the DFC we use

$$u_k(x_k) = K(x(k-p) - x_k)$$

where K is the optimal gain used to stabilize $\hat{x}_k^*$.

4.3.2 Comparing PBC and DFC

The robustness analysis is performed using the Hénon map (4.4) as case study for the comparison between methods.

We define $\hat{a} = 1.4$ and $\hat{b} = 0.3$ for $\hat{f}(k, x_k, 0)$, $b = 0.3$ and vary a for $f(k, x_k, 0)$. We try to stabilize the orbit P2 with both methods for $0.91 < a < 2$, where the limit $a = 0.91$ refers to the bifurcation that originates the UPO P2 and $a = 2$ was used to apply the control schemes in a system without stable solutions. Here, $\nabla_u \hat{f}(k, x_k, u) = \nabla_u f(k, x_k, u) = B = I_n$.

Comparison criteria. The comparison is performed using the maximum, in modulus, Floquet multiplier $|\mu|_{max}$ of the controlled orbit, $\hat{x}_k^*$, and the control effort for one cycle of the steady state trajectory, υ, defined as

$$\upsilon = lim_{k \to +\infty} \sum_{l=1}^{p} \|u_{k+l}(x_{k+l})\|_1$$

$\|\cdot\|_1$ is the norm-1 used to measure the total external effort necessary to stabilization.

Results and analysis The results are shown in Figure 4.10 and $\hat{x}_1^*$ is shown in Figure 4.11 using as initial condition the points of P2 for $a = 1.4$, including the delayed states for the DFC.

Figure 4.10(a) shows that the orbit controlled by the PBC is more stable than the orbit controlled by the DFC. For $a = \hat{a} = 1.4$, as expected, $|\mu|_{max} \approx 0$ for the PBC and this point is not represented in the figure due to the logarithmic scale.

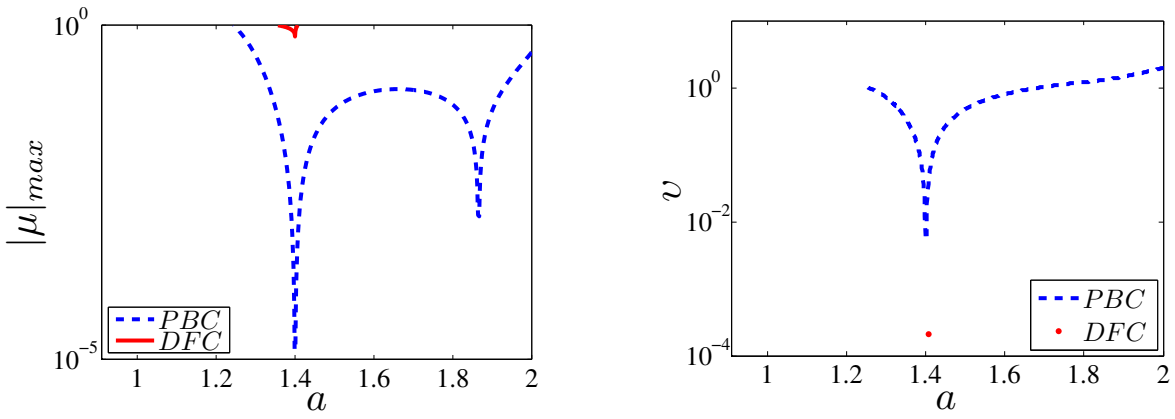

Figure 4.10: Comparison between the PBC with the CL 3 and the DFC stabilizing the $\hat{x}_k^*$ for $b = 0.3$. (a) the maximum, in modulus, Floquet multiplier; (b) the control effort for one cycle of the steady state system.

Figure 4.10(b) shows that the orbit controlled by the DFC presents a steady state control effort approximately equal to zero (not shown due to logarithm scale). The point in red shown in the figure is obtained for a value of a where $|\mu|_{max} \approx 1$ and the convergence is slow. For the PBC we have $\upsilon \approx 0$ for $a = \hat{a} = 1.4$ and a larger control effort for other values.

Figure 4.11 shows the stabilized orbit for both control methods. The analysis of the Figures 4.10 and 4.11 allows to conclude that PBC method is applicable for a larger interval of a, including values where there is not a stable solution for the free system ($a > 1.428$), the controlled orbit is more stable, but the control effort is larger in comparison with the DFC. The choice of the method to be used depends on the performance criteria of the control problem.

4.4 Prediction-based control for non-invertible input matrix

Here we use the PBC to stabilize periodic orbits of the Hénon map (4.4) for a non-invertible input matrix $\nabla_u f(k, x_k, u) = B$ with a control law similar to CL 3 with no need of previous knowledge about the UPO position.

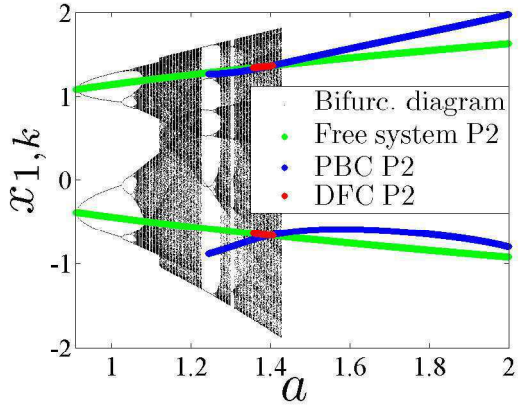

Figure 4.11: Stabilized $\hat{x}_k^*$ using the PBC (blue) and the DFC (red) on the bifurcation diagram (black) of the Hénon map for $b = 0.3$. The orbit x_k^* of the free system is in green
.

Here, the matrices B and $K_k(x_k)$ are given by

$$B = \begin{bmatrix} 1 \\ 0 \end{bmatrix}, \quad K_k(x_k) = \begin{bmatrix} k_{1,k}(x_k) & k_{2,k}(x_k) \end{bmatrix}.$$

In this case we have a scalar control signal (3.26), $u : \mathbb{N} \times \mathbb{R}^2 \to \mathbb{R}$.

The matrix $\nabla_x f(k, x, u_k(x_k))$ for the Hénon map is

$$\nabla_x f(k, x, u_k(x_k)) = \begin{bmatrix} -2x_{1,k} & b \\ 1 & 0 \end{bmatrix}$$

and the matrix $\nabla_x \varphi(k + p, k, x, 0)$ is written as

$$\nabla_x \varphi(k + p, k, x, 0) = \begin{bmatrix} fp_{11,k}(x_k) & fp_{12,k}(x_k) \\ fp_{21,k}(x_k) & fp_{22,k}(x_k) \end{bmatrix}$$

.

Solving (3.39) for

$$T = \begin{bmatrix} 0 & 1 \\ 1 & 0 \end{bmatrix}$$

we obtain

$$k_{1,k}(x_k) = \frac{-bfp_{21,k}(x_k) + 2x_{1,k} - 2fp_{22,k}(x_k)x_{1,k}}{fp_{11,k}(x_k) + fp_{22,k}(x_k) - fp_{11,k}(x_k)fp_{22,k}(x_k) + fp_{12,k}(x_k)fp_{21,k}(x_k) - 1}$$
$$k_{2,k}(x_k) = \frac{bfp_{11,k}(x_k) + 2fp_{12,k}(x_k)x_{1,k} - b}{fp_{11,k}(x_k) + fp_{22,k}(x_k) - fp_{11,k}(x_k)fp_{22,k}(x_k) + fp_{12,k}(x_k)fp_{21,k}(x_k) - 1}.$$

In this case, the matrices $\nabla_x f(k, x, u_k(x_k))$ and $\nabla_u f(k, x_k, u)$ are already in a controllable canonical form. This allows to obtain a constant T and a matrix $K_k(x_k)$. For $B = [0\ 1]'$, $T_k(x_k)$ is not constant and it is necessary to calculate a control gain using the previous knowledge of x_k^*, similar to CL 1 and CL 2.

A numerical example is shown in the Figure 4.12. This example can be compared to the results of Figure 4.9 showing that the convergence rate for the PBC applied for a non-invertible input matrix case has the same magnitude of the convergence rate for the invertible input matrix case. It is also faster than the DFC applied to the invertible input matrix case.

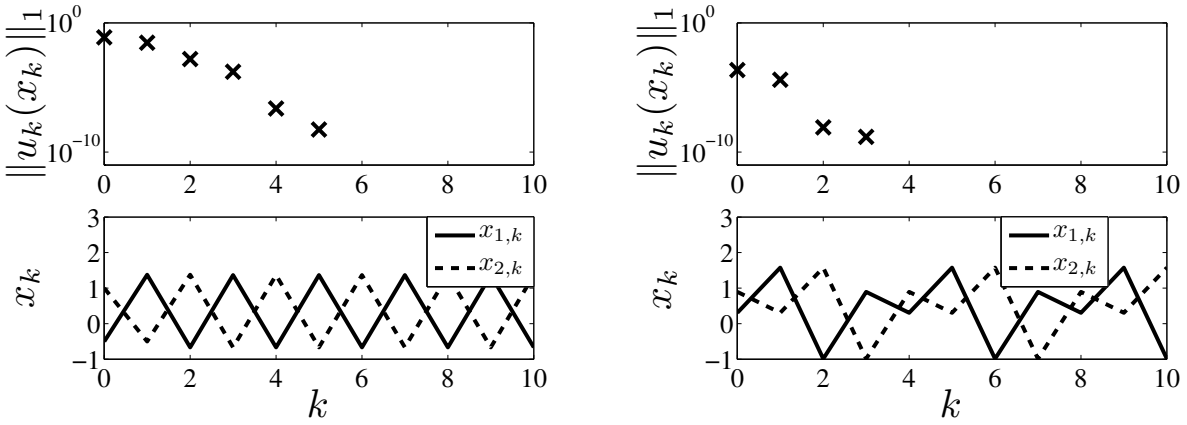

Figure 4.12: Time series of the control effort and state variables of stabilized periodic orbits of the Hénon map using the PBC for a non-invertible input matrix $B = [1\ 0]'$. (a) $p = 2$, $x_0 = [-0.5;\ 1]$; (b) $p = 4$, $x_0 = [0.305;\ 0.893]$.

Chapter 5

Conclusions

In Section 3.4.1, Theorem 3.16 and Lemma 3.15, it was formulated a stability condition for periodic orbits controlled by the PBC in discrete-time systems. This stability condition is used for the formulation of three different control laws in Section 3.4.2. These control laws lead to all Floquet multipliers equal zero and are summarized as:

CL 1: A linear time-invariant control law which depends on the previous knowledge of UPO position;

CL 2: A linear time-varying control law which depends on the previous knowledge of the UPO position;

CL 3: A non-linear time-varying control law which does not depend on the previous knowledge of the UPO position, only its period p;

These control laws are compared using numerical examples in Section 4.1. First of all it is verified that the CL 3 can be applied to find UPOs and its position is used to define the control gain of the CL 1 and CL 2. It was verified that the convergence rate of trajectories to the stabilized orbit is faster for the CL 3 compared to the others control laws. Comparing the basins of attraction it was verified that they are smaller for a periodic orbit stabilized by CL 3. It was verified that when the CL 3 is applied not only one specific orbit is stabilized, but also all the orbits of period integer divisor of p.

The control law 3 is used for a comparison between the PBC and the DFC in Section 4.2. Is is verified that the PBC has a faster convergence rate of trajectories to the stabilized orbit, it has larger basins of attraction, and it stabilizes orbits that are not stabilized by the DFC due to the odd-number limitation and large period.

In Section 4.4 it was numerically tested the robustness of the PBC and the DFC to parametric uncertainties. It was verified that the PBC is much more robust than the DFC using as comparison criterion the range of the parameter error (with respect to the value of the parameter used to design the controllers) for which a stable orbit is achieved. However, it is less robust when using as comparison criterion the variation of the larger magnitude Floquet multiplier and the steady state control effort in the range of the parameter error where both methods leads to stabilization.

The CL 3 was proposed for system with invertible input matrix. In Section 3.4.3 it was proposed a control law that leads the Floquet multipliers to zero without previous knowledge of the UPO position and is applicable to systems with non-invertible input matrix. The condition where this control law can be used is specified in Theorem 3.19. It was verified in Section 4.4 that the convergence rate of this control law is comparable to the CL 3 and faster than the DFC.

Part II

Continuous-time systems

Chapter 6

Introduction

In the present chapter we discuss stabilization of periodic orbits of continuous-time systems. Similarly to Chapter 3, the stabilization methods obtained here use low control effort.

Consider the following continuous-time dynamical system:

$$\dot{x}(t) = f(t, x(t), u(t)), \qquad x(0) \text{ given} \tag{6.1}$$

where $t \in \mathbb{R}^+$, $x : \mathbb{R}^+ \to \mathbb{R}^n$, $u : \mathbb{R}^+ \to \mathbb{R}^m$, $n, m \in \mathbb{N}$ and $f : \mathbb{R}^+ \times \mathbb{R}^n \times \mathbb{R}^m \to \mathbb{R}^n$ is a T-periodic function with respect to time t, that is, by definition

$$\forall t \in \mathbb{R}^+,\ \forall x \in \mathbb{R}^n,\ \forall u \in \mathbb{R}^m, \qquad f(t+T, x, u) = f(t, x, u). \tag{6.2}$$

Moreover, we assume the existence of a T-periodic solution $x^*(t)$ to the free system (6.1), which is the system obtained by setting $u(t) = 0$, $t \geq 0$. In other words,

$$\forall t \in \mathbb{R}^+, \quad x^*(t+T) = x^*(t) \tag{6.3}$$

and

$$\forall t \in \mathbb{R}, \quad \dot{x}^*(t) = f(t, x^*(t), 0_m). \tag{6.4}$$

We assume that this periodic solution is unstable (the stability analysis of periodic orbits is discussed in Section 7.1). Our ultimate goal in this chapter is to synthesize periodic feedback laws $u(t, x(t))$ that stabilize it, that is, such that

$$\forall t \in \mathbb{R}^+, \ \forall x \in \mathbb{R}^n, \quad u(t+T, x) = u(t, x)$$

and such that x^* is a stable solution of the closed-loop system

$$\dot{x}(t) = f(t, x(t), u(t, x(t)) \tag{6.5}$$

with $u : \mathbb{R}^+ \times \mathbb{R}^n \to \mathbb{R}^m$ defined later. Alternatively, we are also interested in simple ways of stabilizing an orbit *close to* the UPO x^* of (6.1).

When the open-loop system (6.1) and the feedback are periodic with respect to time t, the same is true for the closed-loop system (6.5).

The control signal u used in this work has to verify ideally,

$$u(t, x^*(t)) = 0 \qquad t \geq 0. \tag{6.6}$$

The condition (6.6) ensures zero control effort when the trajectory is on the unstable periodic solution x^* of the free system. Regarding the stabilization of trajectories to nearby orbits, this will not be the case. As a matter of fact, in this case x^* will not be a periodic solution of the controlled system.

Non-linear systems with chaotic sets in their state space are examples of dynamical systems that present unstable periodic orbits (UPO). In fact, if there is a chaotic set in the n-dimensional state space formed by $x(t)$, it is known that the chaotic set is composed by an infinite number of UPOs [1, 24]. The number of p-periodic UPOs, defined for the discretized system on the Poincaré map (Appendix A), increases exponentially with p [20].

The stabilization of UPOs embedded in chaotic sets is called *chaos control*. Chaos control aims at eliminating chaotic behaviour from a system that presents a chaotic set, in general, by obtaining stable periodic solutions with low control effort. It may use chaos's

basic characteristics, among which are the sensitive dependence on initial conditions and the infinite number of UPOs embedded in chaotic sets [20, 24].

Another characteristic of chaotic behaviour is that trajectories on chaotic attractors come arbitrarily close to any of the embedded UPOs due to ergodicity [24]. Specific control applications where long transient times are accepted (in return for a low control effort necessity, for example) can take advantage of this characteristics by applying the control signal only when the free system trajectory is in the vicinity of the target UPO. In the present work the ergodicity property of chaos is not used because we are interested in reducing the transient time.

The first idea of stabilizing periodic orbits of chaotic sets in continuous-time dynamical systems was proposed by Pyragas [70]. Pyragas proposed two different continuous-time feedback methods namely proportional feedback control and delayed feedback control.

Proportional feedback control (PFC) This method uses the target UPO itself in the control signal $u(t, x(t))$ and its application depends upon the previous knowledge of the entire target UPO. This is the principal disadvantage of the method and it is more evident in continuous-time systems.

This method will be studied in Section 7.3.1 and the stability properties and design will be discussed in Section 7.4.1.

Delayed feedback control (DFC) This method uses the state of the system delayed by the period T of the target UPO as reference in the control signal. This delayed term makes the closed-loop system a delay differential equation (DDE) with infinite dimension [36].

Different from the PFC, the DFC does not need the knowledge of the entire UPO to be used as reference signal, it is only necessary to know the value of the period and to record the past states. This characteristic contributes to practical applications and to the popularity of the method [74].

Tuning the parameter of the control signal (specifically, the control gain design) can be done experimentally [70]. However a precise analytical stability analysis and design

depends upon the knowledge of the target UPO and is based on the stability properties of DDEs.

A first contribution of this chapter is to apply the method proposed by [10, 23, 51] for stability analysis of DDEs with one fixed delay to the design of a stabilizing control gain for the DFC method. This method simplifies the design because it is based on matrix algebra only (in contrast with previous design methods that use integration of high dimensional differential equations).

The characteristics of the method and a review on the literature is shown in Section 7.3.2. The control gain design is studied in Section 7.4.2.

One topic related to the DFC and commonly discussed in the literature is the *odd number limitation* (discussed in Section 7.3.2). This limitation stimulated alternative methods based on the DFC scheme, one of those methods is the prediction-based control.

Prediction-based control (PBC) and approximate prediction-based control (aPBC) *A second contribution of this chapter is the development of a continuous-time stabilization method inspired by the PBC*[1]. Up to our knowledge, no work has been done based on this approach[2].

The PBC method, initially proposed by Ushio and Yamamoto [91] for discrete-time systems, is based on the prediction of the state one period of the target UPO ahead, computed along the trajectories of the free system. This predicted state is used to compute the control signal.

Computing the future state requires to solve at each time t the free system ODE: this makes the PBC method hardly implementable for continuous-time models. Instead, we introduce the approximate prediction-based control method (aPBC), as follows. Computing the predicted state can be achieved (approximately) by using an implicit Rung-Kutta method [35], which is formulated as a differential algebraic equation (DAE). However, the solution of this DAE has to be computed instantaneously. What we do instead is to build

[1] formulation and initial results have been presented in [13].

[2] A method claiming to stabilize equilibrium points in continuous-time non-linear systems presenting a chaotic set based on predicted states is presented in [6] in a very special case of impulsive control. Stabilization of periodic orbits using some prediction is considered in [82], the predicted value being obtained through a neural network.

an estimator along time of the solution of the implicit Runge-Kutta method, resulting in an ODE with extended dimension.

Overall, the method we propose introduces a dynamical feedback whose state has a dimension equal to the number of points of the Runge-Kutta method adopted, multiplied by the dimension of the initial system to be controlled. The detailed method is presented in Section 7.3.3. Stability analysis and control gain design is done in Section 7.4.3.

Organization of the chapter Stabilization of a periodic orbit for the non-linear system (6.5) using any method studied in this chapter is performed by stabilizing the linear time-periodic (LTP) system that governs the evolution of a perturbed trajectory in the close vicinity of $x^*(t)$. We thus first recall in Section 7.1 basic concepts on the stability analysis of a periodic orbit by its linearised dynamics using Floquet and Lyapunov theories (with special interest to the Floquet theory and monodromy matrices [5]). Stabilization of LTP is thus discussed in Section 7.2. The control laws mentioned before are then extensively presented in Section 7.3. Gain design issues are treated in Section 7.4.

The application and numerical results of the methods are left to Chapter 8. The conclusions are in Chapter 9.

Chapter 7

Feedback stabilization of unstable periodic orbits

7.1 Stability analysis of periodic orbits

In this section we present the Floquet and Lyapunov theories for stability analysis of linear periodic continuous-time systems (see Appendix A).

First we introduce the stability analysis of linear systems in terms of the monodromy matrix and Floquet multipliers. We apply this theory to the stability analysis of periodic orbits of non-linear system by studying the behaviour of a perturbed trajectory governed by the linearised system in the vicinity of the periodic solution. We also introduce the Floquet-Lyapunov transformation and the stability analysis in terms of the Floquet exponents.

The Lyapunov direct method is also studied and related to the Floquet stability analysis.

7.1.1 Floquet stability theory

Here we present the concepts on the stability of linear periodic continuous-time dynamical systems based on the Floquet theory and these results are applied to the local stability of periodic orbits of non-linear continuous-time dynamical systems.

Linear systems

Let us consider a linear continuous-time dynamical system described by the differential equation

$$\frac{dx(t)}{dt} = A(t)x(t), \tag{7.1}$$

where $t \in \mathbb{R}^+$, $x : \mathbb{R}^+ \to \mathbb{R}^n$ is a column vector and $A : \mathbb{R}^+ \to \mathbb{R}^{n\times n}$ (see Appendix A).

Assume that $A(t)$ is a periodic state matrix of period T that satisfies

$$A(t) = A(t+T), \qquad T \in \mathbb{R}, \qquad \forall t. \tag{7.2}$$

The stability of linear periodic systems according to the Floquet theory depends on the eigenvalues of the monodromy matrix (see Appendix A), called the *Floquet characteristic multipliers* $\mu_i \in \mathbb{C}$:

Proposition 7.1 (adapted from Theorems 4.1 and 4.2 in [77])**.** *(i) The system* (7.1) *is asymptotically stable if and only if the characteristic multipliers of* $A(t)$ *have absolute value smaller than* 1*. (ii) The system* (7.1) *is stable if and only if the characteristic multipliers of* $A(t)$ *have absolute value smaller than or equal to* 1 *and those characteristic multipliers with unit-modulus are simple roots of the minimal polynomial of the monodromy matrix* $\Psi(t)$*.* □

See Appendix B for stability definitions.

The state transition matrix or the matrix evolution operator $\Phi(t, t_0)$, $t, t_0 \in \mathbb{R}$ of (7.1) is calculated according to the fundamental matrix definition (see Appendix A and [98]) as follows

$$\begin{aligned} \frac{d\Phi(t,t_0)}{dt} &= A(t)\Phi(t,t_0) \\ \Phi(t_0,t_0) &= I_n. \end{aligned} \tag{7.3}$$

The *monodromy matrix* $\Psi(t)$ is the state transition matrix over a period $[t, t+T]$ [98]:

$$\Psi(t) = \Phi(t+T, t) \tag{7.4}$$

and thus any solution of (7.1) also fulfils:

$$x(t+T) = \Psi(t)x(t). \tag{7.5}$$

Note that $\Psi(t)$ is a periodic matrix with period T, but the characteristic multipliers are constant for all t [5].

The Floquet theory can be used to analyse the stability of periodic orbits of non-linear systems by studying the convergence/divergence of a perturbation, governed by a linear periodic continuous-time system, in the vicinity of the periodic orbit [3, 40].

Application to non-linear systems

Consider a non-linear continuous-time dynamical system described by the differential equation (6.5) with a periodic solution $x^*(t)$ of period T for $u(t, x(t)) = 0$ indicated in (6.2). Here we study the behaviour of a trajectory in the vicinity of $x^*(t)$.

Proposition 7.2 (Stability of periodic orbits of continuous-time systems)**.** *A periodic orbit $x^*(t)$ of the continuous-time dynamical system* (6.5) *is locally asymptotically stable if the linear dynamical system that describes the evolution of a perturbed trajectory in the close vicinity of $x^*(t)$ is asymptotically stable.* □

Proof. Consider a perturbation $\delta x(0) : \mathbb{R} \times \mathbb{R}^n \to \mathbb{R}^n$ applied to the periodic state $x^*(0)$. The initial condition of (6.5), $x(0)$, is defined by

$$x(0) = x^*(0) + \delta x(0). \tag{7.6}$$

The continuous-time evolution $\delta x(t)$ of the initial perturbation $\delta x(0)$ for $u(t, x(t)) = 0$ is obtained substituting the perturbed trajectory (7.6) in (6.5),

$$\frac{dx^*(t)}{dt} + \frac{d\delta x(t)}{dt} = f(t, x^*(t) + \delta x(t), 0).$$

Expanding $f(t, x^*(t) + \delta x(t), 0)$ around $x^*(t)$ for $\delta x(t)$ sufficiently small we obtain

$$f(t, x^*(t) + \delta x(t), 0) \approx f(t, x^*(t), 0) + \nabla_x f(t, x, 0)|_{x=x^*(t)} \delta x(t)$$

$$\frac{d\delta x(t)}{dt} \approx \nabla_x f(t, x, 0)|_{x=x^*(t)} \delta x(t). \tag{7.7}$$

$\nabla_x f(t, x, 0) \in \mathbb{R}^{n\times n}$ is the Jacobian matrix of the system, here a time-periodic matrix due to the periodicity of $\nabla_x f(t, x, 0)|_{x=x^*(t)}$. The stability of $x^*(t)$ is analysed according to the convergence/divergence of $\delta x(t)$ governed by (7.7), reducing the problem to the stability analysis of the linear periodic system (7.1).

Once the equation that governs the perturbation is obtained it is possible to define a continuous-time monodromy matrix $\Psi(t) \in \mathbb{R}^{n\times n}$ related to the periodic orbit $x^*(t)$:

$$\delta x(t + T) = \Psi(t)\delta x(t). \tag{7.8}$$

We calculate the monodromy matrix according to (7.3) and (7.4) using (7.7)

$$\begin{aligned} \Psi(t) &= \Phi(t + T, t) \\ \frac{d\Phi(\tau, t)}{d\tau} &= \nabla_x f(\tau, x, 0)|_{x=x^*(\tau)} \Phi(\tau, t), \qquad \tau \in [t, t + T] \\ \Phi(t, t) &= I_n. \end{aligned} \tag{7.9}$$

The eigenvalues of $\Psi(t)$ (Floquet multipliers) are computed to analyse the stability of the linear system (7.7). If it is asymptotically stable, then $\delta x(t) \to 0$ and $x(0) \to x^*(t)$ as $t \to \infty$. □

7.1.2 Floquet-Lyapunov transformation and Floquet exponents

In this section we present the *Floquet characteristic exponents* defined by the Floquet-Lyapunov transformation and used for stability analysis of linear time-periodic systems. The Floquet-Lyapunov transformation is applied to time-periodic systems obtaining a time-invariant representation.

The results on the Floquet-Lyapunov transformation presented in this section are transcribed from [5]. The application to stability of periodic orbits can be obtained applying the same methodology used in Section 7.1.1.

These exponents are presented here only for continuous-time systems, but there is an equivalent representation for discrete-time systems (see Appendix B). This transformation relates the stability of linear continuous-time invariant systems (determined by the eigenvalues of the state matrix) to the stability of linear periodic continuous-time systems.

Proposition 7.3 (adapted from Theorem 4.1 in [77])**.** *The system* (7.1) *is asymptotically stable if and only if the characteristic exponents,* $\lambda_i \in \mathbb{C}$*,* $i = 1, \ldots, n$*, of* $A(t)$ *have negative real part.* □

Take $S(t)$, a T-periodic invertible space-space transformation,

$$\hat{x}(t) = S(t)x(t)$$

then, the state matrix of (7.1) in the new coordinates is given by

$$\hat{A}(t) = S(t)A(t)S^{-1}(t) + \dot{S}(t)S^{-1}(t). \tag{7.10}$$

It is assumed that $S(t)$ and $S^{-1}(t)$ are continuously differentiable.

The Floquet problem is then to find $S(t)$ (if any) in order to obtain a constant matrix $\hat{A}(t) = \hat{A}$.

From (7.10) it follows that, if $\hat{A}(t) = \hat{A}$ then the transformation $S(t)$ must satisfy

$$\dot{S}(t) = \hat{A}S(t) - S(t)A(t). \tag{7.11}$$

This is a matrix differential equation. Considering t_0 as initial time point and $S(t_0)$ as initial condition, the solution is given by (see intermediate steps in [5, pg. 10])

$$S(t) = e^{\hat{A}(t-t_0)}S(t_0)\Phi(t_0, t). \tag{7.12}$$

Take now $t = t_0 + T$ and impose the periodicity condition $S(t_0 + T) = S(t_0)$ to (7.12):

$$S(t_0) = e^{\hat{A}T} S(t_0) \Phi(t_0, t_0 + T).$$

Thus, the Floquet problem amounts to finding a pair of constant matrices $\hat{A}$ and $\hat{S}$ solving the algebraic equation

$$\hat{S} = e^{\hat{A}T} \hat{S} \Psi^{-1}(t_0). \tag{7.13}$$

The system of algebraic equations (7.13) admits infinitely many solutions $(\hat{S}, \hat{A})$. Taking $\hat{S} = I_n$, then $\hat{A}$ can be obtained from condition

$$e^{\hat{A}T} = \Psi(t_0). \tag{7.14}$$

The eigenvalues of $\Psi(t_0)$ are the Floquet multipliers μ and the eigenvalues of $\hat{A}$ are the Floquet exponents λ. These values are related according to

$$e^{\lambda_i T} = \mu_i, \qquad i = 1, \ldots, n. \tag{7.15}$$

The equivalence between Proposition 7.1 (i) and Proposition 7.3 is verified by (7.15).

7.1.3 Lyapunov stability theory

In this section we present some results on the stability analysis of linear periodic continuous-time systems (7.1) using the Lyapunov direct method.

The stability condition will be presented in terms of a Lyapunov inequality used for time-varying systems. This method is not easily applicable and it was not found a reference in literature that relates it with the Floquet theory as done in Section 3.1.2 for discrete-time systems.

An alternative is to use (7.5) to discretize (7.1) and apply the stability condition presented in Section 3.1.2 for discrete-time systems. This methodology allows to relate the Floquet stability theory with the Lyapunov stability theory.

Stability by a continuous-time Lyapunov inequality

Considering the periodicity of $A(t)$ in (7.1) we have:

Proposition 7.4 (see page 17 in [5]). *The linear periodic continuous-time system* (7.1) *is asymptotically stable if and only if the Lyapunov inequality*

$$\dot{P}(t) > A(t)P(t) + P(t)A'(t) \tag{7.16}$$

admits a periodic positive definite solution $P(t) = P(t+T)$, $P : \mathbb{R} \to \mathbb{R}^{n\times n}$ *and* $P(t)$ *symmetric.* □

The Lyapunov inequality (7.16), valid for time-varying systems, results from the Lyapunov function (7.17) and Theorem 7.5, given below.

We define the stability of time-varying systems in terms of a time-varying Lyapunov function

$$V(t,x) = x'(t)P^{-1}(t)x(t), \tag{7.17}$$

where $V : \mathbb{R} \times \mathbb{R}^n \to \mathbb{R}$.

Theorem 7.5 (Adapted from Theorem 2.4 in [94]). *The continuous-time linear system* (7.1) *is asymptotically stable if a scalar function* $V(t,x)$ *with continuous partial derivatives exists and if the following conditions are met:*

- $V(t,0) = 0$, $\forall t$;
- $V(t,x) > 0$, $\forall t \neq 0$, $\forall x \neq 0$;
- $\dot{V}(t,x) < 0$, $\forall t \neq 0$, $\forall x \neq 0$;
- $V(t_1, x(t_1)) < V(t_0, x(t_0))$, $t_1 > t_0$, *and* $V(t_0, x(t_0)) > 0$, $\forall x \in \mathbb{R}^n$. □

The stability condition of Proposition 7.4 implies the integration of the Lyapunov inequality (7.16) for one period T to verify if a suggested $P(t)$ satisfies the established condition. This reduces the applicability of the proposition. Besides, the relation between the Floquet theory and the Lyapunov direct method is not evident.

An alternative to the Lyapunov inequality (7.16) is the periodic Lyapunov differential equation (7.18), here T-periodic due to $P(t) = P(t+T)$ and $Q(t) = Q(t+T)$ [5].

$$\dot{P}(t) = P(t)A'(t) + A(t)P(t) + Q(t) \tag{7.18}$$

$Q(t)$ a positive definite matrix.

Stability through discrete-time Lyapunov inequality applied to the monodromy matrix

The relation between the Floquet stability and Lyapunov stability is established in Proposition 7.6.

Proposition 7.6. *The origin of the linear periodic continuous-time system* (7.1) *is asymptotically stable if and only if for any* $\tau \in \mathbb{R}$ *the invariant discrete-time Lyapunov inequality*

$$P > \Psi(\tau)P\Psi'(\tau) \tag{7.19}$$

admits a positive definite solution $P \in \mathbb{R}^{n\times n}$*, or equivalently, if and only if the eigenvalues (Floquet multipliers) of* $\Psi(\tau)$ *(monodromy matrix) have modulus less than* 1. □

We emphasize that the stability notion mentioned in Proposition 7.6 is global, as is always the case for linear systems. On the contrary, use of this result on the linearized system obtained in the neighborhood of a given trajectory of a nonlinear system, only ensures local stability in general.

Proof. Given the monodromy matrix $\Psi(\tau)$ of the linear periodic system (7.1), according to (7.5) we have

$$x(\tau + (k+1)T) = \Psi(\tau)x(\tau + kT),$$

and $A(\tau + (k+1)T) = A(\tau + kT)\ \forall k \in \mathbb{N}$.

The exact discretized version of (7.7) for a sample time T (one period) is given by:

$$x_{k+1} = Ax_k$$

where $x_k = x(\tau + kT)$, $k \in \mathbb{N}$ and $A = \Psi(\tau)$.

Applying the Lyapunov inequality for linear invariant discrete-time systems

$$P > APA', \qquad P \in \mathbb{R}^{n\times n},$$

and substituting A by $\Psi(\tau)$ we have (7.19).

$\Psi(t)$ is a time-varying matrix with constant eigenvalues, thus the eigenvalues of $\Psi(t)$ are equal to the eigenvalues of $\Psi(\tau)$. □

7.2 Stabilization of linear time-periodic systems

Consider a linear periodic continuous-time dynamical system described by the following differential equation

$$\frac{dx(t)}{dt} = A(t)x(t) + B(t)u(t), \tag{7.20}$$

with feedback control law

$$u(t) = K(t)x(t), \tag{7.21}$$

$x : \mathbb{R}^+ \to \mathbb{R}^n$ is the state vector, $A : \mathbb{R}^+ \to \mathbb{R}^{n\times n}$ is the state matrix, $B : \mathbb{R}^+ \to \mathbb{R}^{n\times m}$ is the input matrix, $u : \mathbb{R}^+ \to \mathbb{R}^m$ is the input vector and $K : \mathbb{R}^+ \times \mathbb{R}^{m\times n}$ is the control gain matrix, $n, m \in \mathbb{R}$.

The periodicity is verified by $A(t + T) = A(t)$ and $B(t + T) = B(t)$, $T \in \mathbb{R}$.

Definition 7.7 (Stabilization of linear periodic continuous-time systems by state feedback)**.** *Chose a matrix $K(t)$ (possibly periodic of period T) such that the system* (7.20) *with control law* (7.21) *is asymptotically stable, that is, the monodromy matrix* (7.4) *of the closed-loop system* (7.22) *has all the eigenvalues inside the unit cycle.*

$$\frac{dx(t)}{dt} = (A(t) + B(t)K(t))x(t) \tag{7.22}$$

The existence of a stabilizing $K(t)$ depends upon the controllability of (7.20). *Controllability is concerned with the problem of driving a state point to any other state point by*

feeding the system (7.20) *with a suitable input signal.* Controllability is defined formally as follows

Definition 7.8 (Controllability of linear systems, adapted from [85])**.** *(i) System* (7.20)*, or equivalently the pair* $(A(t), B(t))$*, is controllable on the time interval* $[t_1, t_2]$ *if, for each value of* $x^1, x^2 \in \mathbb{R}^n$*, there exists an input* $u(t), t_1 \leq t < t_2$*, such that for* $x(t_1) = x^1$*, one has* $x(t_2) = x^2$*. (ii) For any real* $\tau \geq 0$*, system* (7.20)*, or equivalently the pair* $(A(t), B(t))$*, is controllable in time* τ *if, for each value of* $x^1, x^2 \in \mathbb{R}^n$*, there exist time instants* t_1, t_2*,* $t_2 = t_1 + \tau$ *and an input* $u(t), t_1 \leq t < t_2$*, such that for* $x(t_1) = x^1$*, one has* $x(t_2) = x^2$*. (iii) System* (7.20)*, or equivalently the pair* $(A(t), B(t))$*, is controllable if, for each value of* $x^1, x^2 \in \mathbb{R}^n$*, there exist time instants* t_1, t_2*,* $t_2 > t_1$ *and an input* $u(t), t_1 \leq t < t_2$*, such that for* $x(t_1) = x^1$*, one has* $x(t_2) = x^2$*.* □

The Definition 7.8 is valid only for linear systems where the definition of controllable and reachable states are equivalent. For controllability for nonlinear system see [85].

The design of the control gain $K(t)$ for stabilization of linear periodic continuous-time systems is studied in several references, for example [22, 47, 59, 60, 92, 102]. Here we focus on an optimal $K(t)$ designed using the Lyapunov stability theory [92, 102] or the assignment of the characteristic multipliers of the closed-loop system using the Floquet stability theory [47, 59, 60].

7.2.1 Stabilization by direct Lyapunov method

The problem of stabilization of continuous-time periodic linear systems by the Lyapunov direct method is resumed in Proposition 7.9 following Proposition 7.4.

Definition 7.9 (Asymptotic stabilization by direct Lyapunov method)**.** *Design a control gain matrix* $K(t)$ *of a controllable closed-loop continuous-time linear periodic system described by* (7.22) *that leads to a periodic positive definite symmetric matrix* $P(t) = P(t+T)$*,* $P : \mathbb{R}^+ \to \mathbb{R}^{n \times n}$*, solution of the Lyapunov inequality*

$$\dot{P}(t) > (A(t) + B(t)K(t))P(t) + P(t)(A(t) + B(t)K(t))'. \quad \square$$

A control gain matrix $K(t)$ that satisfies the condition of Definition 7.9 and also minimizes the index function (7.23) is presented in [102].

$$J(u(t)) = \int_0^T (x'(t)\gamma(t)P(t)x(t) + u'(t)R(t)u(t))\,dt \tag{7.23}$$

$\gamma : \mathbb{R}^+ \to \mathbb{R}$ and $R : \mathbb{R} \to \mathbb{R}^{n\times n}$ are T-periodic continuous functions.

Proposition 7.10 (adapted from [102]). *If $K(t) = -R^{-1}(t)B'(t)P(t)$, $P(t)$ and $R(t)$ are T-periodic matrices obtained by the periodic Lyapunov differential equation*

$$\dot{W}(t) = W(t)A_n'(t) + A_n(t)W(t) - S(t), \tag{7.24}$$

$P(t) = W^{-1}(t)$, $S(t) = B(t)R^{-1}(t)B'(t)$, $A_n(t) = A(t) + (1/2)\gamma(t)I_n$, where I_n is the identity matrix of order n and γ a T-periodic scalar function that satisfies

$$\int_0^T \gamma(t)dt > -\ln\left(\min|\mu|\right),$$

where μ_i, $i = 1, \ldots, n$, are the characteristic multipliers of (7.1), then a controllable closed-loop continuous-time linear periodic system described by (7.22) is asymptotically stable. □

Observe that the control law of Proposition 7.10 depends upon the solution of the periodic Lyapunov differential equation (7.24) for each time t. Another optimal control method based on the periodic Lyapunov differential equation that leads to a possible constant control gain matrix is presented in [92].

7.2.2 Eigenvalue assignment by state feedback

Definition 7.11 (Periodic eigenvalue assignment problem). *Consider the continuous-time linear periodic closed-loop system (7.22) and let $(A(t), B(t))$ be controllable. Find periodic $m \times n$ matrices $K(t)$ such that*

$$\Lambda(\Psi(t)) = \Gamma,$$

where $\Psi(t) \in \mathbb{R}^{n\times n}$ *is the monodromy matrix of* (7.22)*,* $\Lambda(\Psi(t)) \in \mathbb{C}^n$ *is the set of eigenvalues of* $\Psi(t)$ *and* $\Gamma \in \mathbb{C}^n$ *is an arbitrary set of* n *complex conjugate numbers.* □

Different strategies for eigenvalues assignment by state feedback of continuous-time linear periodic systems are presented in [22, 47, 59, 60]. A historical review about the theme and other references are presented in [59]. Here we focus on the initial sampled feedback idea presented in [47] and the instantaneous feedback idea presented in [60]. The latter is the most general instantaneous feedback method found in literature.

Eigenvalue assignment via sampled feedback

A methodology for eigenvalue assignment via sampled feedback, called *sampled state periodic hold*, is proposed in [47].

Consider the system (7.20), $(A(t), B(t))$ controllable, with control signal $u(t)$ defined in (7.25) with the state $x(t)$ sampled at each period T.

$$u(t) = K(t)x(iT), \qquad t \in [iT,\ (i+1)T], \tag{7.25}$$

$K : \mathbb{R}^+ \to \mathbb{R}^{m\times n}$, a piecewise and bounded T-periodic function.

More than an eigenvalue assignment, this method allows a whole closed-loop monodromy matrix ($\Psi(t)$) assignment by defining the control gain $K(t)$ as follows

$$K(t) = B'(t)\Phi'(T,t)W^{-1}(T,0)[\Psi(0) - \Phi(T,0)]$$

where $\Psi(0)$ is the desired monodromy matrix at time 0 (remember that the characteristic multipliers are constant), $\Phi(t_2, t_1)$ is the state transition matrix of (7.1) and

$$W(t_2,t_1) = \int_{t_1}^{t_2} \Phi(t_2,\tau)B(\tau)B'(\tau)\Phi'(t_2,\tau)d\tau. \tag{7.26}$$

The main problem of this method is that the state variables are measured only once per cycle. This means that the control law is more sensible to unexpected behaviour between cycles than others with continuous measurement of the state variables.

Eigenvalue assignment via continuous feedback

In this section we exemplify a control method via a continuous feedback control law, as (7.21), for eigenvalue assignment of the controllable closed-loop continuous-time linear periodic system (7.20). The chosen method was proposed in [60] and can assign the entire closed-loop monodromy matrix. The authors claim that the method "can in principle be applied to any continuous-time linear periodic system because it only relies upon properties derived from the Floquet-Lyapunov theory". Other control laws are presented in [22, 59] and references therein.

Before present a resume of the method it is necessary to define the controllability index.

Definition 7.12 (Controllability index, see Definition 6 in [60])**.** *Given two $n \times n$ and $n \times r$ constant matrices M and N, let:*

$$U_k = \begin{bmatrix} N & MN & \dots & M^k N \end{bmatrix}.$$

The controllability index of the pair $\{M, N\}$ is the smallest integer k_0 such that U_{k_0-1} has rank n. □

The method is summarised in the following steps, details are available in the original reference.

1- Assign a new period T_K for the closed-loop system such that

$$\det[W(T_K, 0)] \neq 0.$$

$W(t_2, t_1)$ defined as in (7.26), $T_K = \nu T$ and ν is the controllability index of the pair $\{\Phi(T, 0), W(T, 0)\}$. $\Phi(T, 0)$ is the monodromy matrix of (7.1).

2- Assign the desired monodromy matrix $\Phi_K(T_K, 0)$ of the closed-loop system (7.22) satisfying the relation

$$\det[\Phi_K(T_K, 0)] > 0.$$

3- Choose a pair $\{Y, F\}$ such that

$$Y\Phi_K(T_K, 0) = e^{T_K F},$$

$Y, F \in \mathbb{R}^{n\times n}$.

4- Solve the boundary value problem

$$\frac{d}{dt}[L^{-1}(t)] = -L^{-1}(t)[A(t) + FL^{-1}(t) - B(t)B'(t)\Phi'_K(T_K, t)K_cL^{-1}(t)]$$
$$L^{-1}(0) = I_n, \qquad L^{-1}(T_K) = Y$$

to compute $L^{-1}(t)$. $K_c \in \mathbb{R}^{n\times n}$ and $L : \mathbb{R}^+ \to \mathbb{R}^{n\times n}$ is kT_K-periodic ($k \in \mathbb{Z}$), non-singular for all t and continuous with a piecewise continuous derivative.

5- Compute the control gain

$$K(t) = B'(t)\Phi'(T_K, t)K_cL^{-1}(t).$$

K_c is guaranteed to exist due to controllability.

7.3 Control methods for periodic orbits

Here we detail the control methods studied for stabilization of periodic orbits of continuous-time systems and review the literature about them.

We first explain the PFC, then we explain the DFC and present a review on its principal modifications since proposed by Pyragas [70]. Last we detail the application of the continuous-time PBC, an original contribution of this work.

7.3.1 Proportional feedback control (PFC)

This method uses as reference signal the target UPO itself and the control signal is defined by

$$u(t, x(t)) = K(t, x(t))\,(x^*(t) - x(t))\,. \tag{7.27}$$

$K : \mathbb{R}^+ \times \mathbb{R}^n \rightarrow \mathbb{R}^{m \times n}$ may be a time-varying control gain that depends on the system state such that $x^*(t)$ is stable and condition (6.6) is satisfied. The application of the PFC method depends on the previous knowledge of the target UPO and this is the principal disadvantage of the method. This problem is more evident in continuous-time systems where continuous orbits, not only the discrete p points, should be identified and reconstructed.

Examples of the application of the PFC with a constant scalar control gain K adjusted experimentally are found in [70, 97]. In [97] it is suggested that an approximation of $x^*(t)$ can be obtained experimentally from time series by the methods proposed in [56, 83].

A matrix gain K is used in [4] to stabilize periodic orbits in noisy systems. The gain K is designed by optimization aiming to find the control gain that makes the orbit more stable. An approximation of one point of the periodic orbit is found by minimizing $|x(T) - x(0)|^2$ varying $x(0)$ and T.

Analytical design of the control gain and stability analysis for the PFC can be performed if the system model is available [79, 80]. In this case, an approximation of one point of the UPO can be found using the Newton-Raphson method [68] to find a zero of $(x(t_p) - x(0))$ with adjustable parameter $x(0)$. $x(t_p)$ is the value of the state at the p-th intersection of $x(t)$ with the Poincaré section (Appendix A) defined on $x(0)$.

The design of the PFC control gain in this work is done integrating the variational equation (see [68] and Section 7.4.1) of the closed-loop system around $x^*(t)$ to obtain the monodromy matrix for a value of K. We chose a K that leads to a minimum of the Floquet multiplier with largest magnitude (Section 7.1.1).

7.3.2 Delayed feedback control (DFC)

This method uses the state of the system delayed by the period T of the target UPO as reference. The control signal for the DFC is thus defined

$$u(t, x(t)) = K(t, x(t)) \, (x(t - T) - x(t)) \tag{7.28}$$

and satisfies condition (6.6). $K : \mathbb{R}^+ \times \mathbb{R}^n \to \mathbb{R}^{m \times n}$ is a (possibly time-varying and state-dependent) control gain. The delayed term in the control signal makes (6.5) a delay differential equation with infinite dimension [36].

The application of the DFC depends only upon the ability of recording the value of the past (measured) state variables over a period T of the target UPO. This characteristic makes the method easily applicable.

Experimental constant control gain design. Pyragas [70] initially proposed a constant scalar control gain K. This control gain and an approximation of the period T of the target orbit could be tuned experimentally achieving a stable periodic orbit without a mathematical model. $u(t, x(t))$ does not necessarily go to zero in this case, since T is not accurate.

The practical aspects of the DFC method contributed for its popularity [74]. Application of the DFC with constant gain in practical experiments and theoretical models can be found in review references [73, 79, 80]. In general, a scalar gain K is chosen using the largest Lyapunov exponent, which, on periodic orbits, correspond to the real part of the Floquet exponent (Appendix B). The largest Lyapunov exponent can be estimated numerically from the output time series of a dynamical system or using its mathematical model [95, 101].

Model based constant control gain design. Analytical design of a stabilizing control gain K for the DFC can be performed calculating it as a function of the control gain used to stabilize the same orbit with the PFC [73, 79, 80]. In this case, both the target UPO and a system model should be available.

The design of a DFC constant control gain for systems with a mathematical model available can be performed calculating the closed-loop monodromy matrix. This matrix can be obtained integrating the variational equation of a finite dimensional system around the target periodic orbit for one period of the orbit (see Section 7.1.1 and [68]). For infinite dimensional systems it is necessary to approximate their state by a finite number of variables. In the case of systems controlled with the DFC, the delayed states are

discretized by $n \times N$, $N \in \mathbb{N}$, state variables resulting in a system of dimension $n(1+N)$. This discretization can be done using the finite element method [9, 21, 86, 88], spectral element methods [9,23,51] and collocation methods with different types of approximating polynomials [10, 51], for example.

One of the contributions of this work on the DFC is the application of the method proposed by [10,23,51] to the design of a constant control gain by approximating the closed-loop monodromy matrix using only matrix algebra. The approximation of the monodromy matrix by the integration of the variational equation of the discretized system is time consuming because it is necessary to integrate a system of $[n(1+N)]^2$ equations for one period of the target orbit [68]. An alternative method for stability analysis of periodic delay differential equations with one constant time-delay was proposed in [10,23,51]. This method reduces the approximation of the monodromy matrix of a known UPO to matrix algebra applying the discretization of the delayed states, reducing the computational time and simplifying the numerical stability analysis. The details are discussed in Section 7.4.2 and numerical results in Chapter 8, these results were published in [14].

Adapting DFC. Adapting DFC methods for unknown T were developed in [39, 52]. These methods automatically adjust the value of the time-delay until it matches the period of a periodic orbit, if $u(t, x(t))$ leads to stability. Recently, a novel adapting method based on gradient descendent for applications where the knowledge about T is not precise was developed in [75]. This method is also useful in cases where the system parameters changes in time, leading to changes in the orbit period. The authors claim that this method does not require any complex on-line computation and does not changes the period or position in the state space of the target periodic orbit (only stability).

A method where both, control gain and time-delay, are functions of the system output is presented in [57]. This method is applicable when the system model is unknown and

does not require, a priory, any knowledge about the target UPO. The control signal in [57] is

$$\begin{aligned} u(t, y(t)) &= K(t, y(t))[y(t - \tau(t, y(t))) - y(t)] \\ \frac{d\tau(t, y(t))}{dt} &= -r_1[y(t - \tau(t, y(t))) - y(t)] \\ \frac{dK(t, y(t))}{dt} &= r_2[y(t - \tau(t, y(t))) - y(t)]^2, \end{aligned}$$

$r_1, r_2 \in \mathbb{R}$ are constants to be tuned and $y : \mathbb{R}^+ \to \mathbb{R}$ is an accessible state variable. The control signal is based on the assumption that the trajectories of the controlled system are bounded, which is not guaranteed for typical systems, requiring that $u(t, y(t))$ is forcibly limited (saturated) in applications.

Extended DFC. A popular method derived from the DFC is the extended delayed feedback control, proposed to stabilize orbits with larger periods and larger Floquet multipliers which are not stabilizable by the original DFC [71,73,79,80,84]. This method uses not only one delayed state $x(t-T)$ as in (7.28), but the sum of the, ideally infinite, terms $x(t - mT)$, $m = 1, 2, \ldots, +\infty$, with each term in the sum multiplied by its own constant weight defined by a proper rule. The control signal for the extended DFC is

$$u(t, y(t)) = K \left[(1 - r) \sum_{m=1}^{\infty} r^{m-1} y(t - mT) - y(t) \right], \tag{7.29}$$

where $K, r \in \mathbb{R}$, $|r| < 1$, and $y : \mathbb{R}^+ \to \mathbb{R}$ is an accessible state variable.

Odd-number limitation. The most studied limitation of the DFC is the *odd-number limitation*, defined initially for discrete-time dynamical systems (see Chapter 3, Section 3.3.2) and later to continuous-time dynamical systems in [45, 64, 65, 90]. This limitation refers to orbits with an odd number of real Floquet multipliers grater than +1, initially said to be impossible to stabilize with the original DFC and also a wider class of its modifications.

This limitation was contested by a counter example in [26,27,46]. It is stressed in [79, pg. 139] that the proof presented in [64] is valid for non-autonomous systems while the example presented in [26] refers to an autonomous system. Moreover, the experience with

autonomous systems shows that many of them suffer from this limitation, making this subject still unclear. A recent article [42] treats the limitation on autonomous systems departing from the results obtained in [64]. The analysis results in a more complete formulation of the odd-number limitation that justifies the counter-example presented in [26, 27, 46].

A methodology to stabilize orbits with the odd-number limitation with the extended delayed feedback control was proposed in [72]. The limitation is overcome introducing into the feedback loop an additional unstable degree of freedom. The result is a system with an even number of real Floquet multipliers larger than +1 to be stabilized by an additional term in the shape of the extended DFC. The control signal for the so called extended unstable DFC [72] is

$$\begin{aligned} u(t, y(t)) &= Kw(t, y(t)) - u_e(t, y(t)), \\ \frac{dw(t, y(t))}{dt} &= (\lambda_c^\infty - \lambda_c^0)u_e(t, y(t)) - \lambda_c^0 w(t, y(t)), \end{aligned}$$

$w : \mathbb{R}^+ \times \mathbb{R} \to \mathbb{R}$, $\lambda_c^0, \lambda_c^\infty \in \mathbb{R}$, $\lambda_c^0 > 0$ and $\lambda_c^\infty < 0$, and $u_e(t, y(t))$ is defined as $u(t, y(t))$ in (7.29).

Another method proposed to overcome the odd-number limitation of the DFC and its modifications is the prediction-based control.

7.3.3 Prediction-based (PBC) and approximate prediction-based (aPBC) control

Here we detail the new continuous-time control methods.

Principles and general formulation of the prediction-based control

The PBC is based on the prediction of *the state one period of the target UPO ahead, computed along the trajectories of the free system response.* The control signal of the continuous-time PBC is defined as

$$u(t, x(t)) = K(t, x(t)) \left(\varphi(t + T, t, x(t), 0) - x(t)\right), \tag{7.30}$$

where $\varphi(t_1, t_0, x, 0)$ is the value at time t_1 of the state of (6.5) with $x(t_0) = x$ and $u(t) = 0$, $t_0 \leq t \leq t_1$. In other words, $\varphi(t_1, t_0, x, 0)$ is the value at time t_1 of the state along the trajectory departing from x at time t_0 of the free system ($u(t) \equiv 0$). $K : \mathbb{R}^+ \times \mathbb{R}^n \to \mathbb{R}^{m \times n}$ is the control gain. The issue of designing constant control gain K to stabilize a target UPO $x^*(t)$ is treated in Section 7.4.3.

The general formulation of the PBC method is as follows. The solution of system (6.5) with control signal (7.30) is the solution of the following PDE

$$\frac{\partial X(t,0)}{\partial t} = f(t, X(t,0), K(t, X(t,0)) \left(X(t,T) - X(t,0)\right), \qquad t \geq 0 \tag{7.31a}$$

$$\frac{\partial X(t,Ts)}{\partial s} = Tf(t + Ts, X(t,Ts), 0), \qquad t \geq 0, \qquad s \in [0,1] \tag{7.31b}$$

$$X(0,0) = x(0).$$

The function $X : \mathbb{R}^+ \times [0,T] \to \mathbb{R}^n$ is such that $X(t,0) = x(t)$ and $X(t,T) = \varphi(t + T, t, x(t), 0)$.

Clearly, real-time application of the control structure proposed here depends on the ability to compute $\varphi(t + T, t, x(t), 0)$.

Principles of the approximate prediction-based control method (aPBC)

Apart and before the question of finding a stabilizing gain for PBC method, is the issue of implementing in real time the value of the predicted state $\varphi(t + T, t, x(t), 0)$. Computing the future state $\varphi(t + T, t, x(t), 0)$ requires solving at each time t the free system ODE from time t to $t + T$. This can not be done exactly in real-time. This is why we introduce an approximation of this quantity that can be computed in real time. We call the corresponding feedback law, based on the difference between the present state and the approximate predicted state, approximate prediction-based control.

An important difference compared with the previous methods is the following. While the initial UPO was a solution (with null feedback) of the closed-loop system obtained with PFC, DFC or "exact" (non-implementable) PBC, this is not true any more. In fact,

we have in mind stabilization to a new orbit of the controlled system, *close to* the UPO of the uncontrolled system.

Approximation of the prediction term - 1^{st} step. The first step consists in approximating the solution of (7.31b) by an implicit Runge-Kutta ODE integration method [35], in order to estimate the prediction term, that is, the terminal value

$$X(t,T) = x + T\int_0^1 f\left(t+Ts, X(t,Ts), 0\right) ds, \qquad x \text{ given.} \tag{7.32}$$

To estimate $X(t,T)$ given by (7.32), the state transition map of the free system $\varphi(t_2,t_1,x,0)$ is first approximated by the operator $\mathbf{z}$ defined by

$$\mathbf{z}(t+T,t,x) = x + T\sum_{i=1}^{N} c_i l_i(t) \tag{7.33a}$$

$$l_i(t) = f\left(t+Ts_i, x+T\sum_{j=1}^{N} a_{ij} l_j(t), 0\right), \tag{7.33b}$$

where $i = 1,\ldots,N$, $l_j : \mathbb{R}\times\mathbb{R}^n \to \mathbb{R}^n$ and $a_{ij}, c_i \in \mathbb{R}$ are weights chosen according to the implicit method used [35]. The approximation $\mathbf{z}(t+T,t,x(t))$ of $X(t,Ts)$, $s\in[0,1]$, is calculated at the discretization points $s = s_i$, $i = 1,\ldots,N$.

For simplicity, (7.33b) is written in the vector form (7.34).

$$L(t) = F_T(t,x,L(t)), \tag{7.34}$$

where

$$\forall t \geq 0, \quad L(t) = \begin{bmatrix} l_1(t) \\ \vdots \\ l_N(t) \end{bmatrix} \in \mathbb{R}^{nN},$$

and $F_T : \mathbb{R} \times \mathbb{R}^n \times \mathbb{R}^{nN} \to \mathbb{R}^{nN}$ is defined by:

$$F_T(t, x, L) = \begin{bmatrix} f(t + Ts_1, x + \sum_{j=1}^{N} a_{1j} l_j, 0) \\ \vdots \\ f(t + Ts_N, x + \sum_{j=1}^{N} a_{Nj} l_j, 0), \end{bmatrix}, \qquad \forall x \in \mathbb{R}^n, \quad \forall L \in \mathbb{R}^{nN}.$$

To compute $\mathbf{z}(t+T, t, x)$ through (7.33a), it is necessary to solve the algebraic system of equations (7.34) with unknown $L(t) \in \mathbb{R}^N$. Writing

$$C = \begin{bmatrix} c_1 & \dots & c_N \end{bmatrix}$$

and closing equation (6.5) by

$$u(t, x(t)) = K(t, x(t))(\mathbf{z}(t + T, t, x(t)) - x(t)) = TK(t, x(t))CL(t)$$

yields the differential algebraic equation (DAE),

$$\dot{x}(t) = f(t, x(t), TK(t, x(t))CL(t)), \qquad x(0) = x_0 \tag{7.35a}$$

$$L(t) = F_T(t, x(t), L(t)). \tag{7.35b}$$

The real time solution of the DAE (7.35) requires the computation of $L(t)$, its algebraic term, at each time t — a complicated task indeed. We therefore introduce an observer equation in the sequel, to transform the controlled system into a system of ODEs.

Approximation of the prediction term - 2^{nd} step. We now approximate (7.35b) by solving the nN-dimensional ODE (7.36) whose solution $\hat{L}(t)$ is an estimation of $L(t)$. The initial value $\hat{L}(0)$ is intended to be (precisely) computed off-line to provide good tracking quality for $L(t)$.

$$\frac{d}{dt}\left(\hat{L}(t) - F_T(t, x(t), \hat{L}(t))\right) + k_o\left(\hat{L}(t) - F_T(t, x(t), \hat{L}(t))\right) = 0, \qquad \hat{L}(0) \text{ given.} \tag{7.36}$$

The scalar gain k_o is chosen positive in order that $\hat{L}(t)$ of (7.36) tends asymptotically towards the solution $L(t)$ of (7.35b) when $t \to +\infty$, and typically such that the estimator dynamics is faster than the controlled system dynamics. If indeed the evolution of $\hat{L}(t)$ may be chosen in order to fulfil (7.36), convergence does occur.

From (7.36) we obtain:

$$\dot{\hat{L}}(t) - \Big[\partial_1 F_T(t, x(t), \hat{L}(t)) + \partial_2 F_T(t, x(t), \hat{L}(t))(\mathbf{1}_N \otimes f(t, x(t), 0)) + \partial_3 F_T(t, x(t), \hat{L}(t)) \left(T(A \otimes I_n)\dot{\hat{L}}(t)\right)\Big] + k_o \left(\hat{L}(t) - F_T(t, x(t), \hat{L}(t))\right) = 0, \quad (7.37)$$

where $A = (a_{ij})$ and ∂_i the partial derivative with respect to the i-th variable. I_n is the $n \times n$ identity matrix and $\mathbf{1}_N$ is the column vector of dimension N with all elements equal to 1. $\otimes$ is the Kronecker product.

By determining $\dot{\hat{L}}(t)$ from (7.37) we get (7.38).

$$\dot{\hat{L}}(t) = \Big[I_{nN} - T\partial_3 F_T(t, x(t), \hat{L}(t))(A \otimes I_n)\Big]^{-1} \Big[\partial_1 F_T(t, x(t), \hat{L}(t)) + \partial_2 F_T(t, x(t), \hat{L}(t))(\mathbf{1}_N \otimes f(t, x(t), 0)) - k_o \left(\hat{L}(t) - F_T(t, x(t), \hat{L}(t))\right)\Big]. \quad (7.38)$$

Clearly, solving (7.38), in order to obtain (7.36), requires inversibility of the first factor.

We now define $G_T : \mathbb{R}^n \times \mathbb{R}^n \times \mathbb{R}^{nN} \to \mathbb{R}^{nN}$,

$$G_T(t, x, \hat{L}) = \Big[I_{nN} - T\partial_3 F_T(t, x, \hat{L})(A \otimes I_n)\Big]^{-1} \Big[\partial_1 F_T(t, x, \hat{L}) + \partial_2 F_T(t, x, \hat{L})(\mathbf{1}_N \otimes f(t, x, 0)) - k_o \left(\hat{L} - F_T(t, x, \hat{L})\right)\Big]. \quad (7.39)$$

From (7.35), (7.36), (7.39) and denoting $\hat{l}_i(t)$ the components of $\hat{L}(t)$, the control law we propose yields the following closed-loop system of ODEs:

$$\begin{bmatrix} \dot{x}(t) \\ \dot{\hat{L}}(t) \end{bmatrix} = \begin{bmatrix} f\left(t, x(t), K(t, x(t))TC\hat{L}(t)\right) \\ G_T\left(t, x(t), \hat{L}(t)\right) \end{bmatrix} \qquad x(0) = x_0, \quad \hat{L}(0) = L(0). \quad (7.40)$$

The solution of (7.40) is an approximation of the solution of the PDE given in (7.31).

The ODE (7.40) has two types of state components, corresponding to the controlled system dynamics and to the dynamical state controller. Once $\hat{L}(t)$ stands for a set of unmeasured state variable components, equation (7.36) can be interpreted as a state observer. Notice that this estimator introduces a dynamical feedback whose state has a dimension equal to the number of points of the Runge-Kutta method adopted, multiplied by the dimension of the initial system to be controlled.

In summary, the closed-loop system (6.5)-(7.30) has first been rewritten as the PDE (7.31). The latter provides the possibility of computing the controlled state and the free system response at a future time simultaneously. An approximated solution of the PDE is then calculated computing the future state along the trajectories of the free system using a Runge-Kutta implicit method leading to the DAE (7.35). Instead, of solving this DAE, we prefer to approximate it by the extended ODE (7.40) for real time application.

As mentioned earlier, due to the use of an approximate value of the predicted state, we can only expect approximate stabilization of the initial orbit, or rather, stabilization to an orbit close to the initial one.

Implementation issues

The implicit Runge-Kutta method given in (7.33) is a general formulation used for the integration of differential equations, whose application depends on the choice of a specific implementation. Here we choose the orthogonal collocation [28, 35, 93] as implicit Runge-Kutta method, but there's no doubt other implementations should be experimented.

Collocation methods amount to approximate the prediction term by $\mathbf{z}(t+T, t, x(t))$, where $\mathbf{z}(t+Ts, t, x(t))$ is defined on the whole interval $s \in [0, 1]$ by

$$\mathbf{z}(t+Ts, t, x(t)) = \sum_{j=1}^{N} w_j(s) m_j(t), \qquad m_1(t) = x(t), \quad s \in [0,1], \quad t \geq 0 \tag{7.41}$$

where $m_j : \mathbb{R}^+ \to \mathbb{R}^n$, $j = 1, \ldots, N$, is a column vector. The functions $w_j(s)$ are the Lagrange polynomials

$$w_j(s) = \prod_{i=1, i\neq j}^{N} \frac{s - s_i}{s_j - s_i}, \qquad j = 1, \ldots, N \tag{7.42}$$

attached to the choice of the points $0 = s_1 < s_2 < \cdots < s_{N-1} < s_N = 1$. For simplicity, we choose here Lagrange polynomials but other ones, like Chebyshev or Legendre, could be used.

The link with the implicit Runge-Kutta method is as follows.

Theorem 7.13 (Adapted from Theorem 7.7 in [35] ([34, 96] are cited by [35] as original references))**.** *The collocation method* (7.41) *with Lagrange polynomials* $w_j(s)$ *is equivalent to the* N*-stage implicit Runge-Kutta method* (7.33) *with coefficients*

$$a_{ij} = \int_0^{s_i} w_j(s)ds, \qquad c_j = \int_0^1 w_j(s)ds, \qquad i, j = 1, \ldots, N \quad \square \tag{7.43}$$

It is possible to choose the collocation points in order to fulfill the orthogonality relations:

$$\int_0^1 (1 - s)s \; w_i(s)w_j(s) \; ds = 0, \; i, j = 2, \ldots, N - 1, \; i \neq j. \tag{7.44}$$

Note that for each $j = 1, \ldots, N$, $\varphi(t + Ts_j, t, x(t), 0) \approx \mathbf{z}(t + Ts_j, t, x(t)) = m_j(t)$ as $w_j(s_i) = \delta_j^i$ (with δ_j^i, the Kronecker symbol). A characteristic of the orthogonal collocation method is that each $m_j(t)$ is an approximation of the state that differs from the $l_j(t)$ in (7.33), which are the derivatives.

Equation (7.40) is obtained applying the substitutions provided by (7.41) and Theorem 7.13 with interpolating times s_j obtained by solving (7.44).

7.4 Analysis methods for stabilization of periodic orbits

The discussion of Section 7.1.1 shows that the stability of a periodic orbit is defined by the stability analysis of the linear time-periodic system that governs the dynamics in its vicinity. In particular, the stability of the periodic orbit is defined by the eigenvalues of the monodromy matrix of the linearised system, being asymptotically stable if they have modulus less the one.

Following this, the stabilization of a periodic orbit of the non-linear system (6.5) is performed by stabilizing the linear time-varying system (7.45) that governs the evolution of a perturbed trajectory $\delta x(t) : \mathbb{R}^+ \times \mathbb{R}^n \to \mathbb{R}^n$ in the close vicinity of $x^*(t)$ with initial condition $x(0) = x^*(0) + \delta x(0)$.

$$\frac{d\delta x(t)}{dt} = \Big(\nabla_x f(t, x, u(t, x(t)))|_{x=x(t)} + \nabla_u f(t, x(t), u)|_{u=u(t,x(t))} \, \nabla_x u(t, x)|_{x=x(t)} \Big) \, \delta x(t), \quad \delta x(0) \text{ given.} \tag{7.45}$$

For $x(t) = x^*(t)$, system (7.45) is linear time-periodic and the stabilization of this continuous-time system by state-feedback was studied in Section 7.2.

Here we intend to stabilize a T-periodic orbit $x^*(t)$ of (6.5) by applying a control signal $u(t, x(t))$ that stabilizes the linear system (7.45) and satisfies condition (6.6). The methods for stabilization of linear time-periodic systems exemplified in Section 7.2 do not consider (directly) the characteristics of the non-linear system and condition (6.6).

Three control methods for stabilization of periodic orbits were presented in Section 7.3: PFC with $u(t, x(t))$ defined in (7.27), DFC with $u(t, x(t))$ defined in (7.28) and PBC with $u(t, x(t))$ defined in (7.27). In this section we present the methodology for computation of the closed-loop monodromy matrix for each method, in special for the DFC, where we simplify this computation using the method prosed in [10, 23, 51] for general delayed systems with one constant time delay. A constant control gain for each method will be chosen such that all the Floquet multipliers have modulus less then one.

7.4.1 Stabilization by proportional feedback control

Here we discuss the computation of the closed-loop monodromy matrix as a function of a constant control gain K. A value K is chosen by calculating the monodromy matrix for each K and choosing the one that leads to the more adequate Floquet multipliers.

The purpose is stabilizing $x^*(t)$ in (6.5) by using the feedback control signal (7.27) with a constant control gain $K \in \mathbb{R}^{n\times n}$.

The computation of the monodromy matrix is done by integrating (7.46) for one cycle T.

$$\frac{d\Phi(t,0)}{dt} = \left[\nabla_x f(t,x,u) - \nabla_u f(t,x,u)K\right]_{x=x^*(t)} \Phi(t,0), \quad t \in [0,T], \quad \Phi(0,0) = I_n. \tag{7.46}$$

K is chosen such that all the eigenvalues of the monodromy matrix obtained by (7.46) have modulus less then one.

7.4.2 Stabilization by delayed feedback control

Here we use the method proposed by [10,23,51] to approximate the monodromy matrix of DDEs with one constant time delay to approximate the monodromy matrix of the system controlled with the DFC. This approximation uses only matrix algebra and simplifies the design of a constant control gain.

The aim is to provide an approximation of the monodromy matrix of $x^*(t)$ for (6.5) with the feedback control signal (7.28) and constant control gain $K \in \mathbb{R}^{n\times n}$.

The design of the control gain K for an infinite dimensional system, and specially the computation of the monodromy matrix, implies on the discretization of the past states in time. This results in an ODE of high dimension whose stability analysis and monodromy matrix approximates the same for the original DDE.

Closed-loop monodromy matrix approximation. A finite-dimensional version of the system state is considered by representing it as a vector composed by a discrete-time

approximation of the trajectory from $x(t-T)$ to $x(t)$. This extended state $X(t)$ can be represented as

$$X(t) = \begin{bmatrix} x(t - s_1 T) \\ x(t - s_2 T) \\ \vdots \\ x(t - s_N T) \end{bmatrix}, \tag{7.47}$$

where $s_1 = 0$, $s_i < s_{i+1}$, $i = 1, 2, \ldots, N$, and $s_N = 1$.

The s_i values will be determined by a discretization method and the number of samples N depends on the system dynamics and the value of T. It is now possible to re–write (6.5) for the DFC method as a function of $X(t)$, resulting in:

$$\frac{dX(t)}{dt} = F\left(t, X(t), \left(I_N \otimes K\right)\left(X(t-T) - X(t)\right)\right), \tag{7.48}$$

where $K \in \mathbb{R}^n$ is the control gain, from now constant, I_N is the identity matrix of order N, $\otimes$ is the Kronecker product and

$$F(t, X(t), U(t, X(t))) = \begin{bmatrix} f(t - s_1 T, x(t - s_1 T), K(x(t - (1 + s_1)T) - x(t - s_1 T)) \\ f(t - s_2 T, x(t - s_2 T), K(x(t - (1 + s_2)T) - x(t - s_2 T)) \\ \vdots \\ f(t - s_N T, x(t - s_N T), K(x(t - (1 + s_N)T) - x(t - s_N T)) \end{bmatrix}, \tag{7.49}$$

$F : \mathbb{R}^+ \times \mathbb{R}^{nN} \times \mathbb{R}^{mN} \to \mathbb{R}^{nN}$.

Consider a perturbation $\delta X(0)$ on the periodic state $X^*(0)$ resulting in

$$X(0) = X^*(0) + \delta X(0),$$

where X, X^*, and δX are defined as in (7.47). The evolution $\delta X(t)$ of the initial perturbation $\delta X(0)$ is obtained by substituting the perturbed trajectory in (7.48),

$$\frac{dX^*(t)}{dt} + \frac{d\delta X(t)}{dt} = F(t, X^*(t) + \delta X(t), U(t, X^*(t) + \delta X(t)).$$

Expanding $F(t, X^*(t)+\delta X(t), U(t, X^*(t)+\delta X(t))$ around $X^*(t)$ for $\delta X(0)$ sufficiently small, we obtain

$$\frac{d\delta X(t)}{dt} = \nabla_X F(t, X, U(t, X^*(t)))|_{X=X^*(t)}\, \delta X(t) + \nabla_U F(t, X^*(t), U)|_{U=U(t,X^*(t))}\, (I_N \otimes K)\, (\delta X(t-T) - \delta X(t)). \quad (7.50)$$

We adopt a numerical approximation for $d\delta X(t)/dt$, including the delayed states, in the form

$$\frac{d\delta X(t)}{dt} \approx (D \otimes I_n)\delta X(t), \quad (7.51)$$

where $D \in \mathbb{R}^{N\times N}$ is a differentiation matrix with constant coefficients that can be obtained using finite difference methods [9, 21, 86, 88], spectral methods [9, 23, 51] or a collocation method with different types of approximating polynomials [10, 51].

Substituting (7.51) in (7.50) leads to

$$M_D \delta X(t) = M_A \delta X(t) + M_K(\delta X(t-T) - \delta X(t)), \quad (7.52)$$

where

$$M_D = \begin{bmatrix} D_{ij} \otimes I_n \\ \mathbf{0}_{n\times nN} \quad I_n \end{bmatrix}, \quad (7.53a)$$

$$M_A = \begin{bmatrix} A(t-s_1T) & \mathbf{0}_{n\times n} & \cdots & \mathbf{0}_{n\times n} & \mathbf{0}_{n\times n} \\ \mathbf{0}_{n\times n} & A(t-s_2T) & \cdots & \mathbf{0}_{n\times n} & \mathbf{0}_{n\times n} \\ \vdots & \vdots & \ddots & \vdots & \vdots \\ \mathbf{0}_{n\times n} & \mathbf{0}_{n\times n} & \cdots & A(t-s_{N-1}T) & \mathbf{0}_{n\times n} \\ I_n & \mathbf{0}_{n\times n} & \cdots & \mathbf{0}_{n\times n} & \mathbf{0}_{n\times n} \end{bmatrix}, \quad (7.53b)$$

$$M_K = \begin{bmatrix} B(t-s_1T)K & \mathbf{0}_{n\times n} & \cdots & \mathbf{0}_{n\times n} & \mathbf{0}_{n\times n} \\ \mathbf{0}_{n\times n} & B(t-s_2T)K & \cdots & \mathbf{0}_{n\times n} & \mathbf{0}_{n\times n} \\ \vdots & \vdots & \ddots & \vdots & \vdots \\ \mathbf{0}_{n\times n} & \mathbf{0}_{n\times n} & \cdots & B(t-s_{N-1}T)K & \mathbf{0}_{n\times n} \\ I_n & \mathbf{0}_{n\times n} & \cdots & \mathbf{0}_{n\times n} & \mathbf{0}_{n\times n} \end{bmatrix}, \tag{7.53c}$$

with $i = 1, \ldots, N-1$, $j = 1, \ldots, N$, $A(t-s_iT) = \nabla_x f(t-s_iT, x, u)|_{x=x^*(t-s_iT)}$ and $B(t-s_iT) = \nabla_u f(t-s_iT, x, u)|_{u=u^*(t-s_iT, x^*(t-s_iT))}$. The last lines of the matrices guarantee the periodicity [51].

Now, we define the closed-loop monodromy matrix $\Psi_X(t)$ as the state transition matrix on $X^*(t)$, from $\delta X(t-T)$ to $\delta X(t)$ given by

$$\delta X(t) = \Psi_X(t)\delta X(t-T), \tag{7.54}$$

where $\Psi_X(t) \in \mathbb{R}^{nN\times nN}$.

By equating (7.52) and (7.54) one obtains

$$\Psi_X(t) = (M_D - M_A + M_K)^{-1} M_K. \tag{7.55}$$

Once an approximation for $x^*(t)$ is obtained, the computation of the monodromy matrix is done by matrix algebra operations only. This method reduces considerably the computational effort to approximate the monodromy matrix since it is not necessary to integrate the variational equation (7.46). For the DFC, $\nabla_x f(t, x, K(x(t-T) - x(t))|_{x=x^*(t)}$ in (7.46) is infinite dimensional because of the delayed states, in practice it is a large matrix obtained by discretization of the delayed states.

In Chapter 8 we will discuss an optimization process to design K using (7.55) [14].

Implementation issues

Here we present a method to implement the differentiation matrix D used on the approximation (7.51). We chose the orthogonal collocation method presented in Section 7.3.3.

The collocation method is used here to approximate the past states $x(t-Ts)$, defined on the whole interval $s \in [0,1]$ by

$$x(t-Ts) \approx \sum_{j=1}^{N} w_j(s) m_j(t), \qquad m_1(t) = x(t), \quad s \in [0,1], \quad t \geq 0 \tag{7.56}$$

where $m_j : \mathbb{R}^+ \to \mathbb{R}^n$, $j = 1, \ldots, N$, is a column vector. The functions $w_j(s)$ are the Lagrange polynomials defined in (7.42) attached to the choice of the collocation points $0 = s_1 < s_2 < \cdots < s_{N-1} < s_N = 1$ calculated according to (7.44).

Here, for each $j = 1, \ldots, N$, $x(t - Ts_j) \approx m_j(t)$ as $w_j(s_i) = \delta_j^i$ and their derivative with respect to s is given by

$$\left.\frac{\partial x(t-Ts)}{\partial s}\right|_{s=s_i} \approx \sum_{j=1}^{N} \left.\frac{\partial w_j(s)}{\partial s}\right|_{s=s_i} m_j(t), \qquad i = 1, \ldots, N. \tag{7.57}$$

Note that

$$\left.\frac{\partial x(t-Ts)}{\partial s}\right|_{s=s_i} = \left.\frac{\partial (t-Ts)}{\partial s} \frac{\partial x(t-Ts)}{\partial (t-Ts)}\right|_{s=s_i} = \\ -Tf(t-Ts_i, x(t-Ts_i), u(t-Ts_i, x(t-Ts_i))), \qquad i = 1, \ldots, N. \tag{7.58}$$

Equations (7.57) and (7.58) lead to

$$f(t-Ts_i, x(t-Ts_i), u(t-Ts_i, x(t-Ts_i))) \approx -\frac{1}{T} \sum_{j=1}^{N} \left.\frac{\partial w_j(s)}{\partial s}\right|_{s=s_i} x(t-Ts_i),$$

and $D \in \mathbb{R}^{N \times N}$, in (7.51), is computed as

$$D_{ij} = -\frac{1}{T} \sum_{j=1}^{N} \left.\frac{\partial w_j(s)}{\partial s}\right|_{s=s_i}. \tag{7.59}$$

An example of how to compute the matrix D is in [14] (attached in the Appendix D).

7.4.3 Stabilization by prediction-based control

Once the feedback method has been described in Section 7.3.3, we provide a method to design the control gain $K(t, x(t))$ of system (7.40). It is applied for a constant control gain K and it depends upon the ability of computing the closed-loop monodromy matrix of $x^*(t)$. The computation of this matrix requires the integration of the closed-loop system and its variational equation along a trajectory in the vicinity of $x^*(t)$ (7.60) [68, Appendix B]. To integrate this trajectory, the initial condition is chosen close to $x^*(0)$. Integrating (7.60) over a period yields the corresponding closed-loop monodromy matrix $\Psi(t) = \Phi(t+T, t)$.

$$\frac{d\Phi(t,0)}{dt} = \nabla_x f\left(t, x, K(\varphi(t+T, t, x, 0) - x)\right)|_{x=x^*(t)}\, \Phi(t,0), \quad t \in [0,T], \quad \Phi(0,0) = I_n, \tag{7.60}$$

where

$$\nabla_x f\left(t, x, K(\varphi(t+T, t, x, 0) - x)\right) = \nabla_x f(t,x,u) + K\nabla_u f(t,x,u)(\nabla_x \varphi(t+T,t,x,0) - I_n). \tag{7.61}$$

$\nabla_x \varphi(t+T, t, x, 0)$ is the free system monodromy matrix calculated as in (7.9).

Using (7.60) and (7.61) we compute the closed-loop monodromy matrix of $x^*(t)$ given gain K. The Floquet multipliers are calculated to measure the local stability of the controlled orbit for the chosen K. If the system is controllable, then there is a control gain K that asymptotically stabilizes it.

In practice, we fix K, compute the monodromy matrix by integrating (7.60) with an explicit Runge-Kutta method and $\varphi(t+T, t, x^*(t), 0)$ is calculated integrating the free system over a period T at each step of the integration of (7.60). After that we obtain the corresponding Floquet multipliers of the closed-loop system. Other methods, such that eigenvalue assignment method could be applied. This is the subject of future works.

Alternative time-varying control law

Here we provide the formulation of a time-varying control law, a continuous-time version of control law 3 (CL 3) presented in Section 3.4.2. For now, this control law is not applicable due to the necessity of exact computation of the free system state transition matrix from time t to $t+T$ computed at each time t. The development of this control law may be studied in future works using an approximation of the free system state transition matrix adapting, for example, the method shown in [8].

Theorem 7.14. *Assume that there exists a hyperbolic periodic orbit $x^*(t)$ that is a solution of system (6.5) with $\nabla_u f(t, x(t), u)|_{u=u(t,x(t))}$ invertible for all $t \geq 0$. If the feedback control signal $u(t, x(t))$, defined in (7.30) with $K(t, x(t))$ given by*

$$K(t,x(t)) = \Big(\nabla_u f(t,x(t),u)|_{u=u(t,x(t))}\Big)^{-1} \Big(\Theta - \nabla_x f(t,x,u(t,x(t)))|_{x=x(t)}\Big)\Big(\nabla_x \varphi(t+T,t,x,0)|_{x=x(t)} - I_n\Big)^{-1}, \quad (7.62)$$

is applied to (6.5), then the monodromy matrix of $x^*(t)$ is assigned as $\Psi(t) = e^{\Theta T}$, $\Theta \in \mathbb{R}^{n\times n}$. □

Proof. Consider the Jacobian matrix of the closed-loop system (6.5) with control signal (7.30) calculated on the periodic orbit $x^*(t)$

$$\nabla_x f\left(t,x,K(t,x^*(t))(\varphi(t+T,t,x,0)-x)\right)|_{x=x^*(t)} = \nabla_x f(t,x,u)|_{x=x^*(t)} + \nabla_u f(t,x(t),u)|_{u=u(t,x^*(t))} K(t,x^*(t))(\nabla_x \varphi(t+T,t,x,0)|_{x=x^*(t)} - I_n). \quad (7.63)$$

The derivative of $K(t, x(t))$ on the periodic orbit does not change the calculus of the Jacobian matrix, see the proof of Lemma 3.15 for the arguments on discrete-time systems (easily adaptable for continuous-time systems).

We aim at making

$$\nabla_x f\left(t,x,K(t,x^*(t))(\varphi(t+T,t,x,0)-x)\right)|_{x=x^*(t)} = \Theta, \quad (7.64)$$

where $\Theta \in \mathbb{R}^{n\times n}$ is a constant matrix. If (7.64) is ensured we can calculate the state transition matrix from time t to time $t+T$ as

$$\dot{\Phi}(t+T,t) = \Theta\Phi(t+T,t), \qquad \Phi(t,t) = I_n$$

with solution

$$\Phi(t+T,t) = \Psi(t) = e^{\Theta T}.$$

Using (7.63) and (7.64) for an invertible $\nabla_u f(t,x(t),u)|_{u=u(t,x^*(t))}$ and a hyperbolic $x^*(t)$ we have

$$K(t,x(t)) = \Big(\nabla_u f(t,x(t),u)|_{u=u(t,x^*(t))}\Big)^{-1} \Big(\Theta - \nabla_x f(t,x,u(t,x(t)))|_{x=x^*(t)}\Big)\Big(\nabla_x \varphi(t+T,t,x,0)|_{x=x^*(t)} - I_n\Big)^{-1}. \quad (7.65)$$

Applying (7.65) at any state $x(t)$ we achieve (7.62). □

Chapter 8

Numerical results

8.1 Introduction

Numerical results on the stabilization of periodic orbits using the proportional feedback control (PFC, see Section 7.3.1), delayed feedback control (DFC, see Section (7.3.2)) and prediction-based control (PBC, see Section 7.3.3) in continuous-time systems are presented in this chapter. For practical reasons, the approximate prediction-based control (aPBC, see Section 7.3.3) is applied instead of the PBC. The numerical simulations are chosen in order to evaluate the main characteristics of the methods.

Initially we use a non-autonomous system, the forced van der Pol (vdP) oscillator, characterized on Section 8.2. We also use the Rössler system on Section 8.5, an autonomous system, in order to evaluate the performance of the proposed continuous-time PBC in this case.

The numerical results were obtained using Fortran when characterizing the forced van der Pol oscillator, due to high numerical integration precision and computational effort requirements, and Matlab® when applying feedback control, due to existing functions that facilitate the implementation and possibility of reduction of the numerical integration precision. The reduction of the numerical precision on feedback control systems is related to the fact that they are less sensible to noise, external disturbance and parameters uncertainties [54].

The characteristics of the DFC and PFC are compared using as case study the forced van der Pol oscillator on Section 8.3. The DFC gain is designed using the stability analysis method shown in Section 7.4.2. We first evaluate both control methods for a period $p = 1$ orbit stabilized by both controllers on Section 8.3.2. Then we perform a brief robustness analyses comparing the DFC and PFC for the case of parameters uncertainties on Section 8.3.2. Two situations where the orbits are stabilized by the PFC and are not stabilized by the DFC are shown on Section 8.3.3.

The characteristics of the aPBC are evaluated on Section 8.4. We first apply the aPBC with a large number of collocation points (see Section 7.3.3), the parameters for aPBC are chosen in Section 8.4.1. The aPBC and the DFC are compared in Section 8.4.2. On Section 8.4.3 a situation where an orbit is stabilized by the aPBC and is not stabilized with the DFC is shown. We analyse the behaviour of the aPBC for different numbers of collocation points on Section 8.4.4. On Section 8.5 we stabilize one orbit of the Rössler system using the aPBC and analyse the behaviour of the method for different numbers of collocation points.

8.2 Bifurcation diagram for the forced vdP oscillator and target UPO selection

The forced vdP oscillator is described by the system of ODEs (8.1a).

Forced vdP oscillator

$$\dot{x}(t) = f(t, x(t)) + u(t, x(t)), \tag{8.1a}$$

$$f(t, x(t)) = \begin{bmatrix} x_2(t) \\ a\sin(\omega t) - \eta\left(x_1^2(t) - 1\right) x_2(t) - x_1(t) \end{bmatrix}, \tag{8.1b}$$

where $x : \mathbb{R}^+ \to \mathbb{R}^2$ and $f : \mathbb{R}^+ \times \mathbb{R}^2 \to \mathbb{R}^2$. We follow [16, 17] and choose $\omega = 0.45$ and $\eta = 1$ and use a as an adjustable parameter. The control signal $u(t, x(t))$ is defined on Section 7.3 for each control method (PFC - (7.27); DFC - (7.28); PBC - (7.30)).

Bifurcation diagram. The system dynamic is characterized by a bifurcation diagram (see, for example, Figure 8.1). The bifurcation diagram is composed by the asymptotic behaviour, on the Poincaré map, of one state variable (for example, $x_2(t_k)$) when one parameter of the system is changed in an interval of interest (for example, $0.982 \leq a \leq 0.989$) [68].

For non-autonomous systems, the Poincaré sections are hyperplanes crossed by the trajectory at a constant sampling time. This Poincaré map is also called stroboscopic map. Denoting as t_k the time of the k-th intersection of the Poincaré section by the trajectory, the discretized period of a periodic orbit x^* with period $T = t_{k+p} - t_k$ is $p \in \mathbb{N}$. Observe that for non-autonomous systems there is a fixed ratio between p and T something which is not valid for autonomous systems where there is a possibility of orbits with different T and the same p. Here, $T = t_{k+p} - t_k = p\frac{2\pi}{0.45}$.

Once constructed, the bifurcation diagram can be used for finding chaotic attractors and chaotic saddles (non attracting chaotic sets [43,48]), which are invariant sets composed by an infinite number of UPO's.

Figure 8.1 shows a bifurcation diagram of (8.1a) for $u \equiv 0$ depicting a periodic window (region for $0.9832 < a < 0.98765$). The black points represent attracting chaotic sets to the left and to the right of the window. They are obtained by plotting 200 Poincaré map points for each value of a after dropping the initial transient. The beginning of the periodic window is at a pair of saddle-node bifurcations (SNB) [1] at $a = 0.9832$, where two period-1 ($p = 1$) attractors are simultaneously created. Attractor $A1$ is represented by blue points and attractor $A2$ by green points. Both attractors undergo a period-doubling cascade that leads to chaos. At $a = 0.98765$ a global bifurcation occurs, the merging crises (MC) [1], where a single enlarged chaotic attractor is recovered (black points to the right of MC).

At the SNB, the original chaotic attractor loses stability and becomes the surrounding chaotic saddle (SCS), in light gray. The SCS is numerically obtained by the PIM triple method [66, 76]. At the MC the two chaotic attractors originated from $A1$ and $A2$ lose stability and become band chaotic saddles (BCS1 and BCS2). Many other SNB's are originated inside the periodic window (not represented here). After bifurcations, the

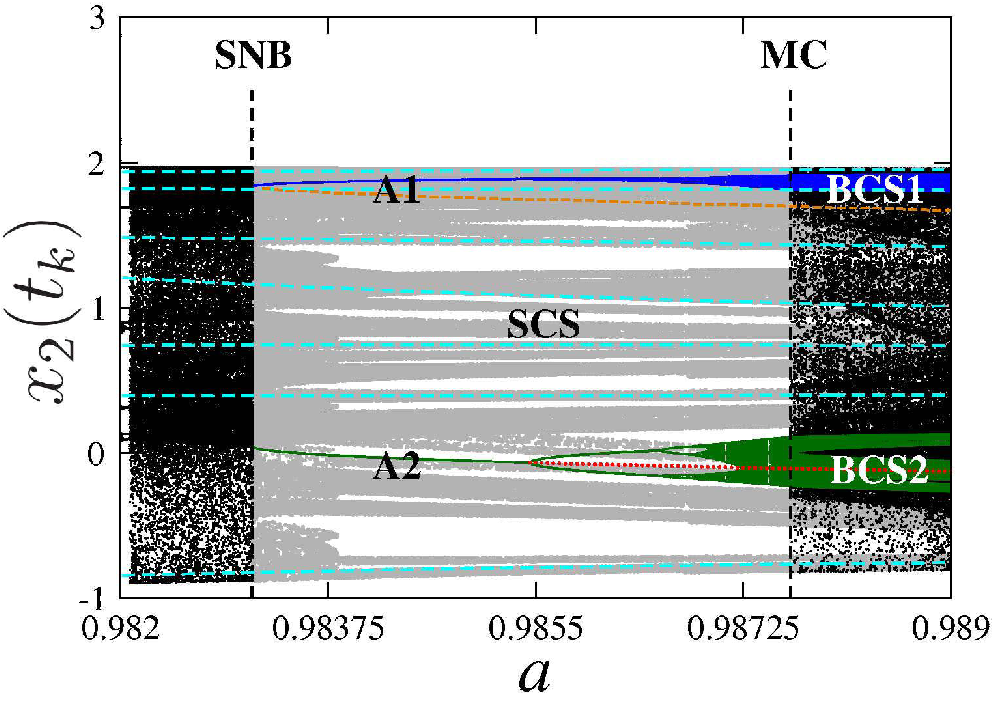

Figure 8.1: Bifurcation diagram of the vdP oscillator using the Poincaré map.

periodic attractors originated by the others SNB's become chaotic attractors and after the MC also become band chaotic saddles. The chaotic attractor (black), after the crises, is composed by the SCS and the BCS originated from the periodic window, specially the BCS1 and BCS2.

More details about the bifurcations diagram are exposed on [16, 17].

8.2.1 Finding the target UPO

The choice of the target UPO depends on performance criteria previously defined in a control project. Some of these criteria can be period, position in the state space, amplitude of oscillation and others. The focus of this work is the stabilization of an existing periodic orbit, specially those that compose a chaotic set. Then, a necessary step is finding a periodic orbit of the free system ($u \equiv 0$), among the existing ones, with desired characteristics. We are interested in orbits with short period and that exists (and are unstable) for the larger interval of a in the bifurcation diagram of Figure 8.1

The application of the DFC depends on the period of the target UPO. The project of the DFC and the PFC and the application of the PFC depend on the target UPO itself. Then, again, there is the necessity of finding UPO's and their periods.

The method used here to find UPOs is the Newton-Raphson method [68,76], a classical method used to find zeros of functions. In this work, the method is used on the Poincaré map to solve

$$\varphi(t_p, t_0, x(t_0), 0) - x(t_0) = 0, \qquad p \in \mathbb{N}, \quad t_p \in \mathbb{R}. \tag{8.2}$$

If condition (8.2) is satisfied then we have an orbit x^* with discrete-time period p and continuous-time period $T = t_p - t_0$.

The Newton-Raphson method is an iterative method, the idea is to adjust an initial guess of $x(t_0)$, close to x^*, until (8.2) is satisfied with some error ($\Delta_x(t_0)$) tolerance. That is, at each iteration the following steps are executed:

$$\begin{aligned} \Delta x(t_0) &= -(\Phi(t_p, t_0) - I)^{-1}(x(t_p) - x(t_0)), \\ x(t_0) &\leftarrow x(t_0) + \Delta x(t_0), \end{aligned}$$

where $\Phi(t_p, t_0)$ is the state transition matrix of the linearized system around $x(t_0)$ for $u \equiv 0$.

The method gives one point $x^*(t_0)$, the entire orbit is approximated by the solution of (8.1a) with $x(0) = x^*(t_0)$.

The UPOs of interest are represented in the Poincaré map in Figure 8.1 for the second state variable. In red dots we have a period-1 orbit (TUPO1) originated from a period-doubling bifurcation which has no real Floquet multiplier grater than +1. The orange dashed line represents a period-1 orbit (TUPO2) originated from a saddle-node bifurcation and with one real Floquet multiplier grater than +1. The light blue dashed line represents a period-7 orbit (TUPO3) with no real Floquet multiplier greater than +1. Among all the orbits that we found, the TUPO3 is the one with smallest period that exists in the entire bifurcation diagram.

Figure 8.2 presents the state space of the target periodic orbits embedded in the chaotic attractor in continuous-time (line) and Poincaré map ($*$) (left column) and their time

Table 8.1: Floquet multipliers and one Poincaré map point for $a = 0.988$ of the three target periodic orbits of the vdP oscillator.

	TUPO1	TUPO2	TUPO3
μ	[-1.872, -0.048]	[4.627, 0.147]	[-25.446, -9×10^{-16}]
$x^*(t_0)$	[0.1588445, -0.1106056]	[0.0771541, 1.6893651]	[0.0439776, 1.8139795]

series (right column) for $a = 0.988$ for the TUPO1, TUPO2 and TUPO3, respectively. The values of the Floquet multipliers computed for this value of a and one point of the orbit (at the Poincaré map) are in Table 8.1.

8.3 Tuning the DFC gain by optimization and comparison with the PFC

In this section, an optimization routine is used for tuning the DFC gain applied to the forced vdP oscillator and the results are compared with the ones obtained using the PFC according to [14]. The control signal $u(t, x(t))$ in (8.1a) is defined as (7.27) for the PFC

$$u(t, x(t)) = K(x^*(t) - x(t)),$$

and (7.28) for the DFC

$$u(t, x(t)) = K(x(t - T) - x(t)).$$

In both cases we use a constant control gain K. The monodromy matrices are computed following the methods shown in Section 7.4 and the Floquet multipliers and exponents are obtained from this matrix (see Section 7.1 and Appendix B).

The optimization is applied to find a control gain K that minimizes the largest, in modulus, Floquet multiplier $|\mu|_{max}$ of the target UPO. The value of $|\mu|_{max}$ is obtained through the solution of the non-linear system (8.1a) and is considered as a scalar cost function. A simplex algorithm [55] is used to solve this optimization problem through the *fminsearch* routine of the Matlab®. A similar optimization process was applied to the PFC in [4].

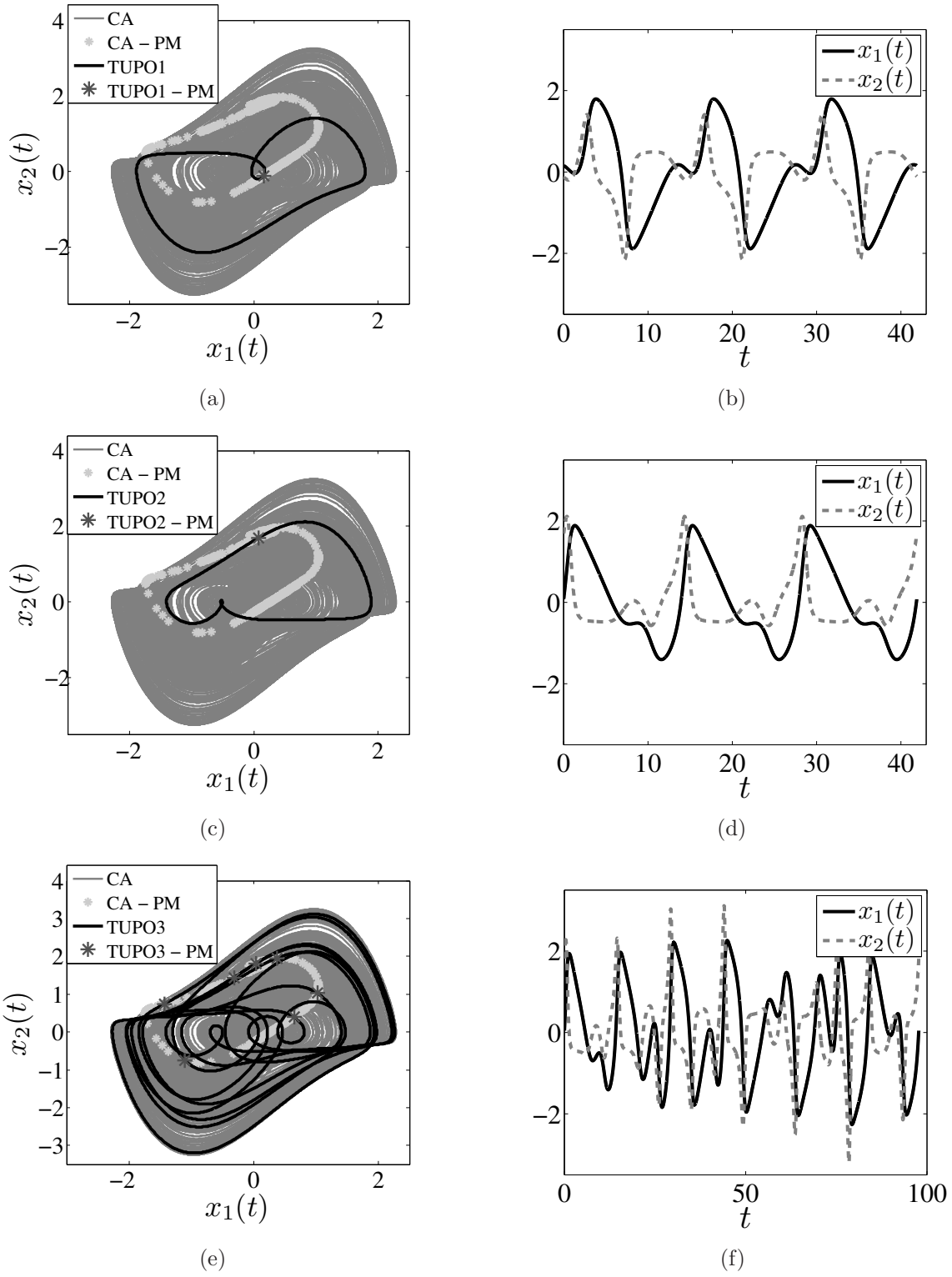

Figure 8.2: Target UPOs (TUPO) 1, 2 and 3 embedded in the chaotic attractor (CA) in the state space (left column) and time series (right column). The time series of TUPOs 1 and 2 are shown for three cycles. The points of the target UPOs and the chaotic attractor in the Poincaré map (PM) are represented by $*$.

Finding a K that minimizes $|\mu|_{max}$ is equivalent to finding a K that makes the orbit more stable (for $|\mu|_{max} < 1$) with faster convergence or less unstable (for $|\mu|_{max} > 1$). Thus, the optimization criterion and the choice of the control gain are related to the stability of the target periodic orbit. Two more parameters are used for the comparison between the DFC and the PFC. The steady state error d is the distance (Euclidean norm) between a reference signal $r(t)$ (which is $x^*(t)$ for the PFC and $x(t-T)$ for the DFC) and $x(t)$ (the current state) for an entire cycle in the close vicinity of the target UPO,

$$d = \lim_{t \to +\infty} \int_t^{t+T} \|r(\tau) - x(\tau)\|_2 d\tau. \tag{8.3}$$

The steady state control effort υ is the measure of the total external effort (norm-1) necessary to keep the trajectory on the close vicinity around one cycle of the target periodic orbit,

$$\upsilon = \lim_{t \to +\infty} \int_t^{t+T} \|u(\tau)\|_1 d\tau. \tag{8.4}$$

Both d and υ are defined for ideally infinity t over one period of the target orbit. For numerical analysis a convergence criterion is applied to obtain a limited and large enough time t. It is defined as the relative difference between d at the current cycle and at the $M \in \mathbb{N}$ past cycles,

$$\left| 1 - \frac{\int_{t-MT}^{t-T} \|r(\tau) - x(\tau)\|_2 d\tau}{M \int_{t-T}^{t} \|r(\tau) - x(\tau)\|_2 d\tau} \right| < \epsilon \tag{8.5}$$

where $\epsilon > 0$ is chosen according to the desired precision.

The values of d and υ are zero for a stabilized orbit using DFC, it will be shown that they are not necessarily zero for orbits stabilized with the PFC and aPBC.

8.3.1 Approximating the monodromy matrix for the DFC

For the DFC method, it is necessary to define the number of samples or delayed states N, which is also the number of collocation points used to approximate the monodromy matrix (see Section 7.4.2). An increase in the number of collocation points results in greater accuracy at the expense of computational time.

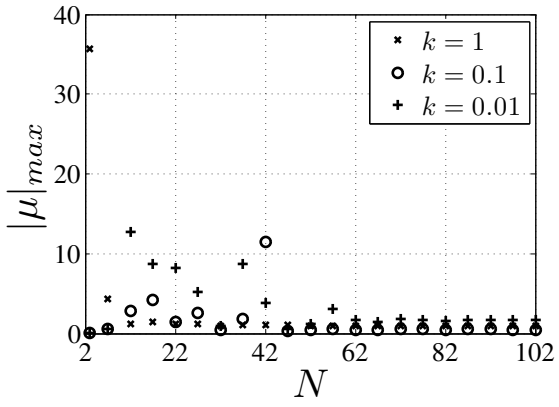

Figure 8.3: Relation between the number of collocation points N and the largest magnitude Floquet multiplier $|\mu|_{max}$ of the TUPO1 stabilized with the DFC and a scalar control gain for $a = 0.988$.

Figure 8.3 plots $|\mu|_{max} \times N$ for $a = 0.988$ and three different values of control gain k for the DFC applied to the TUPO1. N is the number of discretization points and k is a constant scalar using the control gain K, in (7.28) and (7.53c), as[1]

$$K = \begin{bmatrix} k & 0 \\ 0 & 0 \end{bmatrix}, \qquad k \in \mathbb{R}. \tag{8.6}$$

Notice that $u : \mathbb{R}^+ \times \mathbb{R}^2 \to \mathbb{R}^2$ and the control signal may be applied directly to the derivative of each state variable. However, in general, only the first component of the control signal vector is different from zero in this section and the system is not fully actuated.

Observing Figure 8.3 one can notice a considerable reduction on the variation of $|\mu|_{max}$ when increasing N for $N > 82$. We adopt $N = 102$ in the following results on the DFC.

8.3.2 Stabilizing the TUPO1

The first orbit to be stabilized is the TUPO1 for $a = 0.988$ (see Figures 8.2(a) and 8.2(b)) with Floquet multipliers for $u \equiv 0$ shown in Table 8.1. UPOs with short periods are less

[1]The control structure proposed with such choice of gain K amounts to applying the control signal to the derivative of the first state variable. Considering a mechanical system (oscillator), this means applying the external input to velocity instead of acceleration. This point is critical for practical applications, here we compare numerically control methods and the controlled state variable is less relevant.

unstable [20, 29] and, in general, easier to stabilize with the DFC. Another characteristic that favours the stabilization of the TUPO1 with the DFC is that there is not real Floquet multipliers grater than +1. See Section 7.3.2 for a review on the limitations of the DFC. The PFC does not have these limitations.

Before comparing the PFC and the DFC methods, a good approximation for the target UPO is needed, since it leads to more precise results for the PFC ($r(t)$ closer to $x^*(t)$ in (8.3) and (8.4)). We adopt the following procedure:

- A Poincaré point of the orbit is obtained for the free system ($u \equiv 0$) with the Newton-Raphson method. This point is shown in Table 8.1;
- The ODE is integrated from this point during one period to obtain an initial approximation of the whole orbit;
- This first approximation is used to compute the monodromy matrix for the DFC. At this stage it is necessary to search for a control gain k which makes $|\mu|_{max} < 1$;
- With such k, the DFC method is used to control the TUPO1 until the convergence criterion (8.5) be satisfied for $\epsilon = 10^{-10}$. This last step is used to obtain a better approximation of the whole orbit and not just one Poincaré point.

In what follows, the resulting orbit will be denoted by $x^*(t)$ and used in the DFC/PFC optimization processes.

Alternatively, one may obtain a good approximation of $x^*(t)$ by directly applying the DFC while searching for the proper $x(0)$ and k values. But that would require the simultaneous search of $x(0)$ and k and the integration of the trajectory using a DDE integrator. This simultaneous search is much slower than using the suggested procedure. In practical situations where the model equations might not be known, it may be necessary to first use a standard method to estimate the UPO from a time series (e.g., [83]), then apply the DFC to obtain the desired convergence.

Figure 8.4 illustrates the method for finding the scalar control gain k. The magnitude of the Floquet multipliers of the TUPO1 are plotted against k for the DFC (solid lines) and PFC (dashed lines) methods. For the DFC, only the six Floquet multipliers with largest

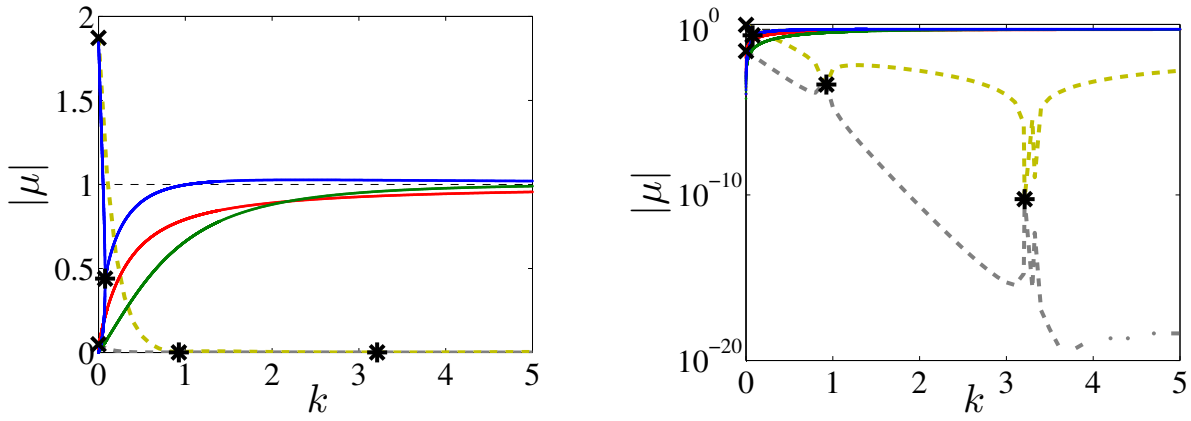

(a) (b)

Figure 8.4: (a) Magnitude of the Floquet multipliers of the TUPO1 at $a = 0.988$ using DFC (solid lines) and PFC (dashed lines). The Floquet multipliers of the orbit for $u \equiv 0$ are represented by $\times$ and the local minima for the stabilized orbit by $*$. (b) is the same as (a) in log-linear scale.

magnitude are plotted. There are two real and four complex conjugate multipliers for $k \lesssim 0.076$, while there are three complex conjugate multipliers for $k \gtrsim 0.076$. Therefore, only three solid lines are visible in the plot of $|\mu|$ in Figure 8.4(a) for most values of k. For the PFC method, there are only two real multipliers. Figure 8.4(b) is the same as Figure 8.4(a), but in log-linear scale.

The stars $(*)$ in Figure 8.4 refer to the values of k found by an optimization process. After plotting $|\mu|$ for several values of k by a scanning process, the optimization method is applied by using as initial conditions the approximated values of k where the local minima of $|\mu|_{max}$ are found. The optimization results are summarized in Table 8.2. From Figure 8.4 and Table 8.2 we observe that the PFC leads to smaller values of $|\mu|_{max}$, even when a diagonal matrix gain K is applied for the DFC with the values obtained by optimization. The diagonal K obtained is a local minimum, no global minimum study has been achieved in this case. This shows that if more elements of matrix (8.6) are not set equal to zero, better results can be obtained for the DFC while the $|\mu|_{max} \approx 0.6 \times 10^{-10}$ shows that a scalar gain leads to very small (close to zero) Floquet multipliers for the PFC in this case.

The crosses $(\times)$ in Figure 8.4 are the values of $|\mu|$ of the TUPO1 for the free system. The UPO is stabilized when $|\mu|_{max} < 1$, which occurs for $0.053 \lesssim k \lesssim 1.031$ for the DFC

Table 8.2: Summary of the optimal results on $|\mu|_{max}$ according to the gain matrix K and the control method for TUPO1.

	DFC		PFC	
K	$\begin{bmatrix} 0.07632510479 & 0 \\ 0 & 0 \end{bmatrix}$	$\begin{bmatrix} -0.003168 & 0 \\ 0 & 0.0674015 \end{bmatrix}$	$\begin{bmatrix} 0.92619140625 & 0 \\ 0 & 0 \end{bmatrix}$	$\begin{bmatrix} 3.2105712890625 & 0 \\ 0 & 0 \end{bmatrix}$
$\|\mu\|_{max}$	0.4395116372	0.1565149475	0.4666610×10^{-3}	0.6×10^{-10}

and for $k \gtrsim 0.1$ for the PFC. For the DFC, it can be shown that the values of $|\mu|$ tend to one when $k \to +\infty$.

Figure 8.4 shows that the range of k for controlling the TUPO1 is larger for the PFC than for the DFC. The DFC method has a slight advantage since $u(t, x(t)) \to 0$ for a stabilized orbit even if the orbit is not completely known (only its period) but a stabilizing gain k is found. Notwithstanding, the orbit stabilized with the PFC is more stable, since smaller values of $|\mu|_{max}$ are found.

The results of stabilization of the TUPO1 for $a = 0.988$ are shown in Figure 8.5(a) for the DFC with the optimal value $k = 0.07632510479$, Figure 8.5(b) for the PFC with the optimal value $k = 0.92619140625$ and Figure 8.5(c) for the PFC with the optimal value $k = 3.2105712890625$. The initial condition is set on $x(0) = [-0.5;\ 0.5]$ (for the DFC, all the delayed states are on x^*), the perturbations decay after an initial transient and the system converges to the periodic regime corresponding to the TUPO1. Figure 8.6 shows the time series of the norm-1 of the control signal $u(t, x(t))$ in a log-linear scale. The initial transients are shorter for PFC than DFC due to $|\mu|_{max}$, but the PFC presents an initial peak on $\|u(t, x(t))\|_1$ that represents a short-time high external effort.

The real (Re) and imaginary (Im) parts of the Floquet multipliers (μ) and exponents (λ) for the DFC can be seen in the root locus chart in Figure 8.7. The crosses ($\times$) are μ (Figure 8.7(a)) and λ (Figure 8.7(b)) for $k = 0$ and the stars ($*$) are the optimal values (minimum of $|\mu|_{max}$ or $\mathrm{Re}(\lambda)_{max}$). The evolution of the six Floquet multipliers and exponents with largest magnitude are represented by the six branches, where the arrows show the flow for increasing k. The dashed circle in Figure 8.7(a) is the unity circle. It is clear that $\mu \to +1$ and $\lambda \to 0$ as $k \to +\infty$.

The relation between the steady state error (d) and k is presented in Figure 8.8(a), This Figure is computed by integrating an initial condition very close to $x^*(t)$ while applying

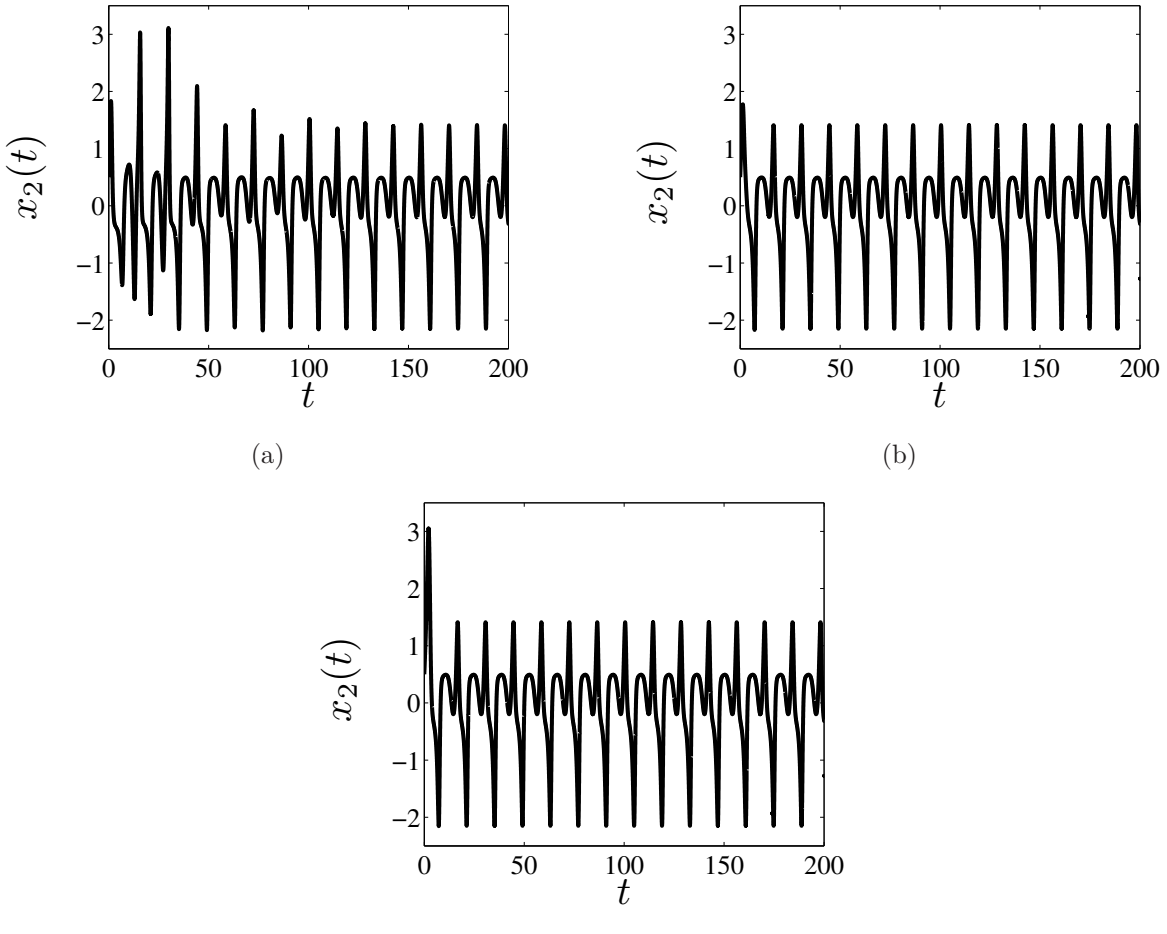

(a)

(b)

(c)

Figure 8.5: Time series of $x_2(t)$ showing the stabilization of the TUPO1 of the vdP system for $a = 0.988$ using (a) DFC with $k = 0.07632510479$; (b) PFC with $k = 0.92619140625$ and (c) PFC with $k = 3.2105712890625$.

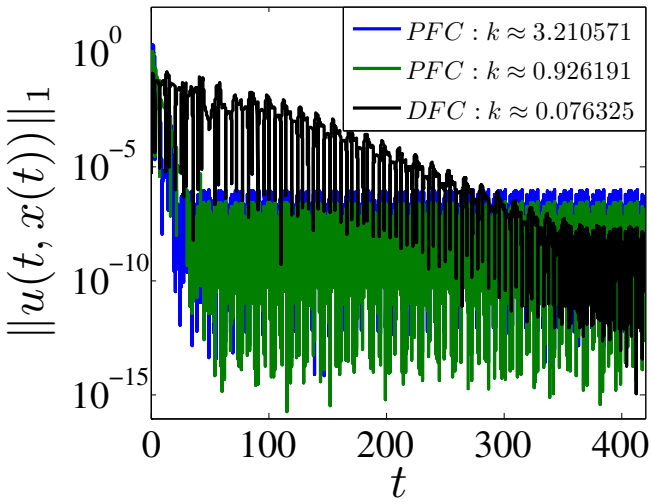

Figure 8.6: Time series of $\|u(t, x(t))\|_1$ of the TUPO1 of the vdP system for $a = 0.988$ using DFC with $k = 0.07632510479$ (black line), PFC with $k = 0.92619140625$ (green line) and PFC with $k = 3.2105712890625$ (blue line).

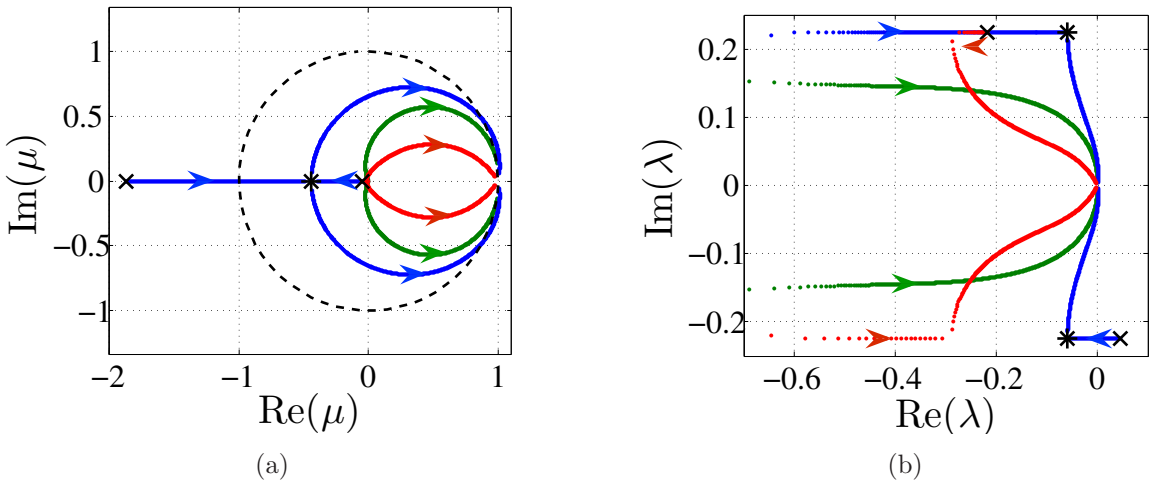

(a) (b)

Figure 8.7: Root locus chart of the TUPO1 controlled by DFC. (a) Floquet multipliers (μ), (b) Floquet exponents (λ).

the DFC/PFC control methods with a relative and absolute integration tolerances equal to 10^{-10}. After convergence of d is reached, we compute one more cycle and plot the final value of d. Note that for the PFC (dashed line) the steady state error is low for all $k \gtrsim 0.1$, as expected from Figure 8.4, which shows that $|\mu|_{max} < 1$ in this region. As for the DFC (solid line), the steady state error is low for $0.053 \lesssim k \lesssim 1$. This is close to the point where $|\mu|_{max}$ becomes greater than one in Figure 8.4. If $|\mu|_{max} \approx 1$, the target UPO is marginally stable/unstable and perturbed trajectories take long time to converge to (or diverge from) it. This is the case of the DFC for $k \gtrsim 1$, where $|\mu|_{max} \gtrsim 1$ according to Figure 8.4(a). Therefore, in Figure 8.8(a), d is not plotted for $k > 1.5$ for the DFC method, since the divergence time is very long. Figure 8.8(b) is the same as Figure 8.8(a), but for the control effort υ.

Notice from Figure 8.8 that when the orbit is stabilized with the DFC, both the steady state error and control effort tend to zero when $t \to +\infty$ (they are close to the integration tolerances). The same is not valid for the PFC where, even with a good approximation of $x^*(t)$ we observe an increase on d and υ when increasing k. Figure 8.9 is used to explain this fact for the PFC. We observe in Figure 8.9(a) that for $k = 0.92619140625$ the stabilized trajectory is very close to the TUPO1 while it becomes more distant when using $k = 3.2105712890625$, Figure 8.9(c). The steady state control signal $k = 0.92619140625$ in Figure 8.9(b) is much smaller than for $k = 3.2105712890625$, Figure 8.9(d). These figures contribute to illustrate the increase of d and υ. For the PFC with large (scalar) control gain we observe that the control signal does not change the stability of x^*, a new stable orbit is created in its vicinity. Similar results were obtained in [4].

The observation of Figures 8.4 and 8.8 shows that the method presented in Section 7.4.2 to compute the monodromy matrix for the DFC is adequate. Given a value of the control gain k, instability/stability are coherent in both figures.

One of the main advantages of a chaos control technique is the small control effort required [67, 70], and in that sense the DFC method provides slightly better results since the control effort always tends to zero as $t \to +\infty$ for a stabilizing k. Since the PFC method requires knowledge of the target UPO position, errors in its estimation always lead to finite d and υ. The errors tend to be larger for longer period UPOs.

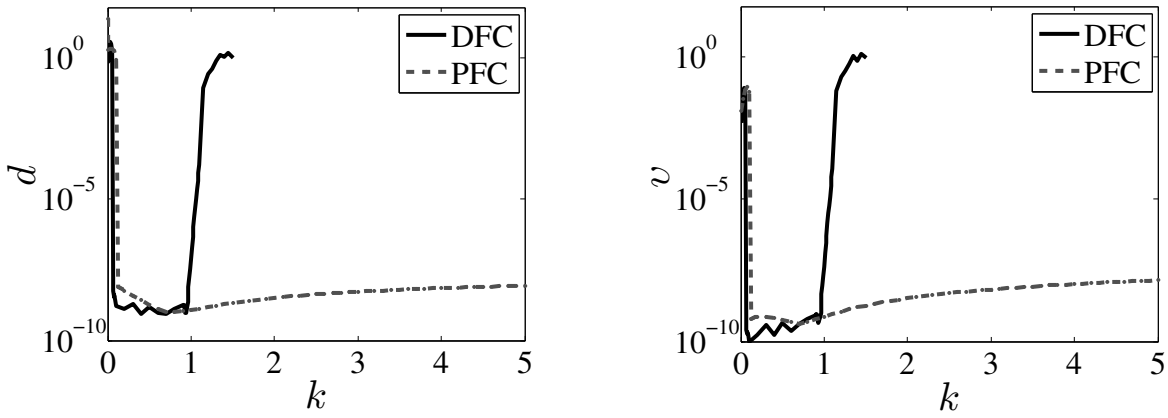

(a) (b)

Figure 8.8: (a) Steady state error d as a function of k for the DFC (solid line) and PFC (dashed line) methods applied to the vdP oscillator with $a = 0.988$; (b) same as (a), but for the control effort v. for DFC and PFC controlling the TUPO1.

A brief robustness analysis of DFC and PFC

In the previous sections, the driver amplitude was set to $a = 0.988$, where the UPO was found and the control methods applied. In the present section, the TUPO1 is found for $a = 0.988$, but the controllers are applied for $a \in \begin{bmatrix} 0.9855 & 0.994 \end{bmatrix}$.

Figures 8.10(a) and 8.10(c) show d and v for the DFC when a is changed. As observed, while the orbit is stabilized, both quantities remain close to the integrator's error tolerance. The values of the six largest magnitude Floquet multipliers $|\mu|$ of the orbit stabilized by the DFC are presented in Figure 8.10(e). These results are obtained by integrating the initial condition until convergence of d is observed. After that, the last T time units of the simulation are used to compute de monodromy matrix and the Floquet multipliers. In all cases, the optimal value $k \approx 0.076325$ is used. Note that the DFC adapts well to parameter changes because the reference $r(t) = x(t - T)$ does not depend upon a system model, it consists of only recorded state values. This characteristic reduces the controller's stability, but increases its robustness to parametric uncertainties.

For the PFC, we test the two values of k where the local minima of $|\mu|_{max}$ are found in Figure 8.4, i. e., $k = 0.92619140625$ and $k = 3.2105712890625$. Figures 8.10(b) and 8.10(d) show the steady state error and the control effort as a function of a. The sudden change in d and v around $a = 0.988$ is due to the proximity of $r(t)$, in (8.3), to the target

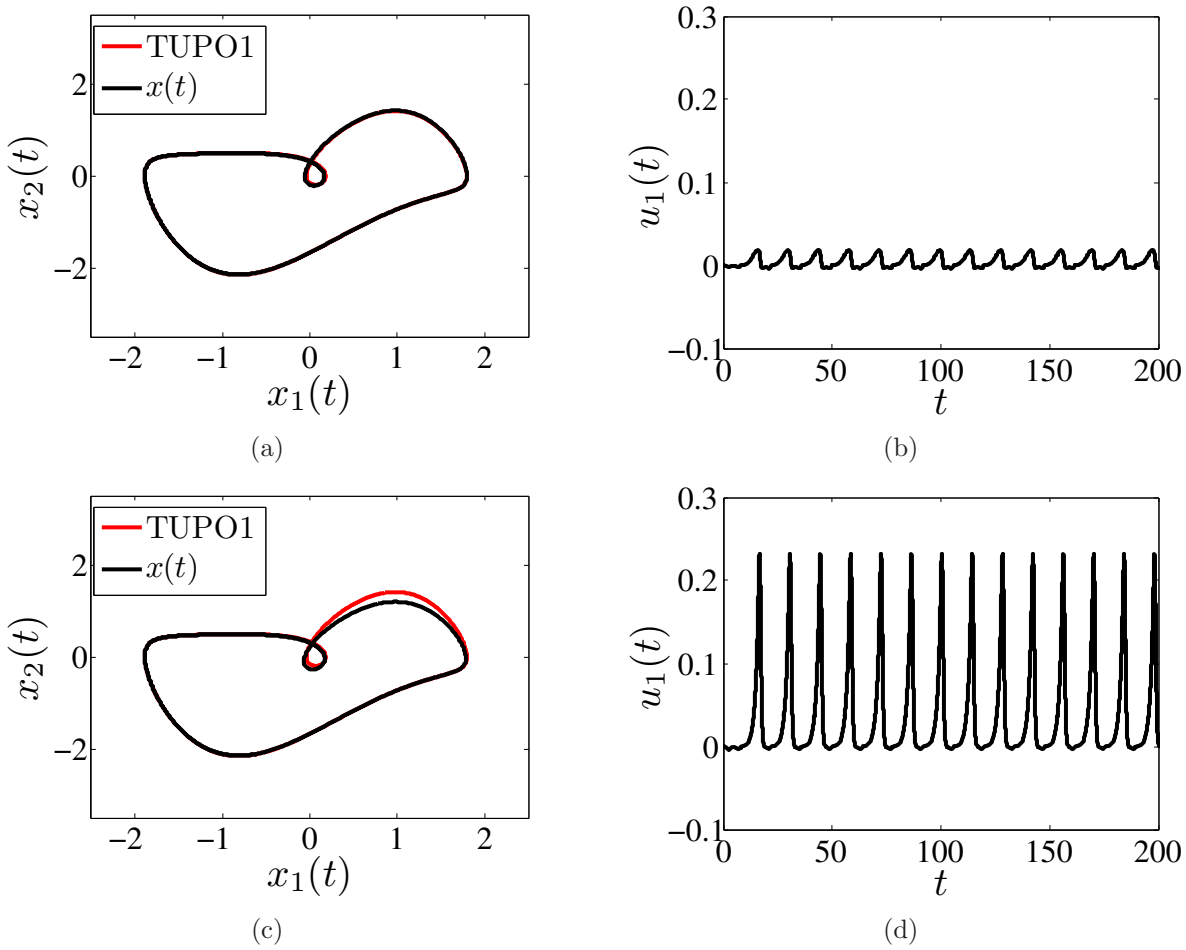

Figure 8.9: TUPO1 stabilized with the PFC. (a) State space trajectory and (b) control signal for $k = 0.92619140625$. (c) State space trajectory and (d) control signal for $k = 3.2105712890625$.

UPO $x^*(t)$. Since in the PFC method $r(t)$ does not self–adapt to changes in the system parameter, the steady state error and control effort are much higher for $a \neq 0.988$. Figure 8.10(f) reveals that $|\mu|_{max}$ is very sensitive to variations in a for $k = 3.2105712890625$, whereas $|\mu|_{max}$ is kept almost constant for $k = 0.92619140625$. Overall, the orbit stabilized with $k = 3.2105712890625$ is more stable, except for large values of a.

As shown in Figure 8.10, even with perturbations in a, the TUPO1 is more stable when controlled with the PFC than the DFC. However, the DFC has a much lower steady state error and control effort for $a \neq 0.988$.

8.3.3 Controlling the TUPO2 and TUPO3

The limitations of the DFC were discussed in Section 7.3.2. Here the orbits TUPO2 and TUPO3 are used to exemplify situations where a constant control gain K for the DFC that stabilizes the target UPO was not found. As shown in Section 8.2.1, the TUPO2 has one real Floquet multiplier grater than +1 and the TUPO3 has a discrete period equal to 7 (long period).

Stabilizing the TUPO2. The Floquet multipliers of the TUPO2 for $u \equiv 0$ and one point of the orbit on the Poincaré map are shown in Table 8.1. This orbit is not stabilized using the DFC with a scalar gain according to the root locus chart of Figure 8.11. Notice that it was shown in the previous example (TUPO1, Figure 8.7(a)) that all the Floquet multipliers of the orbit tend to +1 when increasing the DFC scalar gain k. The same occurs for the TUPO2 as shown in Figure 8.11. The real Floquet multiplier greater than +1 goes straight to +1 through the real axis when increasing k. The corresponding branch of the root locus does not enter the unit circle.

A matrix gain was tried with values obtained by the previous optimization process using the Matlab® routines *fminsearch* and *fmincon* [31,37,58,69]. A scan process varying all the values of the matrix gain was also tried. The final try was using a matrix gain composed by a rotational matrix (composed by sines and cosines) multiplied by a real scalar gain equivalent to the gain used in [26, 27, 46]. After varying both the rotation angle and the gain, a matrix control gain that stabilizes the TUPO2 was not found.

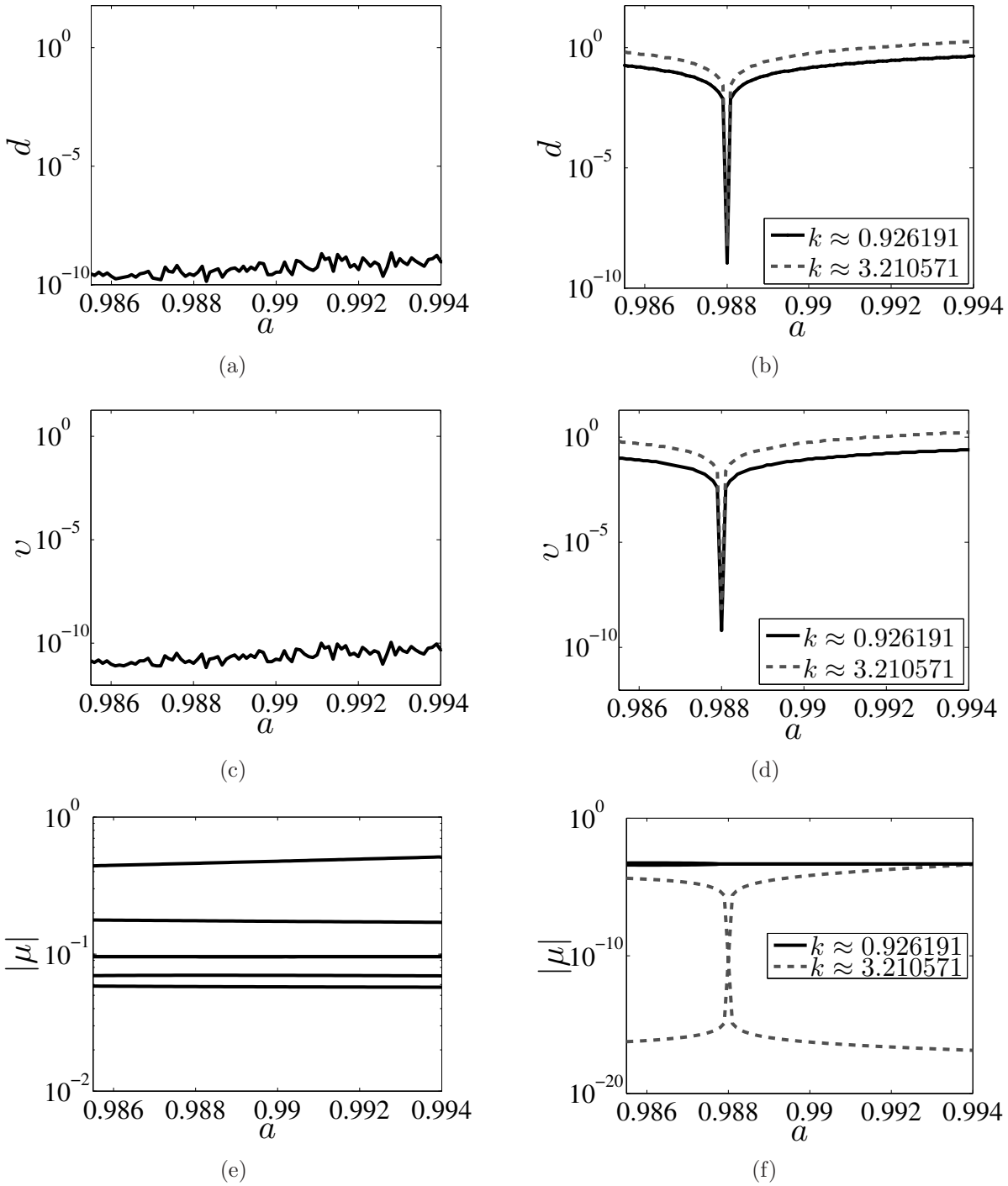

Figure 8.10: The steady state error (a), control effort (c) and magnitude of Floquet multipliers (e) as a function of a for the DFC with $k = 0.07632510479$ stabilizing the TUPO1. The steady state error (b), control effort (d) and magnitude of Floquet multipliers (f) as a function of a for the PFC stabilizing the TUPO1.

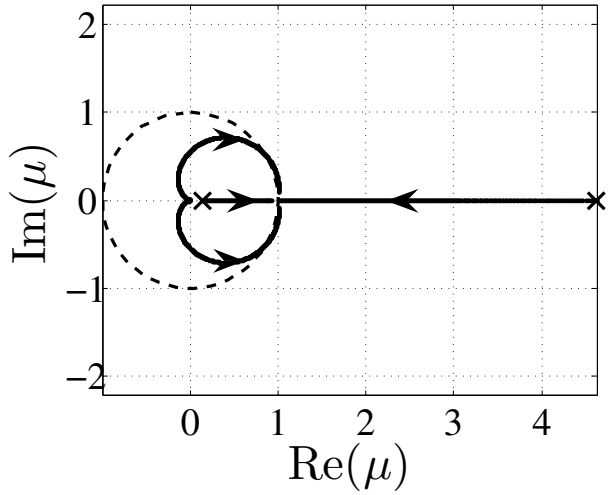

Figure 8.11: Root locus chart of the four largest magnitude Floquet multipliers of the TUPO2 using the DFC. The Floquet multipliers of the free system orbit are represented by (×).

The same orbit is stabilized using the PFC and the modulus of the Floquet multipliers are shown in Figure 8.12 for an interval of k. The orbit used to compute the monodromy matrix was obtained integrating the Poincaré map point for one cycle of the free system once the DFC can not be used to refine its approximation.

Stabilizing the TUPO3. The Floquet multipliers of the TUPO3 for $u \equiv 0$ and one point of the orbit on the Poincaré map are shown in Table 8.1. The root locus chart of the two largest, in modulus, Floquet multipliers of this orbit controlled by a scalar gain with DFC is shown in Figure 8.13. Observe that the branches of the root locus never enter the unity circle, independently of the gain value. A matrix gain that stabilizes the TUPO3 was not found using the optimization proposed. The *fmincon* Matlab® routine was also tried resulting in an unstable orbit.

Comparing the absolute value of the Floquet multiplier in Table 8.1, the TUPO7 is over ten times more unstable then the TUPO1. This does not prove that the orbit is uncontrollable with the DFC, but the result is in agreement with the literature. A possible method that can be used to stabilize this orbit using delayed states is the Extended DFC shown in Section 7.3.2.

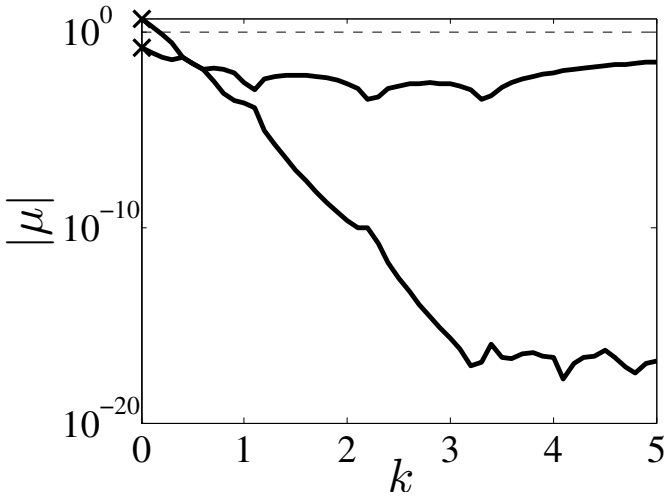

Figure 8.12: Modulus of the Floquet multipliers of the TUPO2 using the PFC. The Floquet multipliers of the free system orbit are represented by (×).

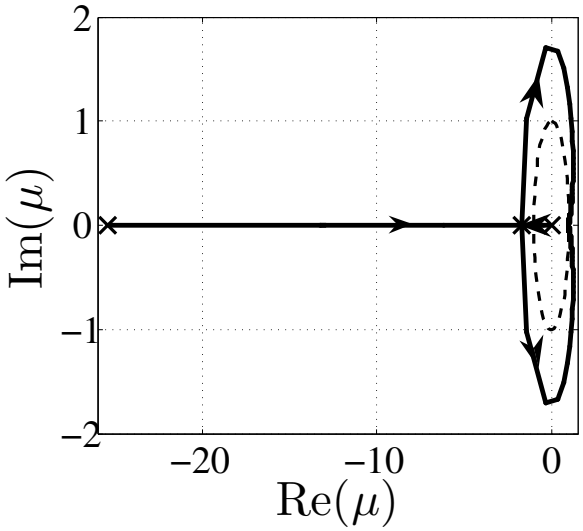

Figure 8.13: Root locus chart of the two largest, in modulus, Floquet multipliers of the TUPO3 controlled by the DFC. The Floquet multipliers of the orbit without control are represented by (×) and a local minimum is represented by (∗).

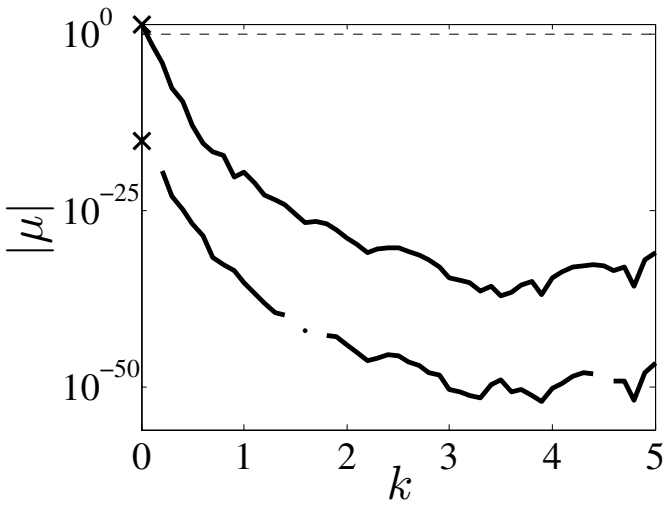

Figure 8.14: Modulus of the Floquet multipliers of the TUPO3 controlled using the PFC. The Floquet multipliers of the orbit without control are represented by (×).

When computing the monodromy matrix of the TUPO3 controlled by the DFC we used the same $N = 102$ collocation points s to discretize *each cycle* of the forcing term ($\frac{2\pi}{0.45}$). The monodromy matrix of the complete $p = 7$ orbit was computed using pN collocation points.

The same orbit is stabilized using the PFC resulting in very small, in modulus, Floquet multipliers. The results on the relation between the modulus of the Floquet multipliers and the control gain are presented in Figure 8.14.

The results of this section exemplify orbits that could no be stabilized by the DFC with a real constant gain. The two situations show characteristic limitations of the DFC that do not affect the performance of the PFC. The only observation on the results using the PFC is that the Floquet multipliers of the TUPO3, the more unstable orbit studied, were changed to very small values and the stabilized orbit became the more stable one.

8.4 Numerical results on the aPBC applied to a non-autonomous system

In this section we provide numerical results on the approximated prediction-based control (aPBC) (see Section 7.3.3) applied to the van der Pol oscillator (8.1b) using the control scheme (8.1a).

The control signal $u(t, x(t))$ for the PBC is defined in (7.30) as

$$u(t, x(t)) = K(t, x(t)) \left(\varphi(t + T, t, x(t), 0) - x(t)\right).$$

The state transition map $\varphi(t + Ts_j, t, x(t), 0)$ is approximated by an implicit Runge-Kutta method using the operator $\mathbf{z}(t+Ts_j, t, x(t))$ in the s_j, $j = 1, 2, \ldots, N$ discretization points. The implicit Runge-Kutta method is solved using the estimator (7.36) resulting in the aPBC (7.40) (see Section 7.3.3 for details).

Here, we apply the aPBC using the orthogonal collocation method (see Section 7.3.3), obtaining $\mathbf{z}(t+Ts_j, t, x(t)) = m_j(t)$, and the estimator (7.36) that leads to $m_j(t) \approx \hat{m}_j(t)$. The control signal of the closed-loop control method (7.40) applied to the system (8.1b) is

$$u(t, x(t)) = K\left(\hat{m}_N(t) - x(t)\right) \tag{8.7}$$

with the constant control gain

$$K = \begin{bmatrix} k & 0 \\ 0 & 0 \end{bmatrix}, \qquad k \in \mathbb{R}. \tag{8.8}$$

As done in Section 8.3, $u : \mathbb{R}^+ \times \mathbb{R}^2 \to \mathbb{R}^2$ is defined with the same dimension of the free system, but only the first component of the control signal vector is different from zero and the system is not fully actuated.

The control signal is designed by approximating the feedback term, leading to the closed-loop system (7.40). The solution of the latter depends on the choice of three parameters: the control gain k, the observer gain k_o and the number of discretization

points for the orthogonal collocation method N. The values k_o and N are directly related to the estimation quality and these two parameters will be tuned first.

8.4.1 Tuning the parameters k_o and N

To evaluate the future state estimation, whose characteristics are related to the parameters k_o and N, we first set $k = 0$. We used as the initial condition $x(0) = [-0.75,\ 0.75]'$. The system is integrated for $t \in [0, T]$ and the points $\hat{m}_N(t + jT/999)$, $j = 0, \ldots, 999$, are collected for different values of k_o and N. One then assesses the convergence by comparison with the solution obtained with $N = 152$ and $k_o = 50$, by computing (8.9),

$$\varepsilon(N, k_o) = \frac{\|\hat{m}_{N,2}^{(152,50)}(\cdot) - \hat{m}_{N,2}^{(N,k_o)}(\cdot)\|_{L^1(0,T)}}{\|\hat{m}_{N,2}^{(152,50)}(\cdot)\|_{L^1(0,T)}}. \tag{8.9}$$

The superscript on $\hat{m}_{N,2}^{(N,k_o)}(t)$ indicates the value of N and k_o used in the estimation and the number 2 in subscript refers to the second value of the 2-dimensional vector $\hat{m}_N(t)$, the one used in the control signal (8.7) due to the control gain (8.8).

Figure 8.15(a) shows $\varepsilon(N, 50)$ for different values of N. Note that the collocation parameters s_i and ω_j are previously computed for each N tested. The computation of ω_j for large N requires intense off-line computational burden and reduces the number of values N tested. These values are computed once for all and are independent of $f(t, x(t))$. The values of $N < 72$ lead to integration instability and are not computed, this instability is exemplified in Figure 8.31 when analysing the effect of small N on stabilization.

Repeating the same process, we evaluate $\varepsilon(152, k_o)$ for different values of k_o, see Figure 8.15(b). Increasing N and k_o results in larger computation effort and trade-off between estimation quality and computation effort should be considered.

Due to the error level shown in Figure 8.15 for $N = 102$ and $k_o = 10$, we adopt these values in the sequel. In Figure 8.16 it is shown $x_2(t)$ and $\hat{m}_{N,2}(t-T)$ (beware the time shift here). In this case it is expected that $x(t) = \varphi(t, t-T, x(t-T), 0) \approx \mathbf{z}(t, t-T, x(t-T)) \approx \hat{m}_N^{(102,50)}(t - T)$ and the proximity of both time-series in Figure 8.16 allows to use $m_j(t)$ instead of $\hat{m}_j^{(102,50)}(t)$.

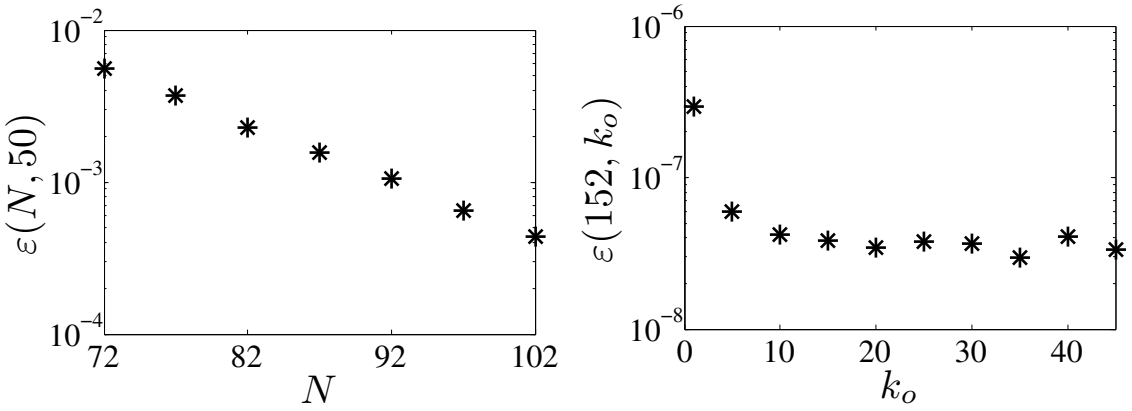

(a) (b)

Figure 8.15: Relative error of the estimated free system response future value using different (a) N and (b) k_o.

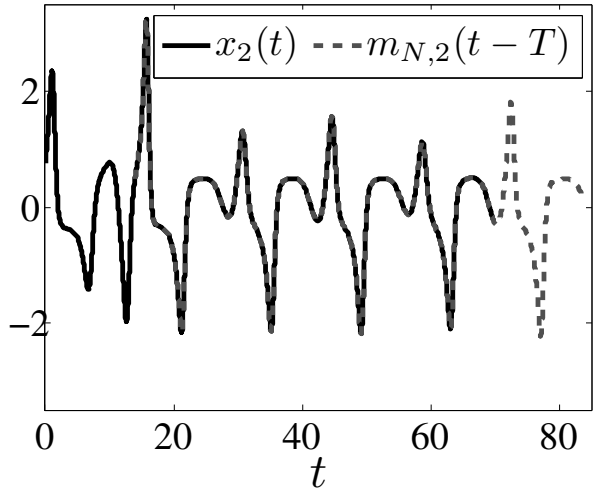

Figure 8.16: Current time and shifted future time trajectory of the system for $k = 0$, $k_o = 10$ and $N = 102$.

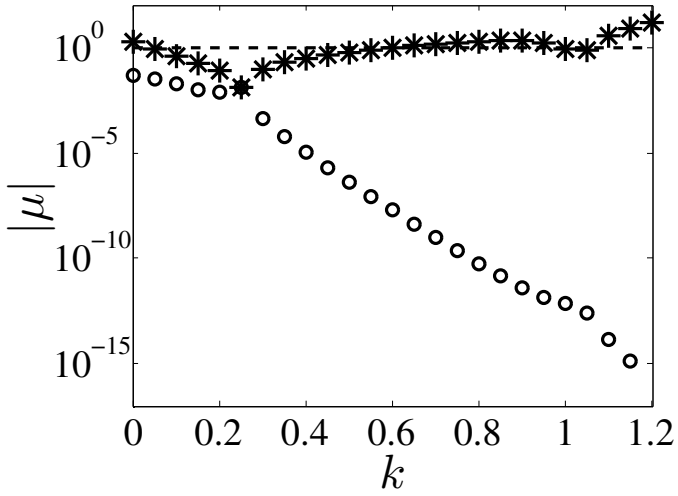

Figure 8.17: Modulus of the Floquet multipliers for different values of k for the TUPO1 controlled by the aPBC.

8.4.2 Stabilizing TUPO1

Once obtained the values of N and k_o we now stabilize the TUPO1. The control gain k is tuned to stabilize the orbit and the results are compared with the one obtained for the DFC.

Tuning of k

Now we tune the feedback gain k. We use (7.60), with $x^*(0) = [0.15884454118,\ 0.110605560432]'$, to obtain a value k that stabilizes the orbit of (7.31). Note that, the estimation with $N = 102$ and $k_o = 10$ being precise, we expect that a stabilizing k for (7.31) will yield stability for a slightly perturbed cycle of (8.1a) with the control signal (8.7).

Figure 8.17 shows the modulus of the two Floquet multipliers $|\mu|$ for different values of k. The stability is achieved when $|\mu| \leq 1$. We choose $k = 0.25$, which results in $|\mu| \approx 0.01213$. All the Floquet multipliers in this case are real numbers.

Comparison with the Delayed Feedback Control

A stabilized trajectory (TUPO1) for $k = 0.25$, $k_o = 10$, $N = 102$ and $x(0) = [-1.5,\ 1.0]'$ is shown in the state space in Figure 8.18. The time series of the controlled orbit is shown in Figure 8.19(a) and 8.19(b) for the first and second state variables, respectively.

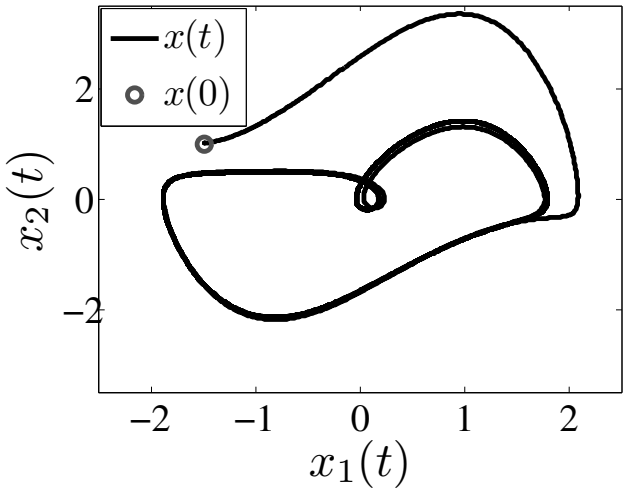

Figure 8.18: Stabilized TUPO1 in the state space for $k = 0.25$.

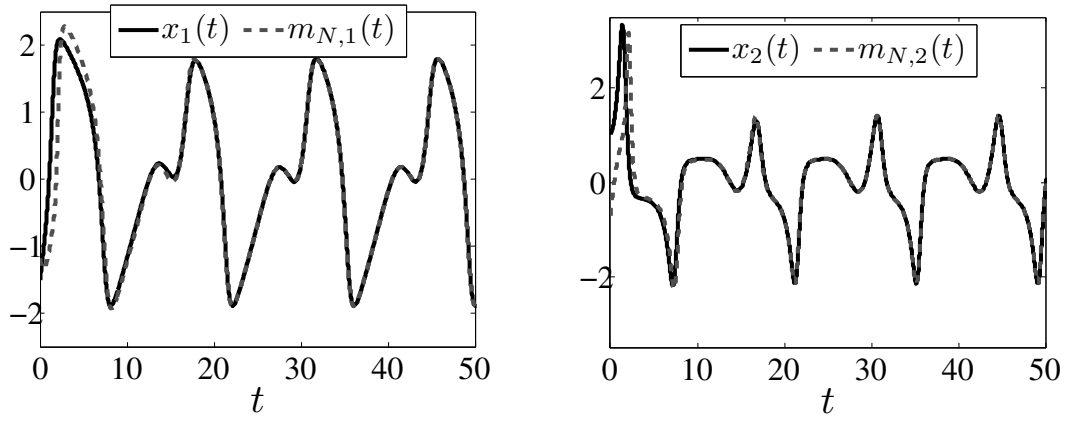

(a) (b)

Figure 8.19: Time series for the (a) first and (b) second state variables of the stabilized TUPO1 with $k = 0.25$.

The control effort applied to stabilize the target orbit is shown in Figure 8.20. The control effort tending to zero and $x(t)$ tending to $m_N(t)$ ensure that the orbit is stabilized.

These results exemplify a successful application of the aPBC to a continuous-time dynamical system using a real-time estimation of the future state dynamics.

The DFC is used here as a classical reference for comparison with the proposed method. From Section 8.3, Table 8.2, we the optimal value $k \approx 0.07632510479$ for the DFC control gain which leads to $|\mu| \approx 0.43951$. Here we observe the first advantage of the proposed method, the largest Floquet multiplier is smaller than the one obtained for the DFC, re-

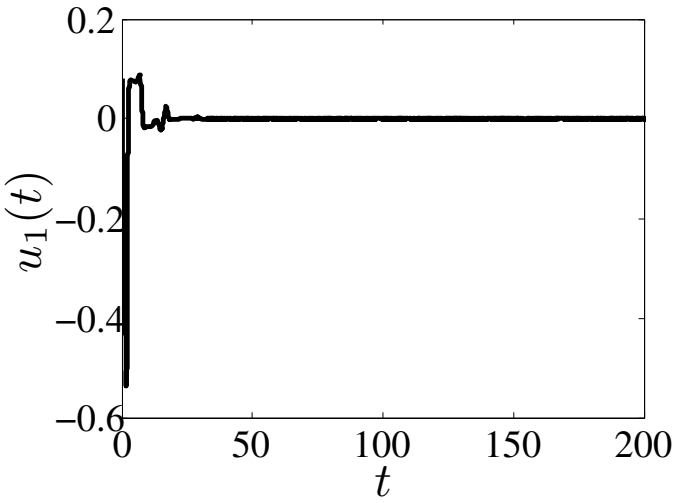

Figure 8.20: Time series of the control effort of the stabilized TUPO1 for $k_c = 0.25$ and $x(0) = [-1.5,\ 1.0]'$.

sulting in a more stable orbit. Notice that better results are expected for the PBC refining the scan in Figure 8.18 or applying optimization. Here the aim is to show applications of the aPBC and compare it with the DFC.

The TUPO1 with $x(0) = [-1.5,\ 1.0]'$ controlled by the DFC in the state space is shown in Figure 8.21(a) and the time series of the control effort is shown in Figure 8.21(b). Comparing these figures with Figures 8.18 and 8.20, respectively, we observe that the convergence of the trajectory to the controlled orbit by the proposed method is much faster than the one controlled by the DFC. This result is in agreement with the calculated $|\mu|$.

A trajectory in state space stabilized by both aPBC and DFC with initial condition $x(0) = [-0.5,\ 0.5]'$ are presented in Figure 8.22. Here we use a different initial condition to show the faster convergence of the aPBC. Although, Figure 8.23, with the norm-1 of the aPBC control effort in a log-linear scale, shows that the DFC control effort shown in Figure 8.6 (same initial condition) is much smaller in steady state. In comparison with the PFC (using optimization), we observe that the aPBC has a similar convergence rate but a larger steady state control effort.

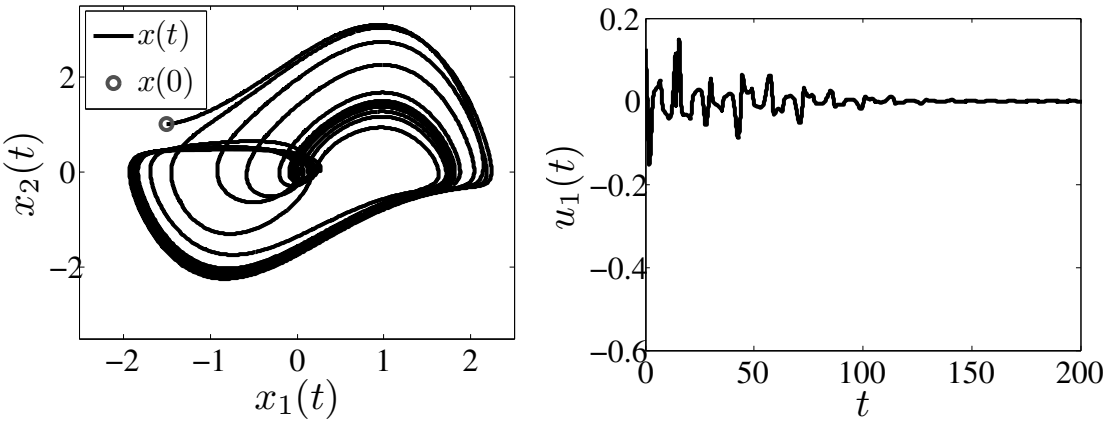

(a) (b)

Figure 8.21: Trajectory with $x(0) = [-1.5,\ 1.0]'$ controlled using the DFC with $k \approx 0.07632510479$. (a) State space and (b) time series of the control effort.

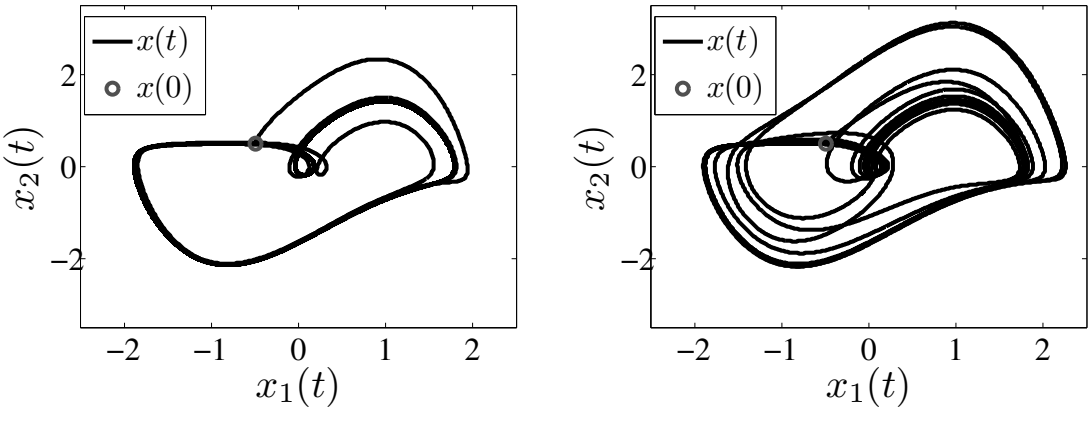

(a) (b)

Figure 8.22: Trajectory with $x(0) = [-0.5,\ 0.5]'$ controlled using (a) aPBC with $k = 0.25$ and (b) DFC with $k \approx 0.07632510479$.

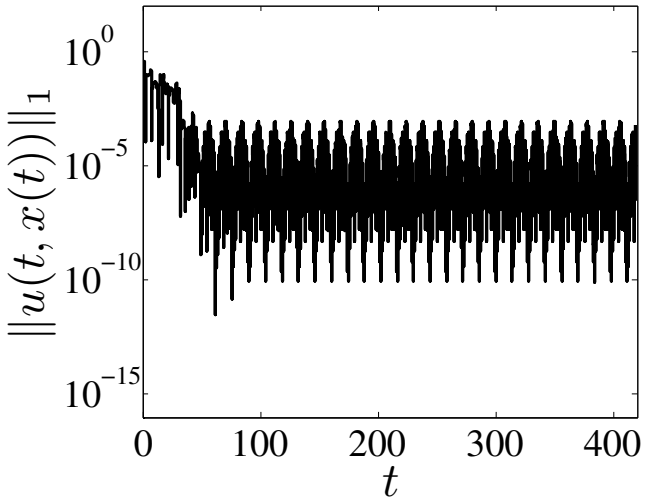

Figure 8.23: Time series of the control effort of the stabilized TUPO1 for $k_c = 0.25$ and $x(0) = [-0.5,\ 0.5]'$.

8.4.3 Stabilizing TUPO2 and TUPO3

In Section 8.3.3 it was shown that the TUPO2 and TUPO3 are not stabilized with the DFC with a constant scalar gain and it was not found a constant matrix gain that stabilizes them. It was also shown that the PFC stabilizes both orbits. Now we evaluate the aPBC controlling both orbits.

stabilizing TUPO2. Figure 8.24 shows the modulus of the Floquet multipliers as a function of the control gain k for the TUPO2 applying the aPBC. It is noticed that the aPBC stabilizes orbits with an odd number of real Floquet multipliers larger than +1. One detail is relevant here, the stabilization is achieved only for negative values of the gain k. Positive values of k make the largest magnitude Floquet multiplier increases and the orbit becomes more unstable.

The TUPO2 stabilized by the aPBC with $k = -0.125$ and initial condition $x(0) = [0.1,\ 1.8]'$ is shown in the state space in Figure 8.25(a). The time series of the control signal is presented in Figure 8.25(b) with $u_2(t) \to 0$ as $t \to +\infty$ indicating stabilization.

stabilizing TUPO3 Figure 8.26 shows the modulus of the Floquet multipliers as a function of the control gain k for the TUPO3 applying the PBC for five different values

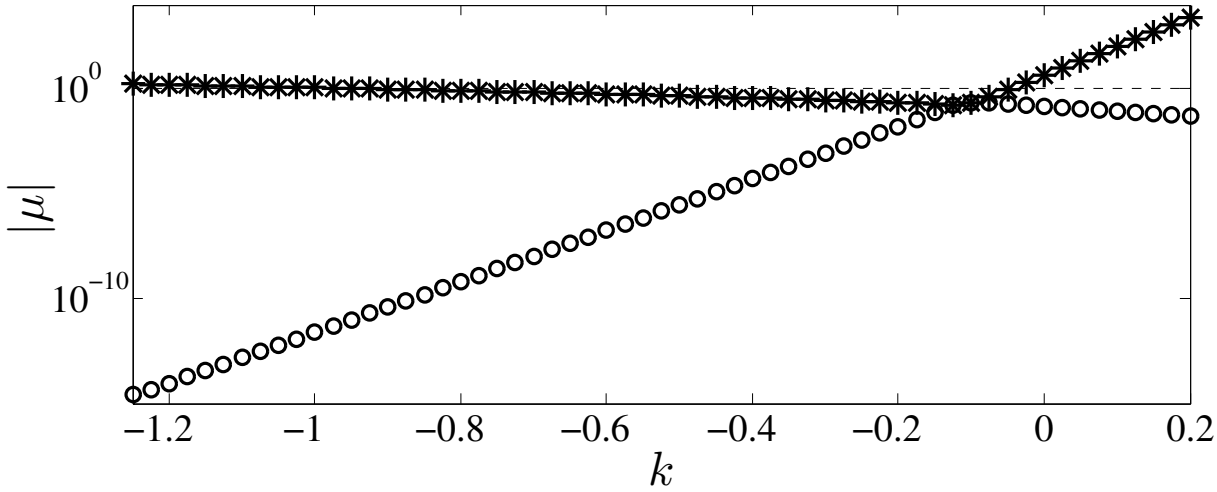

Figure 8.24: Modulus of the Floquet multipliers for different values of k for the TUPO2 controlled by the aPBC.

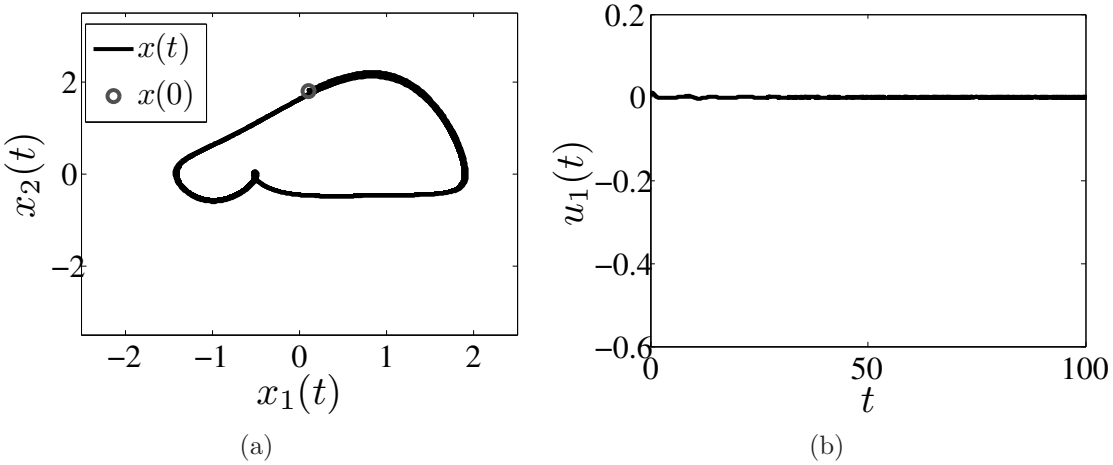

(a) (b)

Figure 8.25: TUPO2 stabilized using the aPBC with $k = -0.125$ and $x(0) = [0.1,\ 1.8]'$. (a) State space and (b) time series of the control effort.

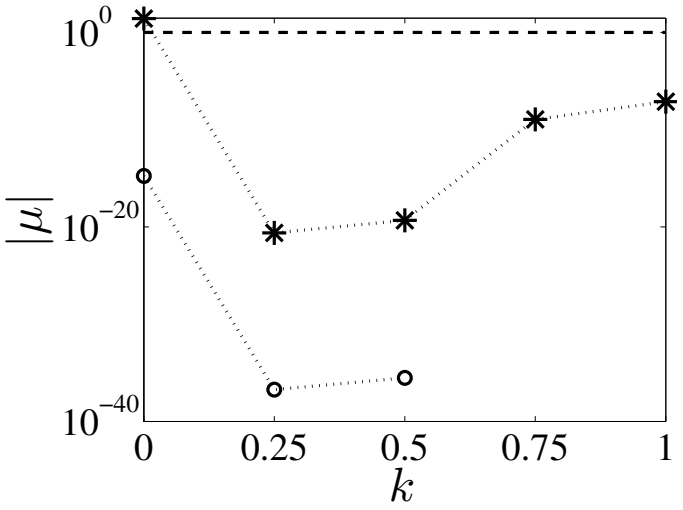

Figure 8.26: Modulus of the Floquet multipliers for different values of k for the TUPO3 controlled by the PBC.

of k. It is noticed that the PBC can stabilize an orbit that is not stabilized by the DFC with the same type o gain due to large period.

From Section 7.4.3 it is noticed that the computation of the Floquet multipliers is done obtaining $\varphi(t+T, t, x(t), 0)$ by an explicit Runge-Kutta integration method at each time step. The obtained $|\mu|_{max} < 1$ indicates that there is no theoretical limitation on the PBC on stabilizing the TUPO3.

However, there is a practical aspect that renders difficult the stabilization of the TUPO3 by the aPBC. When applying the aPBC to a system represented by a set of $n \in \mathbb{N}$ ODEs, the dimension of the closed-loop system is represented by a set of $nN \in \mathbb{N}$ ODEs. Here we are using $N = 102$ for each cycle of the forcing term, which means a set of $7nN = 1428$ ODEs to be solved. For the DFC, which leads to an infinite dimensional closed-loop system, the computational cost comes, predominantly, from memory to record the past states for a delay-time T. For the aPBC the computational cost comes from processing with reasonable error tolerance the set of $7nN$ ODEs.

Two possibilities are considered here:

- Using an implicit Runge-Kutta method that uses less discretization points to precisely approximate $\varphi(t+T, t, x(t), 0)$ than the orthogonal collocation method. This

alternative is not evaluated in this manuscript and is considered a relevant future work on the theme;

- Reduce the number of collocation points N and evaluate the characteristics of the controlled orbit when applying the implicit Runge-Kutta method with less precision. This alternative will be studied following.

8.4.4 Applying the aPBC for a low N

In the previous sections the aPBC was applied using $N = 102$ collocation points per cycle of the forcing term ($t = \frac{2\pi}{0.45}$). In this section we evaluate the characteristics of the TUPO1 stabilized by the aPBC with $N < 102$, $k_o = 10$ and $k = 0.25$. The results are relevant when studying practical aspects of the aPBC.

From Figure 8.15(a) it is observed an increase of $\epsilon(N, 50)$ when decreasing N for $k = 0$. This value means the relative difference between the predicted state $\hat{m}_{N,2}(t)$ and the actual state $x(t)$ for one cycle of a trajectory in the chaotic attractor of the free system. Now we are interested in the characteristics of the closed-loop system, in special the value of d (see (8.3), with $r(t) = \hat{m}_N(t)$) and υ (see (8.4)) as a function of N.

Figure 8.27(a) shows υ when stabilizing the TUPO1 applying the aPBC for different values of N with $k = 0.25$ and $k_o = 10$. The same for d is shown in Figure 8.27(b). Comparing Figure 8.27 with Figure 8.8 it is observed that for any stabilizing k for the DFC/PFC, the steady state error and control effort are smaller than for the aPBC with $k = 0.25$ for different N. These relatively high values for the aPBC are justified by the estimation error of the predicted state and this error decreases exponentially when increasing N.

It is observed in Figure 8.27 that even for a reduction on the number of collocation points, stability of TUPO1 is achieved for $N \geq 67$. The TUPO1 stabilized with the aPBC for $N = 82$ and $N = 67$ and $x(0) = [-1.5,\ 1.0]'$ is shown in Figures 8.28 and 8.29, respectively. Figures 8.28(e) and 8.29(e) show the initial value of the predicted states $m_j(0)$, $j = 1, 2, \ldots, N$ and $\varphi(T, 0, x(0), 0)$. It is observed that $m_j(0)$ is relatively close to $\varphi(T, 0, x(0), 0)$.

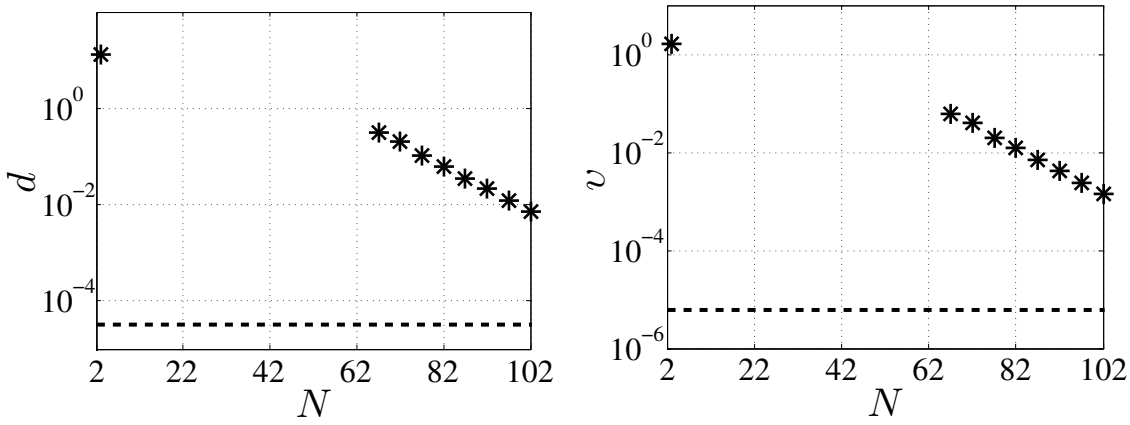

Figure 8.27: (a) d and (b) υ applying aPBC to the TUPO1 for different N with $k = 0.25$ and $k_o = 10$. The bottom dashed line is the value of (a) d and (b) υ computed with $N = 152$ and $k_o = 50$ used as reference.

The high values observed on Figure 8.27 for $N = 3$ are explained in Figure 8.30. It exemplifies a situation where a stable orbit different from TUPO1 is achieved due to the reduced N. The high amplitude periodic control signal in Figure 8.30(b) indicates that this stabilized orbit is not an orbit of the original free system. Figure 8.30(e) shows that $N = 3$ leads to $m_j(0)$ almost unrelated with $\varphi(T, 0, x(0), 0)$ and consequently $u_2(t) = k(\hat{m}_{N,2}(t) - x_2(t))$ is a high amplitude control signal. According to Figure 8.30(a), a trajectory with initial condition $x(0)$ on the TUPO1 (Poincaré point) diverges from it showing that it becomes unstable in this case.

It is noticed from the time-series of the trajectories in Figures 8.28(c), 8.28(d), 8.29(c) and 8.29(d) that in some torsions of the trajectory of the system controlled by the aPBC there is an oscillation on $\hat{m}_N(t)$. This oscillation is generated because small N leads to instability on the predicted state and it reflects in the time-series of the control signal in Figures 8.28(b) and 8.29(b) and the value of υ and d in Figure 8.27.

Another consequence on reducing N is the complete loss of stability of $\hat{m}_N(t)$ and the consequent interruption on the numerical integration of the trajectories. This phenomenon, exemplified in Figures 8.31 and 8.32, occurs even after increasing or reducing the error tolerances of the explicit Runge-Kutta integrator[2]. One of the reasons for this

[2]The simulations present in this work were performed using the Matlab® integration routine ode45 and, in this specific case, it was tested also the routines ode113 and ode15s.

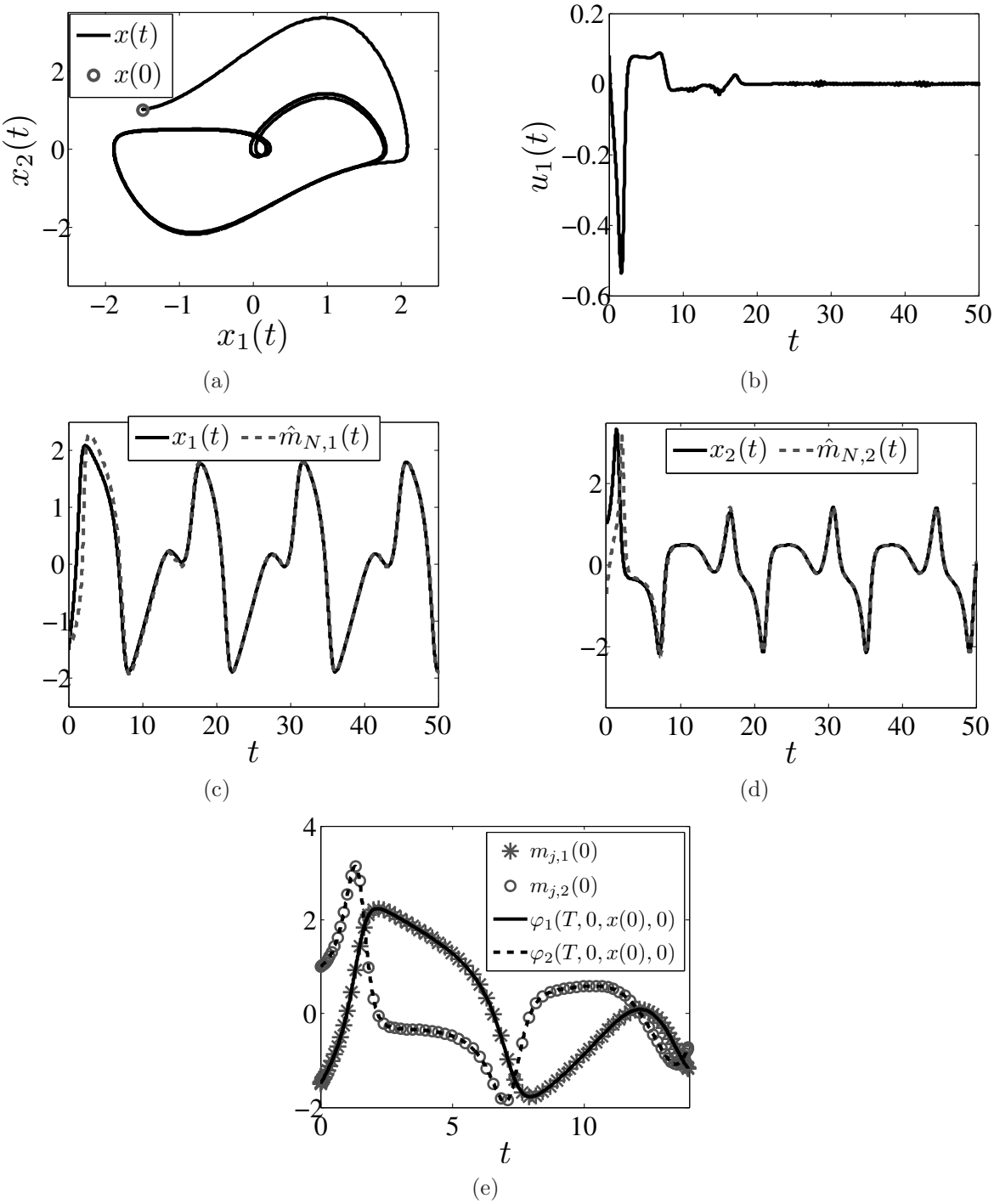

Figure 8.28: aPBC applied with $N = 82$, $k = 0.25$ and $k_o = 10$. (a) Trajectory in state space; (b) time-series of the control signal; (c) and (d) time-series of the actual and predicted state variables; (e) time-series of $\varphi(T, 0, x(0), 0)$ and the initial value of the predicted states $m_j(0)$.

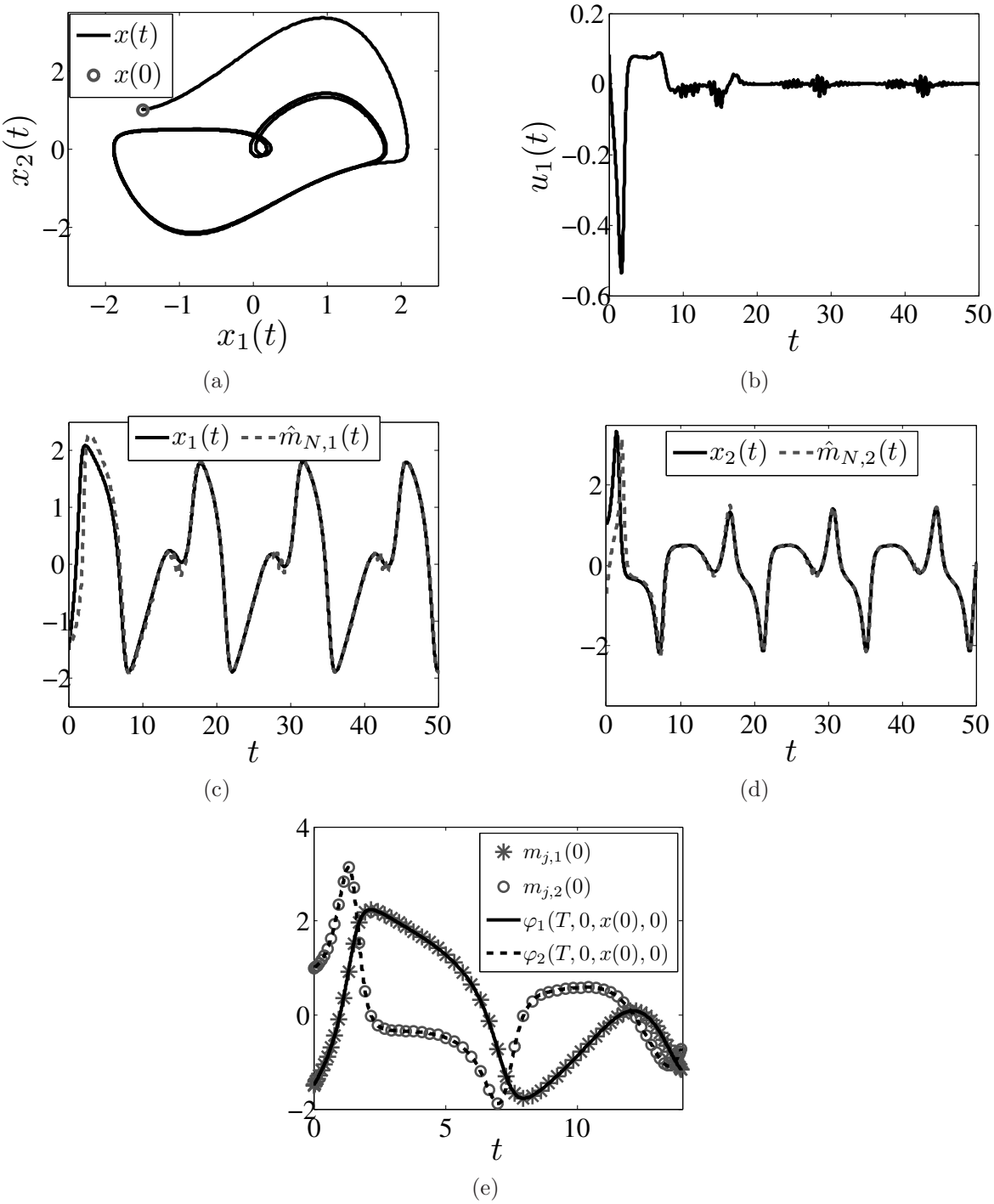

Figure 8.29: aPBC applied with $N = 67$, $k = 0.25$ and $k_o = 10$. (a) Trajectory in state space; (b) time-series of the control signal; (c) and (d) time-series of the actual and predicted state variables; (e) time-series of $\varphi(T, 0, x(0), 0)$ and the initial value of the predicted states $m_j(0)$.

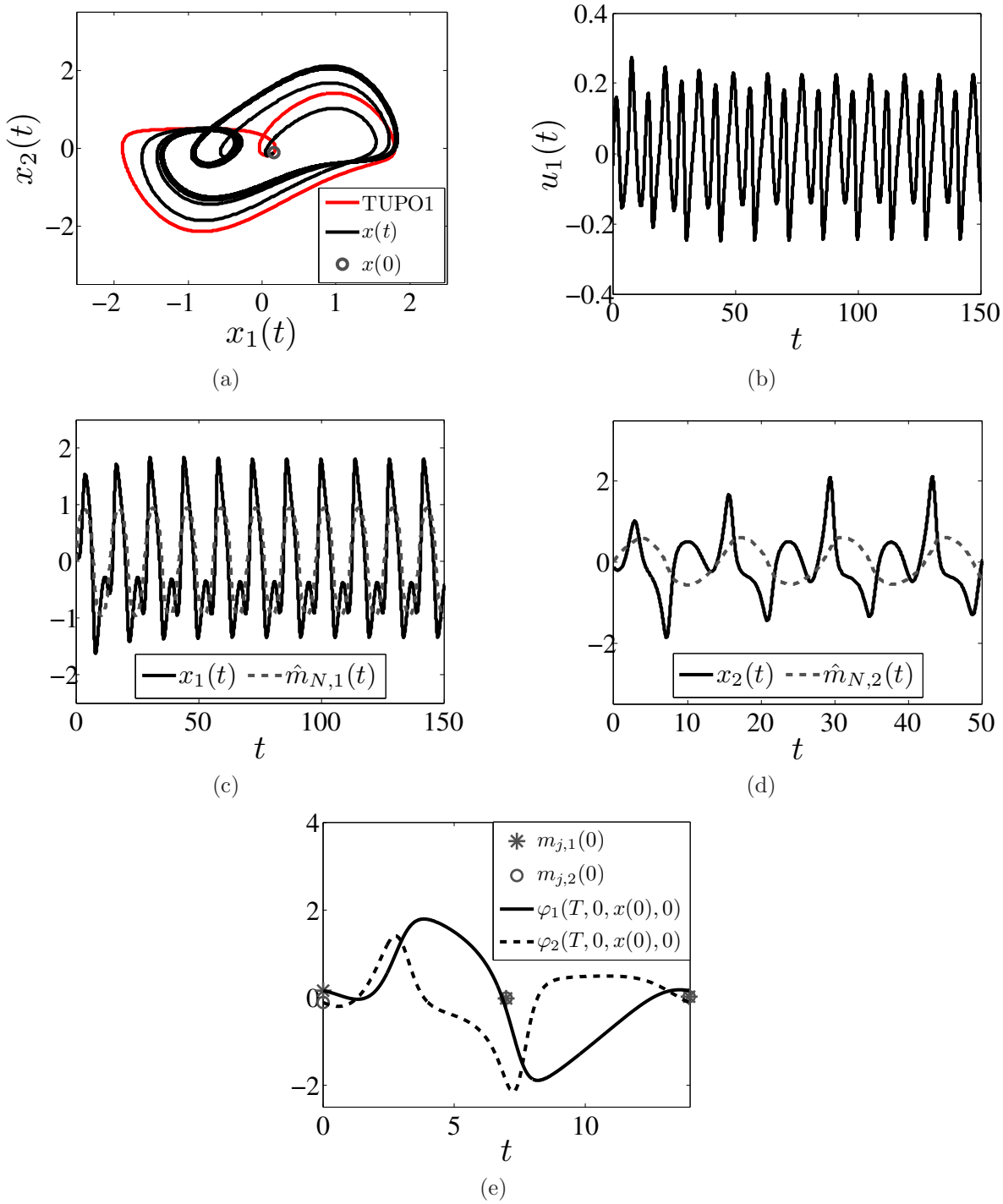

Figure 8.30: aPBC applied with $N = 03$, $k = 0.25$ and $k_o = 10$. (a) Trajectory in state space; (b) time-series of the control signal; (c) and (d) time-series of the actual and predicted state variables; (e) time-series of $\varphi(T, 0, x(0), 0)$ and the initial value of the predicted states $m_j(0)$.

loss of stability is that N is the parameter that rules the implicit Runge-Kutta integration error and Figures 8.31(d), 8.31(e) and 8.32(d) show that $m_N(0)$ is diverging from $\varphi(T, 0, x(0), 0)$ at time T. Another reason is the multiple set of $m_j(t)$ that can be obtained solving (7.35b) ($m_j(t)$ is the special case of $l_j(t)$ when using orthogonal collocation). Two different sets of $m_j(0)$ are exemplified in Figures 8.31(d) and 8.31(e) for $N = 5$. This means that there are, at least, two different solutions for $\hat{m}_j(t)$ and a possible jump of the trajectory from the vicinity of one solution to the other leads to the loss of stability of the estimator. This loss of stability should be investigated in future works.

8.5 Numerical results on the aPBC applied to an autonomous system

In this section we provide numerical results on the approximated prediction-based control (aPBC) (see Section 7.3.3) applied to the Rössler system using the control scheme (8.1a). The goals are (i) to show that the method is applicable to autonomous systems without any modification and (ii) to compare the effect of different numbers of collocation points N on stabilization.

The Rössler system is described by the system of ODEs (8.10).

8.5.1 The Rössler system

$$\dot{x}(t) = f(t, x(t)) + u(t, x(t)), \tag{8.10a}$$

$$f(t, x(t)) = \begin{bmatrix} -x_2(t) - x_3(t) \\ x_1(t) + \beta_1 x_2(t) \\ \beta_2 + x_1(t)x_3(t) - \beta_3 x_3(t) \end{bmatrix}, \tag{8.10b}$$

where $x : \mathbb{R}^+ \to \mathbb{R}^3$ and $f : \mathbb{R}^+ \times \mathbb{R}^3 \to \mathbb{R}^3$. We follow [4] and choose $\beta_1 = 0.2$, $\beta_2 = 0.2$ and $\beta_3 = 4.5$.

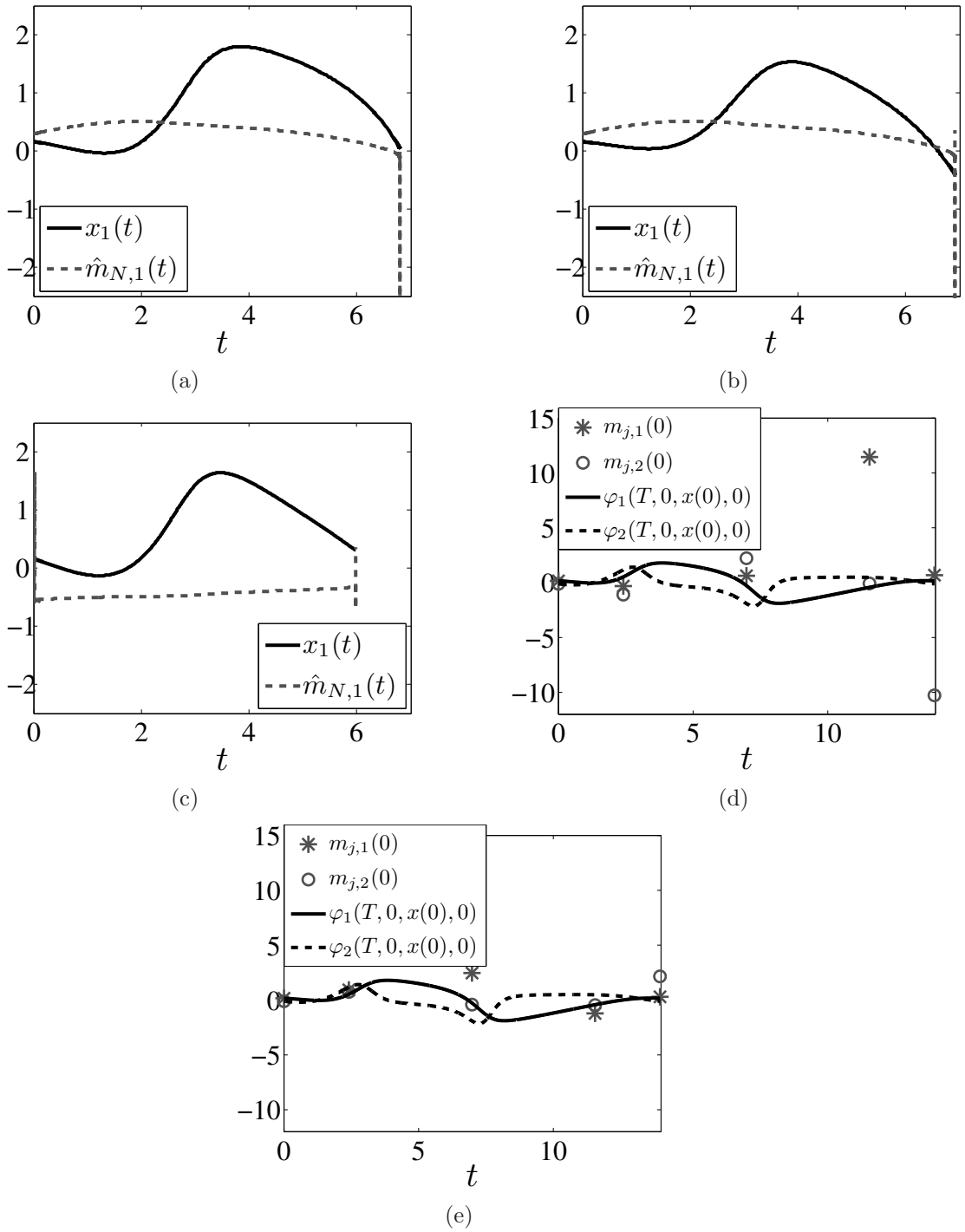

Figure 8.31: Time-series of a trajectory when applying the aPBC with $N = 05$ and (a) $k = 0$ and $k_o = 10$; (b) $k = 0.25$ and $k_o = 10$; (c) $k = 0.25$ and $k_o = 1000$; (d) and (e) time-series of $\varphi(T, 0, x(0), 0)$ and the initial value of the predicted states $m_j(0)$.

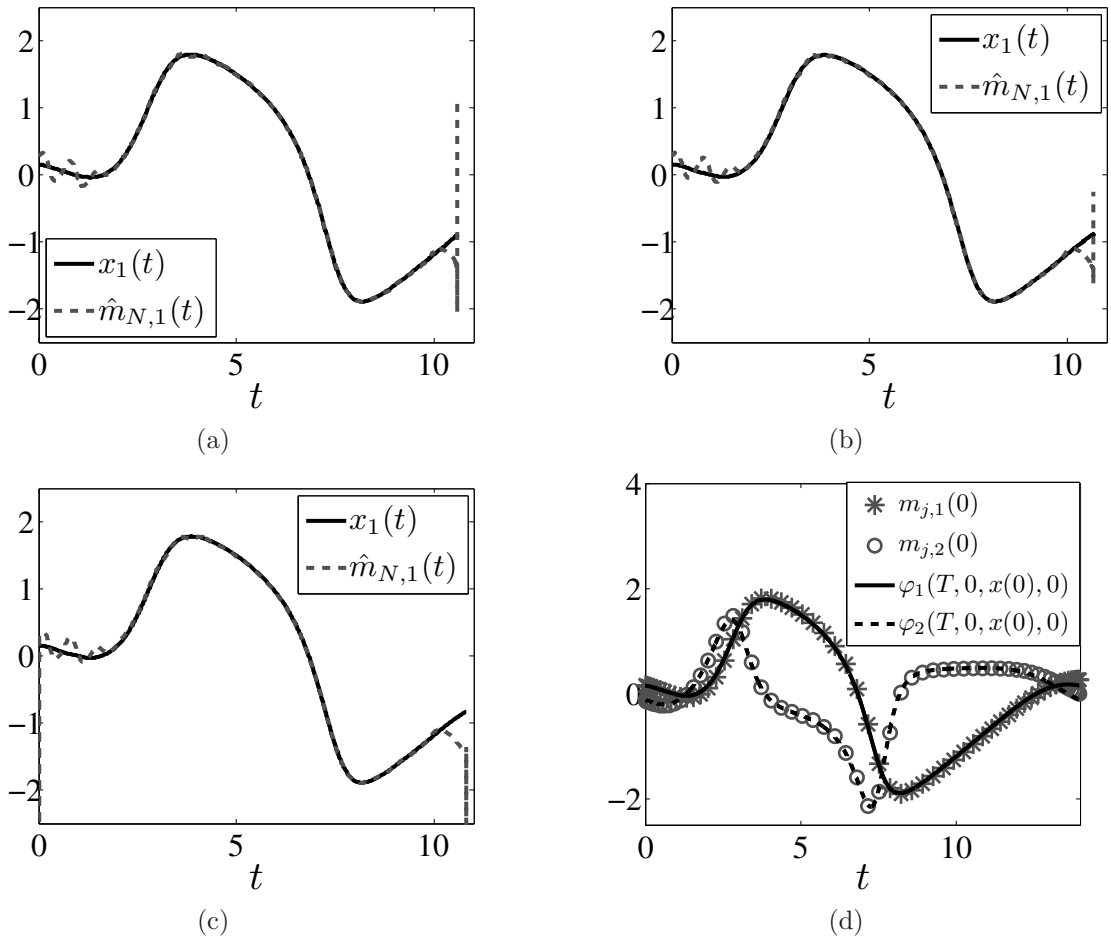

Figure 8.32: Time-series of a trajectory when applying the aPBC with $N = 62$ and (a) $k = 0$ and $k_o = 10$; (b) $k = 0.25$ and $k_o = 10$; (c) $k = 0.25$ and $k_o = 1000$; (d) time-series of $\varphi(T, 0, x(0), 0)$ and the initial value of the predicted states $m_j(0)$.

Table 8.3: Poincaré map point $x(t_0)$, period T and Floquet multipliers μ of a periodic orbit (TUPO4) of the Rössler system.

	TUPO4
$x(t_0)$	$\begin{bmatrix}0 & 5.0206004746 & 1.6806432235\end{bmatrix}'$
T	5.8439698764
μ	$\begin{bmatrix}-1.9182862735 & 1 & -1.8655159319 \times 10^{-11}\end{bmatrix}$

Target period orbit. Following Section 8.2 we should qualitatively analyse the Rössler system in order to find UPOs to stabilize. The first step would be to plot a bifurcation diagram of the system by varying one parameter β_i to find a chaotic attractor and the second step would be finding embedded UPOs. Both steps are avoided once the parameters β_i that lead to chaotic behaviour and one UPO of the chaotic attractor are presented in [4].

A Poincaré section S is defined as

$$S = \{s = (x_1, x_2, x_3) \in \mathbb{R}^3 : x_1 = 0 \text{ and } x_2 \geq 0\}.$$

We apply the Newton-Raphson method to refine the position and period of the orbit and call it TUPO4. Its period T and Floquet multipliers μ are presented in Table 8.3.

The chaotic attractor of the Rössler system in the state space for the chosen parameters and its Poincaré map are presented in Figure 8.33. The TUPO4 in the state space is presented in Figure 8.34(a) and its time series for the three state variables in Figure 8.34(b).

8.5.2 Stabilizing TUPO4

The control signal $u(t, x(t))$ for the aPBC was shown in Section 7.3.3 and its application discussed in Section 8.4 for non-autonomous systems. Here we apply it using the control signal (8.7) with the constant control gain

$$K = \begin{bmatrix}0 & 0 & 0\\ 0 & 0 & 0\\ 0 & 0 & k\end{bmatrix}, \qquad k \in \mathbb{R}. \tag{8.11}$$

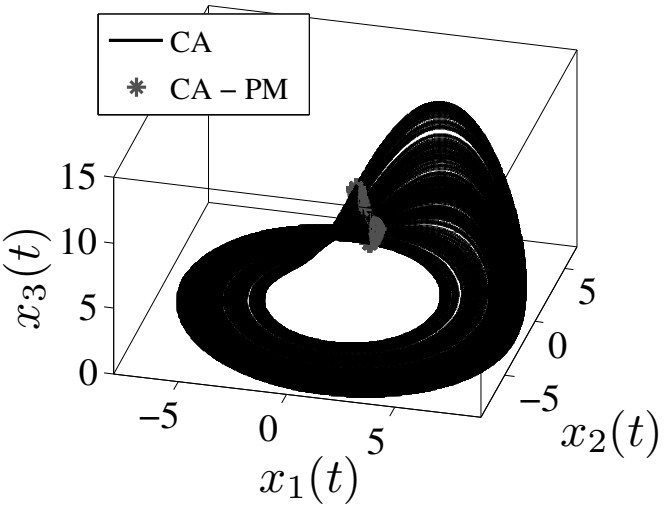

Figure 8.33: Rössler chaotic attractor for $\beta_1 = 0.2$, $\beta_2 = 0.2$ and $\beta_3 = 4.5$ with 200 Poincaré map points ($\star$).

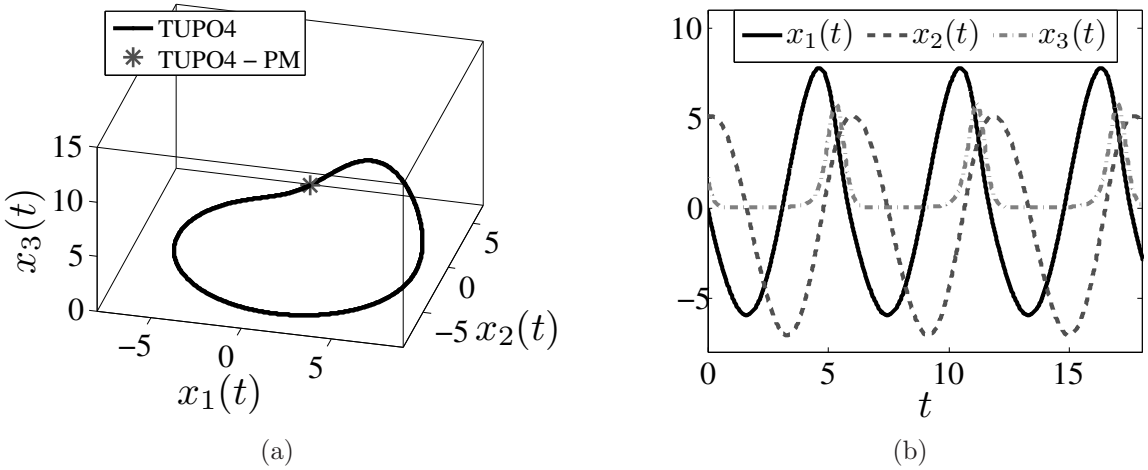

Figure 8.34: TUPO4 of the Rössler system for $\beta_1 = 0.2$, $\beta_2 = 0.2$ and $\beta_3 = 4.5$. (a) State space with Poincaré map ($\star$) and (b) time-series of the state variables.

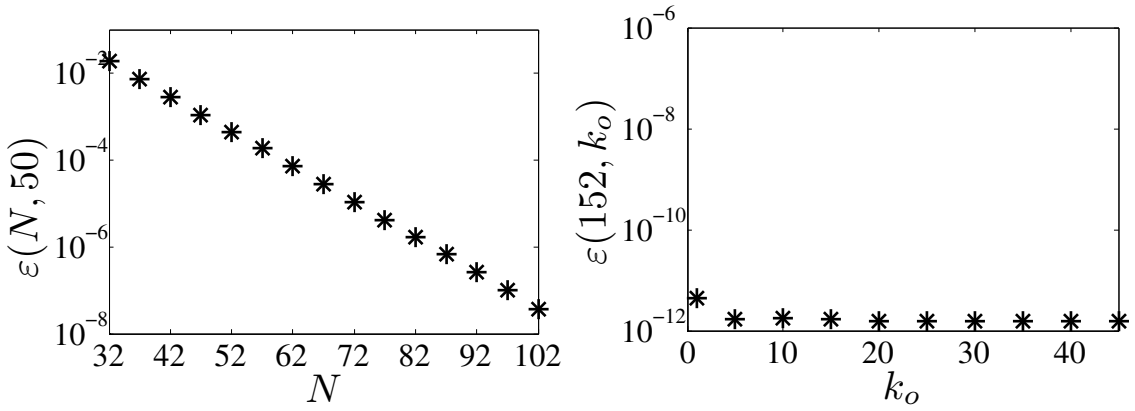

Figure 8.35: Relative error of the estimated free system response future value using different (a) N and (b) k_o.

Notice that $u : \mathbb{R}^+ \times \mathbb{R}^3 \to \mathbb{R}^3$ and the control signal may be applied to the derivative of each state variable resulting in fully actuated system. However, in this section, only the third component of the control signal vector is different from zero according to the choice of the matrix control gain 8.11.

First, the quality of the estimator is evaluated for different values of the observer gain k_o and the number of discretization points for the orthogonal collocation method N for the control gain $k = 0$. Second, the control gain k is tuned using k_o and N that leads to a good estimation quality. Third, the control method is applied for different N and the steady state control effort v and error d are computed for one cycle of the orbit.

Tuning the parameters k_o and N

The procedure shown in Section 8.4.1 is repeated here to characterize the performance of the estimator for different values of the parameters k_o and N for $k = 0$. We used as the initial condition $x(0) = [0, \ -6, \ 0.0375]'$ to compute $\varepsilon(N, k_o)$ in (8.9). The results are shown in Figure 8.35 for different values of (a) N with $k_o = 50$ ($\varepsilon(N, 50)$) and (b) k_o with $N = 152$ ($\varepsilon(152, k_o)$).

The values of $N < 32$ leads to numerical integration instability, except $N = 3$, and are not computed. Here we notice that less collocation points are necessary to obtain estimation quality equivalent to the one obtained for the vdP oscillator (see Figure 8.15).

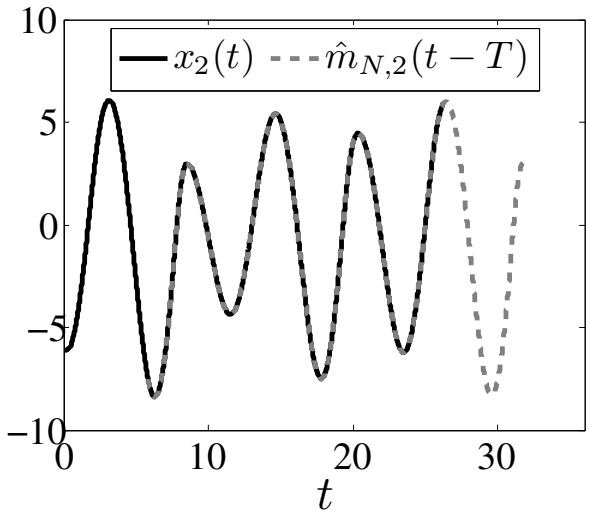

Figure 8.36: Current time and shifted future time trajectory of the Rössler system for $k = 0$, $k_o = 10$ and $N = 102$.

We see that for the vdP we have $\varepsilon(102, 50) \approx 4.4 \times 10^{-4}$ while, for the Rössler system we have $\varepsilon(52, 50) \approx 4.4 \times 10^{-4}$. The values of $\varepsilon(152, k_o)$ for k_o large of the chosen trajectory of the Rössler system also stabilize to a value much smaller than for the vdP oscillator. Notice that $T = 5.8439698764$ (the period of the TUPO4) for Rössler system while $T = 2\pi/0.45$ for the vdP oscillator, but these values of $\varepsilon(152, k_o)$ are much more related with the behaviour of the trajectories than the period itself because the collocation points s_i are computed for a normalized time between 0 and 1.

In Figure 8.36 it is shown $x_2(t)$ and $\hat{m}_{N,2}(t - T)$ (beware the time shift here) for the Rössler system, which can be compared with Figure 8.16.

Tuning of k

Now we tune the feedback gain k that stabilizes the TUPO4. As done in Section 8.4.2, we use $N = 102$ and $k_o = 10$ which leads to an adequate estimation of the future state.

Figure 8.37 shows the modulus of the three Floquet multipliers $|\mu|$ for different values of k. The stability is achieved when $|\mu| \leq 1$ and the value $\mu = 1$ is characteristic of autonomous system trajectories. We choose $k = 1.85$, which results in $|\mu| \approx 0.299 \times 10^{-2}$. All the Floquet multipliers in this case are real numbers.

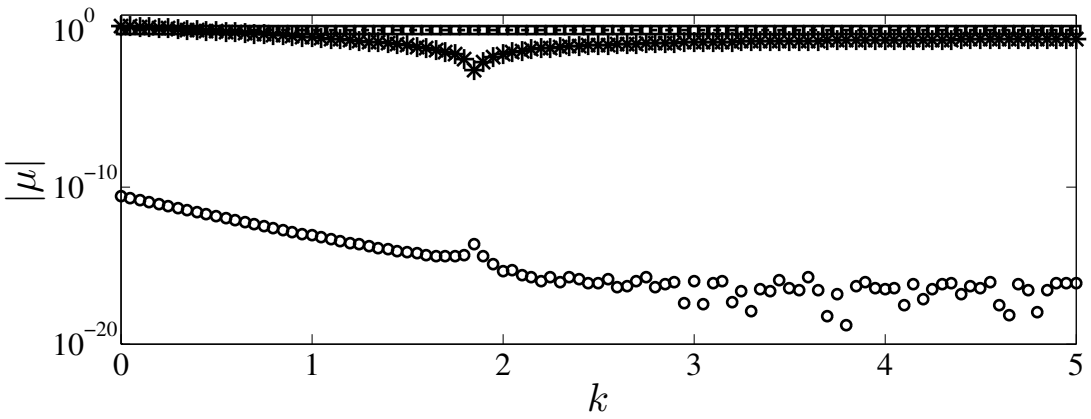

Figure 8.37: Modulus of the Floquet multipliers for different values of k for the TUPO4 controlled by the aPBC.

Applying the aPBC for different values of N

In this section we evaluate the characteristics of the aPBC for different values of N applied to the stabilization of the TUPO4. Here we use $N \leq 102$, $k_o = 10$ and $k = 1.85$.

From Figure 8.35(a) an increase of $\epsilon(N, 50)$ is observed when decreasing N for $k = 0$. This value means the relative difference between the predicted state $\hat{m}_{N,2}(t)$ and the actual state $x(t)$ for one cycle of a trajectory in the chaotic attractor of the free system. Now we are interested in the characteristics of the closed-loop system, in special the value of d (see (8.3), with $r(t) = \hat{m}_N(t)$) and υ (see (8.4)) as a function of N for the TUPO4 stabilized by the aPBC.

Figure 8.38(a) shows υ for different values of $N \geq 32$ with $k = 1.85$ and $k_o = 10$. The same for d is shown in Figure 8.38(b). Values of $3 < N < 32$ where not computed because of numerical integration instabilities, the same observed in Section 8.4.4.

Here we observe that $N \geq 102$ leads to a precise estimation once there is a convergence of υ to the value computed using $N = 152$ and $k_o = 50$ (dashed line). Comparing Figure 8.38 with Figure 8.27 it is observed a great reduction on υ and d for the control method applied to the Rössler system, which is in accordance with what was observed for $\varepsilon(N, 50)$. In fact, N between 47 and 52 leads to a value of d equivalent to the value obtained for $N = 102$ for the vdP oscillator. For the υ this reduction is more significant, with $N = 37$ leading to a value of υ close to the value obtained for $N = 102$ for the vdP. This result is

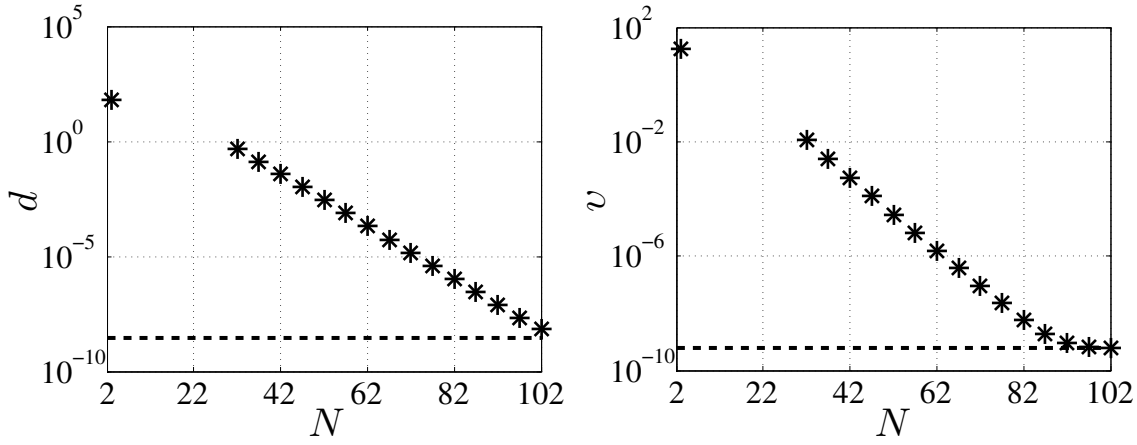

Figure 8.38: (a) d and (b) v applying aPBC to the TUPO4 for different N with $k = 1.85$ and $k_o = 10$. The bottom dashed line is the value of (a) d and (b) v computed with $N = 152$ and $k_o = 50$ used as reference.

important for practical aspects because it shows that, for some systems, the augmented state of the closed-loop system controlled with the aPBC can be reduced significantly (in comparison with the initial results shown for the vdP oscillator).

It is observed in Figure 8.38 that stability of TUPO4 is achieved for $N \geq 32$. The TUPO4 stabilized with the aPBC for $N = 102$, $N = 82$, $N = 52$ and $N = 32$ is shown in Figures 8.39, 8.40, 8.41 and 8.42, respectively, using $x(0) = [0, \ -6, \ 0.0375]'$. Deviation of $\hat{m}_{N,2}(t)$ from $x_2(t)$ is observed in Figure 8.42(d), this deviation reflects the numerical integration instabilities for $N < 32$. The aPBC applied for $N = 3$ with the same initial condition is shown in Figure 8.43. We verify that stabilization is not achieved for $N = 3$, which leads to the high values of v and d observed in Figure 8.38.

By applying $k = 1$, $k_0 = 10$ and $x(0)$ on the Poincaré map point of the TUPO4 for $N = 3$ we have the stable orbit shown in Figure 8.44(a), different from TUPO4 in position, continuous-time period ($T \approx 35.2$) and discrete-time (Poincaré) period ($p = 6$). Figure 8.44(b) shows that the stabilized orbit is not a periodic orbit of the free system (relatively high control effort) and this is confirmed by integrating the free Rössler system for $0 \leq t \leq 35.2$) with initial condition on the stabilized orbit and verifying that it does not close in state space.

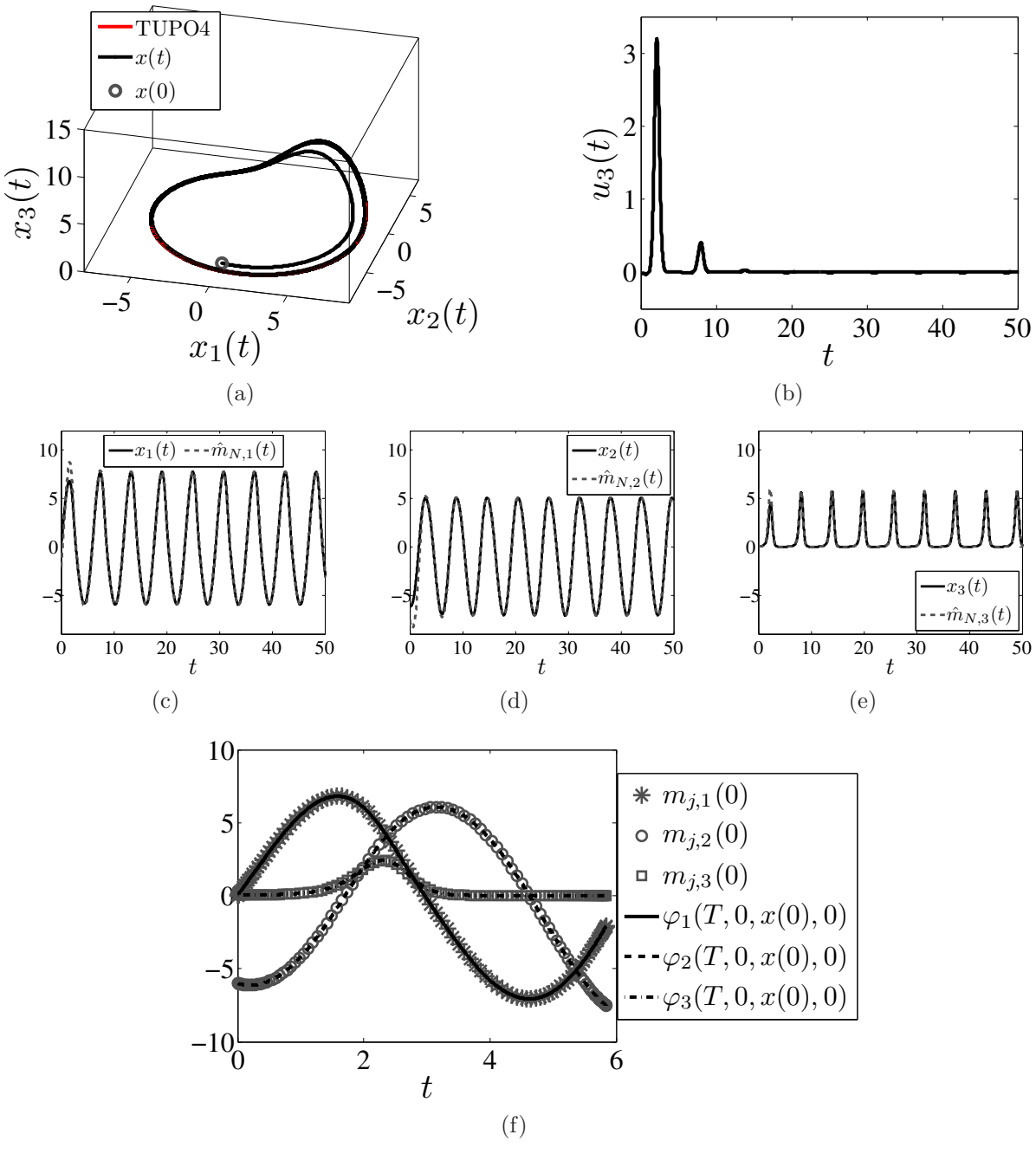

Figure 8.39: aPBC applied with $N = 102$, $k = 1.85$ and $k_o = 10$. (a) Trajectory in state space; (b) time-series of the control signal; (c), (d) and (e) time-series of the actual and predicted state variables; (f) time-series of $\varphi(T, 0, x(0), 0)$ and the initial value of the predicted states $m_j(0)$.

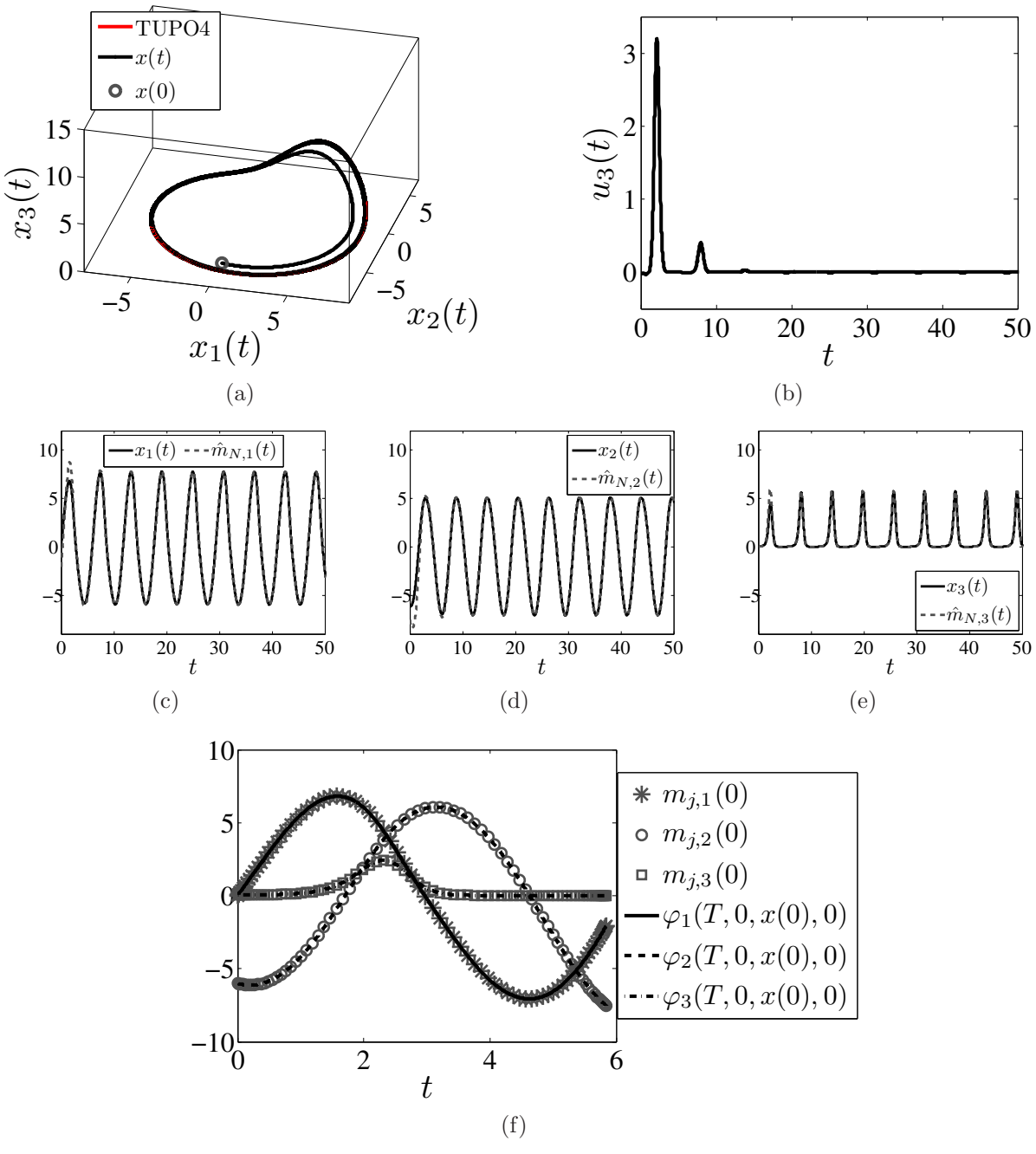

Figure 8.40: aPBC applied with $N = 82$, $k = 1.85$ and $k_o = 10$. (a) Trajectory in state space; (b) time-series of the control signal; (c), (d) and (e) time-series of the actual and predicted state variables; (f) time-series of $\varphi(T, 0, x(0), 0)$ and the initial value of the predicted states $m_j(0)$.

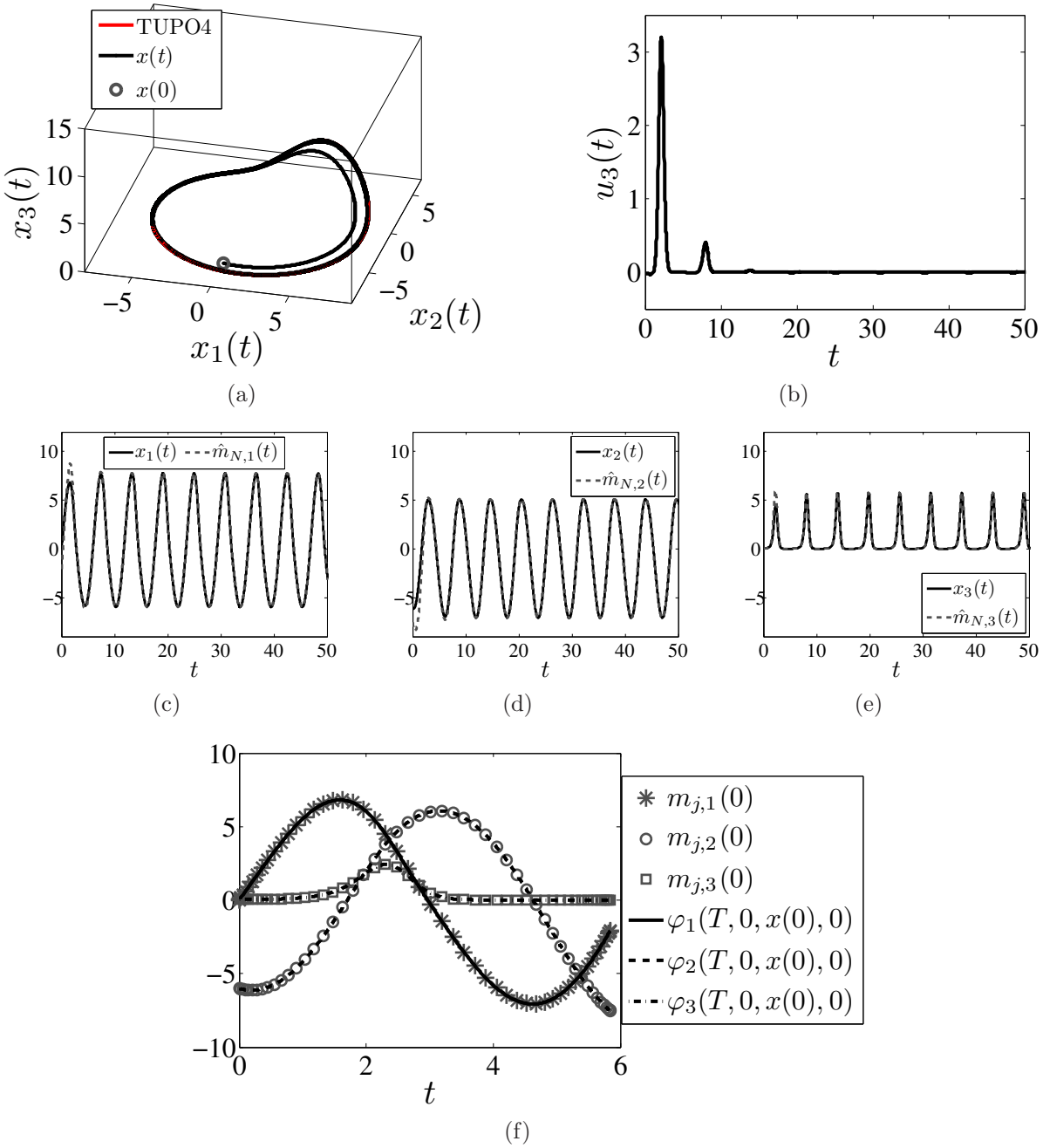

Figure 8.41: aPBC applied with $N = 52$, $k = 1.85$ and $k_o = 10$. (a) Trajectory in state space; (b) time-series of the control signal; (c), (d) and (e) time-series of the actual and predicted state variables; (f) time-series of $\varphi(T, 0, x(0), 0)$ and the initial value of the predicted states $m_j(0)$.

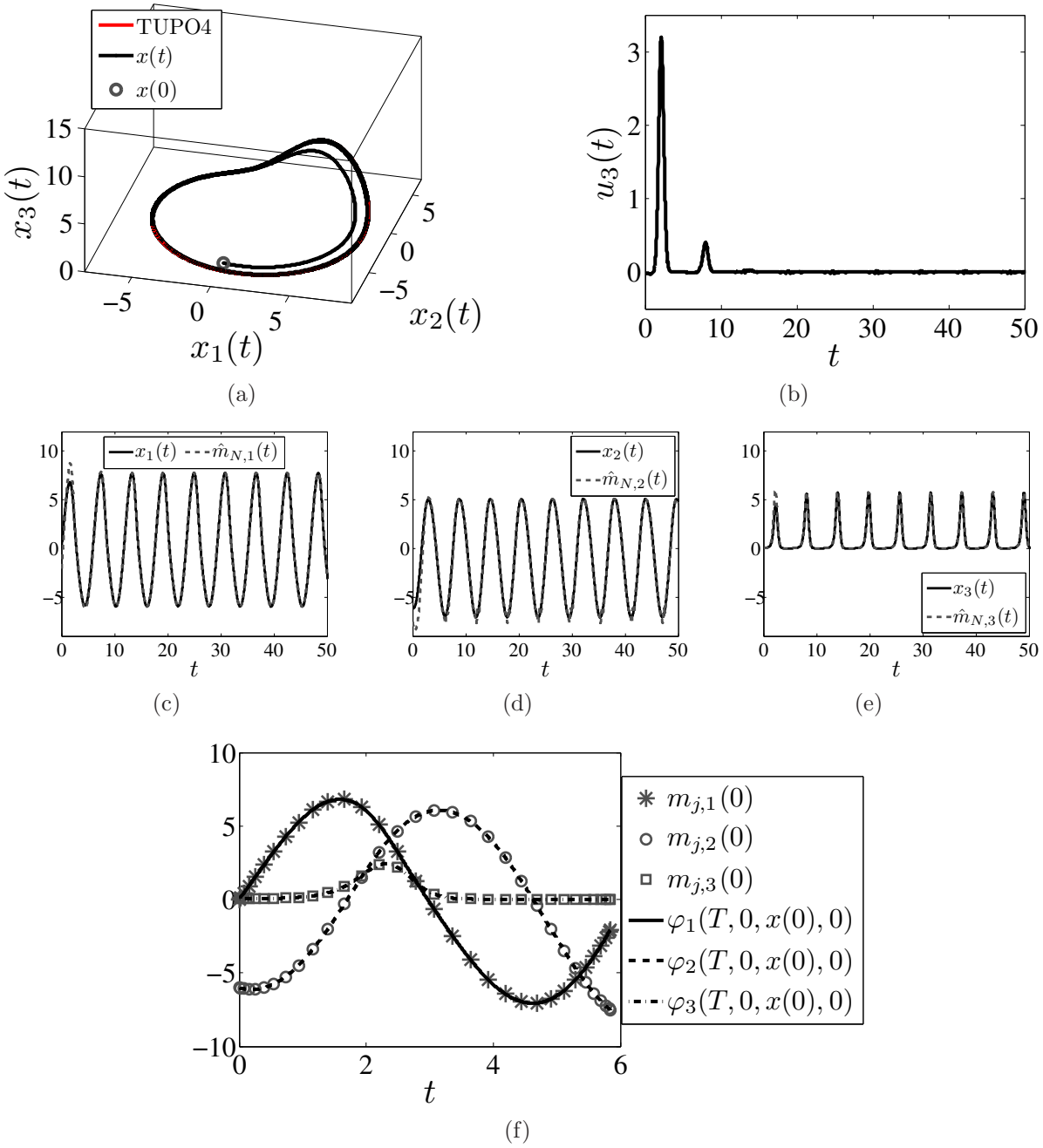

Figure 8.42: aPBC applied with $N = 32$, $k = 1.85$ and $k_o = 10$. (a) Trajectory in state space; (b) time-series of the control signal; (c), (d) and (e) time-series of the actual and predicted state variables; (f) time-series of $\varphi(T, 0, x(0), 0)$ and the initial value of the predicted states $m_j(0)$.

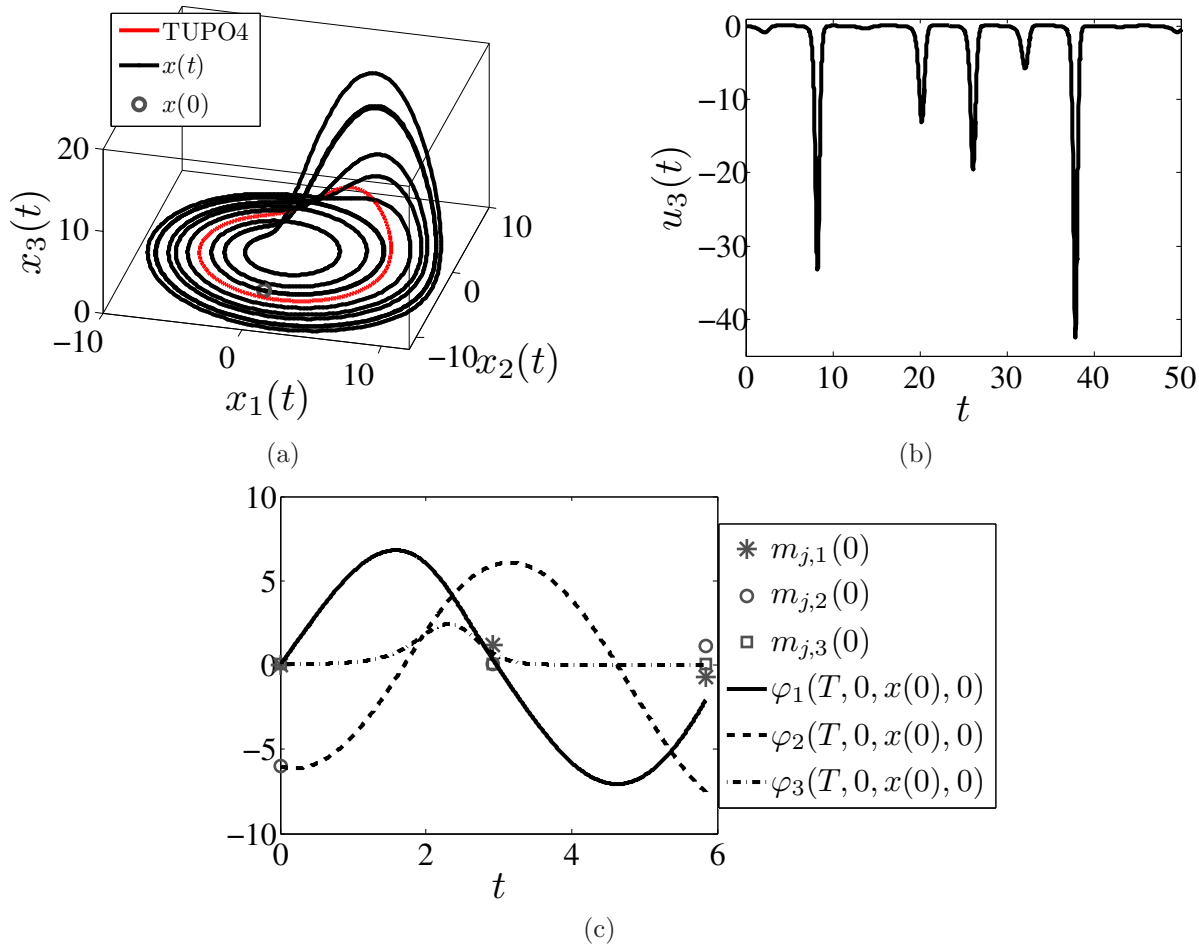

Figure 8.43: aPBC applied with $N = 03$, $k = 1.85$ and $k_o = 10$. (a) Trajectory in state space; (b) time-series of the control signal; (c) time-series of $\varphi(T, 0, x(0), 0)$ and the initial value of the predicted states $m_j(0)$.

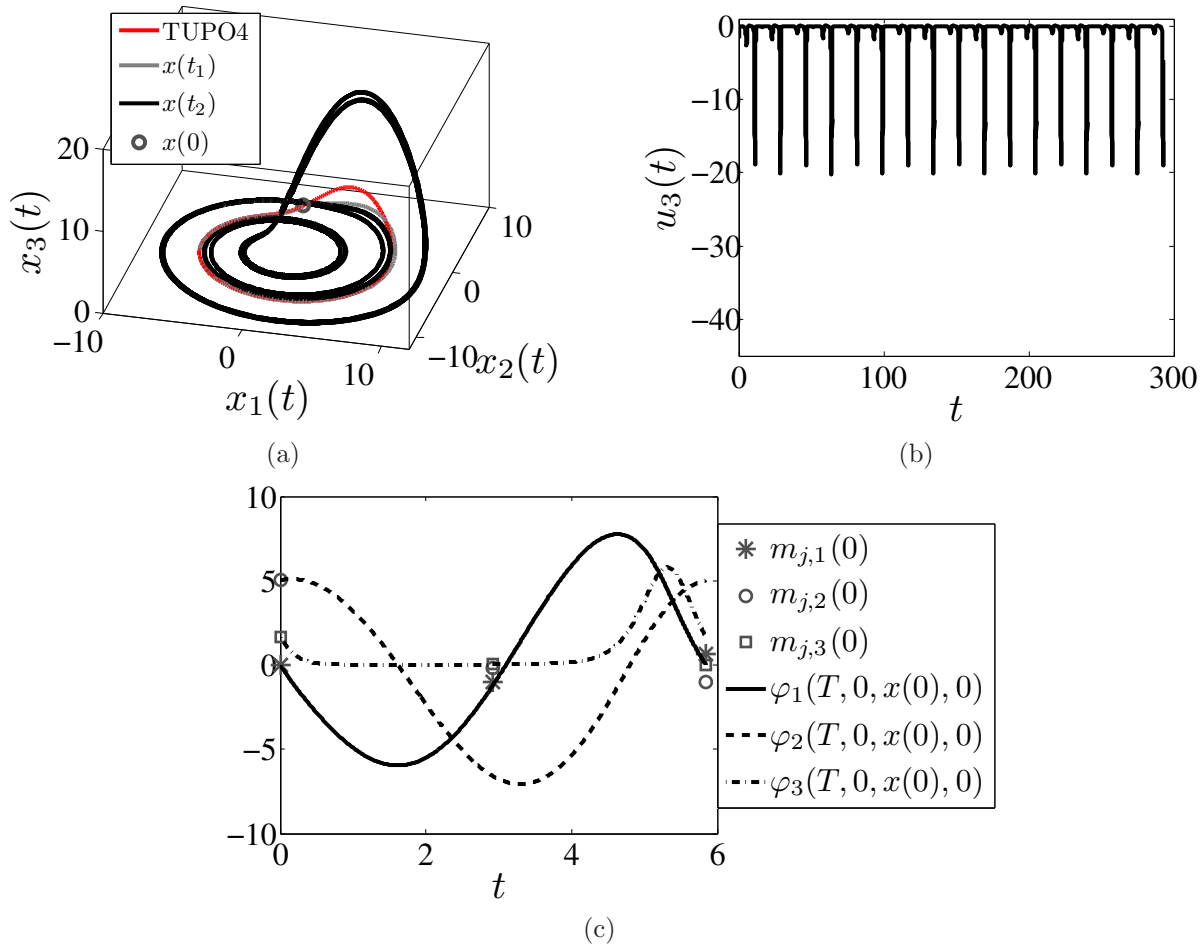

Figure 8.44: aPBC applied with $N = 03$, $k = 1$ and $k_o = 10$. (a) Trajectory in state space with $0 \leq t_1 \leq 7$ and $7 \leq t_2 \leq 293$; (b) time-series of the control signal; (c) time-series of $\varphi(T, 0, x(0), 0)$ and the initial value of the predicted states $m_j(0)$.

Chapter 9

Conclusions

In Part II the stabilization of existing periodic orbits of continuous-time systems using feedback control was studied. The interest is in control methods whose control signal ideally vanishes when the trajectory is on the stabilized periodic orbit. This ideal condition is achieved when the stable periodic orbit is exactly the same (position and period) unstable periodic orbit of the free system. Considering future practical applications of the methods in real systems, we are also interested in a stable periodic orbit in the vicinity of the target UPO.

The proportional feedback control (PFC), delayed feedback control (DFC) and prediction-based feedback control (PBC) were studied to stabilize periodic orbits. The PFC was presented in Section 7.3.1. The DFC was presented in Section 7.3.2 and a method to simplify the stability analysis of closed-loop periodic orbits approximating their monodromy matrices by matrix algebra only was presented in Section 7.4.2. This simplification reduced the computational time to verify the stability of the closed-loop orbit given a control gain and made feasible the application of optimization to control gain design of the continuous-time DFC in Section 8.3. The continuous-time PBC was presented in Section 7.3.3, but its application on continuous and real-time systems is not allowed due to the necessity to compute the future state of the free system trajectories one period ahead at the current time. This problem was solved with the proposition of the approximated prediction-

based control (aPBC) in Section 7.3.3. The aPBC uses an estimator based on implicit Runge-Kutta methods to approximate the free system future states in real-time.

The three methods were compared using a non-autonomous system (forced van der Pol oscillator) in Chapter 8 using three different target UPOs. One orbit (TUPO1) of discrete period 1 without odd number of real Floquet multipliers larger than +1, one orbit (TUPO2) of discrete period 1 with one real Floquet multipliers larger than +1 and one orbit (TUPO3) with discrete period 7, considered a large period. The DFC and PFC control gains were designed using optimization with the largest magnitude Floquet multiplier as a cost function.

Stabilizing TUPO1 of the vdP oscillator. The three methods (PFC, DFC and aPBC) achieved the stabilization of TUPO1 and for this example we can do some affirmations.

Comparing the stability by the largest magnitude Floquet multiplier (Figures 8.4 and 8.17) we observed that the range of stabilizing control gain is larger for the PFC and smaller for the aPBC. The smaller value of the largest Floquet multiplier was obtained using the PFC and the larger with the DFC. A comparison criterion also related with the Floquet multipliers is the convergence rate of nearby trajectories to the stable solution. In this case (Figures 8.6 and 8.23), the best results (faster convergence rate) were obtained for the PFC and the worst for the DFC. We conclude that considering Floquet multipliers and their associated performance characteristics (stability and convergence rate) the best results were obtained for the PFC, the aPBC is in an intermediate situation and the DFC leaded to the worst results.

Comparing the steady state error and control effort (Figures 8.8 and 8.27) we observe that for small control gains the DFC and PFC present similar results. The best result obtained for the aPBC ($k = 0.25$, $k_o = 50$ and $N = 150$ - dashed line in Figure 8.27) is significantly (approximately 10^6 times) worse compared to the DFC and PFC. This result is clearly expected because of the estimation approximations used with the aPBC.

A numerical robustness analysis to one parameter uncertainty comparing the DFC and PFC is shown in Figure 8.10. One may observe that the DFC is more robust to variations

on the forcing term amplitude (a) than the PFC. This is justified by the fact that the PFC depends upon the exact knowledge of the target UPO which changes when a system parameter is modified. The steady state error and control effort increase considerably for $a \neq 0.988$ when using the PFC and this is the main weakness of the method once the exact orbit is never found in real systems. Notwithstanding, the closed-loop stable orbit obtained for the PFC is more stable than the stabilized orbit obtained for the DFC for all tested values of a.

This robustness analysis was not performed for the aPBC (results will be shown in future works), although, the results of Part I and the knowledge about the characteristics of the method can be used for some conclusions. Figures 4.10 and 4.11 show that the PBC has robustness characteristics similar to the PFC, that is, variations on a system parameter increase the steady state control effort and Floquet multipliers of the closed-loop stable orbit. The PBC depends on the system model to predict the free system future states and differences between this model and the real system degrade the closed-loop performance.

The aPBC is a new method for stabilization of periodic orbits proposed in this work and there are still many open questions about it. Several of these questions are outlined in Chapter 10. The numerical simulations were performed to show that it works, that it has some advantages comparing to other methods and evaluate some basic characteristics. The most important characteristic for application of the method is the necessity of the enlarged equation (7.40) composed by the $n(N-1)$ discretized states used for estimation of future states (n is the state-space and N is the number of discretization points). The method used in the numerical examples as implicit Runge-Kutta method is the orthogonal collocation. We concluded that a large N is necessary to obtain a stable solution. Small N leads to numerical integration errors. The relation between steady state error and control effort with the value of N is exponential, that is, reducing N the performance of the controller degrades exponentially.

Stabilizing TUPO2 and TUPO3 of the vdP oscillator. The TUPO2 and TUPO3 were chosen as examples of orbits that can not be stabilized by the DFC. There is not any theoretical limitation for the PFC and PBC on stabilizing them, but there is a practical

limitation for the aPBC. When stabilizing TUPO3 with the aPBC it would be necessary a huge number of discretization points N and this clearly shows the necessity of reducing N, for example, using a different implicit Runge-Kutta method.

Applying the aPBC to an autonomous system Finishing the examples, an autonomous system was used as case study for the aPBC. Basically it was not found any limitation in applying the method for these systems. It was verified again that the steady state error and control effort increase exponentially when decreasing N.

It was shown that for one periodic orbit of the Rössler system it was necessary less discretization points than for periodic orbits of the vdP oscillator to obtain values of d and υ equivalent. This is related to the smoother folds of the Rössler periodic orbit, parts of trajectories with sharp folds require more precise numerical integration. In the case of the implicit Runge-Kutta method the numerical integration precision is directly proportional to N. It is evident in Figure 8.29(c) that on some folds of the TUPO1 of the vdP oscillator the predicted trajectory oscillates around the expected value.

Implementation and discretization issues. For real-time applications, the implementation of the aPBC depends on the ability of computing the control signal between sample times of the sensor measurement. That is, the data should be read by the sensor, it should be processed, the value of the control signal should be computed and delivered to the actuator at the next sample time. A larger number of discretization points N used to predict the future values of the state and consequently a larger dimension of the closed-loop system implies higher computational effort.

When measurement is discrete, use of piecewise constant control is natural and yields to discrete-time system - just as studied in Part I. Due to the future state prediction, the right-hand side of the latter system corresponds to an approximation of the map associated to the (open-loop) continuous-time system with constant input, which maps $x(t)$ to $x(t+T)$. Thus, the analysis provided for discrete-time systems should be related, and to verify this claim is a point for further studies.

Chapter 10

Final comments and suggestions for future research

In this work, local stability of periodic orbits were studied using Floquet theory analyzing the linearized system in the close vicinity of the periodic orbit. It was shown that alternative results can be obtained using Lyapunov stability, although, this method was not applied. The linearized system in the closed vicinity of the periodic orbit is described by a linear time-periodic system, then the stabilization of periodic orbits of non-linear system is reduced to stabilization of this type of linear system. Basically is was shown that these linear systems can be stabilized via eigenvalues assignment using state feedback control methods. However, once the unstable periodic orbit already exists on the non-linear system, this characteristic can be used to stabilize them with ideal zero steady-state control effort.

Three stabilization methods which are ideally capable of achieving stabilization with zero steady state control effort were studied, proportional feedback control (PFC), delayed feedback control (DFC) and prediction-based feedback control (PBC). We are also interested in stable periodic orbits in the close vicinity of the target UPO, which leads to small steady state control effort.

The main contributions of the thesis are development of a new control law for the discrete-time PBC, a new design method for the continuous-time DFC and a new control

method based on the PBC applied to continuous-time system and are summarized in Section 1.1. All the methods studied and proposed were compared by numerical examples in Sections 4 and 8.

Results were provided in discrete and continuous-time systems. For continuous-time systems most of the effort was dedicated to the implementation of the PBC (or aPBC) and the approximation of the closed-loop monodromy matrix for the DFC. The prediction of the future state in the discrete-time case can be done numerically by computing the recursive evolution equation of the system at each time step; this computation is fast and the time between successive steps will be sufficient in most cases. For continuous-time systems the future state shall be obtained in real-time and this may not be done integrating the differential equation with an explicit integration method at each time instant.

Another problem related to the differential equation used to model the continuous-time system dynamics is the computation of the monodromy matrix, necessary for stability analysis and control gain design. This problem is explicitly solved in the case of the DFC, where the closed-loop system is represented by a DDE and has infinite dimension, requiring the discretization of past states to approximate the monodromy matrix. The computation of the monodromy matrix also affects the PBC, notice that for the discrete-time proposed control laws the free system monodromy matrix (or state-transition matrix) is required and readily computed. An equivalent control law for continuous-time systems was proposed, but the requirement of the free system monodromy matrix limited its implementation.

Considerations done in Chapters 5 and 8 allow to affirm that if the DFC method locally stabilizes the target UPO and satisfies the closed-loop system requirements (for example, size of basins of attraction, convergence rate, etc.) due to application simplicity (only necessitates to record past states) and low steady state control effort this method is indicated for stabilization of periodic orbits. Comparing robustness to parameter uncertainties, it was shown that, for a certain interval of the parameter variation, the DFC is the more robust method. Although, it was shown that the DFC has some limitations, not stabilizing certain types of orbits that are stabilized by the other methods. It was also shown that the DFC presents the smaller basins of attraction (at least for the discrete-

time systems), slower convergence rate and leads to the less stable orbits. Then, there are cases where the PFC or PBC/aPBC should be applied.

Comparing the PFC and the PBC/aPBC results in the question: what is the most feasible, to obtain an approximation of the target periodic orbit or to obtain the model of the non-linear system? Even if the orbit can be roughly approximated from time series of the system output, the system model or some control method is necessary to refine this approximation. It is known how to obtain UPOs if the system model is available using Newton-Raphson method. If the periodic orbit is stabilized by the DFC it can be recorded and used with the PFC, this was performed in the numerical simulations of Section 8.3.2 to refine the target orbit approximation. It should be evidenced that the control gain design, generally, requires the system model. Once the system model is obtained, it is possible to increase the control system robustness to parameters uncertainties and it is also possible to adjust the model when a parameter change identified. Resuming, in cases where the DFC does not satisfy the closed-loop system requirements, the PBC/aPBC is a feasible alternative.

Future works and open questions

Use of other techniques to control gain design applied to the methods. It was applied optimization using as cost function the largest magnitude Floquet multiplier to the DFC control gain design and it was proposed a deadbeat controller for the PBC applied to discrete-time systems. For continuous-time systems the PFC and PBC control gain design was performed in a non usual sense. We gave the control gain and computed the Floquet multipliers, then we chose the control gain that leaded to the smaller largest magnitude Floquet multiplier. It would be interesting to apply the direct Lyapunov method or eigenvalues assignment technique studied in Sections 3.2 and 7.2 to the linearized dynamic of the closed-loop system when using DFC, PFC of PBC. These methods may enable that, given the desired Floquet multiplier, the control gain is designed;

Control law for the non-invertible input matrix case applying PBC to discrete-time systems. A control law that does not necessitate previous knowledge about the target UPO and is applicable to discrete-time systems with a non-invertible input matrix was presented in Section 3.4.3. Theorem 3.19 was used to define mathematically the condition for application of the control law. However it is an open question the type of real system that satisfies the theorem and if this type of system is usual in engineering problems. Another open question is the expansion of the theorem to multi input systems;

Robustness analysis of the control methods. Both for discrete and continuous-time systems a numerical robustness analysis to parameters uncertainties of some control methods was performed. Although, it is necessary to do a similar analysis for the aPBC to compare with the other continuous-time controllers. It would be interesting also to analytically discuss the robustness of the aPBC and suggest methodologies to increase it since the prediction model will be subjected to uncertainties in real application;

Analysis of the PBC/aPBC subjected to noise. The prediction of the future state for the PBC/aPBC is based on the evolution in time of the actual value of the state variables. In practical applications this value is affected by noise, for example, the noise associated to the sensors used to measure the state outputs. The implication of this noise should be studied in future works because it decreases the estimation quality and can lead to the instability of the target UPO. Moreover, the proposed control laws for the discrete-time system depends on the cancellation of the linearized dynamics, which will not occur if the system is subjected to noise and this topic should be analyzed;

Design the aPBC control gain. The control gain used with the aPBC was designed for the PBC (for off-line continuous-time systems) and it was shown numerically that it is applicable to the aPBC for large N. That is, for a good estimation of the future state, the PBC control gain can be applied to the aPBC with satisfactory results. But the control gain design directly applied to the aPBC, and that consider the number of discretization points necessary to the approximation of the predicted state, is suggested as future work;

Reducing the number of discretization points for the aPBC. It was pointed as a weakness of the aPBC using orthogonal collocation with Lagrange polynomials that lots of collocation points are necessary to obtain stabilization and this number is related exponentially to the reduction of steady state error and control effort. But, considering future applications the worst point is that it is directly proportional to the number of extended states of the closed-loop system. A necessary future work is applying other methods to reduce N, for example using orthogonal collocation with Chebyshev polynomial or finite elements (maybe associated with orthogonal collocation) or other methods contained in the literature. Another question to be studied is why numerical integration becomes unstable when reducing N, this can be an important point aiming its reduction;

Apply alternative control laws to the aPBC avoiding dependence of previous knowledge of the target UPO. It was proposed in Section 7.4.3 an alternative method for stabilization of periodic orbits using the aPBC without previous knowledge of the target orbit. The suggested method was not applied due to necessity of estimation of the free-system state transition matrix along one period of the target UPO. This estimation and other control laws that do not require previous knowledge about the UPO are suggested as future work;

Basins of attraction for continuous-time systems. The basins of attraction of the stabilized orbits in continuous-time systems were not computed due to computational limitations. These basins of attraction are important for comparison between methods and are expected in future works;

Increase robustness to period uncertainties. Both DFC and aPBC require the previous knowledge of the target orbit period. For non-autonomous systems with forcing term this period is exactly known, however for other systems this is not necessarily true. For example, when applying the Newton-Raphson method it is obtained one point of the target UPO and its period with great precision. In other situations, for example obtaining UPOs from time series, the computed period might be a poor approximation of the real

period. Then, it would be interesting to increase the robustness of the method to this uncertainty, using for example some averaging methods.

Appendices

Appendix A

Dynamical systems - Definitions

The definitions of dynamical systems are presented in this appendix. Only the principal definitions are transcribed here, for a complete text on the subject see [41].

A.1 General concepts of dynamical systems

Definition A.1 (Dynamical system, see Definition 2.1.1 in [41]). *A structure* $\Sigma = (T, U, \mathcal{U}, X, Y, \varphi, \eta)$ *is said to be a dynamical system or state space system with time domain* T*, input value space* U*, input function space* $\mathcal{U}$*, state space* X*, output value space* Y*, state transition map* φ*, and output map* η*, if* T*,* U*,* $\mathcal{U}$*,* X*,* Y *are non void sets,* $T \subset \mathbb{R}$*,* $\mathcal{U} \subset U^T$*, and* $\eta : T \times X \times U \to Y$*,* $\varphi : \mathcal{D}_\varphi \to X$ *(where* $\mathcal{D}_\varphi \subset T^2 \times X \times \mathcal{U}$*) are functions such that the following axioms hold.*

Axiom 1 (Interval). *For every* $t_0 \in T$*,* $x^0 \in X$*,* $u(\cdot) \in \mathcal{U}$ *the life span of* $\varphi(\cdot, t_0, x^0, u(\cdot))$

$$T_{t_0, x^0, u(\cdot)} = \{t \in T; (t, t_0, x^0, u(\cdot)) \in \mathcal{D}_\varphi\}$$

is an interval in T *containing* t_0*.* □

Axiom 2 (Consistency). *For every* $t_0 \in T$*,* $x^0 \in X$*,* $u(\cdot) \in \mathcal{U}$

$$\varphi(t_0, t_0, x^0, u(\cdot)) = x^0. \quad \square$$

Axiom 3 (Causality). *For all* $t_0 \in T$, $x^0 \in X$, $u(\cdot), v(\cdot) \in \mathcal{U}$, $t_1 \in T_{t_0,x_0,u(\cdot)} \cap T_{t_0,x_0,v(\cdot)}$

$$(\forall t \in [t_0, t_1) : u(t) = v(t)) \quad \Rightarrow \quad \varphi(t_1, t_0, x^0, u(\cdot)) = \varphi(t_1, t_0, x^0, v(\cdot)). \quad \square$$

Axiom 4 (Co-cycle property). *If* $t_1 \in T_{t_0,x^0,u(\cdot)}$ *and* $x^1 = \varphi(t_1, t_0, x^0, u(\cdot))$ *for some* $t_0 \in T$, $x^0 \in X$, $u(\cdot) \in \mathcal{U}$ *then* $T_{t_1,x^1,u(\cdot)} \subset T_{t_0,x^0,u(\cdot)}$ *and*

$$\varphi(t, t_0, x^0, u(\cdot)) = \varphi(t, t_1, x^1, u(\cdot)), \quad t \in T_{t_1,x^1,u(\cdot)}. \quad \square$$

$\square$

U^T denotes the set of all functions $u(\cdot) : T \to U$. $\mathcal{U} \subset U^T$ is the set of admissible input functions, in general, it is not possible to admit arbitrary functions $u(\cdot) \in U^T$. We distinguish the notations between input *values* $u \in U$ and input *functions* $u(\cdot) \in \mathcal{U}$. $\mathcal{D}_\varphi$ is called the domain of definition of φ.

See [25] for supplementary reference on dynamical systems.

Definition A.2 (Differentiable system, see Definition 2.1.12 in [41]). *A dynamical system* $\Sigma = (T, U, \mathcal{U}, X, Y, \varphi, \eta)$ *is called differentiable if the following conditions are satisfied.*

- $T \subset \mathbb{R}$ *is an open interval.*
- U, Y *are subsets of* $\mathbb{K}^m$ *and* $\mathbb{K}^p$, X *is an open subset of* $\mathbb{K}^n$.
- *There exists a function* $f : T \times X \times U \to \mathbb{K}^n$ *such that for all* $t_0 \in T$, $x^0 \in X$, $u(\cdot) \in \mathcal{U}$ *the initial value problem*

$$\begin{aligned} \dot{x}(t) &= f(t, x(t), u(t)), \quad t \geq t_0, \quad t \in T \\ x(t_0) &= x^0 \end{aligned} \tag{A.1}$$

has a unique solution $x(\cdot)$ on a maximal open time interval I satisfying $I = T_{t_0,x^0,u(\cdot)}$ and $x(t) = \varphi(t, t_0, x^0, u(\cdot))$, $t \in I$.

- *$\eta : T \times X \times U \to Y$ is continuous.* □

$\mathbb{K}$ is an arbitrary field, either $\mathbb{R}$ or $\mathbb{C}$.

Definition A.3 (Recursive system, see Example 2.1.23 in [41])**.** *Let U, X, Y be non-empty sets, $T = \mathbb{N}$ or $\mathbb{Z}$ and*

$$f : T \times X \times U \to X, \quad \eta : T \times X \times U \to Y$$

be two arbitrary mappings. For any $u(\cdot) \in \mathcal{U} = U^T$, $t_0 \in T$, $x^0 \in X$ let $\varphi(t, t_0, x^0, u(\cdot))$, $t \in T$, $t \geq t_0$ be the unique solution of the recursive (or difference) equation

$$x(t+1) = f(t, x(t), u(t)) \tag{A.2}$$

with initial value $x(t_0) = x^0$. Then $\Sigma = (T, U, \mathcal{U}, X, Y, \varphi, \eta)$ is a discrete-time dynamical system. □

Definition A.4 (Time-periodic function)**.** *If $f(t + \tau, x, u) = f(t, x, u)$, for any $t \in T$, $x \in X$ and $u \in U$, then $f(t, x, u)$ is called a time-periodic function with minimal period τ.* □

Definition A.5 (Poincaré map)**.** *Let $\Sigma = (T, U, \mathcal{U}, X, Y, \varphi, \eta)$ be a differentiable dynamical system defined by a time-periodic function $f(t, x, u)$ with period τ_p for $x = x^*(t)$. A hyperplane $S \subset X$ defined such that $x^*(0) \in S$ and $x(t)$ crosses S transversally in the close vicinity of $x^*(0)$ is called Poincaré section. The Poincaré map $P(x) : S \to S$ is defined by $P^k(x^*(0)) = \{x^*(\tau_k) \in S : x^*(\tau_k) = \varphi(\tau_k, 0, x^*(0), 0)\}$. $\tau_k \in T$ is the time necessary for $\varphi(t, 0, x^*(0), 0)$ to cross S $k \in \mathbb{N}$ times. The discrete period $p \in \mathbb{N}$ is the minimal k such that $P^p(x^*(0)) = x^*(0) = x^*(\tau_p)$.*

A.2 Linear systems

Definition A.6 (Linear system, see Definition 2.1.26 in [41]). *Let $\mathbb{K}$ be an arbitrary field. A dynamical system Σ is said to be $\mathbb{K}$-linear if*

- *U, $\mathcal{U}$, X, Y are vector spaces over $\mathbb{K}$,*
- *the maps*

$$\varphi(t, t_0, \cdot, \cdot) : X \times \mathcal{U} \to X \quad \text{and} \quad \eta(t, \cdot, \cdot) : X \times U \to Y$$

are $\mathbb{K}$-linear for all $t, t_0 \in T$, $t \geq t_0$.

□

The second condition implies that

$$\varphi(t, t_0, 0_X, 0_{\mathcal{U}}) = 0_X, \quad t, t_0 \in T, \quad t \geq t_0$$

where 0_X is the origin in X and $0_{\mathcal{U}}$ the origin in $\mathcal{U}$ (zero function). This means that 0_X is an equilibrium state of Σ under the control $0_{\mathcal{U}}$ whenever Σ is linear.

Remark A.7 (Superposition principle, see page 100 in [41]). *Let $\mathbb{K}$ be an arbitrary field and $\Sigma = (T, U, \mathcal{U}, X, Y, \varphi, \eta)$ a $\mathbb{K}$-linear system, then for every $t_0, t \in T$, $t \geq t_0$ and $\lambda_i \in \mathbb{K}$, $x_i \in X$, $u_i \in U$, $u_i(\cdot) \in \mathcal{U}$, $i = 1, \ldots, k$ we have*

$$\varphi(t, t_0, \sum_{i=1}^{k} \lambda_i x_i, \sum_{i=1}^{k} \lambda_i u_i(\cdot)) = \sum_{i=1}^{k} \lambda_i \varphi(t, t_0, x_i, u_i(\cdot))$$
$$\eta(t, \sum_{i=1}^{k} \lambda_i x_i, \sum_{i=1}^{k} \lambda_i u_i) = \sum_{i=1}^{k} \lambda_i \eta(t, x_i, u_i). \quad \square$$

A special case of the superposition principle is the *decomposition principle*:

$$\varphi(t, t_0, x^0, u(\cdot)) = \varphi(t, t_0, x^0, 0_{\mathcal{U}}) + \varphi(t, t_0, 0_X, u(\cdot)).$$

The decomposition law leads us to introduce the following two families of linear maps. For any pair of times $(t, t_0) \in T^2$, $t \geq t_0$, we define the *evolution operator* $\Phi(t, t_0) : X \to X$ by

$$\Phi(t, t_0)x = \varphi(t, t_0, x, 0_{\mathcal{U}}), \quad x \in X \tag{A.3}$$

and the input-to-state map $\Theta(t, t_0) : \mathcal{U} \to X$ by

$$\Theta(t, t_0)u(\cdot) = \varphi(t, t_0, 0_x, u(\cdot)), \quad u(\cdot) \in \mathcal{U}. \tag{A.4}$$

The Axioms 2 and 4 of a state transition map imply the following basic equations

$$\begin{aligned} \Phi(t, t) &= I_X, \qquad t \in T \\ \Phi(t_2, t_1) \circ \Phi(t_1, t_0) &= \Phi(t_2, t_0), \quad t_0, t_1, t_2 \in T, \quad t_0 \leq t_1 \leq t_2. \end{aligned} \tag{A.5}$$

Let $L^q_{\text{loc}}(T, X)$ be the space of q-integrable functions $x : T \to X$ and $PC(T, X)$ be a space of piecewise continuous functions $x : T \to X$.

Definition A.8 (Linear hyperbolic map, see Definition 1.2.5 in [50])**.** *A linear map of* $\mathbb{K}$ *is called hyperbolic if all of its eigenvalues have absolute values different from one.* □

Definition A.9 (Linear differentiable systems, see Example 2.2.1 in [41])**.** *Let* $T \subset \mathbb{R}$ *be an interval,* $X = \mathbb{K}^n$, $U = \mathbb{K}^m$, $Y = \mathbb{K}^p$, $\mathcal{U}$ *any linear subspace of* $L^1_{loc}(T, \mathbb{K}^m)$*, e.g.* $\mathcal{U} = PC(T, \mathbb{K}^m)$ *and* $A(\cdot) \in PC(T, \mathbb{K}^{n\times n})$*,* $B(\cdot) \in PC(T, \mathbb{K}^{n\times m})$*,* $C(\cdot) \in PC(T, \mathbb{K}^{p\times n})$*,* $D(\cdot) \in PC(T, \mathbb{K}^{p\times m})$*.* $\Sigma = (T, U, \mathcal{U}, X, Y, \varphi, \eta)$ *is a linear differentiable system defined by the matrix-valued functions* $A(\cdot)$*,* $B(\cdot)$*,* $C(\cdot)$*,* $D(\cdot)$ *with state transition map*

$$\varphi(t, t_0, x^0, u(\cdot)) = X(t, t_0)x^0 + \int_{t_0}^{t} X(t, s)B(s)u(s)\, ds, \quad t \in T. \tag{A.6}$$

and output map

$$\eta(t, x, u) = C(t)x + D(t)u.$$

$X(t, t_0)$ is the fundamental matrix associated with the initial value problem with unique solution [41, Corollary 2.1.20]

$$\begin{aligned} \dot{x}(t) &= A(t)x(t) + B(t)u(t), \quad t \in T \\ x(t_0) &= x^0 \end{aligned} \tag{A.7}$$

for all $u(\cdot) \in \mathcal{U}$, $t_0 \in T$, $x^0 \in X$. By definition, $X(t, t_0)$ is the solution of the matrix differential equation

$$\begin{aligned} \frac{dX(t, t_0)}{dt} &= A(t)X(t, t0), \quad t \in T \\ X(t_0, t_0) &= I_n, \end{aligned}$$

where I_n is the identity matrix of order n. □

Let us now determine the linear operators $\Phi(t, t_0)$, $\Theta(t, t_0)$ associated with Σ. As an immediate consequence of (A.3) and (A.6) we obtain for all $t_0, t \in T$

$$\Phi(t, t_0)x = X(t, t_0)x.$$

So the fundamental matrix of (A.7) is just the matrix representation of the evolution operator $\Phi(t, t_0)$ with respect to the standard basis of $\mathbb{K}^n$. We use the same notation $\Phi(t, t_0)$ for both the linear operators and their matrix representations, called *state transition matrix* [33]. Since $\Phi(t, t_0)\Phi(t_0, t) = I_n$ (A.5), the operators $\Phi(t, t_0)$, $t, t_0 \in T$ are invertible. From (A.4) and (A.6) we obtain for all $t_0, t \in T$

$$\Theta(t, t_0)u(\cdot) = \int_{t_0}^{t} \Phi(t, s)B(s)u(s)\, ds, \quad u(\cdot) \in \mathcal{U}.$$

This specifies the relation between the input-to-state operators $\Theta(t, t_0)$ and the evolution operator $\Phi(t, s)$ for the system Σ.

Definition A.10 (Periodic linear differentiable system, adapted from page 12 in [2]). *If* $A(t) = A(t+\tau)$ *and* $B(t) = B(t+\tau)$, $\forall t \in T$, *then the linear differentiable system* (A.7) *assumes the form*

$$\dot{x}(t) = A(t)x(t) + B(t)u(t), \qquad t + \tau \in T_{t,x,u(\cdot)}. \tag{A.8}$$

We call such an equation a linear periodic differentiable system with period τ. □

Definition A.11 (Linear difference systems, see Example 2.2.2 in [41]). *Let* $\mathbb{K}$ *be an arbitrary field,* $U = \mathbb{K}^m$, $X = \mathbb{K}^n$, $Y = \mathbb{K}^p$, $T \subset \mathbb{Z}$ *a time-domain satisfying* $t \in T \Rightarrow t + 1 \in T$, $\mathcal{U} = U^T$, *and* $A(\cdot) = (A(t))_{t\in T}$, $B(\cdot) = ((B(t))_{t\in T}$, $C(\cdot) = (C(t))_{t\in T}$, $D(\cdot) = (D(t))_{t\in T}$ *sequences of* $n\times n$, $n\times m$, $p\times n$, $p\times m$ *matrices over* $\mathbb{K}$. $\Sigma = (T, U, \mathcal{U}, X, Y, \varphi, \eta)$ *is a linear difference system defined by the matrix-valued functions* $A(\cdot)$, $B(\cdot)$, $C(\cdot)$, $D(\cdot)$ *with state transition map*

$$\varphi(t, t_0, x^0, u(\cdot)) = \Phi(t, t_0)x^0 + \sum_{s=t_0}^{t-1} \Phi(t, s+1)B(s)u(s), \quad t \in T_{t_0}$$

and output map

$$\eta(t, x, u) = C(t)x + D(t)u.$$

$\Phi(t, t_0)$ *is the fundamental matrix associated with the initial value problem with unique solution*

$$\begin{aligned} x(t+1) &= A(t)x(t) + B(t)u(t), \quad t \in T \\ x(t_0) &= x^0. \end{aligned} \tag{A.9}$$

for all $u(\cdot) \in \mathcal{U}$, $t_0 \in T$, $x^0 \in X$. *By definition,* $\Phi(t, t_0)$ *is the solution of the matrix product*

$$\Phi(t, t_0) = A(t-1)A(t-2)\dots A(t_0), \quad t, t_0 \in T, t_0 < t.$$

and $\Phi(t_0, t_0) = I_n$ *for all* $t_0 \in T$. □

As done for the linear differentiable system, we call the matrix representation of the evolution operator $\Phi(t, t_0)$ as *state transition matrix*. The associated input-to-state operator $\Theta(t, t_0)$ can again be expressed in terms of the evolution operator $\Phi(t, s)$,

$$\Theta(t, t_0)u(\cdot) = \sum_{s=t_0}^{t-1} \Phi(t, s+1)B(s)u(s), \quad u(\cdot) \in \mathcal{U}, t_0, t \in T, \quad t_0 < t.$$

Definition A.12 (Periodic linear difference system, adapted from page 62 in [2])**.** *If* $A(t) = A(t+\tau)$ *and* $B(t) = B(t+\tau)$, $\forall t \in T$, *then the linear difference system* (A.9) *assumes the form*

$$x(t+1) = A(t)x(t) + B(t)u(t) = A(t+\tau)x(t) + B(t+\tau)u(t), \quad t+\tau \in T_{t,x,u(\cdot)}. \quad \text{(A.10)}$$

We call such an equation a linear periodic difference system with period τ. □

Definition A.13 (Monodromy matrix, adapted from page 74 in [5])**.** *The linear evolution operator matrix of* (A.8) *or* (A.10) *over one period* τ

$$\Psi(t) = \Phi(t+\tau, t), \quad \forall t \in T,$$

is defined as monodromy matrix at time t. □

Appendix B

Stability of dynamical systems

The definitions of stability are presented in this appendix as a complement to the definitions on dynamical systems shown in Appendix A. Only the main definitions are transcribed here, for a complete text on the subject see e.g. [41].

We introduce the basic notations of stability for local flows $\mathcal{F} = (T, X, \varphi)$ on a metric space (X, d). Consider time domains T which are unbounded to the right and assume that the control $\bar{u}(\cdot) \in \mathcal{U}$ is fixed and neglect the output. We study the local flow $\mathcal{F} = (T, X, \varphi)$ determined by the fixed control $\bar{u}(\cdot)$

$$\varphi(t, t_0, x^0) = \varphi(t, t_0, x^0, \bar{u}(\cdot)), \quad t \in T_{t_0}(x^0) := T_{t_0, x^0, \bar{u}(\cdot)}, \quad (t_0, x^0) \in T \times X.$$

Definition B.1 (Local flow, see Definition 3.1.1 in [41]). *$\mathcal{F} = (T, X, \varphi)$ is said to be a local flow with time domain $T \subset \mathbb{R}$ and state transition function φ on a metric space (X, d), if for every $(t_0, x^0) \in T \times X$ there exists $t_+(t_0, x^0) \in (t_0, \infty]$ such that $\varphi(t, t_0, x^0) \in X$ is defined for all $t \in T_{t_0}(x^0) = T \cap [t_0, t_+(t_0, x^0))$ and satisfies for all $(t_0, x^0) \in T \times X$, $t, t_1 \in T_{t_0}(x^0)$, $t \geq t_1$*

- $\varphi(t_0, t_0, x^0) = x^0$.
- $T_{t_1}(\varphi(t_1, t_0, x^0)) = T_{t_1} \cap T_{t_0}(x^0)$ *and* $\varphi(t, t_0, x^0) = \varphi(t, t_1, \varphi(t_1, t_0, x^0))$.

- *The map* $(t, s, x) \mapsto \varphi(t, s, x)$ *is continuous in the sense: If* (t_k, s_k, x^k) *converges in* $T \times T \times X$ *to* (t, s, x) *where* $t \in T_s(x)$, $t > s$, *then* $t_k \in T_{s_k}(x^k)$ *for* k *sufficiently large and* $\lim_{k\to\infty} \varphi(t_k, s_k, x^k) = \varphi(t, s, x)$. □

$\mathcal{F} = (T, X, \varphi)$ is called a *global flow* if additionally $t_+(t_0, x^0) = \infty$ for all $(t_0, x^0) \in T \times X$.

Recall that in any metric space (X, d) the *distance* between a point $x \in X$ and a subset $S \subset X$ is defined by

$$\operatorname{dist}(x, S) = \inf\{d(x, y); y \in S\}.$$

For every t_0, the set of initial states $x^0 \in X$ which generate, at time t_0, trajectories with *infinite life span* is denoted by

$$X_\infty(t_0) = \{x^0 \in X; t_+(t_0, x^0) = \infty\}.$$

B.1 Stability of an equilibrium state

Suppose that $\bar{x}$ is an *equilibrium state* of a local flow $\mathcal{F}$, i.e. $\varphi(t, t_0, \bar{x}) = \bar{x}$ for all $t \in T_{t_0}$, $t_0 \in T$.

Definition B.2 (Open ball)**.** *The open ball of radius* $\delta > 0$ *and centre* $\bar{x} \in X$, *is defined by*

$$B(\bar{x}, \delta) = \{x \in X; d(\bar{x}, x) < \delta\}. \quad \square$$

Definition B.3 (Stability of equilibrium state, see Definition 3.1.8 in [41])**.** *An equilibrium state* $\bar{x}$ *of a local flow* $\mathcal{F}$ *is stable at time* $t_0 \in T$ *if for all* $\epsilon > 0$ *there exists* $\delta = \delta(\epsilon, t_0)$ *such that* $B(\bar{x}, \delta) \subset X_\infty(t_0)$ *and*

$$x^0 \in B(\bar{x}, \delta) \Rightarrow \varphi(t, t_0, x^0) \in B(\bar{x}, \epsilon), \quad t \in T_{t_0}. \quad \square$$

Definition B.4 (Asymptotic stability of an equilibrium state, see Definition 3.1.9 in [41])**.**

- *An equilibrium state $\bar{x}$ of a local flow $\mathcal{F}$ is called attractive at time t_0 if there exists $\rho = \rho(t_0) > 0$ such that $B(\bar{x}, \rho) \subset X_\infty(t_0)$ and*

$$x^0 \in B(\bar{x}, \rho) \Rightarrow \lim_{t\to\infty} \varphi(t, t_0, x^0) = \bar{x}.$$

- *$\bar{x}$ is said to be asymptotically stable at time t_0, if it is stable and attractive at time t_0.*

- *If $\bar{x}$ is attractive the basin of attraction of $\bar{x}$ at time t_0 is given by*

$$\mathcal{A}(t_0, \bar{x}) = \left\{ x^0 \in X_\infty(t_0); \lim_{t\to\infty} \varphi(t, t_0, x^0) = \bar{x} \right\}.$$

  $\bar{x}$ is said to be globally attractive at time t_0 if $\mathcal{A}(t_0, \bar{x}) = X$. □

Definition B.5 (Exponential stability of an equilibrium state, see Definition 3.2.19 in [41])**.** *An equilibrium point $\bar{x}$ of the non-linear system* (A.1) *or* (A.2) *is said to be exponentially stable at time t_0 if it is stable and exponentially attractive at time t_0, i.e. there are $\delta = \delta(t_0) > 0$, $M = M(t_0) > 0$, $\omega = \omega(t_0) < 0$, such that $\varphi(t, t_0, x^0)$ exists for all $t \in T_{t_0}$ and*

$$\|x^0 - \bar{x}\| < \delta \quad \Rightarrow \quad \|\varphi(t, t_0, x^0) - \bar{x}\| \leq M e^{\omega(t-t_0)}, \quad t \in T_{t_0}. \tag{B.1}$$

If $\bar{x}$ is uniformly stable and (B.1) *holds with constants δ, M, ω independent of t_0 then $\bar{x}$ is said to be uniformly exponentially stable.* □

B.2 Stability of a trajectory

Definition B.6 (Stability of a trajectory, see Definition 3.1.6 in [41])**.** *A trajectory $t \mapsto \varphi(t, t_0, \bar{x})$, $\bar{x} \in X_\infty(t_0)$ of a local flow $\mathcal{F}$ is said to be stable at time $t_0 \in T$ if for all $\epsilon > 0$, there exists $\delta = \delta(\epsilon, t_0) > 0$ such that $B(\bar{x}, \delta) \subset X_\infty(t_0)$ and for all $x^0 \in B(\bar{x}, \delta)$*

$$d(\varphi(t, t_0, x^0), \varphi(t, t_0, \bar{x})) < \epsilon, \quad t \in T_{t_0}. \quad \square$$

Definition B.7 (Asymptotic stability of a trajectory, see Definition 3.1.7 in [41]). *A trajectory $t \mapsto \varphi(t, t_0, \bar{x})$, $\bar{x} \in X_\infty(t_0)$ is said to be asymptotically stable at time $t_0 \in T$ if it is stable at time t_0 and there exists $\rho = \rho(t_0) > 0$ such that $B(\bar{x}, \rho) \subset X_\infty(t_0)$ and for all $x^0 \in B(\bar{x}, \rho)$*

$$\lim_{t\to\infty} d(\varphi(t, t_0, x^0), \varphi(t, t_0, \bar{x})) = 0, \quad t \in T_{t_0}. \quad \square \tag{B.2}$$

The trajectory $\varphi(t, t_0, x^0)$ is called *uniformly stable* or *uniformly asymptotically stable* if in the previous definitions δ, ρ do not depend on t_0 and the limit in (B.2) is uniform in t_0. If $\mathcal{F}$ is time-invariant then (asymptotic) stability implies uniform (asymptotic) stability.

B.3 Stability of an invariant set

To describe the asymptotic behaviour of more complicated systems the stability concepts for equilibrium states have to be extended to arbitrary closed[1] invariant subsets of the state space.

Definition B.8 (Invariant set, see Definition 3.1.4 in [41]). *A non-empty subset $S \subset X$ is said to be weakly invariant for $\mathcal{F}$ if $(t_0, x) \in T \times S$ implies $\varphi(t, t_0, x) \in S$ for all $t \in T_{t_0}(x)$. It is said to be invariant for $\mathcal{F}$ if in addition $S \subset X_\infty(t_0)$ for all $t_0 \in T$.* $\square$

Definition B.9 (Stable invariant set, adapted from Definition 3.1.25 in [41]). *A closed invariant subset $\Omega \subset X$ is said to be stable at time t_0 if every neighbourhood W of Ω there exists a neighbourhood V of Ω such that $V \subset X_\infty(t_0)$ and, for each $x^0 \in V$, $\varphi(t, t_0, x^0) \in W$ for all $t \in T_{t_0}$.* $\square$

Definition B.10 (Attractor, adapted from Definition 3.1.25 in [41]). *A closed invariant subset $\Omega \subset X$ is called an attractor at time t_0 if there exists a neighbourhood V of Ω such that $V \subset X_\infty(t_0)$ and $\varphi(t, t_0, x^0) \to \Omega$ as $t \to \infty$ for every $x^0 \in V$.*

The basin of attraction of an attractor Ω at time t_0 is given by

$$\mathcal{A}(t_0, \Omega) = \{x \in X_\infty(t_0); \varphi(t, t_0, x) \to \Omega \text{ as } t \to \infty\}. \quad \square$$

[1] We recall that the closed set of a metric space is any set which contains all the limits of its converging sequences.

B.3.1 Stability of a periodic orbit

Definition B.11 (Periodic orbit)**.** *A closed invariant subset $P \subset X$ of $\mathcal{F}$ is said to be a periodic orbit of period τ if $\varphi(t+\tau, t, x^*) = x^*$ for all $x^* \in P$.* □

Definition B.12 (Asymptotically stable periodic orbit)**.** *A closed invariant subset $P \subset X$ is said to be an asymptotically stable periodic orbit if P is a periodic orbit and P is an attractor.* □

B.4 Stability of linear systems

We consider systems of the form

$$\dot{x}(t) = Ax(t), \quad t \in T, \quad (\text{resp. } x(t+1) = Ax(t), \quad t \in T) \tag{B.3}$$

where $A \in \mathbb{K}^{n\times n}$ and $T = \mathbb{R}_+$ (resp. $T = \mathbb{N}$). The following result relates growth properties of $x(t)$ to the spectrum of A, $\sigma(A)$.

Lemma B.13 (see Lemma 3.3.19 in [41])**.** *Given $A \in \mathbb{K}^{n\times n}$ and $\omega \in \mathbb{R}$. If*

$$\alpha(A) = \max\{\operatorname{Re}\lambda; \lambda \in \sigma(A)\} < \omega, \quad (\textit{resp. } \varrho(A) = \max\{|\lambda|; \lambda \in \sigma(A)\} < e^{\omega})$$

then there exists M, depending on ω such that

$$\|e^{At}\| \leq Me^{\omega t}, \quad t \in \mathbb{R}_+, \quad (\textit{resp. } \|A^t\| \leq Me^{\omega t}, \quad t \in \mathbb{N}).$$ □

Theorem B.14 (see Theorem 3.3.20 in [41])**.** *The system* (B.3) *is asymptotically (or, equivalently, exponentially) stable if and only if* $\operatorname{Re}\lambda < 0$*, in the continuous-time case, or* $|\lambda| < 1$*, in the discrete-time case,* $\lambda \in \sigma(A)$*.* □

The stability of the linear homogeneous systems (B.4a) and (B.4b), derived from (A.7) and (A.9) respectively, with $A(t)$ τ-periodic is determined according to Proposition B.15.

$$\dot{x}(t) = A(t)x(t), \quad t \in T \subset \mathbb{R} \tag{B.4a}$$

$$x(t+1) = A(t)x(t), \quad t \in T \subset \mathbb{Z} \tag{B.4b}$$

with $x(t_0) = x^0$.

Proposition B.15 (see Proposition 3.3.6 in [41])**.** *Suppose the generators $A(\cdot)$ of* (B.4) *are periodic with period $\tau \in T$, $T = \mathbb{R}$ or $\mathbb{Z}$, $\tau > 0 : A(t+\tau) = A(t)$, $t \in T$. Then* (B.4) *is uniformly stable (uniformly asymptotically stable) if and only if the time-invariant discrete time system*

$$\hat{x}(k+\tau) = \Phi(\tau, 0)\hat{x}(k), \quad k \in \mathbb{N}$$

is stable (asymptotically stable) where Φ is the evolution operator generated by (B.4)*.* □

Remark B.16. *According to Definition A.13, the evolution operator $\Phi(\tau, 0)$ on Proposition B.15 is called monodromy matrix.* □

Remark B.17. *The eigenvalues of the monodromy matrix are called Floquet characteristic multipliers or characteristic multipliers or Floquet multipliers $\mu \in \mathbb{C}$ of system* (B.4) *and it is uniformly asymptotically stable if all the Floquet multipliers are inside the open unity circle.* □

Remark B.18. *The Floquet characteristic exponents or characteristic exponents or Floquet exponents $\lambda \in \mathbb{C}$ are calculated as*

$$\mu = \begin{cases} e^{\lambda\tau}, \text{ in the case of } (\text{B.4a}) \\ \lambda^{\tau}, \text{ in the case of } (\text{B.4b}) \end{cases}$$

and system (B.4a) *(or* (B.4b)*) is uniformly asymptotically stable if for all λ associated to all eigenvalues μ of the monodromy matrix,* $\mathrm{Re}(\lambda) < 0$ *(or $|\lambda| < 1$).* □

Appendix C

Monodromy matrix for discrete-time delayed feedback control

In this appendix we provide the necessary equations to the calculus of the monodromy matrix for the system controlled by the DFC with a constant gain matrix K (C.1).

$$x_{k+1} = f(k, x_k, K(x_{k-p} - x_k)) \tag{C.1}$$

$x : \mathbb{N} \to \mathbb{R}^n$, $K \in \mathbb{R}^{n\times n}$, $f : \mathbb{N} \times \mathbb{R}^n \times \mathbb{R}^n \to \mathbb{R}^n$ and $k, p, n \in \mathbb{N}$.

The state vector x_k is not sufficient to represent the dynamics of the closed-loop system with the DFC. We define an extended state vector X_k and control signal U_k as follows:

$$X_k = \begin{bmatrix} x_k \\ x_{k-1} \\ \vdots \\ x_{k-p} \end{bmatrix} \in \mathbb{R}^{n(1+p)}, \quad U_k = \begin{bmatrix} u_k \\ u_{k-1} \\ \vdots \\ u_{k-p} \end{bmatrix} \in \mathbb{R}^{n(1+p)}.$$

The map φ_{est} is defined as in (3.27) using the extended vector state. Observe that x_k and x_{k-p} are the first and last n states of X_k, respectively:

$$X_{k+p} = \varphi_{est}(k + p, k, X_k, U_k(X_k)).$$

The monodromy matrix for the periodic orbit of the extended system is obtained directly from (3.31). We define a new function (C.2), an extension of (3.30) for the DFC, and its Jacobian matrix for each point of the orbit is given by (C.3).

$$\psi_{est}(X,K) \doteq \begin{bmatrix} 0_{n\times np} & 0_{n\times n} \\ I_{np\times np} & 0_{np\times n} \end{bmatrix} X + \begin{bmatrix} f\left(k, \begin{bmatrix} I_{n\times n} & 0_{n\times np} \end{bmatrix} X\right) + K \begin{bmatrix} -I_{n\times n} & 0_{n\times n(p-1)} & I_{n\times n} \end{bmatrix} X \\ - \\ 0_{np\times 1} \end{bmatrix} \tag{C.2}$$

$$\nabla_X \psi_{est}(X,K)\,\big|_{X=X_k^*} = \begin{bmatrix} 0_{n\times np} & 0_{n\times n} \\ I_{np\times np} & 0_{np\times n} \end{bmatrix} + \begin{bmatrix} \nabla_x f(k,x)\,\big|_{x=x_k^*} + K \begin{bmatrix} -I_{n\times n} & 0_{n\times n(p-1)} & I_{n\times n} \end{bmatrix} \\ - \\ 0_{np\times n(1+p)} \end{bmatrix} \tag{C.3}$$

Appendix D

Publications

T. P. Chagas, P.-A. Bliman and K. H. Kienitz, New feedback laws for stabilization of unstable periodic orbits, in *8th IFAC Symposium on Nonlinear Control Systems*, (Bologna, Italy), Set. 2010

New feedback laws for stabilization of unstable periodic orbits

Thiago P. Chagas [*,**] **Pierre-Alexandre Bliman** [*]
Karl H. Kienitz [**]

[*] *INRIA, Rocquencourt BP105, 78153 Le Chesnay cedex, France*
[**] *Dept. of Control and Systems, Instituto Tecnológico de Aeronáutica, 12228-900 São José dos Campos - SP, Brazil*

Abstract: In this note a gain tuning scheme for prediction-based chaos control of discrete-time systems is proposed, extending previous work by T. Ushio and S. Yamamoto. The derived control laws are proved to be stabilizing. Three different time-invariant or time-varying laws are proposed, leading to different convergence rates and sizes for the basins of attraction. The results are illustrated by numerical simulations. A parallel between finding unstable periodic orbits and chaos control is done.

Keywords: Nonlinear systems, Discrete time systems, Prediction-based chaos control, Stability condition, Stabilization, Unstable periodic orbits.

1. INTRODUCTION

Chaos control, originally proposed by Ott *et al.* [10], aims at eliminating chaotic behavior in nonlinear dynamical systems. It specifically uses chaos basic characteristics [3] to obtain stable periodic solutions with small control effort. These characteristics are related to the infinite number of unstable periodic orbits (UPO) embedded in the chaotic sets [2] and these UPOs are the target of the chaos control methods.

Two characteristics of the UPOs proved to be of interest when applying chaos control. The first is the relation period vs. stability and the second is the relation period vs. number of periodic orbits [2, 4]. It is known that the instability (measured, for example, by an unstable Floquet exponent [5]) and the quantity of periodic orbits grow exponentially with period, being more difficult to stabilize longer orbits.

A quite popular chaos control method, discovered by Pyragas, is the Delayed Feedback Control (DFC), see [13] and extensions in [16]. The method is based on ensuring zero error between the actual state and the state delayed by the period of the target UPO. The error is multiplied by a constant and scalar gain properly tuned to take it to zero. The DFC method has the advantage that it does not presuppose prior knowledge of the periodic orbit to be stabilized (except the value of the period itself). It is also known that the DFC, as first proposed, cannot stabilize long periodic orbits [15].

Alternative prediction-based ideas for chaos control has been presented by Ushio and Yamamoto [17], using comparison of the actual state with the *future* state distant from the period of the UPO under consideration, *computed along the trajectories of the open-loop system*. This provides simple ways for developing gain tuning methods [9], see also interesting extension in [12].

The present paper proposes a method to define the gain used in the structure presented in [17]. The difference is that, here, the control scheme is based on improved sufficient stability conditions and leads to stabilizing gains. Three control laws are proposed. They lead to different behaviors in terms of convergence rate and size of attraction basin. One of them (the "third one" below) does not need prior knowledge of the target UPO.

In Section 2 of this note analytical results for a sufficient stability condition of periodic orbits are described. In Section 3 the control laws are proposed. In Section 4 numerical results using the Logistic and Henon maps show the control laws characteristics. The conclusions are presented in Section 5.

2. SUFFICIENT STABILITY CONDITION FOR PERIODIC ORBITS

Consider the nonlinear discrete time dynamical system described by

$$x(k+1) = \phi(x(k)),\ x(k) \in \mathbb{R}^n,\ k, n \in \mathbb{N}. \tag{1}$$

We assume the existence of a hyperbolic periodic orbit x^* of period $p \in \mathbb{N}$ of (1), that orbit x^* satisfies:

$$x^*(k+p) = x^*(k), \quad \forall k \in \mathbb{N}. \tag{2}$$

If there is a chaotic set in the n-dimensional state space formed by $x(k)$, it is known that the chaotic set is composed by an infinite number of UPOs [1, 3] and the number of UPOs per period p increases exponentially with p [2, 4].

Ushio and Yamamoto [17] proposed a control scheme to stabilize UPOs embedded in a chaotic set, which is described by

[1] Support is acknowledged from CAPES in Brazil and COFECUB in France, through the CAPES/COFECUB project "Systèmes oscillatoires en Automatique: modélisation, réduite, analyse, identification et synthèse de commande", n Ma 624/09.

$$x(k+1) = \phi(x(k)) + K(\phi^p(x(k)) - x(k)). \quad (3)$$

Here $K \in \mathbb{R}^{n\times n}$ is a constant gain matrix, p is the period of the target UPO, and ϕ^p is defined recursively by the composition: $\phi^1 = \phi$, $\phi^{q+1} = \phi^q \circ \phi$, $q \in \mathbb{N}$. In the sequel, for any $x \in \mathbb{R}^n, K \in \mathbb{R}^{n\times n}$, we use the notation

$$\psi(x, K) \doteq \phi(x) + K(\phi^p(x) - x). \quad (4)$$

Clearly, any p-periodic orbit of the open-loop system (1) is also a p-periodic orbit of the closed-loop system (3). The main characteristic of this control scheme is the use of the error between the future state at $k+p$ *computed on the open-loop system* and the actual state at k. Similar ideas, using the future state, are also used in [17] (constant matrix gains) and in [12] (constant scalar gains, that can be rendered arbitrarily small by using $(\phi^{m+p}(x(k)) - \phi^m(x(k)))$ in (3) instead of $(\phi^p(x(k)) - x(k))$, for large enough integer m).

The control law we propose in the sequel (the precise definitions are stated in Section 3) are improvements of (3) based on non-constant gains. The new control scheme is defined by

$$x(k+1) = \psi(x(k), K(x(k), k)), \quad (5)$$

for gain $K(x(k), k) \in \mathbb{R}^{n\times n}$ depending a priori both on time and actual state. We will only consider in the remaining the gains K that are differentiable with respect to x. Let us define Ψ, the transition from $x(k)$ to $x(k+p)$, by the following map:

$$x(k+p) = \Psi(x(k), k). \quad (6)$$

By definition, $\Psi(x(k), k)$ is defined recursively as:

$$\begin{aligned} y_k &= x(k) \\ y_{k+l+1} &= \psi(y_{k+l}, K(y_{k+l}, k+l)),\ l = 0, \ldots, p-1 \\ \Psi(x, k) &= y_{k+p}. \end{aligned}$$

Lemma 1. For any point $x^*(k)$, $k \in \mathbb{N}$, of the trajectory x^* of the closed-loop system (5), one has

$$\nabla_x \Psi(x, k)\,\big|_{x=x^*(k)} = \prod_{l=0}^{p-1} \nabla_x \psi(x, K(x^*(k+l), k+l))\,\big|_{x=x^*(k+l)} \quad (7)$$

where, in (7) and in the sequel, the matrices in the product are ordered from right to left for increasing indices l. □

The interest of formula (7) is that no derivative with respect to K appears in the right-hand side. Thus, Lemma 1 provides a simplification in the computation of the Jacobian spectrum: as indicated by (7), the dependence of the gain with respect to the state does not modify the Jacobian in the points of the periodic orbit.

Proof. Computation of the derivative can be made by the general chain rule [8]. By recursion,

$$\nabla_x \Psi(x, k)\,\big|_{x=x^*(k)} = \prod_{l=0}^{p-1} \nabla_x \psi(x, K(x, k+l))\,\big|_{x=x^*(k+l)}\ .$$

Now, using the definition of ψ, see (4), one sees that, for any $k \in \mathbb{N}$, the (i,j)-th component of

$$\nabla_x \psi(x, K(x,k))\,\big|_{x=x^*(k)} - \nabla_x \psi(x, K(x^*(k), k))\,\big|_{x=x^*(k)}$$

is equal to

$$\sum_{j'=1}^{n} \left(\left.\frac{\partial K_{ij'}(x,k)}{\partial x_j}\right|_{x=x^*(k)} \cdot (\phi^p(x^*(k)) - x^*(k))_{j'} \right).$$

As $x^*(k)$ is located on the periodic orbit, we have $\phi^p(x^*(k)) = x^*(k)$, and the last term of the sum is zero. This provides the desired result. □

The UPO x^* of system (1) verifies

$$x^*(k+p) = x^*(k) = \Psi(x^*(k), k). \quad (8)$$

When the gain $K(k)$ is p-periodic, then $\nabla_x \Psi(x^*(k), k)$ is the monodromy matrix associated to the orbit x^* of the closed-loop system (6). In general, the stability of the periodic orbit of system (6) is related to the spectrum of the Jacobian. More precisely, a sufficient stability condition is that the modulus of the eigenvalues are less the 1. Here, our idea is to place all the eigenvalues at zero, with the aim of ensuring fast convergence in the vicinity of the controlled orbit.

Theorem 1. Assume the Jacobian $\nabla_x \psi(x, K(x^*(k), k))\,\big|_{x=x^*(k)}$ is zero at least for one point $x^*(k)$ of the orbit. Then, the periodic orbit x^* is locally orbitally exponentially stable. □

Proof. The proof is obtained by direct observation of the result in Lemma 1: under the conditions of the statement, $\nabla_x \Psi(x, k)\,\big|_{x=x^*(k)} = 0_{n\times n}$, which yields stability of the associated fixed point, and thus stability of the periodic cycle. □

3. STABILIZING CONTROL LAWS

The gain $K(x(k), k)$ will be defined in such a way that the sufficient condition for stability of Theorem 1 is satisfied. As mentioned previously, it will even be imposed that the Jacobian matrix defined for $x^*(k)$ equals zero for each k. As a matter of fact, from Lemma 1,

$$\nabla_x \psi(x, K(x,k))\,\big|_{x=x^*(k)} = 0_{n\times n}$$

is equivalent to

$$\nabla_x \phi(x)\,\big|_{x=x^*(k)} + K(x,k)(\nabla_x \phi^p(x) - I)\,\big|_{x=x^*(k)} = 0_{n\times n}. \quad (9)$$

The values of $K(x^*(k), k)$ selected in the sequel will be shown to fulfill (9).

- *Control law CL 1.* K is a constant matrix defined by:
$$K = -\nabla_x \phi(x)\,\big|_{x=x^*(0)}\ (\nabla_x \phi^p(x) - I)^{-1}\,\big|_{x=x^*(0)}\ . \quad (10)$$

- *Control law CL 2.* $K(k)$ is a time-varying matrix defined for each time $k \in \mathbb{N}$ by:
$$K(k) = -\nabla_x \phi(x)\,\big|_{x=x^*(k)}\ (\nabla_x \phi^p(x) - I)^{-1}\,\big|_{x=x^*(k)}\ . \quad (11)$$

Application of CL 1 or CL 2 necessitates to define which of the orbit point is the point $x^*(0)$. A possible choice is to take $x^*(0)$ as the point of the cycle minimizing the distance from $x(0)$. On the other hand, these two control laws are not intended to be used in practice, as they require prior exact knowledge on the UPO (both explicitly use the target UPO as a reference for the controller; see similar idea for DFC in [13]).

• *Control law CL 3.* $K(x(k))$ is given as

$$K(x(k)) = -\nabla_x \phi(x)\,\big|_{x=x(k)}\,(\nabla_x \phi^p(x) - I)^{-1}\,\big|_{x=x(k)}\,. \tag{12}$$

Contrary to CL 1 and CL 2, the choice CL 3 does *not* require any knowledge on the UPO — except period p. Putting the term (12) in (5) reminds of the Newton-Raphson method [11] applied to the iterative search for zeros of the map $(\phi^p(x) - x)$, which uses the adjustment law $x \leftarrow x + \Delta$, $\Delta = -(\nabla_x \phi^p(x) - I)^{-1}(\phi^p(x) - x)$.

4. NUMERICAL EXAMPLES

The previous laws are now applied to two classical systems.

4.1 Logistic map

The Logistic map is used as a first example for the application of the suggested method. Although the proposed scheme was developed for n-dimensional maps, a 1-dimensional system simplifies the numerical analysis and the comparison between the three control laws. The Logistic map is given by

$$x(k+1) = rx(k)(1 - x(k)). \tag{13}$$

CL 3 is used first, because it does not requires any knowledge on the UPOs. As a matter of fact, it is also used here to find out the latter, and then to find adequate values for CL 1 and CL 2. Figure 1 shows the evolution of the state $x(k)$ and of the control effort $u(k) = K(\phi^p(x(k)) - x(k))$ for specific values of the parameter r of the system, initial condition $x(0)$ and the parameter p of the controller. The main characteristic of the proposed control scheme is that few iteration steps are sufficient to stabilize an UPO. Figure 1 (d) may be compared with [9, Fig. 5], where the obtained convergence is much slower (same initial conditions yield 100 to 200 iterations) with larger control effort. Notice that persistent zero value for u indicates convergence to a UPO of the open-loop system.

Transient iterations of the controlled system using each of the three control laws are compared in Figure 2. The comparison is done using the control effort $u(k)$. The examples shown are limited to trajectories that converge to a period-p orbit, the cases where the trajectory diverges to infinity or converges to a periodic orbit (including fixed points) not corresponding to the uncontrolled system (special situations occurring for CL 1 and CL 2, but also for DFC) are not shown [2]. For the trajectories shown in Figure 2 it is clear that, provided it yields convergence, CL 3 yields faster convergence than the other two. This is specially valid for initial conditions more distant from the period-p UPO.

After comparing the duration of the transients, the size of the basins of attraction (BA) is considered. The BA represents the set of initial conditions that can be stabilized

[2] Notice that system (5) may possess periodic orbits of period p which are *not* periodic orbits of the uncontrolled system (1). However, inspecting the values of u allows to conclude whether this is the case or not. This is in contrast with DFC methods, for which the periodic solutions *of period p* are exactly the periodic solutions of period p of the uncontrolled system.

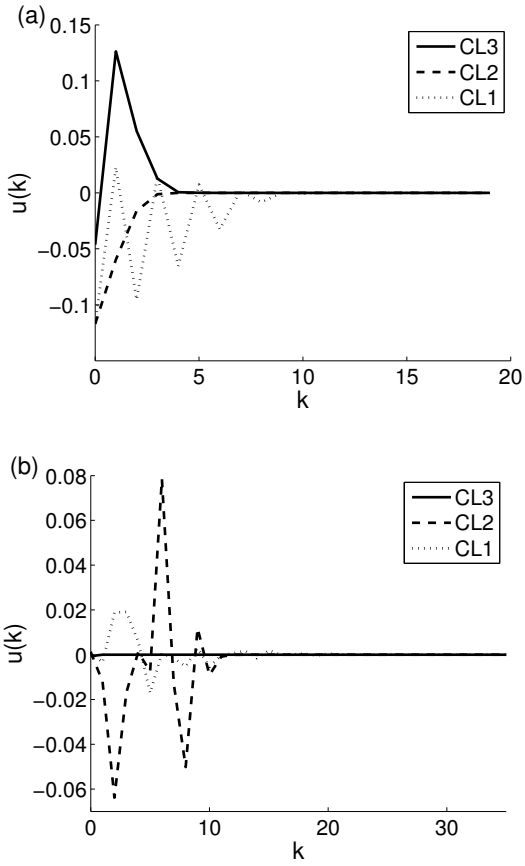

Fig. 2. Comparison of transient steps using the control effort $u(k)$ for the three control laws (legend in figure) studied using the Logistic map with $r = 4$: (a) $x(0) = 0.48$ and $p = 2$; (b) $x(0) = 0.57$ and $p = 5$.

to a given orbit by the controller. The basins of attraction are shown according to their period (2 for Figure 3 (a) and 3 for (b)), to the type of control gain (the lines of the table of graphics) and to the UPOs (grayscale of the basins of attraction for the same gain).

The BAs of the fixed points (FP : period-1 orbits) can be observed for $p = 2$ and $p = 3$. Notice that the BAs of the orbits of periods divisors of p decrease in area for larger values of p. Another observation is that, due to the exponential increase of the quantity of orbits by period and the characteristic of the control law of being valid in the vicinity of the UPO, for larger values of p, more periodic orbits appear and they have smaller BAs, but the space, occupied in the state space by all such BAs is larger. This can be observed in Figure 4.

4.2 Henon map

The Henon map is used to provide an example with dimension grater than 1. In this subsection only CL 3 is analyzed. The Henon map is written

$$x_1(k+1) = a - x_1^2(k) + bx_2(k) \tag{14}$$

$$x_2(k+1) = x_1(k) \tag{15}$$

Figure 5 shows the BAs for p equal to 2, 4 and 7, respectively. As before, the decrease of the size of the BAs referent to the FPs can be observed from Figure 5 (a)

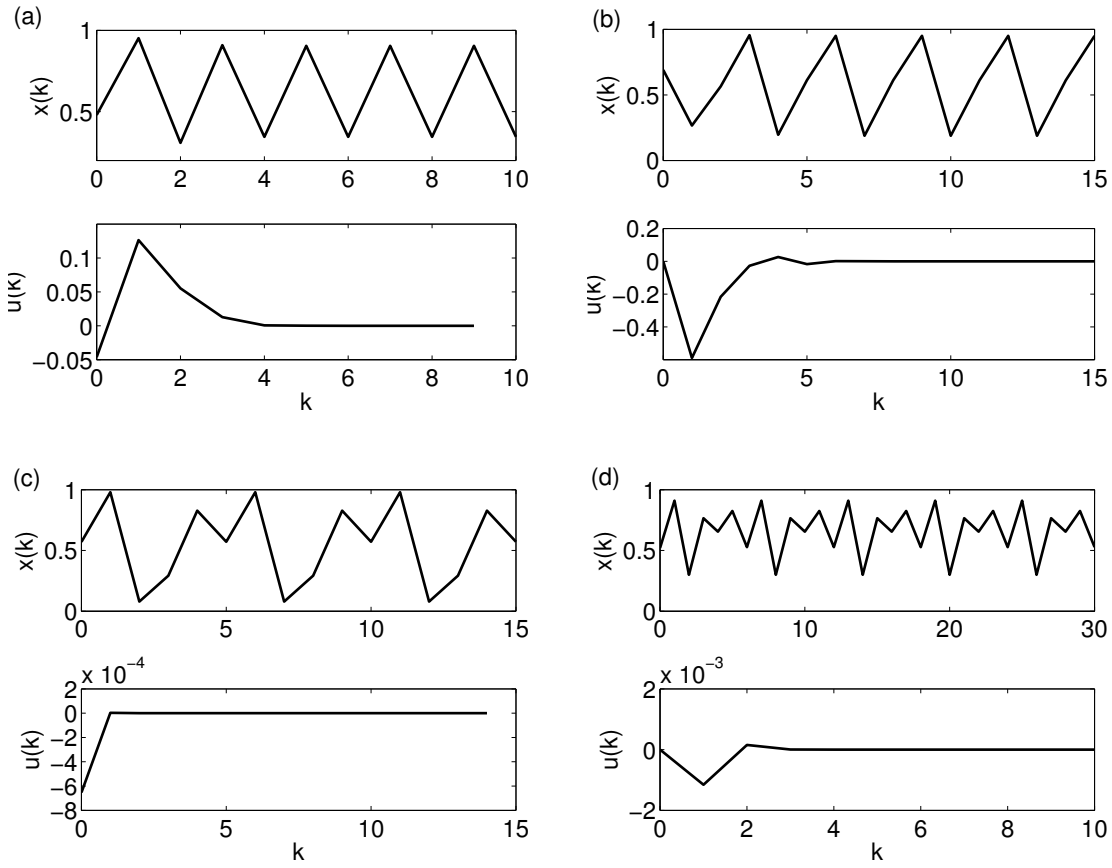

Fig. 1. Example of state $x(k)$ and control effort $u(k)$ evolution for the Logistic map controlled using the gain of CL 3: (a) $r = 4$, $x(0) = 0.48$ and $p = 2$; (b) $r = 4$, $x(0) = 0.69$ and $p = 3$; (c) $r = 4$, $x(0) = 0.57$ and $p = 5$; (d) $r = 3.65$, $x(0) = 0.52$ and $p = 6$.

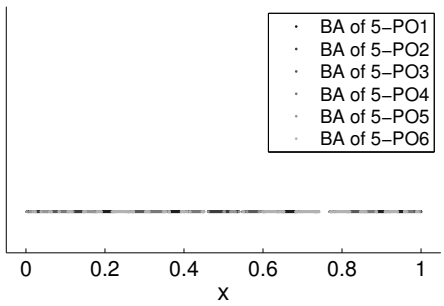

Fig. 4. Basins of attraction (BA) of the Logistic map for CL 3, period $p = 5$ and $r = 4$.

to (b) and, when increasing the value of p the number of attractors increase, the size of each BA decreases and the global size of all the BAs of the set of period-p attractors increase in the state space.

A characteristic better observed in the 2-dimensional example (Figure 5 (b) and (c)) is the fractal basins boundary [1] that suggests that the chaotic attractor of $\phi(x(k))$ became a chaotic saddle [6, 7]. This was expected, as the control term stabilizes periodic orbits whose period is a divisor of p, while there is no reason why the stability of the other UPOs would be modified, composing thus the non attracting chaotic set.

Some examples of the evolution of the state variables and the control effort can be seen in Figure 6. The initial conditions were selected using Figure 5, choosing the ones far from the attractor and in the fractal basin boundaries. Even in these more difficult situations, the number of iterations to get convergence is remarkably small.

5. CONCLUSION

In this paper, a chaos control scheme based on prediction of future states of the system has been proposed, extending some ideas previous formulated by T. Ushio and S. Yamamoto. Based on sufficient stability criterion, the third control law (CL 3), which does not necessitate prior knowledge of the UPO, yields remarkably fast convergence. The method can be used for control purposes, but also directly to find UPOs of the uncontrolled system. The control method developed here can be seen as an application of the Newton-Raphson method to the search for UPOs. Various tests (shown here for periods up to 7, but other simulations, not presented here, have shown similar behavior for larger values) have been conducted, providing large sets of UPOs. The comparison of the present method with the DFC for discrete time systems will be published in a future paper and extension to continuous time systems is in progress.

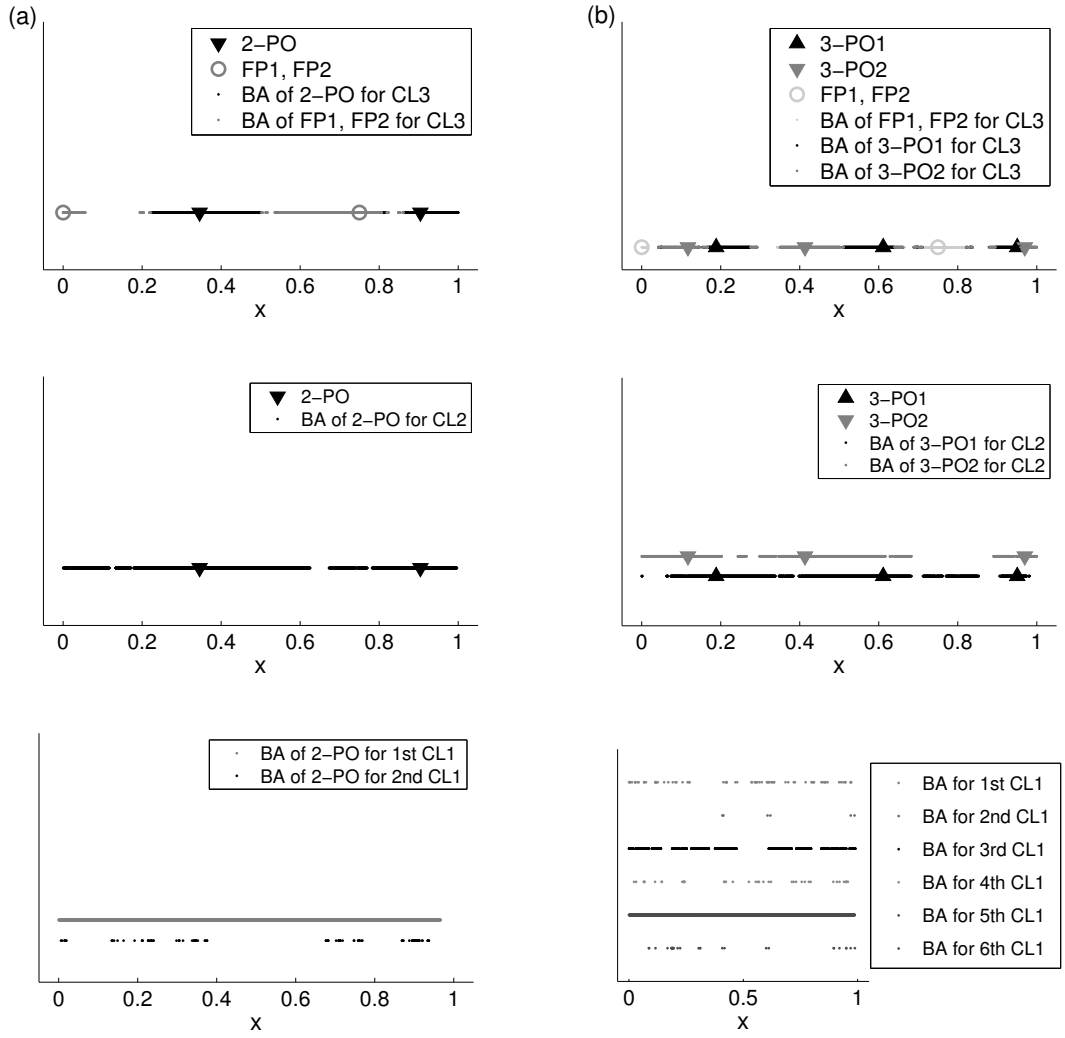

Fig. 3. Basins of attraction (BA) for each control law for periods 2 and 3 of the Logistic map with $r = 4$: (a) (first column) $p = 2$; (b) (second column) $p = 3$. P1 indicates FP and 0 is another FP of the system that does not belong to the chaotic attractor.

REFERENCES

[1] Alligood, K.T., Sauer, T.D. and Yorke, J.A. (1996). *Chaos an introduction to dynamical systems.* Springer-Verlag, New York.

[2] Cvitanović, P. (1988). Invariant Measurement of Strange Sets in Terms of Cycles. *Phys. Rev. Lett.* **61**, 2729–2732.

[3] Devaney, R.L. (1992). *A first course in chaotic dynamical systems: theory and experiment.* Addison-Wesley, New York.

[4] Franceschini, V., Giberti, C. and Zhengi. Z. (1993). Characterization of the Lorenz attractor by unstable periodic orbits. *Nonlinearity* **6**, 251–258.

[5] Hale, J.K. and Lunel, S.M.V. (1993). *Introduction to functional differential equations.* Springer-Verlag, New York.

[6] Hsu, G.-H., Ott, E. and Grebogi, C. (1988). Strange saddles and the dimensions of their invariant manifolds. *Phys. Lett. A* **127**, 199–204.

[7] Kantz, H. and Grassberger, P. (1985). Repellers, semi-attractors, and long-lived chaotic transients. *Physica D* **17**, 75–86.

[8] Kaplan, W. (2003). *Advanced Calculus.* 5th ed., Addison-Wesley, Reading.

[9] Morgül, Ö. (2009). A new generalization of delayed feedback control. *Int. J. Bifurcation and Chaos* **19**, 365–377.

[10] Ott, E., Grebogi, C. and Yorke, J.A. (1990). Controlling chaos. *Phys. Rev. Lett.* **64**, 1196–1199.

[11] Parker, T.S. and Chua, L.O. (1989). *Practical Numerical Algorithms for Chaotic Systems.* Springer-Verlag, New York.

[12] Polyak, B.T. (2005). Stabilizing Chaos with Predictive Control, *Automation and Remote Control* **66**, no. 11, 1791–1804

[13] Pyragas, K. (1992). Continuous control of chaos by self-controlling feedback. *Phys. Lett. A* **170**, 421–428.

[14] Pyragas, K. and Tamaševičius, A. (1993). Experimental control of chaos by delayed self-controlling feedback. *Phys. Lett. A* **180**, 99–201.

[15] Pyragas, K. (1995). Control of chaos via extended delay feedback. *Phys. Lett. A* **206**, 323–330.

[16] Pyragas, K. (2006). Delayed feedback control of chaos. *Phil. Trans. R. Soc. A* **364**, 2309–2334.

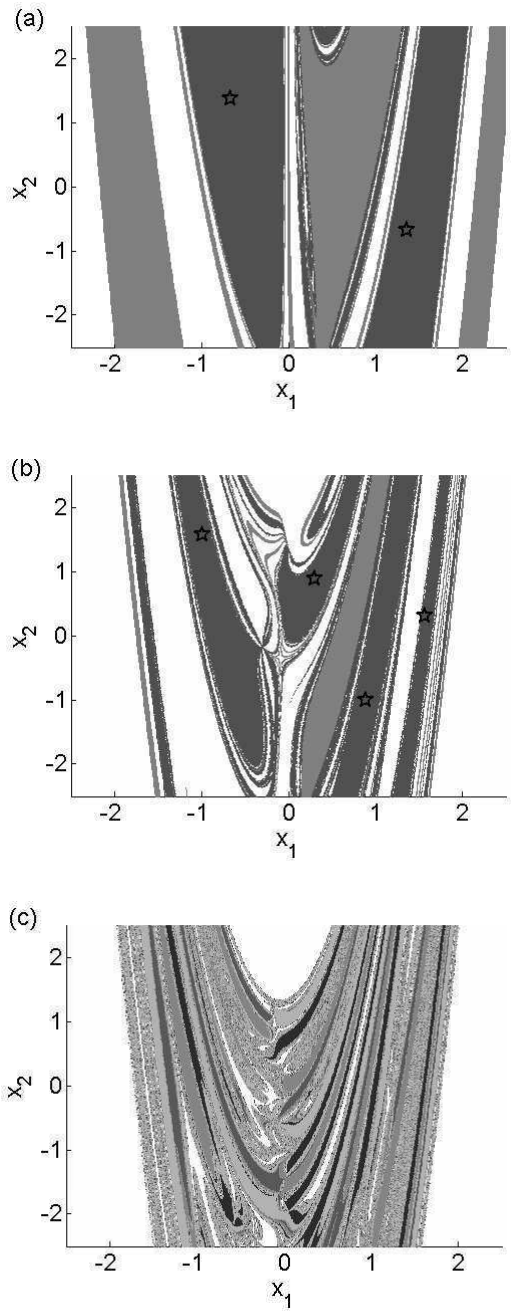

Fig. 5. Basins of attraction (BA) for CL 3 for periods 2, 4 and 7 of the Henon map with $a = 1.4$ and $b = 0.3$: (a) $p = 2$, dark gray represents the BA of $\star$ and light gray the BAs of the FPs; (b) $p = 4$, dark gray represents the BA of $\star$ and light gray the BAs of the period-1 orbits; (c) $p = 7$, 4 BAs.

[17] Ushio, T. and Yamamoto, S. (1999). Prediction-based control of chaos. *Phys. Lett. A* **264**, 30–35.

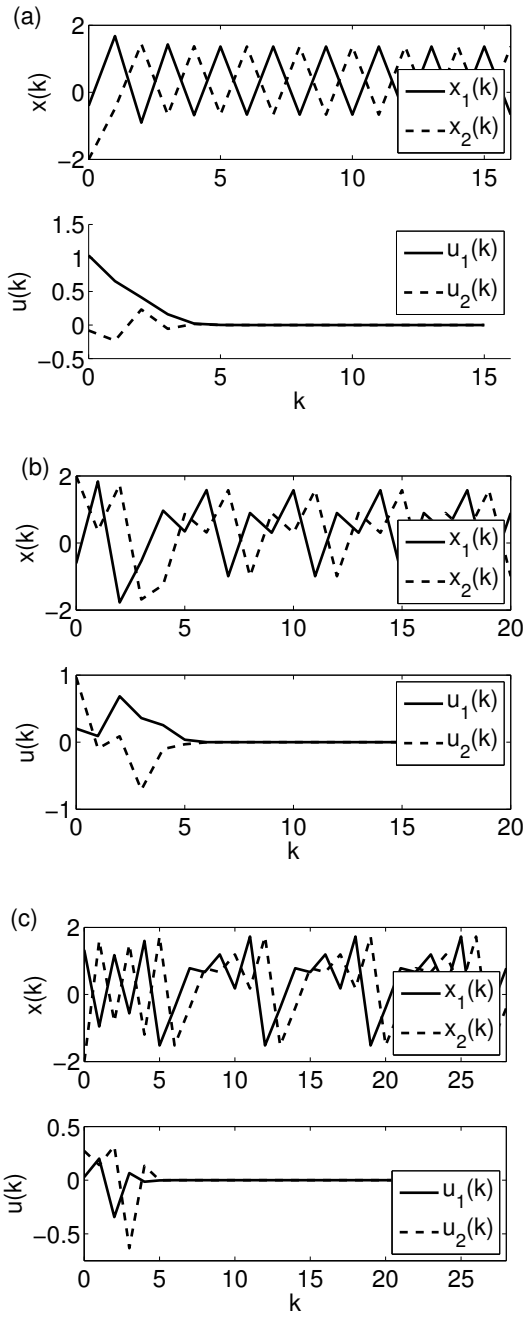

Fig. 6. Example of state $x(k)$ and control effort $u(k)$ evolution for the Henon map controlled using CL 3 with $a = 1.4$ and $b = 0.3$: (a) $x(0) = (-0.4, -2)$ and $p = 2$; (b) $x(0) = (-0.605, 2)$ and $p = 4$; (c) $x(0) = (1.33, -2.045)$ and $p = 7$.

T. P. Chagas, P.-A. Bliman and K. H. Kienitz, Estabilização de órbitas periódicas: comparação entre realimentação de estados atrasados e uma nova lei utilizando estados preditos, in *XVIII Congresso Brasileiro de Automática*, (Bonito, Brazil), Sep. 2010

ESTABILIZAÇÃO DE ÓRBITAS PERIÓDICAS: COMPARAÇÃO ENTRE REALIMENTAÇÃO DE ESTADOS ATRASADOS E UMA NOVA LEI UTILIZANDO ESTADOS PREDITOS.

Thiago P. Chagas*, Pierre-Alexandre Bliman*, Karl H. Kienitz†

*INRIA
Rocquencourt BP105, 78153 Le Chesnay cedex, França

†Dept. de Sistemas e Controle
Instituto Tecnológico de Aeronáutica
12228-900 São José dos Campos, São Paulo, Brasil

Emails: tchagas@ita.br, pierre-alexandre.bliman@inria.fr, kienitz@ita.br

Abstract— In this note a comparison between prediction-based chaos control and delayed feedback control is presented for discrete-time systems. Both controllers are tuned using the Floquet multipliers of the unstable periodic orbits. For the prediction-based chaos control a new control law is proposed which leads to a time-varying gain. The comparison is carried out using the size of the basins of attraction of the controlled orbits and the rate of convergence obtained by numerical simulation.

Keywords— Nonlinear systems, Discrete-time systems, Prediction-based chaos control, Delayed feedback control, Stabilization, Unstable periodic orbits

Resumo— Neste trabalho é feita uma comparação entre dois métodos de controle de caos, um utilizando realimentação com predição dos estados futuros (*prediction-based chaos control*) e outro utilizando realimentação de estados atrasados (*delayed feedback control*). Ambos os controladores são sintonizados considerando os multiplicadores de Floquet das órbitas periódicas instáveis. Uma nova lei de controle é proposta para o *prediction-based chaos control* utilizando um ganho variante no tempo. Como critério de comparação é usado o tamanho das bacias de atração das órbitas controladas e a velocidade de convergência obtidos por simulação numérica.

Palavras-chave— Sistemas não-lineares, Sistemas discretos, Controle de caos, Estabilização, Órbitas periódicas instáveis

1 Introdução

Controle de caos, originalmente proposto por Ott et al. (1990), tem como objetivo comportamento periódico em sistemas originalmente caóticos. Este tipo de controle utiliza características básicas de sistemas caóticos (Devaney, 1992) para obter soluções periódicas estáveis utilizando baixo esforço de controle. Estas características estão relacionadas ao número infinito de órbitas periódicas instáveis (UPO - *unstable periodic orbits*) que compõem os conjuntos caóticos (Cvitanović, 1988). Métodos de controle de caos visam estabilizar estas UPOs.

Duas características das UPOs são de interesse em aplicações de controle de caos. A primeira é a relação período vs. estabilidade e a segunda é a relação período vs. número de órbitas periódicas (Cvitanović, 1988; Franceschini et al., 1993). Sabe-se que a instabilidade (medida, por exemplo, pelos multiplicadores ou pelos expoentes de Floquet (Bittanti and Colaneri, 2008)) e a quantidade de UPOs cresce exponencialmente com o período, sendo órbitas de período mais longo mais difíceis de serem controladas.

Um método de controle de caos muito estudado é o controle por realimentação com atraso (DFC - *Delayed Feedback Control*) proposto por Pyragas (1992) e suas extensões podem ser vistas em Pyragas (2006). Este método baseia-se em garantir um erro nulo entre o estado atual e o estado atrasado pelo período da UPO de interesse. O erro é multiplicado por um ganho que, quando adequado, o leva a zero. O DFC, como originalmente proposto, não controla órbitas de período elevado (Pyragas, 2006). Outra limitação do método é não controlar órbitas que possuam um número ímpar de multiplicadores de Floquet reais e maiores que 1 (Ushio, 1996; Pyragas, 2006).

Ushio and Yamamoto (1999) propuseram uma alternativa ao DFC utilizando o erro entre o estado atual e o estado em um tempo futuro igual ao período da UPO a ser controlada, *obtido através da predição da trajetória para o sistema em malha aberta*. Este erro, assim como no DFC, é multiplicado por um ganho, porém, neste caso o desenvolvimento de procedimentos de sintonização é mais simples (Morgül, 2009; Polyak, 2005) e este não apresenta a limitação do número ímpar de multiplicadores de Floquet reais e maiores que 1. Este método é denominado *Prediction-based chaos control* (PBCC).

Neste trabalho é feita uma comparação entre o DFC e o PBCC. Os ganhos de ambos os controladores são obtidos de forma a minimizar o maior, em módulo, multiplicador de Floquet da órbita a ser controlada (Huijberts et al., 2009). Em especial, para o PBCC, é proposta uma lei de controle que leva a um ganho variante no tempo e

é baseada em uma condição suficiente para estabilização. Através desta lei de controle obtém-se todos os multiplicadores de Floquet iguais a zero, seu valor mínimo (Chagas et al., 2010). Através de simulações numéricas são obtidas as bacias de atração para cada controlador e gráficos de esforço de controle utilizados para controlar algumas órbitas, desta forma pode-se comparar estabilidade e velocidade de convergência para cada método.

Na Seção 2 deste artigo são apresentadas as condições gerais de estabilidade para as órbitas periódicas utilizando o PBCC. Na Seção 3 é apresentada a lei de controle para o PBCC. Na Seção 4 é apresentada a condição para estabilidade a ser utilizada na sintonização do DFC. Na Seção 5 são apresentados os resultados da otimização para sintonização do DFC e também exemplos numéricos para comparação entre os métodos. As conclusões são apresentadas na Seção 6.

2 Estabilidade de órbitas periódicas

Nesta seção são apresentadas condições gerais para estabilização de órbitas utilizando realimentação com predição do estado futuro (PBCC). Dada uma função $\phi : \mathbb{R}^n \to \mathbb{R}^n, n \in \mathbb{N}$, considere o sistema dinâmico não-linear no tempo discreto descrito por

$$x(k+1) = \phi(x(k)), \quad x(k) \in \mathbb{R}^n, \quad k \in \mathbb{N}. \tag{1}$$

Assume-se a existência de uma órbita periódica hiperbólica instável (UPO) de período $p \in \mathbb{N}$ de (1); assim, a trajetória x^* verifica:

$$x^*(k+p) = x^*(k), \quad \forall k \in \mathbb{N}. \tag{2}$$

Caso exista um conjunto caótico no espaço de estados n-dimensional formado por $x(k)$, sabe-se que este conjunto caótico é formado por um número infinito de UPOs (Alligood et al., 1996; Devaney, 1992) e que o número de UPOs por período p cresce exponencialmente com p (Cvitanović, 1988; Franceschini et al., 1993).

O objetivo aqui é estabilizar a UPO x^*. Para isso, considere uma lei de controle do tipo

$$x(k+1) = \phi(x(k)) + K(k)(r(k) - x(k)). \tag{3}$$

Aqui, o sinal $r(k)$ representa o estado predito $\phi^p(x(k))$, *computado para o sistema em malha aberta*. $K(k) \in \mathbb{R}^{n\times n}$ são matrizes de ganho e ϕ^p é definido recursivamente pela composição: $\phi^1 = \phi$, $\phi^{q+1} = \phi^q \circ \phi$, $q \in \mathbb{N}$.

Observa-se que qualquer órbita p-periódica de (1) é também uma órbita p-periódica de (3), pois, sobre a órbita periódica $r(k) = x^*(k)$.

A transição de $x(k)$ a $x(k+p)$ é definida pelo mapeamento Ψ a seguir:

$$x(k+p) = \Psi(x(k), k), \tag{4}$$

onde $\Psi(x(k), k)$ é definido recursivamente como:

$$\begin{array}{lcl} y_k & = & x(k) \\ y_{k+l+1} & = & \phi(y_{k+l}) + K_{k+l}(r_{k+l} - y_{k+l}) \\ \Psi(x,k) & = & y_{k+p}, \end{array} \tag{5}$$

para $l = 0, \ldots, p-1$. Observe que a UPO x^* do sistema (1) satisfaz

$$x^*(k+p) = x^*(k) = \Psi(x^*(k), k) \tag{6}$$

e sua estabilidade, em geral, é definida pelos autovalores da matriz Jacobiana $\nabla_x \Psi(x,k)\big|_{x=x^*(k)}$, sendo estável se todos apresentarem módulo menor ou igual a 1. Estes autovalores são os multiplicadores de Floquet (Bittanti and Colaneri, 2008).

3 Definição da lei de controle para o PBCC

A lei de controle apresentada a seguir é definida a partir de uma condição suficiente para estabilização de UPO (Chagas et al., 2010). Aqui aloca-se *todos* os autovalores de $\nabla_x \Psi(x,k)\big|_{x=x^*(k)}$ em zero. Em (3), o ganho passa a ser dependente do estado atual, $K(x(k), k)$.

Para qualquer $x \in \mathbb{R}^n$ e $K(x(k), k) \in \mathbb{R}^{n\times n}$, utiliza-se a seguinte notação

$$\psi(x, K) \doteq \phi(x) + K(x)(\phi^p(x) - x) \tag{7}$$

e o sistema dinâmico no tempo discreto em malha fechada (3), controlado utilizando o PBCC, é definido por

$$x(k+1) = \psi(x(k), K(x(k), k)). \tag{8}$$

Para definição da lei de controle, primeiro deve-se obter $\nabla_x \Psi(x,k)\big|_{x=x^*(k)}$ para o PBCC.

Lema 1 Em qualquer ponto $x^*(k)$, $k \in \mathbb{N}$, da trajetória x^* em malha fechada (8), tem-se que,

$$\begin{array}{l} \nabla_x \Psi(x,k)\big|_{x=x^*(k)} = \\ \prod_{l=0}^{p-1} \nabla_x \psi(x, K(x^*(k+l), k+l))\big|_{x=x^*(k+l)} \end{array} \tag{9}$$

onde, em (9) e no restante do trabalho, as matrizes no produtório são ordenadas *da direita para esquerda* com o incremento do índice l. ■

Para demonstração do Lema 1, consultar o Anexo. O objetivo da fórmula (9) é mostrar que a derivada de $K(x(k), k)$ em relação à $x(k)$ não aparece no lado direito da equação. Assim, o Lema 1 proporciona uma simplificação no cálculo do espectro de autovalores da Jacobiana: como indica (9), a dependência do ganho em relação ao estado não modifica a Jacobiana nos pontos da órbita periódica.

Neste trabalho busca-se obter o espectro de autovalores de $\nabla_x \Psi(x,k)\big|_{x=x^*(k)}$ igual a zero e uma possível solução é dada pelo Teorema 2.

Teorema 2 Assume-se que a Jacobiana $\nabla_x \psi(x, K(x^*(k), k))\,\big|_{x=x^*(k)}$ é igual a zero ao menos em um ponto $x^*(k)$ da órbita periódica. Então, $\nabla_x \Psi(x, k)\,\big|_{x=x^*(k)} = 0$ para qualquer $k \in \mathbb{N}$, e a órbita periódica x^* é localmente orbitalmente exponencialmente estável. ■

Ver demonstração do Teorema 2 em Anexo. O ganho $K(x(k), k)$ será definido de forma que a condição suficiente para estabilidade do Teorema 2 seja satisfeita. Será imposto que a Jacobiana definida para $x^*(k)$ seja igual a zero para cada k. A hipótese do Teorema 2 é equivalente a $0_{n\times n} = \nabla_x \phi(x)\,\big|_{x=x^*(k)} + K(x, k)(\nabla_x \phi^p(x) - I)\,\big|_{x=x^*(k)}$.

Por consequência, de acordo com Chagas et al. (2010), escolhe-se:

$$K(x(k), k) = \\ -\nabla_x \phi(x)\,\big|_{x=x(k)}\,(\nabla_x \phi^p(x) - I)^{-1}\,\big|_{x=x(k)}\,. \tag{10}$$

Resumindo, a lei de controle PBCC traz um comportamento em malha fechada definido pelas equações (3) a (10), com $r(k) = \phi^p(x(k))$. Esse sistema verifica a hipótese do Teorema 2: com a escolha da realimentação (10), a UPO x^* é localmente orbitalmente exponencialmente estável. Observa-se que a lei de realimentação (10) não pressupõe conhecimento da UPO x^* (exceto o período p) e que o sistema (7)-(10) é autônomo.

4 Sintonia do ganho para o DFC

Para aplicação do DFC, em (3), $r(k)$ é substituído por $x(k-p)$, porém, a mesma análise realizada na Seção 3 não é válida para o DFC devido à utilização do estado atrasado na realimentação. Além disso, o vetor de estados $x(k)$ não é suficiente para representar completamente a dinâmica do sistema controlado. Neste caso será utilizado o vetor de estados estendido definido por $z(k) = \begin{pmatrix} x(k)' & x(k-1)' & \dots & x(k-p)' \end{pmatrix}' \in \mathbb{R}^{n(1+p)}$.

O objetivo nesta seção é encontrar a matriz cujos autovalores são os multiplicadores de Floquet considerando o vetor de estados estendido da órbita controlada utilizando o DFC.

O mapeamento Ψ_{est} é defino como em (4) e (5) utilizando o vetor de estados estendidos. Observe que $x(k)$ (resp. $r(k)$) é representado pelos n primeiros (resp. últimos) estados de $z(k)$:

$$z(k+p) = \Psi_{est}(z(k), k)$$

A derivada de $\Psi_{est}(z(k), k)$ em relação a z, cujos autovalores são os multiplicadores de Floquet desejados, pode ser obtida diretamente de (9). Para isso defini-se uma nova função (11), sendo este uma extensão de (7), e sua Jacobiana para cada ponto da órbita é dada por (12) (ver página seguinte).

5 Exemplos numéricos

Como estudo de caso será utilizado o mapa de Henon descrito por

$$\begin{aligned} x_1(k+1) &= a - x_1^2(k) + b x_2(k) \\ x_2(k+1) &= x_1(k). \end{aligned} \tag{13}$$

O primeiro passo para comparação entre os métodos é encontrar as UPOs de interesse para aplicar um método de otimização e obter um valor adequado de K para o DFC. Aqui observa-se a primeira vantagem do PBCC utilizando a lei de controle proposta na Seção 3, este método também pode ser utilizado para encontrar UPOs em conjuntos caóticos (Chagas et al., 2010). Órbitas de baixo período podem ser facilmente encontradas analiticamente no sistema em questão, porém, a lei de controle proposta para o PBCC automatiza o processo.

Na Tabela 1 é apresentada uma lista de UPOs de período até 6, nela constam o seu período e seus autovalores para o sistema sem controle. Neste trabalho, em (13), foi utilizado $a = 1.4$ e $b = 0.3$ e não existem órbitas de período 3 e 5 para esses valores de parâmetros.

Para aplicar a otimização para o DFC foi utilizada a função *fminsearch* do MATLAB® com condições iniciais para os elementos da matriz K entre -1 e 1. Foi feito o cálculo dos autovalores de $\nabla_z \Psi_{est}(z, K)\,\big|_{z=z^*(k)}$, obtido seus módulos e utilizado como custo o maior desses autovalores em módulo. Os valores para a matriz K e o maior autovalor de cada órbita controlada são mostrados na Tabela 2.

Para as órbitas de período 6 e o ponto fixo P1.2 não foi encontrado um ganho K que as estabilize red com o DFC. Além disso, observa-se que o módulo do maior autovalor para a órbita P4 é próximo de 1. Este fato está de acordo com as limitações do DFC apresentadas na literatura, órbitas de período elevado e órbitas com um número ímpar de multiplicadores de Floquet reais e maiores que 1 não são controláveis utilizando este método. Sabe-se que órbitas com expoente de Floquet real e maior que 1 são originadas a partir de bifurcações sela-nó, sendo o caso das órbitas P1.2 e P6.2. As outras UPOs apresentadas originam-se de bifurcações de duplicação de período.

Na Figura 1 são mostradas as bacias de atração das órbitas periódicas controladas com o DFC. Como condição inicial para os estados atrasados foi utilizada a posição da órbita a ser controlada, sendo que no caso da P2 e P4 foram realizadas, respectivamente, 2 e 4 simulações para cada bacia, variando a ordem dos valores de $x(k-1) \dots x(k-p)$ para cada simulação. A bacia de atração da órbita P4 não foi mostrada porque, em uma varredura de valores iniciais de x com um passo de 0.005, nenhuma das condições inicias tendeu à órbita. Mesmo sendo esta estável, sua bacia de atra-

UPO	P1.1	P1.2	P2	P4	P6.1	P6.2
Período	1	1	2	4	6	6
Autovalores	[-1.9237, 0.1559]	[3.2598, -0.0920]	[-3.0101, -0.0299]	[-8.6394, -0.0009]	[-27.5147, -2×10^{-5}]	[28.1250, 2×10^{-5}]

Tabela 1: UPOs de período até 6 para o mapa de Henon.

UPO	P1.1	P2	P4
K	[-0.46897 0.42973; 0.39570 -0.40845]	[0.60000 -0.20000; 0.60000 -0.31394]	[-0.75154 0.08726; -1.16867 -0.21465]
Maior Autovalor	-0.0940 ± 0.3713i	-0.5380 ± 0.3745i	-0.6849 ± 0.6612i

Tabela 2: Ganho K e maior, em módulo, autovalor para UPOs do mapa de Henon controladas por DFC.

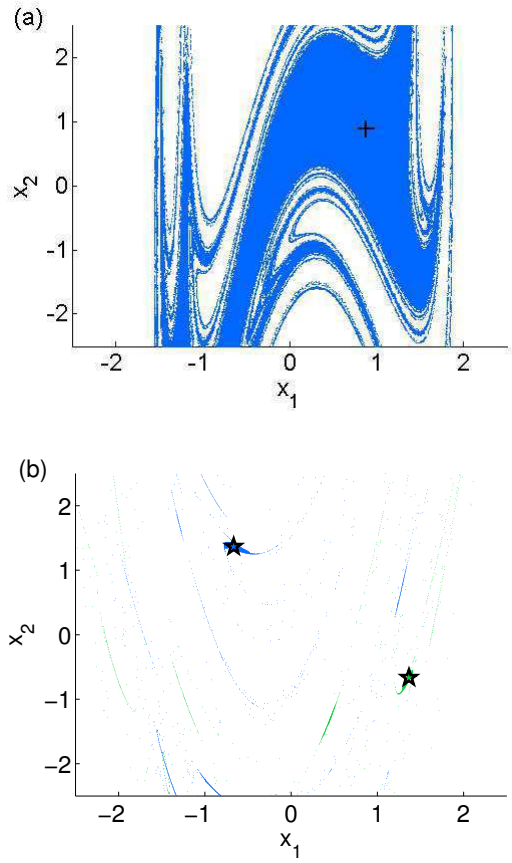

Figura 1: Bacias de atração das órbitas controladas com o DFC para o mapa de Henon. (a) P1.1 (+), (b) P2 ($\star$)

ção se limita à uma vizinhança muito pequena da órbita. Na Figura 1 (b), para cada condição inicial dos estados estendidos foi utilizada uma cor (azul ou verde) para a bacia de atração de P2.

As bacias de atração para o PBCC são apresentadas na Figura 2. Observa-se que com este método todas as órbitas de período p e seus divisores são controladas para um mesmo valor de p utilizado na lei de controle. Por isso, para cada figura apresentada há mais de uma bacia. As bacias de P1.1 e P1.2 são mostradas nas Figuras 2 (b) e (c) sugerindo que cada bacia das órbitas divisoras de p perdem tamanho com o incremento de p. A bacia da órbita P2 não foi incluída na figura 2 (c), assim como as bacias das órbitas P1.1, P1.2 e P2 não foram incluídas na Figura 2 (d). A órbita P1.2 não compõe o atrator caótico presente no mapa de Henon para $a = 1.4$ e $b = 0.3$, porém esta também foi controlada.

Com o aumento do período aumenta-se exponencialmente o número de órbitas que compõem o conjunto caótico e estas, em geral, são mais instáveis que as órbitas de menor período (Cvitanović, 1988; Franceschini et al., 1993). Por isso, a bacia de cada órbita de período p diminui com o aumento do período, porém, o espaço ocupado pelo conjunto das bacias de órbitas de mesmo período aumenta no espaço de estados.

Na Figura 3 é mostrado o somatório do módulo do esforço em cada direção para controlar as órbitas P2 e P4 utilizando o DFC e o PBCC. O esforço de controle é definido por $u(k) = K(k)(r(k) - x(k))$ e a convergência para a UPO de interesse é indicada por $u(k) < 10^{-10}$ (pre-

$$\psi_{est}(z,K) \doteq \begin{bmatrix} 0_{n\times np} & 0_{n\times n} \\ I_{np\times np} & 0_{np\times n} \end{bmatrix} z + \begin{bmatrix} \phi\left(\begin{bmatrix} I_{n\times n} & 0_{n\times np} \end{bmatrix} z\right) + K \begin{bmatrix} -I_{n\times n} & 0_{n\times n(p-1)} & I_{n\times n} \end{bmatrix} z \\ \hline 0_{np\times 1} \end{bmatrix} \quad (11)$$

$$\nabla_z \psi_{est}(z,K)\big|_{z=z^*(k)} = \begin{bmatrix} 0_{n\times np} & 0_{n\times n} \\ I_{np\times np} & 0_{np\times n} \end{bmatrix} + \begin{bmatrix} \nabla_x \phi(x)\big|_{x=x^*(k)} - K & 0_{n\times n(p-1)} & K \\ \hline 0_{np\times n(1+p)} \end{bmatrix} \quad (12)$$

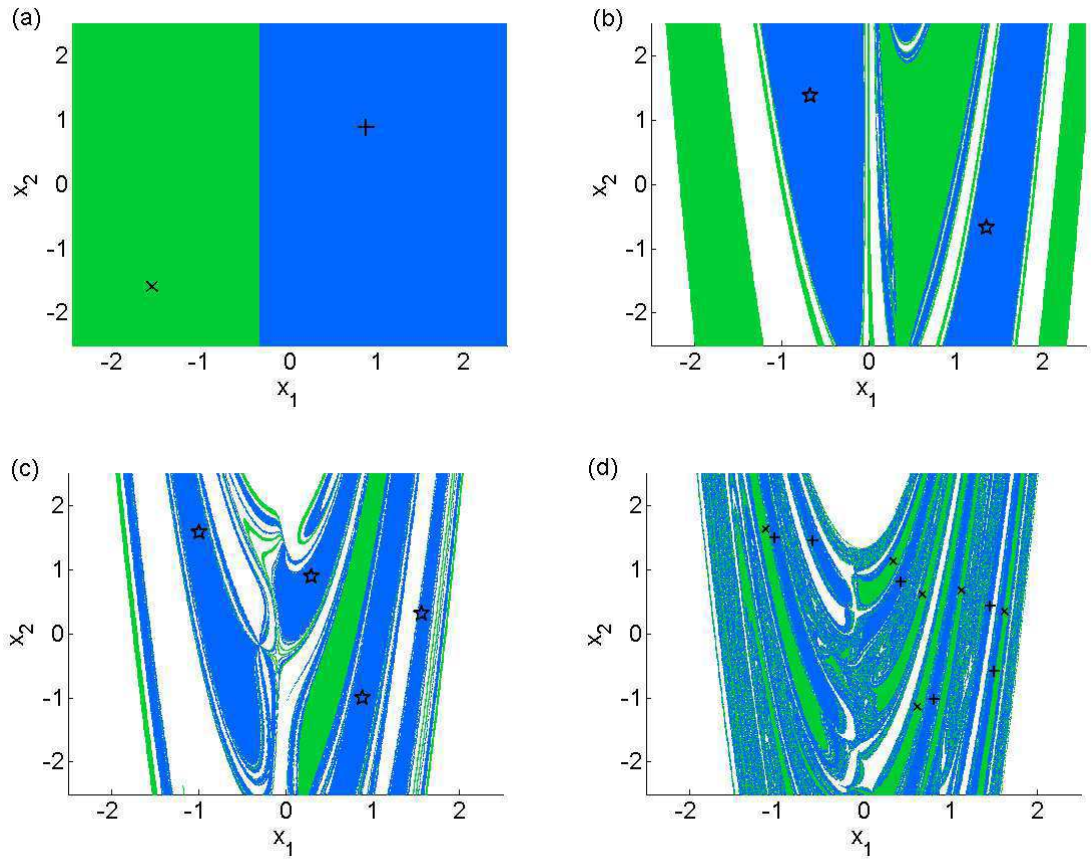

Figura 2: Bacias de atração para órbitas controladas do mapa de Henon utilizando o PBCC. (a) $p = 1$, P1.1 (+) e sua bacia em azul e P1.2 (×) e sua bacia em verde; (b) $p = 2$, P2 ($\star$) e sua bacia em azul e as bacias dos pontos fixos em verde; (c) $p = 4$, P4 ($\star$) e sua bacia em azul e as bacias dos pontos fixos em verde; (d) $p = 6$, P6.1 (×) e sua bacia em verde e P6.2(+) e sua bacia em azul.

cisão máxima utilizada para visualização dos dados). Foi utilizada uma escala logarítmica no eixo vertical para uma melhor comparação da velocidade de convergência para a UPO utilizando cada um dos métodos, por isso, apenas são mostrados os pontos relativos ao esforço de controle onde $|u_1(k)| + |u_2(k)| > 10^{-10}$. Para melhor visualização dos resultados, na Figura 3 (b) os dados relativos ao DFC foram mostrados a cada 10 pontos. Observa-se que em ambos os casos a trajetória controlada com o PBCC converge mais rapidamente para o atrator. Isto ocorre mesmo com os estados estendidos do DFC sendo inicializados de acordo com o ponto da órbita mais próximo da condição inicial de x. Verifica-se também que o esforço de controle quando utilizado o PBCC apresenta menor amplitude que quando utilizado o DFC.

6 Conclusões

Neste trabalho foi apresentada uma comparação entre o *Predictive-based chaos control* (PBCC) e o *Delayed feedback control* (DFC). Para o PBCC foi proposta uma nova lei de controle com um ganho variante no tempo e calculado para cada valor do estado durante a evolução da trajetória controlada. O ganho do controlador DFC foi sintonizado buscando-se um mínimo para o maior, em módulo, multiplicador de Floquet para a órbita controlada.

Verificou-se que o PBCC não apresenta as limitações conhecidas para o DFC, são elas: não controlar órbitas que apresentem um número ímpar de multiplicadores de Floquet reais e maiores que 1 e não controlar órbitas de período elevado. Além disso, as bacias de atração das órbitas controladas e a velocidade de convergência para o atrator são maiores quando utilizado o PBCC quando comparadas com o DFC, necessitando também de um menor esforço de controle.

Para a aplicação do PBCC é necessária a predição do estado futuro do sistema sem controle, isto torna o método dependente do modelo para aplicação. Já o DFC pode ser aplicado sem a necessidade de um modelo, pois, depende apenas dos estados atrasados. Esta característica é favorável ao DFC, porém, uma sintonização adequada do ganho do controlador depende de um modelo para uma formulação analítica ou para sintonização por métodos numéricos. Em relação ao conhecimento prévio da dinâmica do sistema, o PBCC, com a lei de controle proposta, apresenta a característica de

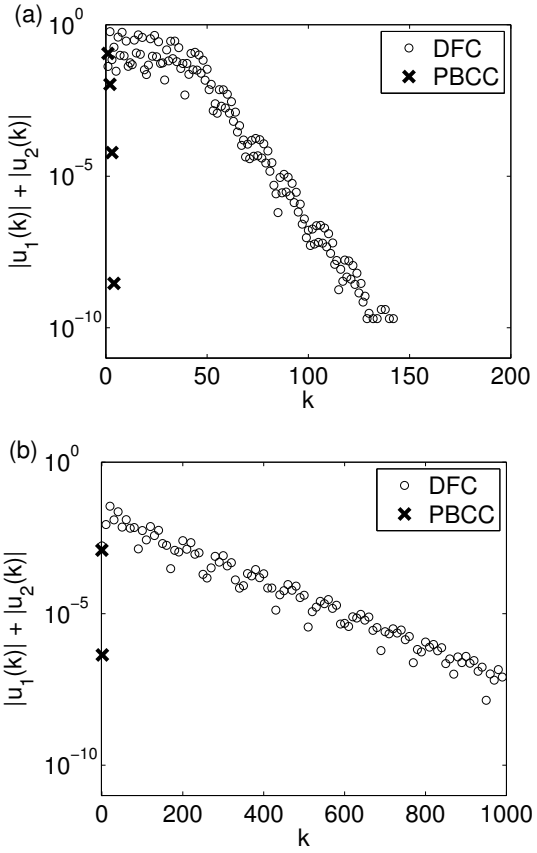

Figura 3: Esforço utilizado para controlar órbitas do mapa de Henon utilizando o DFC e o PBCC. (a) $p = 2$, x0=[-0.42; 1.25]; (b) $p = 4$, x0=[0.304; 0.893].

não depender da posição da órbita a ser controlada, sendo útil para aplicações onde estas órbitas não são conhecidas.

A escolha da função custo para otimização do ganho do DFC favorece a estabilidade local da órbita controlada, porém, não garante um máximo para o tamanho da sua bacia de atração. Desta forma, não é excluída a possibilidade de serem obtidos resultados melhores que os apresentados na comparação.

Agradecimentos

Este trabalho contou com o suporte do projeto CAPES/COFECUB nº MA 624/09.

Referências

Alligood, K. T., Sauer, T. D. and Yorke, J. A. (1996). *Chaos an introduction to dynamical systems*, Springer-Verlag, New York.

Bittanti, S. and Colaneri, P. (2008). *Periodic Systems: Filtering and Control*, Springer Verlag, London.

Chagas, T. P., Bliman, P.-A. and Kienitz, K. H. (2010). New feedback laws for stabilization of unstable periodic orbits, *8th IFAC Symposium on Nonlinear Control Systems*.

Cvitanović, P. (1988). Invariant measurement of strange sets in terms of cycles, *Physical Review Letters* **61**: 2729–2732.

Devaney, R. L. (1992). *A first course in chaotic dynamical systems: theory and experiment*, Addison-Wesley, New York.

Franceschini, V., Giberti, C. and Zheng, Z. (1993). Characterization of the Lorentz attractor by unstable periodic orbits, *Nonlinearity* **6**: 251–258.

Huijberts, H., Michiels, W. and Nijmeijer, H. (2009). Stabilizability via Time-Delayed Feedback: An Eigenvalue Optimization Approach, *SIAM Journal on Applied Dynamical Systems* **8**(1): 1–20.

Morgül, Ö. (2009). A new generalization of delayed feedback control, *International Journal of Bifurcation and Chaos* **19**(1): 365–377.

Ott, E., Grebogi, C. and Yorke, J. A. (1990). Controlling chaos, *Physical Review Letters* **64**: 1196–1199.

Polyak, B. T. (2005). Stabilizing chaos with predictive control, *Automation and Remote Control* **66**(11): 1791–1804.

Pyragas, K. (1992). Continuous control of chaos by self-controlling feedback, *Physics Letters A* **170**: 421–428.

Pyragas, K. (2006). Delayed feedback control of chaos, *Royal Society of London Philosophical Transactions Series A* **364**: 2309–2334.

Ushio, T. (1996). Limitation of delayed feedback control in nonlinear discrete-time systems, *IEEE Transactions on Circuits and Systems I - Regular Papers* **43**(9): 815–816.

Ushio, T. and Yamamoto, S. (1999). Prediction-based control of chaos, *Physics Letters A* **264**: 30–35.

Anexo

Demonstração do Lema 1: O cálculo da derivada é feito através da forma geral da regra da cadeia. Por recursão, $\nabla_x \Psi(x,k)\,\big|_{x=x^*(k)} = \prod_{l=0}^{p-1} \nabla_x \psi(x, K(x,k+l))\,\big|_{x=x^*(k+l)}$.

Utilizando a definição de ψ em (7), percebe-se que, para qualquer $k \in \mathbb{N}$, o (i,j)-ésimo componente de $\nabla_x \psi(x, K(x,k))\,\big|_{x=x^*(k)} -$

$\nabla_x \psi(x, K(x^*(k), k))\,\big|_{x=x^*(k)}$, com $i = 1, \ldots, n$, é igual a

$$\sum_{j'=1}^{n} \left(\frac{\partial K_{ij'}(x,k)}{\partial x_j}\bigg|_{x=x^*(k)} \cdot (\phi^p(x^*(k)) - x^*(k))_{j'} \right).$$

O somatório acima visa simplificar o produto do tensor $\frac{\partial K(x,k)}{\partial x}\Big|_{x=x^*(k)}$ pelo vetor $(\phi^p(x^*(k)) - x^*(k))$.

Como $x^*(k)$ está localizado sobre a órbita periódica, tem-se $\phi^p(x^*(k)) = x^*(k)$ e o último termo dentro do somatório é zero. Tem-se então o resultado desejado.

Demonstração do Teorema 2: A demonstração é obtida por uma observação direta do Lema 1: sob a condição do Teorema 2 tem-se $\nabla_x \Psi(x,k)\,\big|_{x=x^*(k)} = 0_{n\times n}$, o que garante a estabilidade do ponto fixo associado e obtêm-se a estabilidade da órbita periódica.

T. P. Chagas, P.-A. Bliman and K. H. Kienitz, A new method for stabilizing unstable periodic orbits of continuous-time systems. Application to control of chaos, in *51st IEEE Conference on Decision and Control*, (Maui, USA), Dec. 2012

51st IEEE Conference on Decision and Control
December 10-13, 2012. Maui, Hawaii, USA

A new method for stabilizing unstable periodic orbits of continuous-time systems. Application to control of chaos

Thiago P. Chagas, Pierre-Alexandre Bliman and Karl H. Kienitz

Abstract— **This work presents a new method of stabilization for unstable periodic orbits of continuous-time dynamical systems. The principle of this method is to use feedback term based on the difference between the actual state value and the future state value computed along the trajectories of the uncontrolled system. To compute the value of the latter, an implicit Runge-Kutta ODE integration method is used, giving rise to a time-varying dynamical controller. The stability of the control method is defined in terms of the Floquet theory and the conditions for calculation of the monodromy matrix are presented. Numerical results are obtained using the forced Van der Pol oscillator as case study and the orthogonal collocation method as implicit Runge-Kutta method.**

I. INTRODUCTION

The erratic nature of chaotic systems is an undesired characteristic in many engineering applications, however, some properties of chaotic sets favour applications where the desired behaviour is a periodic oscillation. The sensitive dependence on initial conditions and the presence of a dense set of unstable periodic orbits (UPOs) embedded in chaotic sets [1] are characteristics of chaotic sets that lead to the concept of chaos control [2]. The sensitive dependence on initial conditions allows that small perturbations are sufficient to stabilize one of the many existent periodic solutions. The fact that the periodic orbit is already a solution of the system contributes to a very low control effort, and this appears as a realistic way to confine the evolution of the system to certain restricted part of the state space.

A variety of numerical evaluations of chaos control have been conducted since the introduction of the concept by Ott et al. [2]. For a review, see [3]. Pyragas [4] proposed a continuous-time feedback chaos control based on the difference between the current time system state and the time delayed system state, the Delayed Feedback Control (DFC). Apart from its attractive simplicity, this method became popular because of its practical aspects [5]. Its limitations (see " [6]–[9] but also [10]) stimulated the development of alternative feedback methods, e.g. the Prediction-Based Chaos Control (PBCC) [11].

The PBCC, originally proposed for discrete-time dynamical systems, uses the difference between the current time system state and the state computed at a time located one period ahead of the current time, along the free system trajectories. This control scheme does not present the limitations of DFC and its stability characteristics are easier to define [12]–[14].

While the present paper is mainly interested by control of chaos, we want to stress that both DFC and PBCC are control methods that may be used in principle for stabilization of any discrete-time system having unstable periodic orbits.

Here we develop a continuous-time PBCC, using feedback term based on the future state of the uncontrolled system. The method proposed to compute the latter is based on an implicit Runge-Kutta integration method [15], and the controlled system is an ODE system. More precisely, orthogonal collocation method [15]–[17] is used, resulting in tight prediction of the future state. Control gain synthesis is based on Floquet theory and Floquet multipliers [13], [18]. These ideas are successfully applied numerically to the Van der Pol (VdP) oscillator as case study, and comparison with DFC is achieved.

The paper is structured as follows. Section II presents the principles and general formulation of the proposed method. Section III is dedicated to the orthogonal collocation method applied to the general formulation. The method to calculate the stabilizing control gain is presented in Section IV. The numerical results are presented in Section V and conclusions are given in Section VI.

II. PRINCIPLES AND GENERAL FORMULATION

Consider the following continuous-time dynamical system

$$\dot{x}(t) = f(t, x(t)), \quad t \geq 0 \tag{1}$$

where $x : [0, +\infty) \to \mathbb{R}^n$ and $f : [0, +\infty) \times \mathbb{R}^n \to \mathbb{R}^n$ are column vectors and $n \in \mathbb{N}$. The function f is assumed T-periodic with respect to the time variable, for given $T > 0$.

We assume the existence of an unstable periodic orbit (UPO) as solution of (1). Thus, there is a trajectory x^* that satisfies

$$x^*(t + T) = x^*(t), \quad \forall t \in \mathbb{R}. \tag{2}$$

We attempt here to stabilize the UPO x^* by use of a continuous-time version of the Prediction-Based Chaos Control (PBCC) presented in [11], [13]. The feedback control term is applied as indicated in (3)

$$\dot{x}(t) = f(t, x(t)) + Bu(t), \quad x(0) = x_0. \tag{3}$$

Our contribution is to compute $u(t)$ as a *dynamical state-feedback* defined as

$$u(t) = K_c \left(\mathbf{x}(t + T, t, x(t)) - x(t)\right). \tag{4}$$

This project has been funded by CAPES-COFECUB (project Ma 624/09), FAPESP (grant 2011/17610-0) and Université Paris-Sud Orsay. T.P. Chagas is with Universidade Estadual de Santa Cruz (UESC), 45662-900 Ilhéus-BA, Brazil; Instituto Tecnológico de Aeronáutica (ITA), 12228-900 São José dos Campos-SP, Brazil; Inria, 78153 Le Chesnay cedex, France, thchagas@gmail.com. P.-A. Bliman is with Inria, pierre-alexandre.bliman@inria.fr. K.H. Kienitz is with ITA, kienitz@ieee.org

$x : [0, +\infty) \to \mathbb{R}^n$ is the state of the system to be stabilized and, by definition, for any $x \in \mathbb{R}^n$, any $t' \geq t$, $\mathbf{x}(t', t, x)$ is *the value at time t' of the solution of the free system* (1) *departing at time t from x*. $\mathbf{x}(t', t, x)$ is the state transition map of (1) [19]. $B \in \mathbb{R}^{n\times q}$ is the input matrix and $K_c \in \mathbb{R}^{q\times n}$ is the control gain matrix. Observe that the UPO $x^*(t)$ of (1) is also a periodic orbit of (3)-(4) that we intend to stabilize using adequate control gain K_c.

The coupled system is solution of the following PDE

$$\frac{\partial X(t,0)}{\partial t} = f(t, X(t,0)) + BK_c\left(X(t,T) - X(t,0)\right),\ t \geq 0 \tag{5a}$$

$$\frac{\partial X(t,Ts)}{\partial s} = Tf(t+Ts, X(t,Ts)),\ t \geq 0, s \in [0,1] \tag{5b}$$

$$X(0,0) = x_0.$$

The function $X : [0, +\infty) \times [0, T] \to \mathbb{R}^n$ is such that $X(t, 0) = x(t)$ and $X(t, T) = \mathbf{x}(t + T, t, x(t))$.

Real-time application of the control structure proposed here depends on the ability to compute $\mathbf{x}(t + t, t, x(t))$. The first step consists in approximating the solution of (5b) by an implicit Runge-Kutta ODE integration method [15], in order to estimate the terminal value

$$X(t,T) = x + T\int_0^1 f\left(t + Ts, X(t,Ts)\right) ds,\ x \text{ given} \tag{6}$$

For this, the operator $\mathbf{x}$ is first approximated by the operator $\mathbf{y}$ defined by

$$\mathbf{y}(t+T,t,x) = x + T\sum_{i=1}^{N} c_i l_i(t) \tag{7a}$$

$$l_i(t) = f\left(t + Ts_i, x + T\sum_{j=1}^{N} a_{ij} l_j(t)\right), \tag{7b}$$

where $i = 1, \ldots, N$, $l_j : [0, +\infty) \times \mathbb{R}^n \to \mathbb{R}^n$ and $a_{ij}, c_i \in \mathbb{R}$ are weights chosen according to the implicit method used. The approximation $\mathbf{y}(t+T, t, x(t))$ of $X(t, Ts)$, $s \in [0, 1]$, is calculated at the discretization points $s = s_i$, $i = 1, \ldots, N$.

For simplicity, equation (7b) is written with the vector unknown $L(t) = \begin{bmatrix} l_1(t)' & \ldots & l_N(t)' \end{bmatrix}' \in \mathbb{R}^{nN}$:

$$L(t) = F_T(t, x, L(t)), \quad t \geq 0 \tag{8}$$

where $F_T : [0, +\infty) \times \mathbb{R}^n \times \mathbb{R}^{nN} \to \mathbb{R}^{nN}$ is defined in (9).

To compute $\mathbf{y}(t + T, t, x)$ through (7a), it is necessary to solve the algebraic system of equations (8) with unknown $L(t) \in \mathbb{R}^N$. Writing $C = \begin{pmatrix} c_1 & \ldots & c_N \end{pmatrix}$ and closing equation (3) by $u(t) = K_c(\mathbf{y}(t + T, t, x(t)) - x(t))$ yields a differential algebraic equation (DAE), namely:

$$\dot{x}(t) = f(t, x(t)) + TBK_cCL(t), \quad x(0) = x_0 \tag{10a}$$

$$L(t) = F_T(t, x(t), L(t)). \tag{10b}$$

We propose now to approximate (10b) by solving the nN-dimensional ODE (11). The initial value $\hat{L}(0)$ is intended to be (precisely) computed off-line.

$$\frac{d}{dt}\left(\hat{L}(t) - F_T(t, x(t), \hat{L}(t))\right) + k_o\left(\hat{L}(t) - F_T(t, x(t), \hat{L}(t))\right) = 0, \tag{11}$$

Provided $k_o > 0$ and (10b) possesses a unique solution $L(t)$ for any t, x_0, the solution of (11), if it exists, tends asymptotically towards $L(t)$ when $t \to +\infty$. Writing $A = (a_{ij})$; ∂_i the partial derivative with respect to the i-th variable; I_n the identity matrix; $\mathbf{1}_N$ the vector with elements equal to 1 and $\otimes$ the Kronecker product, (11) writes as (12), with $G_T : \mathbb{R} \times \mathbb{R}^n \times \mathbb{R}^{nN} \to \mathbb{R}^{nN}$. Introducing (11) instead of (10b) in (10a) finally yields

$$\begin{bmatrix} \dot{x}(t) \\ \dot{\hat{L}}(t) \end{bmatrix} = \begin{bmatrix} f(t, x(t)) + TBK_cC\hat{L}(t) \\ G_T(t, x(t), \hat{L}(t)) \end{bmatrix}, \quad x(0) = x_0 \tag{13}$$

The ODE (13) has two types of state components, corresponding to the controlled system dynamics and to the dynamical state controller. The solution of (13) is an approximation of the solution of (5).

III. Approximation and implementation

The implicit Runge-Kutta method given in (7) is a general formulation used for the integration of differential equations, whose application depends on the choice of a specific implementation. Here we take the orthogonal collocation [15]–[17] as implicit Runge-Kutta method, but there's no doubt other implementations should be experimented.

A. Orthogonal collocation method

Now, $\mathbf{y}(t+T, t, x)$ in (7) is replaced by $\mathbf{z}(t+T, t, x)$, with $\mathbf{z}(t + T, t, x)$ defined on the whole interval $[t, t + T]$ by:

$$\mathbf{z}(t+Ts,t,x) = w_0(s)x + \sum_{i=1}^{N+1} w_i(s)m_i(t),\ s \in [0,1], t \geq 0 \tag{14}$$

where $m_i : [0, +\infty) \to \mathbb{R}^n$, $i = 1, \ldots, N + 1$, is a column vector. The choice of the weight polynomials $w_i(s)$, $i = 0, \ldots, N+1$ gives different properties to the collocation method. We choose here Lagrange polynomials:

$$w_i(s) = \prod_{j=0, j\neq i}^{N+1} \frac{s - s_j}{s_i - s_j}, \quad i = 0, \ldots, N + 1. \tag{15}$$

but other ones, like Chebyshev or Legendre, could be used. The collocation points verify $0 = s_0 < s_1 < \cdots < s_N < s_{N+1} = 1$, and are taken in order to fulfil the orthogonality relations:

$$\int_0^1 (1-s)s\, w_i(s)w_j(s)\, ds = 0,\ i, j = 1, \ldots, N,\ i \neq j. \tag{16}$$

Note that the state for each time $t + Ts_i$ is approximated as $\mathbf{z}(t + Ts_i, t, x) \approx m_i(t)$ for any $i = 0, \ldots, N + 1$, as $w_i(s_j) = \delta_i^j$ (with δ_i^j, the Kronecker symbol). A characteristic of the orthogonal collocation method is that each $m_i(t)$ is an approximation of the state that differs from the $l_i(t)$ in

$$F_T(t,x,L) = \left[f(t+Ts_1, x+\textstyle\sum_{j=1}^{N} a_{1j}l_j)' \quad \dots \quad f(t+Ts_N, x+\sum_{j=1}^{N} a_{Nj}l_j)'\right]', \quad x\in\mathbb{R}^n,\ L\in\mathbb{R}^{nN} \tag{9}$$

$$\dot{\hat{L}}(t) = \left[I_{nN} - T\partial_3 F_T(t,x(t),\hat{L}(t))(A\otimes I_n)\right]^{-1}\left[\partial_1 F_T(t,x(t),\hat{L}(t)) + \partial_2 F_T(t,x(t),\hat{L}(t))(\mathbf{1}_N\otimes f(t,x(t))) - k_o\left(\hat{L}(t) - F_T(t,x(t),\hat{L}(t))\right)\right] := G_T(t,x(t),\hat{L}(t)) \tag{12}$$

$$\left.\frac{\partial \mathbf{z}(t+Ts,t,x)}{\partial s}\right|_{s=s_j} \approx \left.\frac{\partial w_0(s)}{\partial s}\right|_{s=s_j} x + \sum_{i=1}^{N+1}\left.\frac{\partial w_i(s)}{\partial s}\right|_{s=s_j} m_i(t) \approx Tf(t+Ts_j, m_j(t)). \tag{17}$$

(7), which are the derivatives. The derivative $\frac{\partial \mathbf{z}(t+Ts,t,x)}{\partial s}$ at s_j, $j=1,\dots,N+1$ verifies formula (17).

From this is deduced the following matrix equation with unknown $M(t)$, which parallels (10b):

$$(W_0\otimes I_n)x(t) + (W\otimes I_n)M(t) = H_T(t,M(t)) \tag{18}$$

where $w(s) = [w_1(s)\ \dots\ w_{N+1}(s)]'$ and

$$W_0 = \left[\left.\frac{\partial w_0(s)}{\partial s}\right|_{s=s_1} \quad \cdots \quad \left.\frac{\partial w_0(s)}{\partial s}\right|_{s=s_{N+1}}\right]',$$

$$W = \left[\left.\frac{\partial w(s)}{\partial s}\right|_{s=s_1} \quad \cdots \quad \left.\frac{\partial w(s)}{\partial s}\right|_{s=s_{N+1}}\right]',$$

$$M(t) = \begin{bmatrix} m_1(t) & \cdots & m_{N+1}(t)\end{bmatrix}',$$

$$H_T(t,M) = \begin{bmatrix} Tf(t+Ts_1, m_1) \\ \vdots \\ Tf(t+Ts_{N+1}, m_{N+1})\end{bmatrix}.$$

Here, $W_0\in\mathbb{R}^{(N+1)}$, $W\in\mathbb{R}^{(N+1)\times(N+1)}$, $M:\mathbb{R}\to\mathbb{R}^{n(N+1)}$, $H_T:\mathbb{R}\times\mathbb{R}^{n(N+1)}\to\mathbb{R}^{n(N+1)}$. H_T depends on the choice of the s_i, $i=1,\dots,N$, but, for simplicity, this dependence is not explicit here.

B. Solution of the orthogonal collocation method using the observer

The solution of the algebraic equation (18) is done using the observer (11) resulting in (19) which can be written in turn as (20). With an appropriate choice of $\hat{M}(0)$ and k_o, the state $\hat{M}(t)$ converges to the solution of (18).

Following equation (13), the feedback term effectively implemented yields the closed-loop system

$$\begin{bmatrix}\dot{x}(t)\\ \dot{\hat{M}}(t)\end{bmatrix} = \begin{bmatrix} f(t,x(t)) + BK_c\left[\hat{m}_{N+1}(t) - x(t)\right] \\ Q_T(t,x(t),\hat{M}(t))\end{bmatrix},\ x(0)=x_0. \tag{21}$$

Equation (21), the equivalent of (13) for the orthogonal collocation implementation, gives an approximate solution of (3)-(4).

IV. Control gain design

Now that the feedback method has been exposed, we provide a method to design the control gain K_c. It depends upon the ability of calculating the closed-loop monodromy matrix of $x^*(t)$. The calculus of this matrix requires the integration of the closed-loop system and its variational equation along a trajectory in the vicinity of $x^*(t)$ [20, Appendix B]. To integrate this trajectory, initial condition is chosen as close as possible to $x^*(0)$. Integrating over a period yields the corresponding monodromy matrix. The Floquet multipliers, the eigenvalues of the monodromy matrix, are used to analyze the orbit stability [18]. Computation of the monodromy matrix using an implicit Runge-Kutta method was not studied.

For illustration purposes, a special structure for B and K_c will be used. This structure results on a scalar gain that reduces the calculus complexity and enables to evaluate numerically the relation between the Floquet multipliers and the control gain.

$$B = \begin{bmatrix}0 & \cdots & 0 & 1\end{bmatrix}',\quad K_c = k_c\begin{bmatrix}0 & \cdots & 0 & 1\end{bmatrix}$$

The integration of the variational equation depends on the Jacobian matrix at $x^*(t)$, obtained by linearising (3)-(4), i.e.:

$$\left\{\nabla_x f(t,x(t)) + BK_c\left[\phi(t+T,t) - I_n\right]\right\}_{x(t)=x^*(t)} \tag{22}$$

where $\phi(t+T,t)|_{x(t)=x^*(t)}$, the monodromy matrix of $x^*(t)$ for the free system (1), is calculated for each integration step of (3)-(4). Using (22) we compute the closed-loop monodromy matrix of $x^*(t)$ given gain k_c. The Floquet multipliers are calculated to measure the local stability of the controlled orbit for the chosen k_c. In practice, we fix k_c and obtain the corresponding Floquet multipliers.

V. Numerical results

In this section we apply the proposed solution to the forced Van der Pol (VdP) oscillator. The function $f(t,x)$ in (1) is given by

$$f(t,x) = \begin{bmatrix} x_2 \\ a\sin(\omega t) - \mu(x_1^2-1)x_2 - x_1\end{bmatrix}. \tag{23}$$

In this example the parameters $a=0.988$, $\omega=0.45$ and $\mu=1$ were chosen such that a chaotic attractor exists [21] and consequently a infinite number of UPOs [22].

The control scheme (3) is applied, with $u(t)$ defined in (4) $B=[0\ 1]'$ and $K_c = k_c[0\ 1]$, resulting in

$$\begin{bmatrix}\dot{x}_1(t)\\ \dot{x}_2(t))\end{bmatrix} = f(t,x(t)) + \begin{bmatrix} 0 \\ k_c\left[\mathbf{x}_2(t+T,t,x(t)) - x_2(t)\right]\end{bmatrix} \tag{24}$$

The period of the forcing term is taken here as $T=\frac{2\pi}{0.45}$. Each periodic orbit of system (23) has period multiple of T. The target UPO $x^*(t)$ chosen here is an orbit of period T. This simplifies the analysis, but this does not reduce the generality of the method.

The feedback designed by approximating the feedback term, leading to the closed-loop system (21). The solution

$$\frac{d}{dt}\left[(W\otimes I_n)\hat{M}(t)+(W_0\otimes I_n)z(t)-H_T(t,\hat{M}(t))\right]+k_o\left[(W\otimes I_n)\hat{M}(t)+(W_0\otimes I_n)x(t)-H_T(t,\hat{M}(t))\right]=0 \quad (19)$$

$$\dot{\hat{M}}(t)=\left[(W\otimes I_n)-\partial_2 H_T(t,\hat{M}(t))\right]^{-1}\left\{\partial_1 H_T(t,\hat{M}(t))-(W_0\otimes I_n)f(t,x(t))\right.$$
$$\left.-k_o\left[(W\otimes I_n)\hat{M}(t)+(W_0\otimes I_n)x(t)-H_T(t,\hat{M}(t))\right]\right\}:=Q_T(t,x(t),\hat{M}(t)) \quad (20)$$

of the latter depends on the choice of three parameters: the control gain k_c, the observer gain k_o and the number of intermediate discretization points for the orthogonal collocation method N. The values k_o and N are directly related to the estimation quality and these two parameters will be tuned first.

A. Tuning the parameters k_o and N

To evaluate the future state estimation, whose characteristics are related to the parameters k_o and N, we first set $k_c = 0$. We used as the initial condition $x_0 = [-0.75,\ 0.75]'$. The system is integrated for $t \in [0, T]$ and the points $\hat{m}_{N+1}(t + jT/999)$, $j = 0, \ldots, 999$, are collected for different values of k_o and N. One then assesses the convergence by comparison with the solution obtained with $N = 150$ and $k_o = 50$, by computing (25), where the superscript on $\mathbf{z}_2^{(N,k_o)}$ indicates the value of N and k_o used in the estimation. In Figure 1(a) is given $\varepsilon(N, 50)$ for different values of N.

Note that the collocation parameters s_i, W_0 and W are previously calculated for each N tested. The computation of large matrices W_0 and W requires intense off-line computational burden and reduces the number of values N tested, but these matrices are calculated once for all and are independent of f.

Repeating the same process, we evaluate $\varepsilon(150, k_o)$ for different values of k_o, see Figure 1(b). Increasing N and k_o results in larger computation effort and trade-off between estimation quality and computation effort should be considered.

Due to the error level shown in Figure 1 for $N = 100$ and $k_o = 10$, we adopt these values in the sequel. In Figure 2 is shown $x_2(t)$ and $\mathbf{z}_2(t, t - T, x(t - T))$ (beware the time shift here). In this case it is expected that $x(t) = \mathbf{x}(t, t - T, x(t - T))$ and the proximity of both time series in Figure 2 allows to use $\mathbf{x}$ instead of $\mathbf{z}$.

B. Tuning of k_c

Now we tune the feedback gain. We use (22), with $x^*(0) = [0.15884454118,\ 0.110605560432]'$, to obtain a value k_c that stabilizes the orbit of (5). Note that, the estimation with $N = 100$ and $k_o = 10$ being precise, we expect that a stabilizing k_c for (5) will yield stable slightly perturbed cycle for (21).

Figure 3 shows the modulus of the two Floquet multipliers $|\mu|$ for different values of k_c. The stability is achieved when $|\mu| \leq 1$. We chose $k_c = 0.5$, which results in $|\mu| \approx 0.315 \times 10^{-2}$.

Stabilized trajectory for $k_c = 0.5$, $k_o = 10$, $N = 100$ and $x_0 = [-0.75,\ 0.75]'$ is shown in the state space in Figure 4.

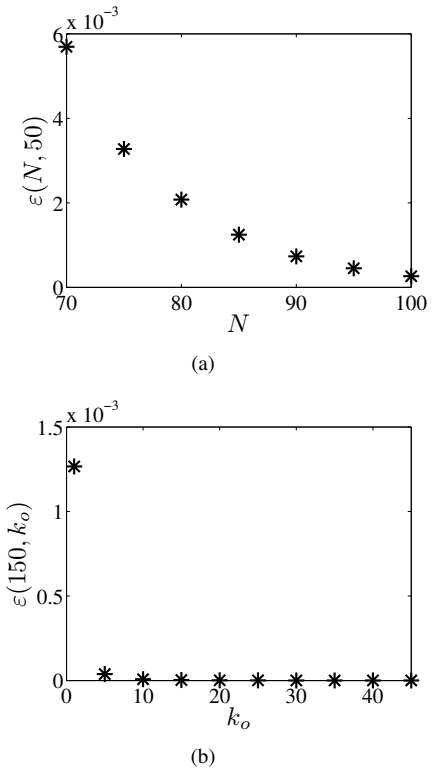

Fig. 1. Error between the estimated free system response future value using different values of (a) N and (b) k_o.

The time series of the controlled orbit is shown in Figure 5(a) and 5(b) for the first and second state variables, respectively.

The control effort applied to stabilize the target orbit is shown in Figure 6. The control effort tending to zero and $x(t)$ tending to $\mathbf{x}(t+T, t, x(t))$ ensure that the orbit is stabilized.

These results exemplify a successful application of the PBCC to a continuous-time dynamical system using a real-time estimation of the future state dynamics.

C. Comparison with the Delayed Feedback Control

The DFC will be used here as a classical reference for comparison with the proposed method. The control signal to be applied on (3), with $B = [0\ 1]'$, for the DFC is defined as

$$u(t) = K_d\left(x(t-T) - x(t)\right). \quad (26)$$

where the matrix $K_d = [0\ k_d]$ is chosen, $k_d \in \mathbb{R}$.

The value $k_d \approx 0.061992542246$ is obtained by optimization using as cost function the largest Floquet multiplier in modulus [23], resulting in $|\mu| \approx 0.3535$. Here we observe the first advantage of the proposed method, the largest Floquet

$$\varepsilon(N,k_o)=\frac{\|\mathbf{z}_2^{(150,50)}(.,0,x(0))-\mathbf{z}_2^{(N,k_o)}(.,0,x(0))\|_{L^1(0,T)}}{\|\mathbf{z}_2^{(150,50)}(.,0,x(0))\|_{L^1(0,T)}} \tag{25}$$

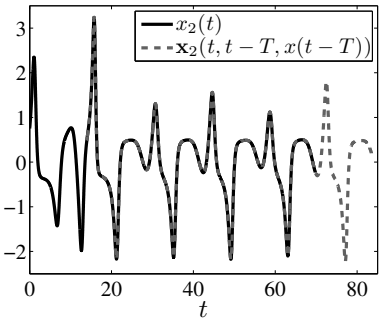

Fig. 2. Current time and shifted future time trajectory of the system for $k_c = 0$, $k_o = 10$ and $N = 100$.

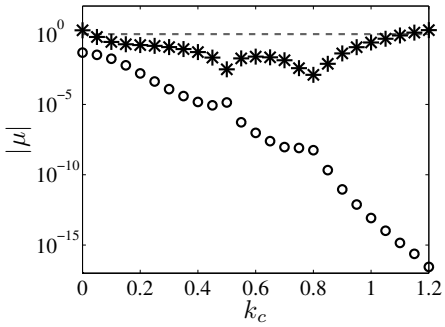

Fig. 3. Modulus of the Floquet multipliers for different values of k_c.

multiplier is closer to zero than the one obtained for the DFC, resulting in a more stable orbit.

The trajectory with $x_0 = [-0.75,\ 0.75]'$ controlled by the DFC in the state space is shown in Figure 7(a) and the time series of the control effort is shown in Figure 7(b). Comparing these figures with Figures 4 and 6, respectively, we observe that the convergence of the trajectory to the controlled orbit by the proposed method is much faster than the one controlled by the DFC. This result is in agreement with the calculated $|\mu|$.

VI. Conclusions

A new stabilization method for unstable periodic orbits of continuous-time dynamical systems has been presented. The principle of this method is to use a feedback term based on the difference between the actual state value and the future state value computed along the trajectories of the uncontrolled system.

The method consists in approximating the predicted free system response by use of an implicit Runge-Kutta method, resulting in a closed-loop DAE. The algebraic equation is solved using an observer which leads to an extended ODE.

The orthogonal collocation method was used as implicit Runge-Kutta method and was applied to the forced Van der Pol oscillator. The results shown here were obtained with $N = 100$ collocation points to guarantee good estimation, although stabilization of the periodic orbit was obtained for $N \geq 70$.

To predict trajectories of chaotic systems requires special care, due to the sensitive dependence on initial conditions, and this explains the large values employed here. Nevertheless, the large closed-loop ODE system obtained induces high computational effort. Reducing the number of collocation points by using different implicit Runge-Kutta

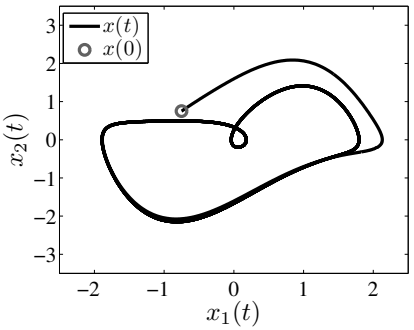

Fig. 4. Stabilized orbit in the state space for $k_c = 0.5$.

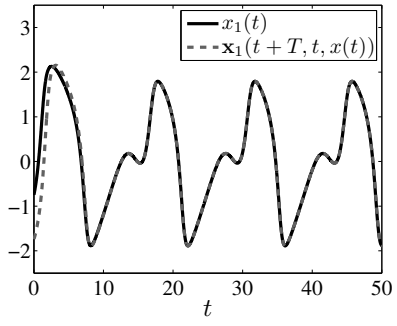

(a)

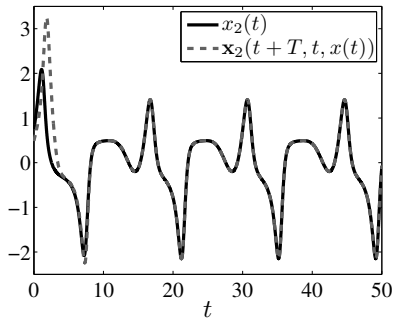

(b)

Fig. 5. Time series for the (a) first and (b) second state variables of a stabilized orbit with $k_c = 0.5$.

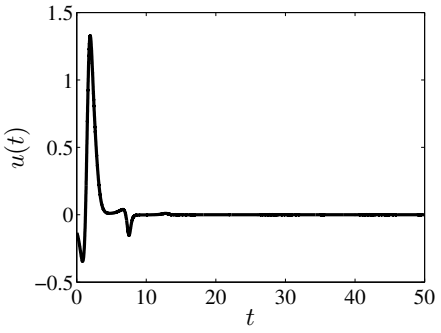

Fig. 6. Time series of the control effort of a stabilized orbit for $k_c = 0.5$.

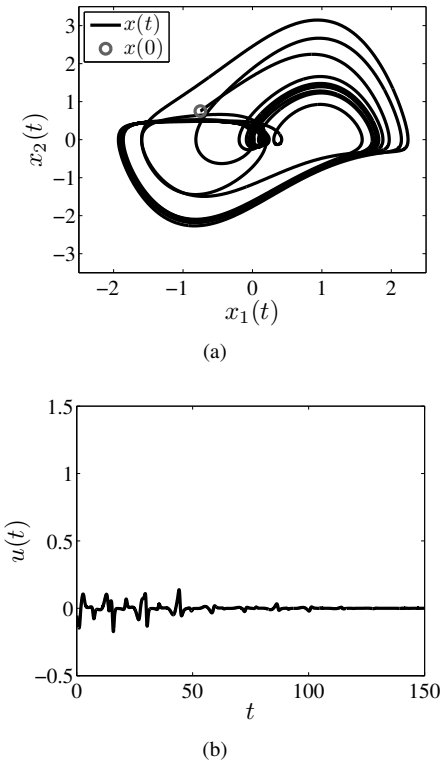

Fig. 7. Trajectory controlled using the DFC with $k_d \approx 0.061992542246$. (a) State space and (b) time series of the control effort.

methods (based e.g. on Chebyshev polynomials or finite element method) certainly needs to be the object of future research in order to arrive to satisfying implementation of the new control principle proposed here.

The real-time estimation of the future state of the free system response can be used in regular systems where periodic orbits or fixed points are to be controlled with different control structures. Modifications of the method can be applied, for example, in model-based predictive controllers. The observer software can be embedded in a dedicated processor and used in parallel with the measurement of the system outputs in practical systems applications.

A method for the control gain determination was also presented based on the Floquet theory. The linearized system, which is a requisite for the monodromy matrix computation, was presented and a stabilizing control gain calculated. A controlled orbit was exemplified and comparison with the DFC was done evidencing the advantages of the proposed method.

REFERENCES

[1] R. L. Devaney, *A first course in chaotic dynamical systems: theory and experiment*. New York: Addison-Wesley, 1992.

[2] E. Ott, C. Grebogi, and J. A. Yorke, "Controlling chaos," *Physical Review Letters*, vol. 64, pp. 1196–1199, Mar. 1990.

[3] E. Schöll and H. G. Schuster, *Handbook of Chaos Control*. John Wiley & Sons, 2008.

[4] K. Pyragas, "Continuous control of chaos by self-controlling feedback," *Physics Letters A*, vol. 170, pp. 421–428, Nov. 1992.

[5] K. Pyragas and A. Tamaševičius, "Experimental control of chaos by delayed self-controlling feedback," *Physics Letters A*, vol. 180, pp. 99–102, Aug. 1993.

[6] T. Ushio, "Limitation of delayed feedback control in nonlinear discrete-time systems," *IEEE Transactions on Circuits and Systems I - Regular Papers*, vol. 43, no. 9, pp. 815–816, SEP 1996.

[7] W. Just, T. Bernard, M. Ostheimer, E. Reibold, and H. Benner, "Mechanism of Time-Delayed Feedback Control," *Physical Review Letters*, vol. 78, no. 2, pp. 203–206, Jan. 1997.

[8] H. Nakajima, "On the stability of delayed feedback control of chaos," in *36th IEEE Conference on Decision and Control*, St. Petersburg, Russia, Dec. 1997, pp. 411–414.

[9] ——, "On analytical properties of delayed feedback control of chaos," *Physics Letters A*, vol. 232, pp. 207–210, Jul. 1997.

[10] B. Fiedler, V. Flunkert, M. Georgi, P. Hövel, and E. Schöll, "Refuting the Odd-Number Limitation of Time-Delayed Feedback Control," *Physical Review Letters*, vol. 16, p. 114101, Mar. 2007.

[11] T. Ushio and S. Yamamoto, "Prediction-based control of chaos," *Physics Letters A*, vol. 264, pp. 30–35, Dec. 1999.

[12] Ö. Morgül, "A new generalization of delayed feedback control," *International Journal of Bifurcation and Chaos*, vol. 19, no. 1, pp. 365–377, JAN 2009.

[13] T. P. Chagas, P.-A. Bliman, and K. H. Kienitz, "New feedback laws for stabilization of unstable periodic orbits," in *8th IFAC Symposium on Nonlinear Control Systems*, Bologna, Italy, Set. 2010.

[14] ——, "Estabilização de órbitas periódicas: comparação entre realimentação de estados atrasados e uma nova lei utilizando estados preditos," in *XVIII Congresso Brasileiro de Automática*, Bonito, Brazil, Sep. 2010.

[15] E. Hairer, S. P. Norsett, and G. Wanner, *Solving Ordinary Differential Equation I: Nonstiff Problems*. Berlin: Springer Verlag, 2008.

[16] J. Viladsen and M. L. Michelsen, *Solution of Differential Equation Models by Polynomial Approximation*. Englewood Cliffs: Prentice-Hall, 1978.

[17] A. B. Finlayson, *The Method of Weighted Residuals and Variational Principles*. London: Academic Press, 1972.

[18] S. Bittanti and P. Colaneri, *Periodic Systems: Filtering and Control*. London: Springer Verlag, 2008.

[19] D. Hinrichsen and A. J. Pritchard, *Mathematical Systems Theory I: Modelling, State Space Analysis, Stability and Robustness*, ser. Texts in Applied Mathematics. Springer, 2010, no. v. 1.

[20] T. S. Parker and L. O. Chua, *Practical Numerical Algorithms for Chaotic Systems*. New York: Springer-Verlag, 1989.

[21] A. C.-L. Chian, F. A. Borotto, E. L. Rempel, and C. Rogers, "Attractor merging crisis in chaotic business cycles," *Chaos, Solitons and Fractals*, vol. 24, pp. 869–875, 2005.

[22] P. Cvitanović, "Invariant measurement of strange sets in terms of cycles," *Physical Review Letters*, vol. 61, pp. 2729–2732, Dec. 1988.

[23] T. P. Chagas, B. A. Toledo, E. L. Rempel, A. C.-L. Chian, and J. A. Valdivia, "Optimal feedback control of the forced van der pol system," *Chaos, Solitons & Fractals*, vol. 45, no. 9-10, pp. 1147 – 1156, 2012.

T. P. Chagas, B. A. Toledo, E. L. Rempel, A. C.-L. Chian and J. A. Valdivia, Optimal feedback control of the forced van der Pol system, *Chaos, Solitons & Fractals*, vol. 45, no. 9-10, pp. 1147-1156, 2012

Chaos, Solitons & Fractals 45 (2012) 1147–1156

Contents lists available at SciVerse ScienceDirect

Chaos, Solitons & Fractals

Nonlinear Science, and Nonequilibrium and Complex Phenomena

journal homepage: www.elsevier.com/locate/chaos

Optimal feedback control of the forced van der Pol system

T.P. Chagas [a,b,c], B.A. Toledo [b,d,*], E.L. Rempel [b,e], A.C.-L. Chian [e,f], J.A. Valdivia [d,g]

[a] Santa Cruz State University (UESC), 45662-900 Ilhéus-BA, Brazil
[b] Institut of Aeronautical Technology (ITA), 12228-900 São José dos Campos-SP, Brazil
[c] Institut National de Recherche en Informatique et en Automatique (INRIA), Rocquencourt BP105, 78153 Le Chesnay cedex, France
[d] Departamento de Física, Facultad de Ciencias, Universidad de Chile, Casilla 653, Santiago, Chile
[e] National Institute for Space Research (INPE) and World Institute for Space Environment Research (WISER), 12227-010 São José dos Campos-SP, Brazil
[f] Observatoire de Paris, LESIA, CNRS, 92190 Meudon, France
[g] Centro para el Desarrollo de la Nanociencia y la Nanotecnología, CEDENNA, Avenida Libertador Bernardo O'Higgins 3363, Estación Central, Santiago, Chile

ARTICLE INFO

Article history:
Received 3 April 2012
Accepted 15 June 2012
Available online 20 July 2012

ABSTRACT

A simple feedback control strategy for chaotic systems is investigated using the forced van der Pol system as an example. The strategy regards chaos control as an optimization problem, where the maximum magnitude Floquet multiplier of a target unstable periodic orbit (UPO) is used as a cost function that needs to be minimized. Thus, the method obtains the optimal control gain in terms of the stability of the target UPO. This strategy was recently proposed for the proportional feedback control (PFC) method. Here, it is extended to the highly popular delayed feedback control (DFC) method. Since the DFC method treats the system as a delay-differential equation whose phase space is infinite-dimensional, the characteristic multipliers are found through a truncation in the number of delayed states. Control of a target UPO is achieved for several values of the forcing amplitude. We compare the DFC and PFC methods in terms of stability of the controlled orbit, steady state error and control effort.

1. Introduction

The erratic nature of chaotic systems may be an undesired characteristic in many applications, where one usually expects the system to behave in a predictable way. However, some properties of chaotic sets favor applications where the desired behavior is a periodic oscillation. The sensitive dependence on initial conditions and the presence of a dense set of unstable periodic orbits (UPOs) embedded in chaotic sets leads to the concept of chaos control, where small perturbations are sufficient to stabilize one of the many unstable periodic states. Moreover, since trajectories on chaotic attractors come arbitrarily close to any of the embedded UPOs due to ergodicity, there is no need to apply external forces to drive the system to the proximity of the desired state and the control effort from then on is ideally very low, constrained by the noise level. A wealth of numerical and experimental applications of chaos control have been conducted since the introduction of the concept by Ott et al. [1]. For a review, see Sanjuán and Grebogi [2].

Pyragas [3] proposed two chaos control methods based on state feedback control. These control schemes became an alternative to the well known OGY method [1], which is based on small time-dependent perturbations to an accessible system parameter to stabilize different UPOs. The methods proposed by Pyragas became popular because of their practical aspects [4], in particular, for being continuous-time control schemes and depending on perturbations of a state variable, in contrast to the OGY method, which depends on the existence of a system parameter that should be constantly changed and is based on

* Corresponding author at: Departamento de Física, Facultad de Ciencias, Universidad de Chile, Casilla 653, Santiago, Chile.
E-mail address: btoledo@macul.ciencias.uchile.cl (B.A. Toledo).

0960-0779/$ - see front matter © 2012 Elsevier Ltd. All rights reserved.
http://dx.doi.org/10.1016/j.chaos.2012.06.004

Poincaré maps, so the parameter perturbations become time-discrete. This leads to restrictions when applying the OGY method to systems with noise [4].

The two methods proposed by Pyragas [3] are the proportional feedback control (PFC) and the delayed feedback control (DFC). The PFC uses a control signal based on the difference between the coordinates of the current state and the target UPO in the phase space. The DFC uses a feedback control signal based on the difference between the system state at a time t (current state) and the state at a time $t - T$ (delayed state), where T is the period of the orbit that must be stabilized (target UPO). Although simpler to implement experimentally, the DFC method has some known limitations to control UPOs with long periods [5], as well as UPOs with an odd number of real Floquet multipliers greater than unity [6]. The long-period limitation could be overcome by using, for example, the extended delayed feedback control [5]. The odd number limitation can be treated with the addition of an unstable degree of freedom to the system [7]. Note that even for the original DFC method, the odd number limitation has been contested with a counter example [8].

This work proposes a feedback control strategy through a case study of the forced van der Pol system, which is a widely studied nonlinear oscillator with applications to electrical circuits [9], biology [10], and economy [11], to name a few. We follow Asenjo et al. [12] and regard the control task as an optimization problem, which allows us to obtain the control gain that minimizes the largest magnitude Floquet multiplier of an unstable periodic orbit. Previously, Fouladi and Valdivia [13] had introduced a similar control method based on optimization. Asenjo et al. [12] investigated the optimal control strategy for the PFC method. Here, we extend their strategy to the DFC and compare it to the PFC, considering important aspects for real systems, such as steady state error and steady state control effort. A difficulty arises when computing the Floquet multipliers for the DFC method. The control law for this method leads to a delay-differential equation (DDE), whose phase space is infinite-dimensional. Hence, we compute the spectrum of Floquet multipliers by assuming an approximation where the continuous infinite-dimensional system is represented by a finite number of delayed states. We also evaluate the robustness of the controllers by considering parametric uncertainties.

In Section 2, the feedback control problem is defined and the PFC and DFC methods are described. This section, together with Appendices A,B,C describe the practical details employed to study the stability of the controlled periodic solutions. Section 3 describes our control strategy based on stability, steady state error, and control effort. The numerical results comparing the PFC and DFC are reported for the van der Pol system. The conclusions are given in Section 4.

2. Problem definition

Consider a continuous-time n-dimensional dynamical system described by the following system of differential equations

$$\frac{d\mathbf{x}(t)}{dt} = \mathbf{f}(t, \mathbf{x}(t)), \quad \mathbf{x}(0) = \mathbf{x}_0, \tag{1}$$

where $t \in \mathbb{R}$, $\mathbf{x} \in \mathbb{R}^n$ and $\mathbf{f} : \mathbb{R} \times \mathbb{R}^n \to \mathbb{R}^n$ is a smooth function. Let $\mathbf{x}^*(t)$ be an unstable periodic orbit of Eq. (1).

Our goal is to stabilize the target UPO $\mathbf{x}^*(t)$ using the following control structure

$$\frac{d\mathbf{x}(t)}{dt} = \mathbf{f}(t, \mathbf{x}(t)) + B\mathbf{u}(t), \tag{2}$$

where $\mathbf{u}(t) \in \mathbb{R}^n$ is a column vector representing the control signal and $B \in \mathbb{R}^{n\times n}$ is the input matrix, a coupling control coefficient. Here, we use $B = I_n$, where I_n is the identity matrix of order n. The control signal is defined as

$$\mathbf{u}(t) = K_c(\mathbf{r}(t) - \mathbf{x}(t)), \tag{3}$$

where $\mathbf{r}(t) \in \mathbb{R}^n$ is a reference signal that depends on the control method and $K_c \in \mathbb{R}^{n\times n}$ is a gain matrix that must be carefully chosen to stabilize $\mathbf{x}^*(t)$.

2.1. Proportional feedback control

The proportional feedback control is a method that uses the target orbit $\mathbf{x}^*(t)$ as reference. For this control scheme the value of $\mathbf{r}(t)$ in Eq. (3) is substituted by $\mathbf{x}^*(t)$, so $\mathbf{u}(t)$ is defined by

$$\mathbf{u}(t) = K_c(\mathbf{x}^*(t) - \mathbf{x}(t)).$$

The stability of the controlled orbit can be studied from the $n \times n$ monodromy matrix of the system, $\Phi_{\mathbf{x}^*}(t)$, obtained by the usual method of integrating the variational equation (4) from time 0 to T,

$$\frac{d\phi_{\mathbf{x}}(t,0)}{dt} = \nabla_{\mathbf{x}}[\mathbf{f}(t, \mathbf{x}(t)) + K_c(\mathbf{x}^*(t) - \mathbf{x}(t))]_{\mathbf{x}(t)=\mathbf{x}^*(t)}\phi_{\mathbf{x}}(t,0), \tag{4}$$

where $\phi_{\mathbf{x}}(t, t_0)$ is the state transition matrix, with $\phi_x(0,0) = I_n$, and $\Phi_{\mathbf{x}^*} = \phi_{\mathbf{x}}(T, 0)$, where T is the period of the target orbit, $\mathbf{x}^*(0) = \mathbf{x}^*(T)$ [14]. The eigenvalues of the monodromy matrix are the Floquet multipliers and describe how a perturbation in the periodic orbit grows with time. Orbits with at least one Floquet multiplier with magnitude greater than one are unstable.

2.2. Delayed feedback control

The delayed feedback control (DFC) is a method to stabilize UPOs based on reducing the error between the state of the controlled system at time t and its state at the delayed time $t - T$. For the DFC method, $\mathbf{r}(t) = \mathbf{x}(t - T)$ in Eq. (3), that is, the reference signal is the delayed state. Thus, $\mathbf{u}(t)$ is defined by

$$\mathbf{u}(t) = K_c(\mathbf{x}(t - T) - \mathbf{x}(t)). \tag{5}$$

The controlled system, Eq. (2), with $\mathbf{u}(t)$ given by Eq. (5) is a delay-differential equation (DDE). The state of this kind of dynamical system is represented by an infinite number of state variables representing the trajectory from $\mathbf{x}(t - T)$ to $\mathbf{x}(t)$. This implies that the phase space is infinite dimensional.

A finite-dimensional version of the system state is considered by representing it as a vector composed by a discrete-time approximation of the trajectory from $\mathbf{x}(t-T)$ to $\mathbf{x}(t)$. This extended state $X(t)$ is necessary for the stability analysis of the UPO and for estimating an optimal value for the control gain K_c, and can be represented as

$$X(t) = \begin{bmatrix} \mathbf{x}(t-s_0T) \\ \mathbf{x}(t-s_1T) \\ \vdots \\ \mathbf{x}(t-s_NT) \\ \mathbf{x}(t-s_{N+1}T) \end{bmatrix}, \tag{6}$$

where $s_0 = 0$, $s_i < s_{i+1}$, $i = 0,1,\ldots,N$, and $s_{N+1} = 1$. The s_i values are determined by the discretization method, which in our case is the orthogonal collocation method, described in Appendix B. The number of samples N depends on the system dynamics and the value of T. It is now possible to rewrite Eq. (2) for the DFC method as a function of $X(t)$ resulting in:

$$\frac{dX(t)}{dt} = F(t,X(t)) + (I_{N+2} \otimes BK_c)(X(t-T) - X(t)), \tag{7}$$

where I_{N+2} is the identity matrix of order $N+2$, $\otimes$ is the Kronecker product and

$$F(t,X(t)) = \begin{bmatrix} \mathbf{f}(t-s_0T, \mathbf{x}(t-s_0T)) \\ \mathbf{f}(t-s_1T, \mathbf{x}(t-s_1T)) \\ \vdots \\ \mathbf{f}(t-s_NT, \mathbf{x}(t-s_NT)) \\ \mathbf{f}(t-s_{N+1}T, \mathbf{x}(t-s_{N+1}T)) \end{bmatrix}. \tag{8}$$

By using the discrete approximation of the delayed states $X(t)$ and their derivatives ($dX(t)/dt = DX(t)$, see Appendices B and C) it is possible to obtain a monodromy matrix of the controlled UPO. Since stability must be achieved also for the delayed states, the monodromy matrix has order $n(N+2)$ for the DFC method. In this case, the variational equation constitutes a system with $[n(N+2)]^2$ equations, and its integration is time consuming. For this reason, we calculate the monodromy matrix according to the method introduced in Refs. [15,16], whereby $\Phi_{X^*(t)}$ is obtained by matrix algebra operations only. The method is described in Appendix A.

Unlike the PFC method, which requires prior knowledge of the position of the target UPO in the phase space, application of the DFC method requires only the period of the UPO. Nonetheless, the position of the UPO $\mathbf{x}^*(t)$ is used to compute the monodromy matrix employed in the stability analysis and control gain design (see Eq. (A.12) in Appendix A). In practice, one can use the DFC method itself with an arbitrary choice of K_c to control/find $\mathbf{x}^*(t)$. One could even use $\mathbf{x}(t)$ instead of $\mathbf{x}^*(t)$ in the monodromy matrix to find K_c, when $\mathbf{x}(t)$ is close to $\mathbf{x}^*(t)$, i.e., small $|\mathbf{x}(t) - \mathbf{x}(t-T)|_2$. These ideas will be explored somewhere else.

We adopt a scalar control gain, so that the gain matrix K_c is

$$K_c = \begin{bmatrix} k_c & [0]_{1,j} \\ [0]_{i,1} & [0]_{i,j} \end{bmatrix}, \quad k_c \in \mathbb{R},\ i,j = 2,\ldots,n-1 \tag{9}$$

and is represented by k_c hereafter.

3. Numerical results

In this section the DFC and PFC methods are applied to the forced van der Pol (vdP) oscillator, described by the following system of ODEs

$$\begin{aligned} \dot{x}_1(t) &= x_2(t), \\ \dot{x}_2(t) &= a\sin(\omega t) - \eta(x_1^2(t) - 1)x_2(t) - x_1(t). \end{aligned} \tag{10}$$

We follow Chian et al. [17] and choose $\omega = 0.45$, $\eta = 1$ and use a as the only adjustable parameter. All simulations are performed with Matlab's dde23 integrator with a local error tolerance equal to 10^{-10}. This integrator can be used for both ODEs and DDEs [18].

Since we are working with a periodically driven system, the natural choice of Poincaré map is a stroboscopic map

$$P : \mathbf{x}(t) \to \mathbf{x}(t+T_1), \tag{11}$$

where T_1 is the driver period.

Unstable periodic orbits of discrete-time period p in the Poincaré map (in contrast to continuous-time period T) are found as fixed points of the p-th iteration of the Poincaré map, $P^p(\mathbf{x}(t))$, with the secant method, by solving

$$\mathbf{x}(t) - P^p(\mathbf{x}(t)) = 0, \quad n \in \mathbb{N}, \tag{12}$$

which returns one Poincaré point of a period-p UPO, $\mathbf{x}^*$. The entire trajectory is approximated by solving Eq. (1) with $\mathbf{x}_0 = \mathbf{x}^*(0)$.

The target UPO can also be found by an optimization routine, minimizing $\|\mathbf{x}(T) - \mathbf{x}_0\|^2$, with $\mathbf{x}(T)$ obtained by integrating equation (1), as done in Asenjo et al. [12], in which case the minimization is over $\mathbf{x}_0$ and T. Alternatively, the DFC method can be used to find the UPO, as mentioned in the previous section.

To choose the control gain k_c, three characteristics of the controlled orbit can be analyzed: its stability, the steady state error and the steady state control effort.

The stability analysis is done by using the Floquet multipliers (μ), which are the roots of the polynomial $\det(\mu I_{n(N+2)} - \Phi_{\mathbf{x}^*}) = 0$, where $\Phi_{\mathbf{x}^*}$ is the monodromy matrix and $I_{n(N+2)}$ the identity matrix.

The steady state error d_{cl} is the distance (Euclidean norm) between $\mathbf{r}(t)$ (the reference signal) and $\mathbf{x}(t)$ (the current state) for an entire cycle of the target UPO,

$$d_{cl} = \int_t^{t+T} \|\mathbf{r}(\tau) - \mathbf{x}(\tau)\| d\tau. \tag{13}$$

Successful control implies that $d_{cl} \to 0$ as $t \to \infty$. In practice, t has a finite value and a convergence criterion for d_{cl} is defined as the relative difference between d_{cl} at the current cycle (d_{cl_0}) and at the N_{cl} past cycles $d_{cl_{-i}}$, $i = 1,2,\ldots,N_{cl}$,

$$\frac{\left|N_{cl}d_{cl_0} - \sum_{i=1}^{N_{cl}} d_{cl_{-i}}\right|}{|N_{cl}d_{cl_0}|} < \epsilon. \tag{14}$$

The steady state control effort, the measure of the effort necessary to keep the trajectory on the close vicinity of the target periodic orbit, is given by the integral of $\|\mathbf{u}(t)\|$, as defined in Eq. (3), along the orbit,

$$u_{cl} = \int_t^{t+T} \|\mathbf{u}(\tau)\| d\tau. \tag{15}$$

Therefore, successful control implies that $u_{cl} \to 0$ as $t \to \infty$.

With the above definitions, the control gain k_c is chosen according to the performance criteria and optimization.

We chose as our target orbit a p-1 UPO which, for $a = 0.988$, has Floquet multipliers $\mu_1 \approx -1.872$ and $\mu_2 \approx -0.048$. Fig. 1(a) shows a projection of the phase-space trajectory of the target UPO at $a = 0.988$ and Fig. 1(b) shows the time-series of $x_2(t)$.

3.1. Adjusting the number of collocation points

For the DFC method, it is necessary to define the number of samples or delayed states N, which is also the number of collocation points used to approximate the matrix D,

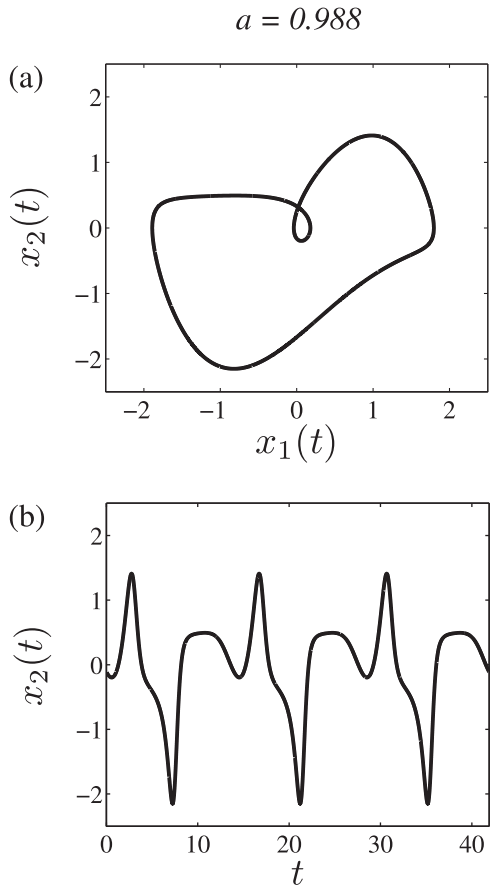

Fig. 1. (a) Projection of the phase-space trajectory of the period-1 target UPO at $a = 0.988$; (b) the time-series of the x_2 component of the target UPO.

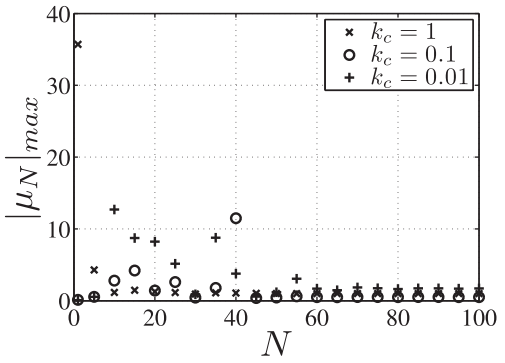

Fig. 2. Relation between the number of collocation points N and the largest magnitude Floquet multiplier of the target UPO, $|\mu|_{max}$, for $a = 0.988$.

which is the differential operator used in the stability analysis of the controlled UPO (see Eq. (A.4) in Appendix A). An increase in the number of collocation points results in greater accuracy at the expense of computational time. Fig. 2 plots $|\mu|_{max} \times N$ for $a = 0.988$ and three different values of k_c, where $|\mu|_{max}$ is the largest magnitude Floquet multiplier of the p-1 UPO. Fig. 2 suggests that $N > 80$ is adequate for this work. We adopt $N = 100$ in all the following results.

3.2. Controlling the target orbit

Before comparing the PFC and DFC methods, a good approximation for the target UPO is needed, since it is necessary for the PFC method. We adopt the following procedure. First, a Poincaré point of the orbit is obtained for the uncontrolled system ($k_c = 0$) with the secant method. For the target UPO at $a = 0.988$ we obtain $(x_1, x_2) = (0.15884454118, -0.110605560432)$. Next, this point is integrated for one period to obtain an initial approximation for the whole orbit. Then, this orbit is used to compute the monodromy matrix for the DFC method. At this stage it is necessary to search for a control gain k_c that stabilizes the target UPO. We search for any k_c which makes $|\mu|_{max} < 1$. With such k_c, the DFC method is used to control the UPO until the convergence criteria of Eq. (14) is satisfied for $\epsilon = 10^{-10}$. This last step is necessary to obtain a good approximation for the whole orbit and not just one Poincaré point, as in the case of the secant method. In what follows, the resulting orbit will be denoted by $\mathbf{x}^*(t)$ and used in the DFC/PFC optimization process. Alternatively, one may obtain $\mathbf{x}^*(t)$ by skipping the secant method step and directly applying the DFC while searching for the proper $\mathbf{x}(0)$ and k_c values, but that would require a search in the $(\mathbf{x}(0) \times k_c)$ space using a DDE integrator with delayed states, which is much slower than using the secant method to find the initial point in the $\mathbf{x}(t)$ space using Eq. (1) and without delayed states. In practical situations where the model equations might not be known, it may be necessary to first use a standard method to estimate the UPO from a time series (e.g., Ref. [19]), then apply the DFC to obtain the desired convergence.

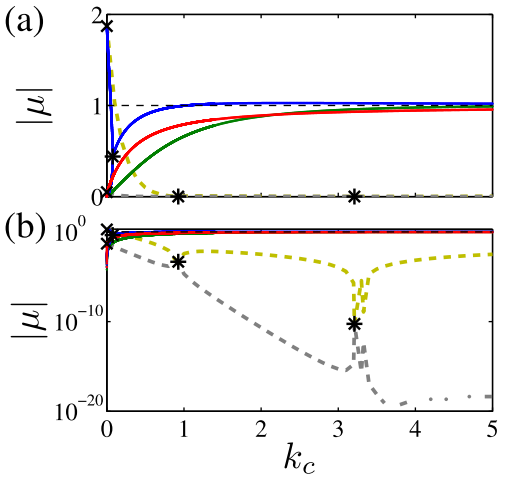

Fig. 3. (a) Magnitude of the Floquet multipliers of the target UPO at $a = 0.988$ using DFC (solid line) and PFC (dashed line). The Floquet multipliers of the orbit without control are represented by $(\times)$ and their local minima for the controlled orbit by $(*)$ and (b) the same as (a), but in log-linear scale.

Fig. 3 illustrates the method for finding k_c. The magnitude of the Floquet multipliers of the target UPO are plotted against k_c for the DFC (solid lines) and PFC (dashed lines) methods. For the DFC, only the six Floquet multipliers with largest magnitude are plotted. There are two real and four complex conjugate multipliers for $k_c \lesssim 0.076$, while there are three complex conjugate multipliers for $k_c \gtrsim 0.076$. Therefore, only three solid lines are visible in the plot of $|\mu|$ in most of Fig. 3(a). For the PFC method, there are only two real multipliers. Fig. 3(b) is the same as Fig. 3(a), but in log-linear scale.

The stars $(*)$ in Fig. 3 refer to the values of k_c found by an optimization process. After plotting $|\mu|$ for several values of k_c by a scanning process, an optimization method is applied by using as initial conditions the approximated values of k_c where the local minima of $|\mu|_{max}$ are found, and using the largest magnitude Floquet multiplier as a cost function [12]. We use the simplex search method [20] and find one minimum for the DFC at $k_c = 0.07632510479$ ($|\mu|_{max} \approx 0.4395$) and two minima for the PFC, at $k_c = 0.92619140625$ ($|\mu|_{max} \approx 0.4667 \times 10^{-3}$) and $k_c = 3.2105712890625$ ($|\mu|_{max} \approx 0.5532 \times 10^{-10}$). The crosses $(\times)$ in Fig. 3 represent the values of $|\mu|$ for the target UPO without control ($k_c = 0$). The UPO is stabilized when $|\mu|_{max} < 1$, which occurs for $0.053 \lesssim k_c \lesssim 1.031$ for the DFC and for $k_c \gtrsim 0.1$ for the PFC. For the DFC, it can be shown that the values of μ tend to one when $k_c \to \infty$.

Fig. 3 shows that the range of k_c for controlling the target UPO is larger for the PFC than for the DFC. However, this may not be an advantage in practice, since one usually hopes to obtain control by applying small perturbations to the system. In that case, the DFC method has a slight advantage, reducing the control effort. Notwithstanding, the orbit controlled with the PFC is more stable, since smaller values of $|\mu|_{max}$ are found. The results of stabilization of the target UPO of the vdP system for $a = 0.988$ are shown in Fig. 4 for (a) the DFC with the optimal value

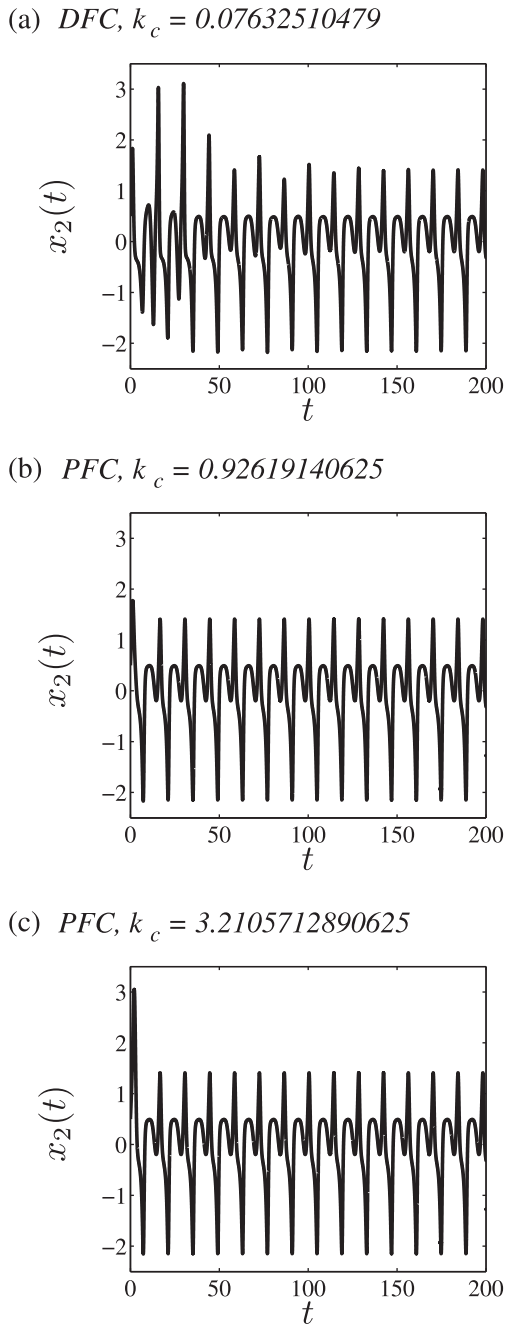

Fig. 4. Time series of the controlled $x_2(t)$ showing the stabilization of the target UPO of the vdP system for $a = 0.988$ using (a) DFC with $k_c = 0.07632510479$, (b) PFC with $k_c = 0.92619140625$ and (c) PFC with $k_c = 3.2105712890625$.

$k_c = 0.07632510479$, (b) the PFC with $k_c = 0.92619140625$ and (c) the PFC with $k_c = 3.2105712890625$. The initial condition is set on $(x_1, x_2) = (-0.5, 0.5)$ (for the DFC, all the delayed states are on the $x^*(t)$), the perturbations decay after an initial transient and the system converges to the periodic regime corresponding to the target UPO. Fig. 5 shows the time series of the magnitude of the control signal $\mathbf{u}(t)$

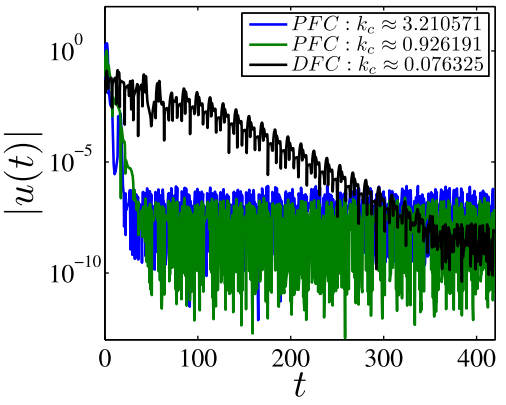

Fig. 5. Time series of the magnitude of the control signal $\mathbf{u}(t)$ of the target UPO of the vdP system for $a = 0.988$ using DFC with $k_c = 0.07632510479$ (black line), PFC with $k_c = 0.92619140625$ (green line) and PFC with $k_c = 3.2105712890625$ (blue line). (For interpretation of the references to colour in this figure legend, the reader is referred to the web version of this article.)

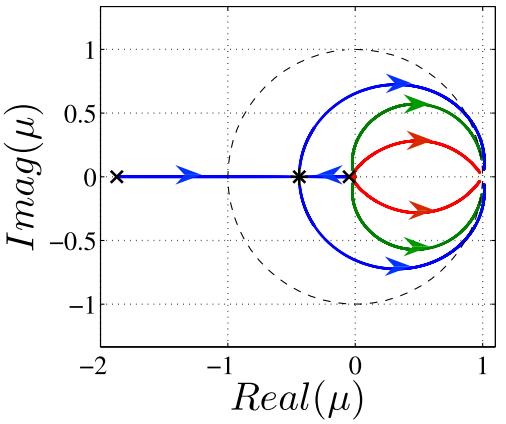

Fig. 6. Root locus chart of the target UPO controlled by the DFC with the Floquet multipliers.

in log-linear scale. The initial transients are shorter for PFC than for DFC in these particular examples, but the PFC presents an initial peak on $\|\mathbf{u}(t)\|$ that represents a short-time high external effort.

The real and imaginary parts of the Floquet multipliers (μ) for the DFC can be seen in the root locus chart in Fig. 6. The cross ($\times$) represents μ for $k_c = 0$ and the star ($*$) represents the optimal value (minimum of $|\mu|_{max}$). The evolution of the six Floquet multipliers with largest magnitude are represented by the six branches, where the arrows show the flow for increasing k_c. The dashed circle in Fig. 6 is the unity circle. It is clear that $\mu \to +1$ as $k_c \to \infty$.

The relation between the steady state error (d_{cl}) and k_c is presented in Fig. 7(a). This figure is computed by integrating an initial condition on $\mathbf{x}^*(t)$ while applying the DFC/PFC control method. After convergence of d_{cl} is reached, we compute one more cycle and plot the final value of d_{cl}. Note that for the PFC (dashed line) the steady state error is low for all $k_c \gtrsim 0.1$, as expected from Fig. 3, which shows that $|\mu|_{max} < 1$ in this region. As for the DFC

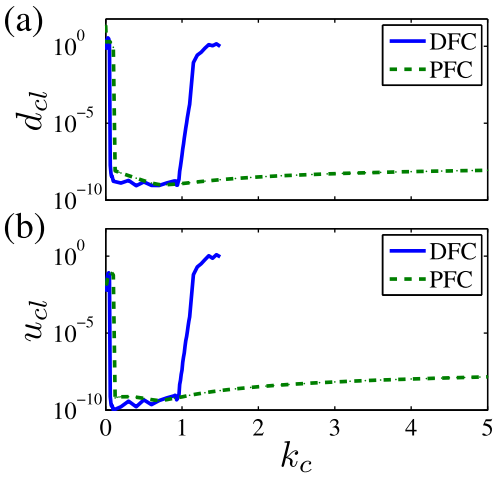

Fig. 7. (a) Steady state error d_{cl} as a function of k_c for the DFC (solid line) and PFC (dashed line) methods; (b) same as (a), but for the control effort u_{cl}. The control parameter is $a = 0.988$.

(solid line), the steady state error is low for $0.053 \lesssim k_c \lesssim 1$. This is close to the point where $|\mu|_{max}$ becomes greater than one in Fig. 3. If $|\mu|_{max} \approx 1$, the target UPO is marginally stable/unstable and perturbed trajectories take a long time to converge to (or diverge from) it. This is the case of the DFC for $k_c \gtrsim 1$, where $|\mu|_{max} \gtrsim 1$ according to Fig. 3(a). Therefore, in Fig. 7, d_{cl} is not plotted for $k_c > 1.5$ for the DFC method, since the divergence time is very long. Fig. 7(b) is the same as Fig. 7(a), but for the control effort u_{cl}.

One of the main advantages of a chaos control technique, is the small control effort required [1,3], and in that sense the DFC method provides slightly better results, since for small values of k_c it generates smaller steady state error d_{cl} and control effort u_{cl}. In fact, supposing that it is possible to find some k_c which is able to control the UPO, in the DFC method the control effort always tends to zero as $t \to +\infty$, as opposed to the PFC method that requires exact knowledge of the target UPO position. Errors in its estimation always lead to finite d_{cl} and u_{cl}, and the errors tend to be larger for longer period UPOs.

3.3. A brief robustness analysis of DFC and PFC

A control method is usually limited by parametric uncertainties when applied to real systems. The source of these uncertainties can be a parametric error between the model used to project the controller and the real system where it will be applied. Furthermore, changes in the parameter of a real system, due to work cycles, for example, are also sources of parametric error. In the previous sections, the driver amplitude was set to $a = 0.988$, where the UPO was found and the control methods applied. In the present section, the target UPO $\mathbf{x}^*(t)$ is found for $a = 0.988$, but the controller is applied for $a \in [0.9855, 0.994]$.

Fig. 8(a) and (b) show d_{cl} and u_{cl} for the DFC when a is changed. As observed, while the orbit is controlled, both quantities remain close to the integrator's error tolerance.

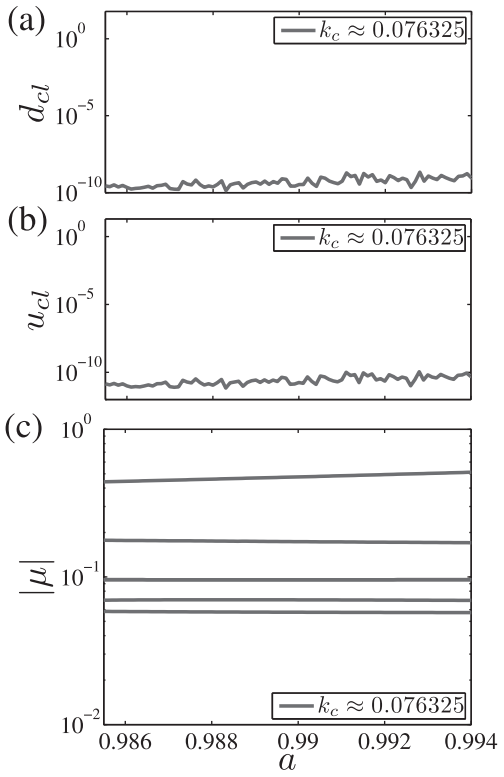

Fig. 8. The steady state error (a), control effort (b) and magnitude of Floquet multipliers (c) as a function of a for the DFC.

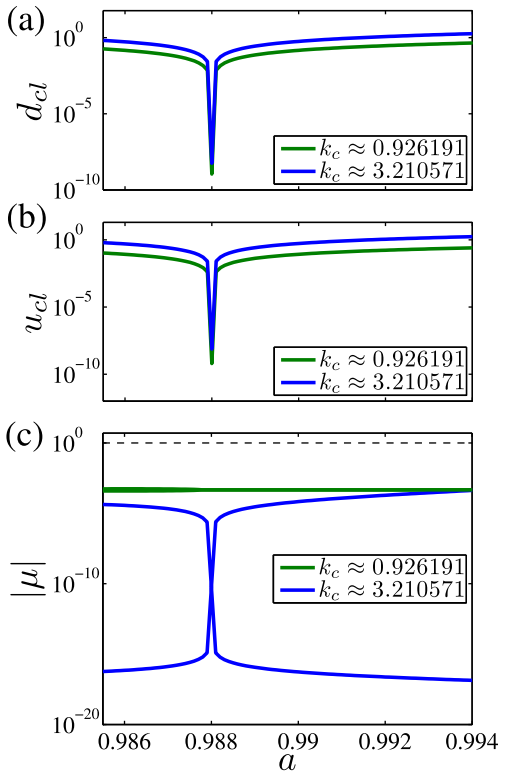

Fig. 9. The steady state error (a), control effort (b) and magnitude of Floquet multipliers (c) as a function of a for the PFC.

The values of the six largest magnitude Floquet multipliers $|\mu|$ of the system controlled with the DFC are presented in Fig. 8(c). These results are obtained by integrating the initial condition until convergence of d_{cl} is observed. After that, the last T time units of the simulation are used to calculate the monodromy matrix and the Floquet multipliers. In all cases, the optimal value $k_c \approx 0.076325$ is used. Note that the DFC adapts well to parameter changes because the reference $\mathbf{r}(t)$ is changed accordingly. This characteristic reduces the controller's stability, but increases its robustness to parametric uncertainties.

For the PFC, we test the two values of k_c where the local minima of $|\mu|_{max}$ are found in Fig. 3, *i.e.*, $k_c = 0.92619140625$ and $k_c = 3.2105712890625$. Fig. 9(a) and (b) show the steady state error and the control effort as a function of a. The sudden change in d_{cl} and u_{cl} around $a = 0.988$ is due to the proximity of the target UPO, $\mathbf{r}(t)$, defined by Eq. (3). Since in the PFC method $\mathbf{r}(t)$ does not self-adapt to changes in the control parameter, the steady state error and control effort are much higher for $a \neq 0.988$. Fig. 9(c) reveals that $|\mu|_{max}$ is very sensitive to variations in a for $k_c = 3.2105712890625$, whereas $|\mu|_{max}$ is kept almost constant for $k_c = 0.92619140625$. Overall, the orbit controlled with $k_c = 3.2105712890625$ is more stable, except for large values of a.

As shown in Figs. 8 and 9, even with perturbations in a, the p-1 UPO is more stable for the PFC method than for the DFC method. However, the DFC has a much lower steady state error and control effort.

4. Conclusions

Chaos control of the forced van der Pol system was studied using proportional feedback control (PFC) and delayed feedback control (DFC). We devise a control strategy whereby the target unstable periodic orbit (UPO) is chosen according to its stability properties. Then the optimal control gain is found by minimizing the stability (Floquet) multipliers of the target UPO. We adopt the optimization strategy proposed by Asenjo et al. [12] and extend it to the DFC method. Since the computation of the monodromy matrix for the DFC method through the integration of the variational equation is highly expensive, we propose the use of the method introduced by Deshmukh et al. [15], whereby the monodromy matrix can be readily obtained using algebraic operations only.

Our results reveal that the magnitude of the Floquet multipliers of the UPO controlled by the PFC method are much smaller than when the DFC method is employed. The PFC also shows a wider range of the control gain for which the UPO can be controlled. In spite of that, the DFC method results in smaller control effort, specially under parametric uncertainties, and this is a highly desired property in real applications. Even small perturbations in the control parameter result in a control effort u_{cl} of the order of 10^{-1} or 10^{0} for the PFC (Fig. 9(b)), whereas for the DFC, u_{cl} is of the order of the integrator's error tolerance, 10^{-10} (Fig. 8(b)). An experimental realization of the DFC method is simpler than the PFC, since the latter requires the use of

a specially designed periodic oscillator for the control signal. In applications where the model equations are not known and the PFC is to be used due to its stability properties, an approximation of the target UPO can be found from time series analysis and/or the DFC method itself.

Besides the previously mentioned applications on electrical circuits [9], biology [10] and economy [11], control of the van der Pol equation is also relevant for fusion plasmas [21]. Recently, the extended time-delayed feedback control method was applied to a natural cardiac pacemaker described by a modified Van der Pol equation, where chaos must be avoided to prevent behavior associated with critical cardiac pathologies [22]. The analysis described in the present paper can be readily applied to those systems.

Acknowledgments

T.P.C. acknowledges support from CAPES (Brazil). B.A.T. acknowledges support from FAPESP (Brazil). E.L.R. acknowledges support from FAPESP (Brazil) and CNPq (Brazil). A.C.L.C. acknowledges support from CNPq (Brazil), and acknowledges the award of a Marie Curie International Incoming Fellowship and the hospitality of Paris Observatory. J.A.V acknowledges support from Fondecyt Grant 1110135 (Chile).

Appendix A. Stability analysis for the DFC method

This appendix describes a method to study the stability of unstable periodic solutions of Eq. (7), reproduced below

$$\frac{dX(t)}{dt} = F(t, X(t)) + (I_{N+2} \otimes BK_c)(X(t-T) - X(t)), \tag{A.1}$$

where T is the period of the orbit, $B \in \mathbb{R}^{n\times n}$ is a matrix of coupling control coefficients, $K_c \in \mathbb{R}^{n\times n}$ is the control gain matrix, I_{N+2} is the identity matrix of order $N+2$, $\otimes$ is the Kronecker product and

$$X(t) = \begin{bmatrix} \mathbf{x}(t-s_0T) \\ \mathbf{x}(t-s_1T) \\ \vdots \\ \mathbf{x}(t-s_NT) \\ \mathbf{x}(t-s_{N+1}T) \end{bmatrix} \tag{A.2}$$

and

$$F(t, X(t)) = \begin{bmatrix} \mathbf{f}(t-s_0T, \mathbf{x}(t-s_0T)) \\ \mathbf{f}(t-s_1T, \mathbf{x}(t-s_1T)) \\ \vdots \\ \mathbf{f}(t-s_NT, \mathbf{x}(t-s_NT)) \\ \mathbf{f}(t-s_{N+1}T, \mathbf{x}(t-s_{N+1}T)) \end{bmatrix}, \tag{A.3}$$

where $\mathbf{x} \in \mathbb{R}^n$, $\mathbf{f} : \mathbb{R} \times \mathbb{R}^n \to \mathbb{R}^n$, $s_0 = 0$, $s_i < s_{i+1}$, $i = 0,1,\ldots,N$, and $s_{N+1} = 1$.

First, we adopt a numerical approximation for $dX(t)/dt$, including the delayed states, in the form

$$\frac{dX(t)}{dt} = DX(t), \tag{A.4}$$

where $D \in \mathbb{R}^{n(N+2)\times n(N+2)}$ is a differential operator matrix that can be obtained using finite difference methods [23], spectral methods [23,15] or a collocation method with different types of approximating polynomials [16]. For simplicity, we employ the orthogonal collocation method with the Lagrange polynomial [24,25]. The method is described in Appendix B and exemplified in Appendix C.

Having defined $X(t)$ and $dX(t)/dt = DX(t)$, we obtain the monodromy matrix of the periodic orbit $X^*(t)$ of period T using the method introduced in Refs. [15,16].

Consider a perturbation $Y(0)$ on the periodic state $X^*(0)$ resulting in

$$X(0) = X^*(0) + Y(0), \tag{A.5}$$

where X, X^*, and Y are defined as in Eq. (A.2). The evolution $Y(t)$ of the initial perturbation $Y(0)$ is obtained by substituting the perturbed trajectory in Eq. (A.1),

$$\frac{dX^*(t)}{dt} + \frac{dY(t)}{dt} = F(t, X^*(t) + Y(t)) + (I_{N+2} \otimes BK_c) \times (Y(t-T) - Y(t)). \tag{A.6}$$

By expanding $F(t, X^*(t) + Y(t))$ around $X^*(t)$ for $Y(0)$ sufficiently small, we obtain

$$\frac{dY(t)}{dt} = \nabla_X F(t, X(t))|_{X(t)=X^*(t)} Y(t) + (I_{N+2} \otimes BK_c)(Y(t-T) - Y(t)). \tag{A.7}$$

We use Eq. (A.4) to approximate dY/dt

$$\frac{dY(t)}{dt} = DY(t). \tag{A.8}$$

Substituting (A.8) in (A.7) leads to

$$M_D Y(t) = M_A Y(t) + M_{K_c}(Y(t-T) - Y(t)), \tag{A.9}$$

where

$$M_D = \begin{bmatrix} D_{j,i} \\ \mathbf{0}_{n\times n(N+1)} \;\; I_n \end{bmatrix},$$

$$M_A = \begin{bmatrix} A(t-s_0T) & \mathbf{0}_{n\times n} & \cdots & \mathbf{0}_{n\times n} & \mathbf{0}_{n\times n} \\ \mathbf{0}_{n\times n} & A(t-s_1T) & \cdots & \mathbf{0}_{n\times n} & \mathbf{0}_{n\times n} \\ \vdots & \vdots & \ddots & \vdots & \vdots \\ \mathbf{0}_{n\times n} & \mathbf{0}_{n\times n} & \cdots & A(t-s_{N+1}T) & \mathbf{0}_{n\times n} \\ I_n & \mathbf{0}_{n\times n} & \cdots & \mathbf{0}_{n\times n} & \mathbf{0}_{n\times n} \end{bmatrix},$$

$$M_{K_c} = \begin{bmatrix} BK_c & \mathbf{0}_{n\times n} & \cdots & \mathbf{0}_{n\times n} & \mathbf{0}_{n\times n} \\ \mathbf{0}_{n\times n} & BK_c & \cdots & \mathbf{0}_{n\times n} & \mathbf{0}_{n\times n} \\ \vdots & \vdots & \ddots & \vdots & \vdots \\ \mathbf{0}_{n\times n} & \mathbf{0}_{n\times n} & \cdots & BK_c & \mathbf{0}_{n\times n} \\ I_n & \mathbf{0}_{n\times n} & \cdots & \mathbf{0}_{n\times n} & \mathbf{0}_{n\times n} \end{bmatrix}, \tag{A.10}$$

with $i = 1,2,\ldots,n(N+2)$, $j = 1,2,\ldots,n(N+1)$, and $A(t-s_iT) = \nabla_{\mathbf{x}} \mathbf{f}(t-s_iT, \mathbf{x}(t-s_iT))|_{\mathbf{x}(t-s_iT)=\mathbf{x}^*(t-s_iT)}$. The last lines of the matrices guarantee the periodicity [16].

Now, define the monodromy matrix Φ_{X^*} as the state transition matrix on $X^*(t)$, from $Y(t-T)$ to $Y(t)$ given by

$$Y(t) = \Phi_{X^*(t)} Y(t-T), \tag{A.11}$$

where $\Phi_{X^*(t)} \in \mathbb{R}^{n(N+2)\times n(N+2)}$.

By equating (A.9) and (A.11) one readily obtains

$$\Phi_{X^*(t)} = (M_D - M_A + M_{K_c})^{-1} M_{K_c}. \quad \text{(A.12)}$$

Appendix B. Orthogonal collocation method

This appendix describes the use of the orthogonal collocation method to obtain the differential operator matrix D used in Eq. (A.4) of Appendix A.

Consider the system of differential equations given by

$$\frac{d\mathbf{x}(t)}{dt} = \mathbf{f}(t, \mathbf{x}(t)), \quad \text{(B.1)}$$

where $\mathbf{x} : [0, +\infty) \to \mathbb{R}^n$ and $\mathbf{f} : [0, +\infty) \times \mathbb{R}^n \to \mathbb{R}^n$ are column vectors. The solution of Eq. (B.1) at time $T \geqslant 0$, for an initial condition $\mathbf{x}(t_0)$, is

$$\mathbf{x}(t_0 + T) = \mathbf{x}(t_0) + \int_{t_0}^{t_0+T} \mathbf{f}(\tau, \mathbf{x}(\tau)) d\tau. \quad \text{(B.2)}$$

The solution (B.2) of (B.1) can be approximated using the collocation method by

$$\mathbf{x}(t_0 + T) \approx w_0(s)\mathbf{x}(t_0) + \sum_{i=1}^{N+1} w_i(s)\mathbf{m}_i(t_0), \quad \text{(B.3)}$$

where $s \in \mathbb{R}$, $w_i(s)$ are weight polynomials, and $\mathbf{m}_i \approx \mathbf{x}(t_0 + Ts_i)$ represent the state vector for each time $t_0 + Ts_i$, where $s_i \in [\,0 \quad 1\,]$ are the collocation points, including $s_0 = 0$ and $s_{N+1} = 1$, which are used to discretize the solution time interval from $t_0 + Ts_0$ to $t_0 + Ts_{N+1}$. The quality of the approximation (B.3) is proportional to N.

The choice of $w_i(s)$ provides different properties for the collocation method. In this work we adopt the Lagrange polynomials

$$w_i(s) = \prod_{j=0, j\neq i}^{N+1} \frac{s - s_j}{s_i - s_j}, \quad i = 0, \ldots, N+1. \quad \text{(B.4)}$$

For the orthogonal collocation method, the values of s_i are obtained in such a way as to ensure the orthogonality of the polynomials w_i [24], and are given by the solutions of

$$\int_0^1 w_i(s) w_j(s)[1 - s] s ds = 0, \quad i, j = 1, \ldots, N, \; i \neq j. \quad \text{(B.5)}$$

The derivative $\partial\mathbf{x}(t_0 + Ts)/\partial s$ at each collocation point s_j is

$$\left.\frac{\partial \mathbf{x}(t_0+Ts)}{\partial s}\right|_{s=s_j} \approx \left.\frac{\partial w_0(s)}{\partial s}\right|_{s=s_j} \mathbf{x}(t_0) + \sum_{i=1}^{N+1} \left.\frac{\partial w_i(s)}{\partial s}\right|_{s=s_j} \mathbf{m}_i(t_0), \quad \text{(B.6)}$$

with

$$\left.\frac{\partial \mathbf{x}(t_0 + Ts)}{\partial s}\right|_{s=s_j} = \frac{\partial(t_0 + Ts)}{\partial s} \cdot \left.\frac{\partial \mathbf{x}(t_0 + Ts)}{\partial(t_0 + Ts)}\right|_{s=s_j} \approx T\mathbf{f}(t_0 + Ts_j, \mathbf{m}_j(t_0)). \quad \text{(B.7)}$$

Eqs. (B.6) and (B.7) form the matrix equation

$$H_T(t_0, X(t_0)) = (W_1 \otimes I_n)\mathbf{x}(t_0) + (W_2 \otimes I_n)X(t_0), \quad \text{(B.8)}$$

where I_n is a $n \times n$ identity matrix, $\otimes$ is the Kronecker product and

$$W_1 = \begin{bmatrix} \left.\frac{\partial w_0(s)}{\partial s}\right|_{s=s_1} \\ \vdots \\ \left.\frac{\partial w_0(s)}{\partial s}\right|_{s=s_{N+1}} \end{bmatrix} \in \mathbb{R}^{(N+1)},$$

$$X(t_0) = \begin{bmatrix} \mathbf{m}_1(t_0) \\ \vdots \\ \mathbf{m}_{N+1}(t_0) \end{bmatrix} \in \mathbb{R}^{n(N+1)},$$

$$W_2 = \begin{bmatrix} \left.\frac{\partial w(s)}{\partial s}\right|_{s=s_1} \\ \\ \vdots \\ \\ \left.\frac{\partial w(s)}{\partial s}\right|_{s=s_{N+1}} \end{bmatrix} \in \mathbb{R}^{(N+1)\times(N+1)},$$

$$H_T(t_0, X) = \begin{bmatrix} T\mathbf{f}(t_0 + Ts_1, \mathbf{m}_1) \\ \\ \vdots \\ \\ T\mathbf{f}(t_0 + Ts_{N+1}, \mathbf{m}_{N+1}) \end{bmatrix}.$$

Here $w(s) = (w_1(s), \ldots, w_{N+1}(s))$ and $H_T : \mathbb{R}^{n(N+1)} \to \mathbb{R}^{n(N+1)}$ depends on the choice of the discrete times $t_0 + Ts_1, \ldots, t_0 + Ts_{N+1}$, but, for simplicity, this dependence is not explicit here.

The solution of (B.8) with unknown $X(t_0) \in \mathbb{R}^{n(N+1)}$ is an approximated solution of

$$\left.\frac{d\mathbf{x}(t_0 + Ts)}{d(t_0 + Ts)}\right|_{s=s_j} = f(t_0 + Ts_j, \mathbf{x}(t_0 + Ts_j)), \quad j = 1, \ldots, N+1$$

with unknown $\mathbf{x}(t_0 + Ts_j)$, given $\mathbf{x}(t_0)$.

By including the state at time $t_0 + Ts_0$ in Eq. (B.8) one obtains

$$\begin{bmatrix} T\mathbf{f}(t_0 + Ts_0, \mathbf{x}(t_0)) \\ \\ H_T(t_0, X) \end{bmatrix} = \left(\begin{bmatrix} \left.\frac{\partial w_0(s)}{\partial s}\right|_{s=s_0} & \left.\frac{\partial w(s)}{\partial s}\right|_{s=s_0} \\ \\ W_1 & W_2 \end{bmatrix} \otimes I_n \right) \begin{bmatrix} \mathbf{x}(t_0) \\ \\ X(t_0) \end{bmatrix}. \quad \text{(B.9)}$$

Eq. (B.9) represents

$$\begin{bmatrix} \frac{d\mathbf{x}(t_0+Ts_0)}{d(t_0+Ts)} \\ \\ \vdots \\ \\ \frac{d\mathbf{x}(t_0+Ts_{N+1})}{d(t_0+Ts)} \end{bmatrix} \approx D \begin{bmatrix} \mathbf{x}(t_0 + Ts_0) \\ \\ \vdots \\ \\ \mathbf{x}(t_0 + Ts_{N+1}) \end{bmatrix},$$

with

$$D = \frac{1}{T} \begin{bmatrix} \left.\frac{\partial w_0(s)}{\partial s}\right|_{s=s_0} & \left.\frac{\partial w(s)}{\partial s}\right|_{s=s_0} \\ \\ W_1 & W_2 \end{bmatrix} \otimes I_n \in \mathbb{R}^{n(N+2)\times n(N+2)}, \quad \text{(B.10)}$$

the differential matrix operator generated using the orthogonal collocation method.

Appendix C. Example of calculation of *D*

Here we show an example of the calculation of the differential operator matrix D, described in Appendix B, for $N = 3$.

The $w_j(s)$ polynomials, $j = 0,\ldots N+1$, are calculated using Eq. (B.4) and defining $s_0 = 0$ and $s_4 = 1$,

$$w_0(s) = \frac{(s-s_1)(s-s_2)(s-s_3)(s-1)}{s_1 s_2 s_3},$$
$$w_1(s) = \frac{s(s-s_2)(s-s_3)(s-1)}{s_1(s_1-s_2)(s_1-s_3)(s_1-1)},$$
$$w_2(s) = \frac{-s(s-s_1)(s-s_3)(s-1)}{s_2(s_1-s_2)(s_2-s_3)(s_2-1)},$$
$$w_3(s) = \frac{s(s-s_1)(s-s_2)(s-1)}{s_3(s_1-s_3)(s_2-s_3)(s_3-1)},$$
$$w_4(s) = \frac{-s(s-s_1)(s-s_2)(s-s_3)}{(s_1-1)(s_2-1)(s_3-1)}.$$

Using the above expressions for $w_1(s)$, $w_2(s)$ and $w_3(s)$, the values of s_1, s_2 and s_3 are found by a numerical solution of Eq. (B.5). By using the simplex search method [20] to minimize the error function $\left|\int_0^1 w_1(s)w_2(s)[1-s]sds\right| + \left|\int_0^1 w_1(s)w_3(s)[1-s]sds\right| + \left|\int_0^1 w_2(s)w_3(s)[1-s]sds\right|$, we found $s_1 \approx 0.17267$, $s_2 = 0.5$ and $s_3 \approx 0.82733$. These s_i values are substituted in the $w_j(s)$ polynomials and they are differentiated with respect to s,

$$\frac{\partial w_0(s)}{\partial s} = 56s^3 - 105s^2 + 60s - 10,$$
$$\frac{\partial w_1(s)}{\partial s} \approx \frac{-392s^3}{3} + 228.0780s^2 - 113.7447s + 13.5130,$$
$$\frac{\partial w_2(s)}{\partial s} = \frac{448s^3}{3} - 224s^2 + \frac{256s}{3} - \frac{16}{3},$$
$$\frac{\partial w_3(s)}{\partial s} \approx \frac{-392s^3}{3} + 163.9220s^2 - 49.5886s + 2.8203,$$
$$\frac{\partial w_4(s)}{\partial s} = 56s^3 - 63s^2 + 18s - 1.$$

Using these values in Eq. (B.10) for $N = 3$ leads to

$$D \approx \frac{1}{T}\begin{bmatrix} -10.0000 & 13.5130 & -5.3333 & 2.8203 & -1.0000 \\ -2.4820 & -0.0000 & 3.4915 & -1.5275 & 0.5180 \\ 0.7500 & -2.6732 & 0 & 2.6732 & -0.7500 \\ -0.5180 & 1.5275 & -3.4915 & 0.0000 & 2.4820 \\ 1.0000 & -2.8203 & 5.3333 & -13.5130 & 10.0000 \end{bmatrix} \otimes I_n.$$

References

[1] Ott E, Grebogi C, Yorke JA. Controlling chaos. Phys Rev Lett 1990;64:1196–9.
[2] Sanjuán MAF, Grebogi C, editors. Recent progress in controlling chaos. Singapore: World Scientific; 2010.
[3] Pyragas K. Continuous control of chaos by self-controlling feedback. Phys Lett A 1992;170:421–8.
[4] Pyragas K, Tamaševičius A. Experimental control of chaos by delayed self-controlling feedback. Phys Lett A 1993;180:99–102.
[5] Pyragas K. Control of chaos via extended delay feedback. Phys Lett A 1995;206:323–30.
[6] Just W, Bernard T, Ostheimer M, Reibold E, Benner H. Mechanism of time-delayed feedback Control. Phys Rev Lett 1997;78(2):203–6.
[7] Pyragas K. Control of chaos via an unstable delayed feedback controller. Phys Rev Lett 2001;86:2265–8.
[8] Fiedler B, Flunkert V, Georgi M, Hövel P, Schöll E. Refuting the odd-number limitation of time-delayed feedback control. Phys Rev Lett 2007;98:114101.
[9] Van der Pol B, Van der Mark J. Frequency demultiplication. Nature 1927;120:363–4.
[10] FitzHugh R. Impulses and physiological states in theoretical models of nerve membranes. Biophys J 1961;1:445–66.
[11] Chian AC-L. Complex systems approach to economic dynamics. Berlin: Springer-Verlag; 2007.
[12] Asenjo F, Toledo BA, Muñoz V, Rogan J, Valdivia JA. Optimal control in a noisy system. Chaos 2008;18:033106.
[13] Fouladi A, Valdivia JA. Period control of chaotic systems by optimization. Phys Rev E 1997;55:1315–20.
[14] Pyragas K. Delayed feedback control of chaos. Philos Trans Roy Soc A 2006;364:2309–34.
[15] Deshmukh V, Butcher EA, Bueler E. Dimensional reduction of nonlinear delay differential equations with periodic coefficients using Chebyshev spectral collocation. Nonlinear Dynam 2008;52(1–2):137–49.
[16] Khasawneh FA, Mann BP, Butcher EA. Comparison between collocation methods and spectral element approach for the stability of periodic delay systems. In: Ninth IFAC workshop on time delay systems, vol. 9, Prague, Czech Republic, IFAC, 2010.
[17] Chian AC-L, Rempel EL, Rogers C. Complex economic dynamics: chaotic saddle, crisis and intermittency. Chaos Solitons Fract 2006;29:1194–218.
[18] Shampine LF, Thompson S. Solving DDEs in MATLAB. Appl Numer Math 2001;37:441–58.
[19] So P, Ott E, Schiff SJ, Kaplan DT, Sauer T, Grebogi C. Detecting unstable periodic orbits in chaotic experimental data. Phys Rev Lett 1996;76:4705–8.
[20] Lagarias JC, Reeds JA, Wright MH, Wright PE. Convergence properties of the Nelder–Med simplex method in low dimensions. SIAM J Optim 1998;9(1):112–47.
[21] Semenov IB, Mitrishkin YV, Subbotin AA, Vertinskii AG, Marusov NL, Sushin IS. A van der Pol coupled-oscillator model as a basis for developing a system for suppressing MHD instabilities. Plasma Phys Rep 2006;32:114–8.
[22] Ferreira BB, de Paula AS, Savi MA. Chaos control applied to heart rhythm dynamics. Chaos Solitons Fract 2011;44:587–99.
[23] Butcher EA, Bobrenkov OA. On the Chebyshev spectral continuous time approximation for constant and periodic delay differential equations. Commun Nonlinear Sci Numer Simul 2011;16(3):1541–54.
[24] Viladsen J, Michelsen ML. Solution of differential equation models by polynomial approximation. Englewood Cliffs: Prentice-Hall; 1978.
[25] Hairer E, Norsett SP, Wanner G. Solving ordinary differential equation I: nonstiff problems. Berlin: Springer Verlag; 2008.

Appendix E

Resumo estendido

E.1 Introdução

O principal problema avaliado neste trabalho é a estabilização de órbitas periódicas de sistemas dinâmicos não-lineares utilizando controle por realimentação de estados ou por realimentação de saída. O objetivo dos métodos de controle propostos é uma oscilação periódica estável, o que difere do objetivo mais usual em sistemas de controle que é um ponto de equilíbrio estável.

Os métodos de controle aqui considerados são aplicados a sistemas que apresentam órbitas periódicos instáveis (UPOs - *unstable periodic orbits*) no espaço de estado e estas UPOs são as órbitas a serem estabilizadas. Os métodos foram propostos de forma que a oscilação estável resultante seja obtida com baixo esforço de controle, uma vez que o sinal de controle é projetado de modo a tender para zero quando a trajetória tende à órbita estabilizada.

Os métodos de controle utilizados para estabilização das órbitas periódicas são *proportional feedback control* (PFC), *delayed feedback control* (DFC) e *prediction-based control* (PBC) e a principal diferença entre eles é a referência usada para compor o sinal de controle. O PFC, proposto por Pyragas [70], utiliza como referência a própria UPO alvo (órbita a ser estabilizada). Esta órbita é encontrada antes da aplicação e imprecisões na sua aproximação implicam maior esforço de controle. O DFC, proposto por Pyragas [70],

utiliza como referência o estado atrasado pelo período da UPO alvo e apenas o seu período é necessário para a aplicação. O PBC utiliza como referência o estado predito um período da órbita alvo à frente de trajetórias da resposta livre do sistema e exige um modelo do sistema para a aplicação.

A estabilização de uma órbita periódica de um sistema não-linear pode ser simplificada para a estabilização de um sistema linear periódico no tempo. Este sistema linear é obtido pela linearização das trajetórias na vizinhança da órbita periódica e sua análise de estabilidade pode ser realizada utilizando a teoria da estabilidade Floquet. Assim, a estabilidade local da órbita periódica do sistema não-linear é definida pela estabilidade do sistema linear associado.

O trabalho é divido em duas partes, a primeira dedicada a sistemas de tempo discreto e a segunda a sistemas de tempo contínuo. Nos capítulos seguintes deste resumo serão abordadas as principais contribuições de cada parte, a proposição dos problemas de controle a serem abordados e a teoria necessária para a sua compreensão. Para sistemas de tempo discreto as principais contribuições são referentes ao PBC e apenas este método é abordado no resumo. Para sistemas de tempo contínuo as principais contribuições são referentes ao DFC e ao PBC e apenas estes métodos são abordados no resumo.

E.2 Sistemas de tempo discreto

Considere o seguinte sistema dinâmico de tempo discreto:

$$x_{k+1} = f(k, x_k, u_k), \quad x_0 \text{ dado} \tag{E.1}$$

onde $x : \mathbb{N} \to \mathbb{R}^n$, $u : \mathbb{N} \to \mathbb{R}^m$, $k, m, n \in \mathbb{N}$ e $f : \mathbb{N} \times \mathbb{R}^n \times \mathbb{R}^m \to \mathbb{R}^n$ é uma função p-periódica no tempo k, isto é, por definição

$$\forall k \in \mathbb{N}, \quad \forall x \in \mathbb{R}^n, \quad \forall u \in \mathbb{R}^m, \qquad f(k+p, x, u) = f(k, x, u). \tag{E.2}$$

Assume-se ainda a existência de uma solução p-periódica x_k^* da resposta livre do sistema (E.1), isto é, o sistema obtido fazendo $u_k = 0$, $k \geq 0$. Em outras palavras

$$\forall k \in \mathbb{N}, \qquad x_{k+p}^* = x_k^* \tag{E.3}$$

e

$$\forall k \in \mathbb{N}, \qquad x_{k+1}^* = f(k, x_k^*, 0_m). \tag{E.4}$$

Assume-se que esta solução periódica é instável. O principal objetivo aqui é projetar leis de controle com realimentação p-periódica $u_k(x_k)$ que estabilizem esta órbita, tal que

$$\forall k \in \mathbb{N}, \quad \forall x \in \mathbb{R}^n, \qquad u_{k+p}(x) = u_k(x)$$

e tal que x^* seja uma solução estável do sistema em malha fechada

$$x_{k+1} = f(k, x_k, u_k(x_k)). \tag{E.5}$$

O objetivo desta parte é a proposição de diferentes formas adequadas de definir $u : \mathbb{N} \times \mathbb{R}^n \to \mathbb{R}^m$.

O sinal de controle u utilizado neste trabalho deve, idealmente, verificar,

$$u_k(x_k^*) = 0, \qquad k \geq 0. \tag{E.6}$$

Isto é, sobre a órbita periódica o esforço de controle é nulo e a solução periódica instável x_k^* de $f(k, x_k, 0)$ é uma solução periódica estável de (E.5).

A Seção E.2.1 é dedicada à análise de estabilidade de órbitas periódica utilizando a teoria de Floquet. A Seção E.2.2 é dedicada à nova lei de controle proposta para o PBC, a qual será utilizada para estabilizar x_k^*.

E.2.1 Teoria de estabilidade de Floquet

Nesta seção serão apresentados os conceitos de estabilidade de sistemas dinâmicos lineares periódicos de tempo discreto baseados na teoria de Floquet e estes resultados são aplicados para análise de estabilidade local de órbitas periódicas de sistemas dinâmicos não-lineares em tempo discreto.

Sistemas Lineares

Considere um sistema dinâmico linear de tempo discreto descrito pela equação a diferenças

$$x_{k+1} = A_k x_k, \tag{E.7}$$

onde $k \in \mathbb{N}$, $x : \mathbb{N} \to \mathbb{R}^n$ é um vetor coluna e $A : \mathbb{N} \to \mathbb{R}^{n \times n}$. Assume-se que A_k é uma matriz de estados p-periódica, isto é

$$A_k = A_{k+p}, \quad \forall k \in \mathbb{N}. \tag{E.8}$$

A estabilidade de sistemas periódicos lineares de acordo com a teoria de Floquet [5] depende dos autovalores da *matriz de monodromia* (detalhes no *Appendix* A), chamados de *multiplicadores característicos de Floquet* $\mu_i \in \mathbb{C}$, $i = 1, \ldots, n$:

Proposição E.1 (consultar *Proposition* 3.1)**.** (*i*) *O sistema* (E.7) *é assintoticamente estável se e somente se os multiplicadores característicos de* A_k *têm valor absoluto menor que* 1*.* (*ii*) *O sistema* (E.7) *é estável se e somente se os multiplicadores característicos de* A_k *têm valor absoluto menor ou igual a* 1 *e os multiplicadores característicos com valor absoluto iguais a* 1 *são raízes simples do polinômio mínimo da matriz de monodromia* Ψ_k*.* □

Consultar *Appendix* B para as definições de estabilidade.

A matriz de monodromia Ψ_k é calculada como a seguir:

$$\Psi_k = \prod_{l=0}^{p-1} A_{k+l} \tag{E.9}$$

com as matrízes no produtório ordenadas da direita para a esquerda com o aumento de l.

A teoria de Floquet pode ser utilizada para analisar a estabilidade de órbitas periódicas de sistemas não-lineares estudando a convergência/divergência de uma perturbação, governada pelo sistema linear, na vizinhança da órbita periódica [3, 40].

Aplicação em sistemas não-lineares

Considere o sistema dinâmico não-linear de tempo discreto descrito pela equação a diferenças (E.5) com solução p-periódica x_k^* para $u_k(x_k) = 0$ indicada em (E.2). Aqui é estudado o comportamento de uma trajetória na vizinhança de x_k^*.

Proposição E.2 (Estabilidade de órbitas periódicas de sistemas de tempo discreto - consultar *Proposition* 3.2)**.** *Uma órbita periódica x_k^* do sistema dinâmico recursivo* (E.5) *é localmente assintoticamente estável se o sistema dinâmico linear que descreve a evolução de uma trajetória perturbada na vizinhança de x_k^* for assintoticamente estável.* □

E.2.2 Estabilização utilizando prediction-based control

Prediction-based control ou controle baseado em prediç ao. Este método, proposto por Ushio e Yamamoto [91], utiliza um sinal de controle definido por

$$u_k(x_k) = K_k(x_k) \left(\varphi(k+p, k, x_k, 0) - x_k\right), \tag{E.10}$$

onde $\varphi(k_1, k_0, x, 0)$ é o valor do estado de (E.5) no tempo k_1 com $x_{k_0} = x$ e $u_k = 0$, $k_0 \leq k \leq k_1$. Em outras palavras, $\varphi(k_1, k_0, x, 0)$ é o valor no tempo k_1 do estado ao longo da trajetória partindo de x no tempo k_0 da resposta livre do sistema ($u_k \equiv 0$).

A contribuição do presente trabalho no domínio de sistemas de tempo-discreto é a proposição de um método para definir o ganho do PBC. Os resultados foram inicialmente publicados em [12]. O esquema de controle mostrado aqui é baseado em uma condição suficiente para estabilidade e leva à proposição de ganhos para o controlador.

Condição suficiente de estabilidade Uma condição suficiente para a estabilidade de órbitas periódicas de sistemas diâmicos de tempo discreto controlados pelo PBC é definida

baseada no espectro de Ψ_k. O resultado obtido no Teorema E.4 a seguir possibilita o desenvolvimento de leis de controle para a estabilização de UPOs utilizando o PBC.

De acordo com (E.5) e (E.10), o sistema dinâmico de tempo discreto em malha fechada controlado utilizando o PBC é definido por

$$x_{k+1} = \varphi(k+1, k, x_k, u_k(x_k)) = f(k, x_k, K_k(x_k)(\varphi(k+p, k, x_k, 0) - x_k)). \tag{E.11}$$

Na sequência, para quaisquer $x \in \mathbb{R}^n$ e $K \in \mathbb{R}^{q\times n}$, $q \in \mathbb{N}$, utiliza-se a notação

$$\begin{aligned} \psi(k, x, K) &\doteq f(k, x, u_k(x)) \\ u_k(x) &= K(\varphi(k+p, k, x, 0) - x). \end{aligned} \tag{E.12}$$

O primeiro passo para a definição da condição suficiente para estabilidade de órbitas periódicas é obter a matriz de monodromia Ψ_k correspondente ao sistema (E.12). Esta matriz, para o sistema em malha fechada, é calculada de acordo com o Lema proposto E.3.

Lema E.3 (consultar *Lemma* 3.15)**.** *Para qualquer ponto p-periódico x_k^*, $k \in \mathbb{N}$, da trajetória x^* do sistema em malha fechada* (E.11)*, tem-se*

$$\Psi_k = \prod_{l=0}^{p-1} \nabla_x \psi(k+l, x, K_{k+l}(x_{k+l}^*))\big|_{x=x_{k+l}^*} \tag{E.13}$$

e as matrizes do produtório são ordenadas da direita para a esquerda aumentando o índice l. □

O interesse na fórmula (E.13) *é que nenhuma derivada de $K_k(x_k)$ relativa a x_k aparece no lado direito da equação.* Assim, o Lema E.3 possibilita uma simplificação na computação do espectro da matriz de monodromia: como indicado por (E.13), a dependência do ganho em relação ao estado não modifica a matriz Jacobiana $\nabla_x \psi(k, x, K_k(x))$ nos pontos da órbita periódica.

A simplificação obtida do Lema E.3 é utilizada no Teorema E.4 para definir uma condição suficiente para estabilidade de uma órbita periódica de (E.11).

Teorema E.4 (consultar *Theorem* 3.16)**.** *Assumindo que a matriz Jacobiana* $\nabla_x \psi(k, x, K_k(x_k^*))\,\big|_{x=x_k^*}$ *do sistema* (E.11) *é zero em pelo menos um ponto da órbita periódica* x_k^**. Então, a órbita periódica* x^* *é localmente assintoticamente exponencialmente estável.* □

O Teorema E.4 reduz o problema de estabilização de órbitas periódicas de sistemas dinâmicos de tempo discreto controlados pelo PBC ao problema de fazer todos os elementos da matriz Jacobiana da órbita iguais a zero em um ponto da órbita (utilizando a simplificação proposta no Lema E.3). O próximo passo é definir uma matriz de ganho $K_k(x_k)$ que leve ao resultado desejado.

Leis de controle. Serão apresentadas aqui leis de controle para estabilizar UPOs utilizando PBC propostas para sistemas dinâmicos de tempo discreto cuja matriz de entrada seja inversível.

Teorema E.5 (Consultar *Theorem* 3.17)**.** *Se* $\nabla_u f(k, x, u)$ *for uma matriz inversível para* $x = x_k^*$*,* $u = u_k(x_k^*)$ *e para cada* $k \in \mathbb{N}$ *e o mapa linear que descreve a evolução de uma perturbação na vizinhança de uma trajetória do sistema* (E.11) *para* $u_k(x_k) = 0$ *for hiperbólico, então existe um ganho de controle* $K_k(x_k)$ *que satisfaz o Teorema E.4.* □

Do Lema E.3 e de (E.12),

$$\nabla_x \psi(k, x, K_k(x))|_{x=x_k^*} = 0_n$$

é equivalente a

$$\nabla_x f(k, x, u_k(x_k^*))|_{x=x_k^*} + [\nabla_u f(k, x, u) K_k(x)(\nabla_x \varphi(k+p, k, x, 0) - I_n)]_{x=x_k^*, u=u_k(x_k^*)} = 0_n. \tag{E.14}$$

Se $\nabla_u f(k, x, u)$ e $(\nabla_x \varphi(k+p, k, x, 0) - I_n)$ forem inversíveis para $x = x_k^*$, $u = u_k(x_k^*)$ e cada valor de $k \in \mathbb{N}$, $K_k(x_k)$ pode ser isolada no lado direito da equação (E.14). Este é o caso se $\nabla_x \varphi(k+p, k, x, 0)$ for hiperbólico (consultar *Appendix* A).

Os valores de $K_k(x_k)$ escolhidos em seguida satisfazem o Teorema E.5.

• **Lei de controle LC 1.** *$K(x_0^*)$ uma matriz constante definida por:*

$$K(x_0^*) = -(\nabla_u f(0, x_0^*, u)|_{u=u_0(x_0^*)})^{-1} \nabla_x f(0, x, u_0(x_0^*))|_{x=x_0^*} (\nabla_x \varphi(p, 0, x, 0) - I_n)^{-1}\big|_{x=x_0^*}. \tag{E.15}$$

Este ganho resulta em uma lei de controle linear e invariante no tempo cuja determinação depende do conhecimento da UPO a ser estabilizada.

• **Lei de controle LC 2.** *$K_k(x_k^*)$ é uma matriz variante no tempo definida para tempo $k \in \mathbb{Z}$ por:*

$$\begin{aligned} &K_k(x_k^*) = \\ &-(\nabla_u f(k, x_k^*, u)|_{u=u_k(x_k^*)})^{-1} \nabla_x f(k, x, u_k(x_k^*))|_{x=x_k^*} (\nabla_x \varphi(k+p, k, x, 0) - I_n)^{-1}\big|_{x=x_k^*}, \end{aligned} \tag{E.16}$$

Este ganho resulta em uma lei de controle linear periódica cuja determinação também depende do conhecimento da UPO a ser estabilizada.

• **Lei de controle LC 3.** *$K_k(x_k)$ é dado como*

$$\begin{aligned} &K_k(x_k) = \\ &-(\nabla_u f(k, x_k, u)|_{u=u_k(x_k)})^{-1} \nabla_x f(k, x, u_k(x_k))|_{x=x_k} (\nabla_x \varphi(k+p, k, x, 0) - I_n)^{-1}\big|_{x=x_k}. \end{aligned} \tag{E.17}$$

Ao contrário da LC 1 e da LC 2, a escolha da LC 3 não requer conhecimento prévio da UPO (exceto o período p). O cálculo de $K_k(x_k)$ depende apenas do estado atual da trajetória.

Uma vantagem da LC 3 é não ser necessário encontrar a UPO antes de estabiliza-la. Outra vantagem é que, durante o projeto do ganho do controlador para LC 1 ou

LC 2 (ou qualquer outro método de controle que depende da posição da UPO), erros na aproximação da UPO levam a ganhos do controlador menos precisos. O PBC com a LC 3 pode ser aplicado para encontrar (ou refinar, para aproximações imprecisas) UPOs quando utilizando outros métodos de controle.

E.2.3 Outros resultados

Outros resultados e revisão da literatura são encontrados na *Part* I do texto. Destaca-se a proposição de uma lei de controle para o caso de um sistema com matriz de entrada não inversível (*Section* 3.4.3) e os resultados numéricos (*Chapter* 4).

Nos resultados numéricos foi feita uma comparação entre as leis de controle para o caso da matriz de entrada inversível, uma comparação entre o PBC utilizando a LC 3 e o DFC, uma breve análise de robustez a incertezas paramétricas comparando o PBC utilizando a LC 3 e o DFC e também foi mostrada uma aplicação para o PBC no caso do sistema que não apresenta uma matriz de entrada inversível.

E.2.4 Conclusões

As conclusões apresentadas para a *Part* I (*Chapter* 5) foram obtidas para resultados numéricos realizados e resumidas a seguir:

- A LC 3 pode ser aplicada para encontrar UPOs. Uma vez encontrada a UPO, sua posição é utilizada para definir o ganho para as LC 1 e LC 2;
- Caso as três leis de controle estabilizem uma UPO, a LC 3 é a que apresenta a maior velocidade de convergência das trajetórias à vizinhança da órbita e a menor bacia de atração;
- Comparando-se o PBC utilizando a LC 3 e o DFC, verifica-se que o primeiro apresenta maior velocidade de convergência das trajetórias à vizinhança da órbita estabilizada, maior bacia de atração e estabiliza órbitas não estabilizáveis com o DFC;

- Verificou-se que o PBC é mais robusto que o DFC utilizando como critério de comparação o intervalo de erro paramétrico (erro em relação ao valor do parâmetro utilizado para projetar os controladores) para o qual uma órbita estável é obtida. No entanto, é menos robusto quando utilizando como critério de comparação a variação do multiplicador Floquet de maior magnitude e o esforço de controle em regime permanente para o intervalo de erro paramétrico em que ambos os métodos conduzem à estabilização;

- Foi verificado que a velocidade de convergência de trajetórias para a órbita estabilizada para a lei de controle proposta para o PBC para o caso da matriz de entrada não inversível é próxima à obtida utilizando a LC 3.

E.3 Sistemas de tempo contínuo

Considere o seguinte sistema dinâmico de tempo contínuo:

$$\dot{x}(t) = f(t, x(t), u(t)), \qquad x(0) \text{ dado} \tag{E.18}$$

onde $t \in \mathbb{R}^+$, $x : \mathbb{R}^+ \to \mathbb{R}^n$, $u : \mathbb{R}^+ \to \mathbb{R}^m$, $n, m \in \mathbb{N}$ e $f : \mathbb{R}^+ \times \mathbb{R}^n \times \mathbb{R}^m \to \mathbb{R}^n$ é uma função T-periódica em relação ao tempo t, isto é, por definição

$$\forall t \in \mathbb{R}^+,\ \forall x \in \mathbb{R}^n,\ \forall u \in \mathbb{R}^m, \qquad f(t+T, x, u) = f(t, x, u). \tag{E.19}$$

Assume-se ainda a existência de uma solução T-periódica $x^*(t)$ da resposta livre do sistema (E.18), isto é, o sistema obtido fazendo $u(t) = 0$, $t \geq 0$. Em outras palavras,

$$\forall t \in \mathbb{R}^+, \quad x^*(t+T) = x^*(t) \tag{E.20}$$

e

$$\forall t \in \mathbb{R}, \quad \dot{x}^*(t) = f(t, x^*(t), 0_m). \tag{E.21}$$

Assume-se que esta solução periódica é instável. O principal objetivo aqui é projetar leis de controle com realimentação periódicas $u(t, x(t))$ que estabilizem esta órbita, isto é, tal que

$$\forall t \in \mathbb{R}^+, \ \forall x \in \mathbb{R}^n, \quad u(t+T, x) = u(t, x)$$

e tal que x^* seja uma solução estável do sistema em malha fechada correspondente. Há também o interesse em formas simples de estabilizar uma órbita próxima à UPO x^* de (E.18).

O sinal de controle u utilizado neste trabalho deve, idealmente, satisfazer,

$$u(t, x^*(t)) = 0 \qquad t \geq 0. \tag{E.22}$$

A condição (E.22) garante esforço de controle nulo quando a trajetória está sobre a solução periódica instável x^* da resposta livre do sistema. Para o caso de estabilização sobre uma órbita na vizinhança da órbita inicial x^* esta condição não é satisfeita. Entretanto, o esforço de controle permanecerá pequeno na vizinhança deste novo atrator.

A Seção E.3.1 é dedicada à análise de estabilidade de órbitas periódicas utilizando a teoria de Floquet. A Seção E.3.2 é dedicada aos métodos de controle DFC e PBC e às principais contribuições do trabalho para sistemas de tempo contínuo.

E.3.1 Teoria de estabilidade de Floquet

Nesta seção serão apresentados os conceitos de estabilidade de sistemas dinâmicos lineares periódicos de tempo contínuo baseados na teoria de Floquet e estes resultados são aplicados para análise de estabilidade local de órbitas periódicas de sistemas dinâmicos não-lineares em tempo contínuo.

Sistemas Lineares

Considere um sistema dinâmico linear de tempo contínuo descrito pela equação diferencial

$$\frac{dx(t)}{dt} = A(t)x(t), \tag{E.23}$$

onde $t \in \mathbb{R}^+$, $x : \mathbb{R}^+ \to \mathbb{R}^n$ é um vetor coluna e $A : \mathbb{R}^+ \to \mathbb{R}^{n \times n}$. Assume-se que $A(t)$ é uma matriz de estados periódica de período T

$$A(t) = A(t+T), \qquad T \in \mathbb{R}, \qquad \forall t. \tag{E.24}$$

A estabilidade de sistemas lineares periódicos de acordo com a teoria de Floquet depende dos autovalores da *matriz de monodromia* (detalhes no *Appendix* A), chamados de *multiplicadores característicos de Floquet* $\mu_i \in \mathbb{C}$:

Proposição E.6 (consultar *Proposition* 7.1)**.** *(i) O sistema* (E.23) *é assintoticamente estável se e somente se os multiplicadores característicos de* $A(t)$ *possuírem valor absoluto menor que* 1*. (ii) O sistema* (E.23) *é estável se e somente se os multiplicadores característicos de* $A(t)$ *possuírem valor absoluto menor ou igual a* 1 *e os multiplicadores característicos com valor absoluto iguais a* 1 *são raízes simples do polinômio mínimo da matriz de monodromia* $\Psi(t)$*.* □

Consultar *Appendix* B para definições de estabilidade.

A matriz de transição de estados $\Phi(t, t_0)$, $t, t_0 \in \mathbb{R}$ de (E.23) é calculada como a seguir (consultar *Appendix* A)

$$\begin{aligned} \frac{d\Phi(t,t_0)}{dt} &= A(t)\Phi(t,t_0) \\ \Phi(t_0,t_0) &= I_n. \end{aligned} \tag{E.25}$$

A *matriz de monodromia* $\Psi(t)$ é definida como

$$\Psi(t) = \Phi(t+T, t). \tag{E.26}$$

A teoria de Floquet pode ser utilizada para analisar a estabilidade de órbitas periódicas de sistemas não-lineares estudando a convergência/divergência de uma perturbação, governada pelo sistema linear, na vizinhança da órbita periódica [3, 40].

Aplicação a sistemas não-lineares

Considere um sistema dinâmico não-linear de tempo contínuo descrito pela equação diferencial (E.18) com solução periódica $x^*(t)$ de período T para $u(t, x(t)) = 0$ indicada em (E.19). Aqui é estudado o comportamento de uma trajetória na vizinhança de $x^*(t)$.

Proposição E.7 (Estabilidade de órbitas periódicas de sistemas de tempo contínuo - consultar *Proposition* 7.2)**.** *Uma órbita periódica $x^*(t)$ do sistema dinâmico de tempo contínuo* (E.18) *é localmente assintoticamente estável se o sistema dinâmico linear que descreve a evolução de uma trajetória perturbada na vizinhança de $x^*(t)$ for assintoticamente estável.* □

E.3.2 Métodos de controle para órbitas periódicas

Serão descritas aqui as principais contribuições do trabalho para o DFC e o PBC, em especial a proposição do *approximate prediction-based control* (aPBC). O PFC é utilizado para comparação.

Delayed feedback control (DFC)

Este método utiliza o estado do sistema atrasado do período T da UPO alvo como referência para compor $u(t, x(t))$. O sinal de controle para o DFC é então definido como em [70]

$$u(t, x(t)) = K(t, x(t)) \left(x(t - T) - x(t)\right) \tag{E.27}$$

e satisfaz a condição (E.22). $K(t, x(t)) \in \mathbb{R}^+ \times \mathbb{R}^n \to \mathbb{R}^{n \times n}$ é o ganho do controlador. O termo atrasado no sinal de controle faz de (E.18) uma equação diferencial com atraso, de dimensão infinita [36].

A aplicação do DFC requer apenas armazenamento dos valores passados das variáveis de estado durante um período T da UPO alvo. Esta característica faz o método facilmente aplicável.

Uma das contribuições contida na tese é a aplicação do método proposto em [10,23,51] para o projeto numérico de um ganho constante para o DFC. *A principal vantagem do*

método é a redução do problema de cálculo da matriz de monodromia de uma órbita controlada utilizando DFC a apenas álgebra matricial. Como consequência tem-se a redução no tempo de computação dos multiplicadores de Floquet para o sistema em malha fechada.

A redução do tempo de computação promovida pelo método permite o projeto numérico do ganho constante para o DFC utilizando otimização. Como função de custo utiliza-se o multiplicador Floquet de maior magnitude da órbita a ser estabilizada em função do ganho do DFC.

Este método proposto é descrito a seguir.

Aproximação da matriz de monodromia de uma órbita para o sistema controlado utilizando o DFC. Neste resumo serão apresentados apenas os passos para se obter a matriz de monodromia utilizando o método proposto. Detalhes e justificativas estão disponíveis na Seção 7.4.2.

A matriz de monodromia $\Psi_X(t) \in \mathbb{R}^{nN \times nN}$ é aproximada utilizando E.28:

$$\Psi_X(t) = (M_D - M_A + M_K)^{-1} M_K. \tag{E.28}$$

onde $n \in \mathbb{N}$ é a dimensão do sistema a ser controlado e $N \in \mathbb{N}$ é a quantidade de pontos de discretização s_i, com $s_1 = 0$, $s_i < s_{i+1}$, $i = 1, 2, \ldots, N$, e $s_N = 1$, utilizados para aproximar os estados atrasados $x(t - s_i T)$. A matriz de monodromia é computada para um novo sistema cujo estado é dado por (detalhes na Seção 7.4.2):

$$X(t) = \begin{bmatrix} x(t - s_1 T) \\ x(t - s_2 T) \\ \vdots \\ x(t - s_N T) \end{bmatrix}, \tag{E.29}$$

Considere o sistema linear que descreve a evolução de uma trajetória perturbada $\delta X(t)$ na vizinhança de $X^*(t)$ (órbita periódica descrita utilizando (E.29)):

$$\frac{d\delta X(t)}{dt} = \nabla_X F(t, X, U(t, X^*(t)))|_{X=X^*(t)}\, \delta X(t) + \nabla_U F(t, X^*(t), U)|_{U=U(t,X^*(t))}\, (I_N \otimes K)\, (\delta X(t-T) - \delta X(t)), \quad \text{(E.30)}$$

com

$$F(t, X(t), U(t, X(t))) = \begin{bmatrix} f(t - s_1 T, x(t - s_1 T), K(x(t - (1 + s_1)T) - x(t - s_1 T)) \\ f(t - s_2 T, x(t - s_2 T), K(x(t - (1 + s_2)T) - x(t - s_2 T)) \\ \vdots \\ f(t - s_N T, x(t - s_N T), K(x(t - (1 + s_N)T) - x(t - s_N T)) \end{bmatrix}.$$

Adota-se uma aproximação numérica para $d\delta X(t)/dt$ na forma

$$\frac{d\delta X(t)}{dt} \approx (D \otimes I_n)\delta X(t), \quad \text{(E.31)}$$

onde $D \in \mathbb{R}^{N \times N}$ é uma matriz de diferenciação com coeficientes constantes que reflete a forma de discretizar os estados atrasados utilizados para computar a matriz de monodromia. A matriz D pode ser obtida utilizando diferenças finitas [9, 21, 86, 88], métodos espectrais [9, 23, 51] ou método da colocação com diferentes tipos de polinômios [10, 51].

Substituindo (E.31) em (E.30) tem-se

$$M_D \delta X(t) = M_A \delta X(t) + M_K(\delta X(t-T) - \delta X(t)), \quad \text{(E.32)}$$

onde

$$M_D = \begin{bmatrix} D_{ij} \otimes I_n \\ \mathbf{0}_{n \times nN} \quad I_n \end{bmatrix},$$

$$M_A = \begin{bmatrix} A(t-s_1T) & \mathbf{0}_{n\times n} & \cdots & \mathbf{0}_{n\times n} & \mathbf{0}_{n\times n} \\ \mathbf{0}_{n\times n} & A(t-s_2T) & \cdots & \mathbf{0}_{n\times n} & \mathbf{0}_{n\times n} \\ \vdots & \vdots & \ddots & \vdots & \vdots \\ \mathbf{0}_{n\times n} & \mathbf{0}_{n\times n} & \cdots & A(t-s_{N-1}T) & \mathbf{0}_{n\times n} \\ I_n & \mathbf{0}_{n\times n} & \cdots & \mathbf{0}_{n\times n} & \mathbf{0}_{n\times n} \end{bmatrix},$$

$$M_K = \begin{bmatrix} B(t-s_1T)K & \mathbf{0}_{n\times n} & \cdots & \mathbf{0}_{n\times n} & \mathbf{0}_{n\times n} \\ \mathbf{0}_{n\times n} & B(t-s_2T)K & \cdots & \mathbf{0}_{n\times n} & \mathbf{0}_{n\times n} \\ \vdots & \vdots & \ddots & \vdots & \vdots \\ \mathbf{0}_{n\times n} & \mathbf{0}_{n\times n} & \cdots & B(t-s_{N-1}T)K & \mathbf{0}_{n\times n} \\ I_n & \mathbf{0}_{n\times n} & \cdots & \mathbf{0}_{n\times n} & \mathbf{0}_{n\times n} \end{bmatrix},$$

com $i = 1, \ldots, N-1$, $j = 1, \ldots, N$, $A(t-s_iT) = \nabla_x f(t-s_iT, x, u)|_{x=x^*(t-s_iT)}$ e $B(t-s_iT) = \nabla_u f(t-s_iT, x, u)|_{u=u^*(t-s_iT, x^*(t-s_iT))}$. As últimas linhas das matrizes garantem a periodicidade [51].

Define-se a matriz de monodromia em malha fechada $\Psi_X(t)$ como a matriz de transição de estados em $X^*(t)$, de $\delta X(t-T)$ a $\delta X(t)$, dada por

$$\delta X(t) = \Psi_X(t)\delta X(t-T), \tag{E.34}$$

onde $\Psi_X(t) \in \mathbb{R}^{nN\times nN}$.

A equação (E.28) é obtida de (E.32) e (E.34).

Prediction-based control (PBC)

O PBC é baseado na predição dos *estados um período da UPO alvo a frente, computada através de trajetórias da resposta livre do sistema.* O sinal de controle para o PBC de tempo contínuo é definido como

$$u(t, x(t)) = K(t, x(t)) \left(\varphi(t+T, t, x(t), 0) - x(t)\right), \tag{E.35}$$

onde $\varphi(t_1, t_0, x, 0)$ é o valor no tempo t_1 do estado de (E.18) com $x(t_0) = x$ e $u(t) = 0$, $t_0 \leq t \leq t_1$. $K(t, x(t))$ é o ganho do controlador.

A solução do sistema (E.18) com sinal de controle (E.35) é solução da seguinte EDP

$$\frac{\partial X(t,0)}{\partial t} = f(t, X(t,0), K(t, X(t,0)))\,(X(t,T) - X(t,0))\,, \qquad t \geq 0 \tag{E.36a}$$

$$\frac{\partial X(t,Ts)}{\partial s} = Tf(t + Ts, X(t,Ts), 0), \qquad t \geq 0, \qquad s \in [0,1] \tag{E.36b}$$

$$X(0,0) = x(0).$$

A função $X : \mathbb{R}^+ \times [0,T] \to \mathbb{R}^n$ é tal que $X(t,0) = x(t)$ e $X(t,T) = \varphi(t+T, t, x(t), 0)$.

Claramente, a aplicação em tempo real da estrutura de controle aqui proposta depende da possibilidade de computar $\varphi(t+T, t, x(t), 0)$.

Princípios do método *approximate prediction-based control* (aPBC)

Computar o estado futuro $\varphi(t+T, t, x(t), 0)$ requer obter a solução a cada tempo t da resposta livre da EDO do sistema (E.18) ($u \equiv 0$) do tempo t ao $t+T$. Isto não pode ser feito de forma exata em tempo real e por isso é introduzida uma aproximação desse valor. Aqui é proposto um novo método de controle realimentado baseado na diferença entre o estado no tempo atual e uma aproximação do estado predito, o *approximate prediction-based control* (aPBC).

Devido à aproximação utilizada, da aplicação do aPBC é esperada a estabilização de uma nova órbita do sistema controlado, próxima à UPO do sistema sem controle.

Passo 1: Aproximação do termo predito. O primeiro passo consiste em aproximar a solução de (E.36b) por um método implícito de Runge-Kutta para integração de EDOs [35] para estimar o termo predito, isto é, o valor final de

$$X(t,T) = x + T\int_0^1 f\,(t + Ts, X(t,Ts), 0)\,ds, \qquad x \text{ dado.} \tag{E.37}$$

Para aproximar $X(t,T)$ dado por (E.37), o mapa de transição de estados da resposta livre do sistema $\varphi(t_2,t_1,x,0)$ é primeiro aproximado pelo operador $\mathbf{y}$ definido por

$$\mathbf{y}(t+T,t,x) = x + T\sum_{i=1}^{N} c_i l_i(t) \tag{E.38a}$$

$$l_i(t) = f\left(t+Ts_i, x+T\sum_{j=1}^{N} a_{ij}l_j(t), 0\right), \tag{E.38b}$$

onde $i=1,\ldots,N$, $l_j : \mathbb{R}\times\mathbb{R}^n \to \mathbb{R}^n$ e $a_{ij}, c_i \in \mathbb{R}$ são pesos escolhidos de acordo com o método implícito utilizado [35]. A aproximação $\mathbf{y}(t+T,t,x(t))$ de $X(t,Ts)$, $s\in[0,1]$, é calculada nos pontos de discretização $s=s_i$, $i=1,\ldots,N$.

Por simplicidade, (E.38b) é escrita na forma do vetor (E.39).

$$L(t) = F_T(t,x,L(t)), \tag{E.39}$$

onde

$$\forall t \geq 0, \quad L(t) = \begin{bmatrix} l_1(t) \\ \vdots \\ l_N(t) \end{bmatrix} \in \mathbb{R}^{nN},$$

e $F_T : \mathbb{R}\times\mathbb{R}^n\times\mathbb{R}^{nN} \to \mathbb{R}^{nN}$ é definida por:

$$F_T(t,x,L) = \begin{bmatrix} f(t+Ts_1, x+\sum_{j=1}^{N} a_{1j}l_j, 0) \\ \vdots \\ f(t+Ts_N, x+\sum_{j=1}^{N} a_{Nj}l_j, 0), \end{bmatrix}, \qquad \forall x\in\mathbb{R}^n, \quad \forall L\in\mathbb{R}^{nN}.$$

Para computar $\mathbf{y}(t+T,t,x)$ utilizando (E.38a) é necessário resolver o sistema de equações algébricas (E.38b) com incógnita $L(t)\in\mathbb{R}^N$. Escrevendo

$$C = \begin{bmatrix} c_1 & \ldots & c_N \end{bmatrix}$$

e fechando a malha de (E.18) utilizando

$$u(t, x(t)) = K(t, x(t))(\mathbf{y}(t + T, t, x(t)) - x(t)) = TK(t, x(t))CL(t)$$

resulta na equação algébrico-diferencial (EAD),

$$\dot{x}(t) = f(t, x(t), TK(t, x(t))CL(t)), \qquad x(0) = x_0 \tag{E.40a}$$

$$L(t) = F_T(t, x(t), L(t)). \tag{E.40b}$$

A solução em tempo real da EAD (E.40) requer que $L(t)$, sua parte algébrica, seja computada a cada tempo t. É então proposta a introdução do observador a seguir para transformar o sistema controlado em um sistema de EDOs.

Passo 2: Aproximação do termo de predição. Agora (E.40b) é aproximada resolvendo a EDO de dimensão nN (E.41) cuja solução $\hat{L}(t)$ é uma estimação de $L(t)$. O valor inicial $\hat{L}(0)$ deve ser previamente (e precisamente) computado para possibilitar uma boa qualidade de rastreio para $L(t)$.

$$\frac{d}{dt}\left(\hat{L}(t) - F_T(t, x(t), \hat{L}(t))\right) + k_o\left(\hat{L}(t) - F_T(t, x(t), \hat{L}(t))\right) = 0, \qquad \hat{L}(0) \text{ dado.} \tag{E.41}$$

O ganho escalar k_o é escolhido positivo de forma que $\hat{L}(t)$ de (E.41) tenda assintoticamente à solução $L(t)$ de (E.40b) quando $t \to +\infty$, e tipicamente tal que a dinâmica do estimador seja mais rápida que a dinâmica do sistema controlado. Se de fato a evolução de $\hat{L}(t)$ for escolhida de forma a satisfazer (E.41), será verificada a convergência.

De (E.41) é obtido:

$$\dot{\hat{L}}(t) = \left[I_{nN} - T\partial_3 F_T(t, x(t), \hat{L}(t))(A \otimes I_n)\right]^{-1}$$
$$\left[\partial_1 F_T(t, x(t), \hat{L}(t)) + \partial_2 F_T(t, x(t), \hat{L}(t))(\mathbf{1}_N \otimes f(t, x(t), 0)) - k_o\left(\hat{L}(t) - F_T(t, x(t), \hat{L}(t))\right)\right]. \tag{E.42}$$

onde $A = (a_{ij})$ e ∂_i é a derivada parcial relativa à i-ésima variável. I_n é a matriz identidade $n \times n$ e $\mathbf{1}_N$ é o vetor coluna de dimensão N com todos os elementos iguais a 1. $\otimes$ é o produto de Kronecker.

A solução de (E.42), para se obter (E.41), requer a inversibilidade do primeiro fator. $G_T : \mathbb{R}^n \times \mathbb{R}^n \times \mathbb{R}^{nN} \to \mathbb{R}^{nN}$ definida como,

$$G_T(t, x, \hat{L}) = \Big[I_{nN} - T\partial_3 F_T(t, x, \hat{L})(A \otimes I_n)\Big]^{-1} \Big[\partial_1 F_T(t, x, \hat{L}) + \partial_2 F_T(t, x, \hat{L})(\mathbf{1}_N \otimes f(t, x, 0)) - k_o\left(\hat{L} - F_T(t, x, \hat{L})\right)\Big]. \quad \text{(E.43)}$$

De (E.40), (E.41), (E.43) e denotando $\hat{l}_i(t)$ como os componentes de $\hat{L}(t)$, a lei de controle proposta resulta no seguinte sistema de EDOs em malha fechada:

$$\begin{bmatrix} \dot{x}(t) \\ \dot{\hat{L}}(t) \end{bmatrix} = \begin{bmatrix} f\left(t, x(t), K(t, x(t))TC\hat{L}(t)\right) \\ G_T\left(t, x(t), \hat{L}(t)\right) \end{bmatrix} \qquad x(0) = x_0, \quad \hat{L}(0) = L(0). \qquad \text{(E.44)}$$

A solução de (E.44) é uma aproximação da solução da EAD dada em (E.40).

E.3.3 Conclusões

As conclusões apresentadas para a *Part* II (*Chapter* 9) foram obtidas dos resultados numéricos comparando o PFC, DFC e PBC/aPBC e resumidas a seguir:

- Considerando os multiplicadores de Floquet e as características de desempenho a eles associadas (estabilidade e velocidade de convergência de trajetórias à solução estabilizada), os melhores resultados foram obtidos para o PFC, o aPBC apresentou resultados intermediários e o DFC os piores resultados;
- Considerando o erro e esforço de controle em regime os resultados obtidos com o aPBC foram significativamente inferiores comparados com os outros métodos;
- O DFC foi o método que apresentou maior robustez a erros paramétricos dentre os métodos testados;

- Não foram encontradas limitações teóricas para o PFC e o PBC/aPBC, ao contrário do DFC que possui limitações descritas na literatura;

- Foi identificada uma limitação prática para o aPBC. Para o sistema em malha fechada, devido à necessidade de estender o estado em relação ao estado do sistema sem controle, a predição do estado futuro para órbitas de período longo necessita de um alto esforço computacional. Este ponto deverá ser foco de esforços futuros, com a experimentação de novas leis de controle;

- Caso o DFC estabilize a órbita alvo e satisfaça as especificações de desempenho, este é o método mais indicado para aplicação devido à sua simplicidade. Caso seja necessário utilizar outro método de controle, o aPBC é o mais indicado por utilizar um modelo do sistema para obter o estado futuro e compor o sinal de controle. Isto é considerado uma vantagem em relação à necessidade da órbita alvo para o PFC.

Appendix F

Résumé étendu

F.1 Introduction

Le principal problème étudié dans ce travail est la stabilisation des orbites périodiques de systèmes dynamiques à l'aide de contrôle non linéaire par rétroaction (*feedback*) d'état ou de sortie. L'objectif des méthodes de contrôle proposées est de stabiliser le système sur une solution périodique stable, ce qui diffère de l'objectif des problèmes de contrôle plus habituels de stabilisation sur un point d'équilibre stable.

Les méthodes de contrôle considérées ici sont appliquées aux systèmes présentant des orbites périodiques instables (UPOs - *unstable periodic orbits*) dans l'espace d'état et ces UPOs sont les orbites à stabiliser. Les méthodes proposées sont telles que l'oscillation stable résultante est obtenue avec un effort de contrôle faible, car le signal de contrôle est conçu de façon à tendre vers zéro lorsque la trajectoire tend vers l'orbite stabilisée.

Les méthodes de contrôle utilisées ici pour la stabilisation des orbites périodiques sont la commande proportionnelle *proportional feedback control* (PFC), la commande retardée *delayed feedback control* (DFC) et la commande à base de prédiction *prediction-based control* (PBC). La principale différence entre elles est la référence utilisée pour définir le signal de contrôle. La PFC, proposée par [70], utilise comme référence l'orbite à stabiliser. Cette orbite doit être trouvée avant l'application de la loi de commande et des inexactitudes dans sa détermination induisent un plus grand effort de contrôle. La DFC, proposée par

Pyragas [70], utilise comme référence l'état retardé d'une période, et seule la période doit être onnue pour son application. La PBC utilise comme référence un état prédit une période en avance, le long des trajectoires de la réponse du système libre, et la connaissance d'un modèle du système est nécessaire pour l'implémentation.

La stabilisation de l'orbite périodique d'un système non linéaire peut être simplifiée pour la stabilisation d'un certain système linéaire périodique en temps. Ce système linéaire est obtenu par linéarisation des trajectoires au voisinage de l'orbite périodique et l'analyse de sa stabilité peut être effectuée à l'aide de la théorie de stabilité de Floquet. La stabilité locale de l'orbite périodique du système non linéaire est déduite de la stabilité du système linéaire associé.

Le manuscrit est divisé en deux parties, la première consacrée aux systèmes en temps discret et la deuxième aux systèmes en temps continu. Dans les paragraphes suivant le présent résumé seront discutées les principales contributions de chaque partie, les problèmes de contrôle à traiter et la théorie nécessaire à leur compréhension. Pour les systèmes en temps discret les principales contributions sont liées au PBC et seule cette méthode est discutée dans ce résumé. Pour les systèmes en temps continu les principales contributions sont liées au DFC et au PBC et seules ces méthodes sont discutées dans ce résumé.

F.2 Systèmes en temps discret

On considère le système dynamique en temps discret:

$$x_{k+1} = f(k, x_k, u_k), \quad x_0 \text{ donnée} \tag{F.1}$$

où $x : \mathbb{N} \to \mathbb{R}^n$, $u : \mathbb{N} \to \mathbb{R}^m$, $k, m, n \in \mathbb{N}$ et $f : \mathbb{N} \times \mathbb{R}^n \times \mathbb{R}^m \to \mathbb{R}^n$ est une fonction p-périodique dans le temps k, c'est-à-dire, par définition

$$\forall k \in \mathbb{N}, \quad \forall x \in \mathbb{R}^n, \quad \forall u \in \mathbb{R}^m, \qquad f(k+p, x, u) = f(k, x, u). \tag{F.2}$$

On suppose l'existence d'une solution p-périodique x_k^* de la réponse libre du système (F.1), à savoir, le système obtenu en faisant $u_k = 0$, $k \geq 0$. En d'autres termes

$$\forall k \in \mathbb{N}, \qquad x_{k+p}^* = x_k^* \tag{F.3}$$

et

$$\forall k \in \mathbb{N}, \qquad x_{k+1}^* = f(k, x_k^*, 0_m). \tag{F.4}$$

On suppose que cette solution périodique est instable. L'objectif principal est ici de concevoir des lois de rétroaction $u_k(x_k)$ qui stabilisent cette orbite, c'est à dire, telles que

$$\forall k \in \mathbb{N}, \quad \forall x \in \mathbb{R}^n, \qquad u_{k+p}(x) = u_k(x)$$

et telles que x^* est une solution stable du système en boucle fermée

$$x_{k+1} = f(k, x_k, u_k(x_k)) \tag{F.5}$$

avec $u : \mathbb{N} \times \mathbb{R}^n \to \mathbb{R}^m$ définie dans les sections suivantes.

Le signal de contrôle u utilisée dans ce travail devrait idéalement vérifier

$$u_k(x_k^*) = 0, \qquad k \geq 0. \tag{F.6}$$

Sur l'orbite périodique l'effort de contrôle est ainsi égal à zéro, et la solution périodique instable x_k^* de $f(k, x_k, 0)$ est une solution périodique stable de (F.5).

La Section F.2.1 est consacrée à l'analyse de la stabilité des orbites périodiques en utilisant la théorie de Floquet. La Section F.2.2 est consacrée à la nouvelle loi de contrôle proposée pour le PBC, qui sera utilisée pour stabiliser x_k^*.

F.2.1 Théorie de la stabilité de Floquet

Cette section présente les concepts de stabilité des systèmes dynamiques linéaires à temps discret périodiques, basés sur la théorie de Floquet, et ces résultats sont appliqués à

l'analyse de la stabilité locale des orbites périodiques de systèmes dynamiques non linéaires à temps discret.

Systèmes linéaires

On considère un système dynamique linéaire décrit par l'équation suivante.

$$x_{k+1} = A_k x_k, \tag{F.7}$$

où $k \in \mathbb{N}$, $x : \mathbb{N} \to \mathbb{R}^n$ est un vecteur colonne et $A : \mathbb{N} \to \mathbb{R}^{n \times n}$. On suppose que A_k est une matrice d'état p-périodique, à savoir

$$A_k = A_{k+p}, \quad \forall k \in \mathbb{N}. \tag{F.8}$$

La stabilité des systèmes périodiques linéaires selon la théorie de Floquet [5] dépend des valeurs propres de la *matrice de monodromie* (détails dans l'Annexe A), appelé *multiplicateurs caractéristique Floquet* $\mu_i \in \mathbb{C}$, $i = 1, \ldots, n$:

Proposition F.1 (voir la *Proposition* 3.1)**.** (*i*) *Le système* (F.7) *est asymptotiquement stable si et seulement si les multiplicateurs caractéristiques de* A_k *ont une valeur absolue inférieure à* 1. (*ii*) *Le système* (F.7) *est stable si et seulement si les multiplicateurs caractéristiques de* A_k *ont une valeur absolue inférieure ou égale à* 1 *et si les multiplicateurs caractéristiques avec une valeur absolue égale à* 1 *sont des racines simples du polynôme minimal de la matrice de monodromie* Ψ_k. □

Se reporter à l'Annexe B pour la définition de la stabilité. La matrice de monodromie Ψ_k est calculée comme suit:

$$\Psi_k = \prod_{l=0}^{p-1} A_{k+l} \tag{F.9}$$

où les matrices dans le multiplicande sont ordonnées de droite à gauche lorsque l croît.

La théorie de Floquet peut être utilisée pour analyser la stabilité des orbites périodiques de systèmes non linéaires par l'étude de la convergence / divergence d'une perturbation, régie par un système linéaire, aux alentours de l'orbite périodique [3, 40].

Application aux systèmes non linéaires

On considère le système dynamique non linéaire à temps discret décrit par l'équation aux différences (F.5) avec une solution p-périodique x_k^* par $u_k(x_k) = 0$ indiquée en (F.2). On étudie ici le comportement d'une trajectoire aux alentours de x_k^*.

Proposition F.2 (Stabilité des orbites périodiques de systèmes en temps discret - se reporter à la *Proposition* 3.2)**.** *Une orbite périodique x_k^* du système dynamique récursif* (F.5) *est localement asymptotiquement stable si le système dynamique linéaire qui décrit l'évolution d'une trajectoire perturbée dans le voisinage de x_k^* est asymptotiquement stable.* □

F.2.2 Stabilisation par prediction-based control (PBC)

Prediction-based control. La méthode proposée par Ushio et Yamamoto [91] utilise un signal de contrôle défini par

$$u_k(x_k) = K_k(x_k)\left(\varphi(k+p, k, x_k, 0) - x_k\right), \tag{F.10}$$

où $\varphi(k_1, k_0, x, 0)$ est la valeur de l'état de (F.5) à l'instant k_1 avec $x_{k_0} = x$ et $u_k = 0$. En d'autres termes, $\varphi(k_1, k_0, x, 0)$ est la valeur de l'état au temps k_1 calculé le long de la trajectoire de la réponse libre du système ($u_k \equiv 0$) partant de x à l'instant k_0.

La contribution de ce travail dans le domaine des systèmes en temps discret est de proposer une méthode pour régler le gain du PBC. Les résultats ont été publiés à l'origine en [12]. Le système de contrôle représenté ici est basé sur une condition suffisante pour la stabilité et conduit à la proposition de gains pour le contrôleur.

Condition suffisante de stabilité Une condition suffisante de stabilité des orbites périodiques des systèmes dynamiques en temps discret contrôlé par PBC est définie, basée sur le spectre de Ψ_k. Le résultat obtenu au Théorème F.4 ci-dessous permet le développement de lois de contrôle pour la stabilisation des UPOs par PBC.

Selon (F.5) et (F.10), le système dynamique à temps discret contrôlé par PBC est défini par

$$x_{k+1} = \varphi(k+1, k, x_k, u_k(x_k)) = f(k, x_k, K_k(x_k)(\varphi(k+p, k, x_k, 0) - x_k)). \tag{F.11}$$

Pour tout $x \in \mathbb{R}^n$ et $K \in \mathbb{R}^{q \times n}$, $q \in \mathbb{N}$, nous utilisons la notation

$$\begin{aligned} \psi(k, x, K) &\doteq f(k, x, u_k(x)) \\ u_k(x) &= K(\varphi(k+p, k, x, 0) - x). \end{aligned} \tag{F.12}$$

La première étape pour définir la condition suffisante de stabilité des orbites périodiques est d'obtenir Ψ_k. Cette matrice pour le système en boucle fermée, est calculée d'après le Lemme F.3.

Lemme F.3 (se reporter au *Lemma* 3.15)**.** *Pour n'importe quel point p-périodique x_k^*, $k, p \in \mathbb{N}$, de la trajectoire x^* du système en boucle fermée* (F.11)*, on a*

$$\Psi_k = \prod_{l=0}^{p-1} \nabla_x \psi(k+l, x, K_{k+l}(x_{k+l}^*))\big|_{x=x_{k+l}^*} \tag{F.13}$$

et les matrices du multiplicande sont ordonnés de droite à gauche lorsque l'indice l croît. □

L'intérêt de la formule (F.13) *est qu'aucune dérivée de $K_k(x_k)$ par rapport à x_k n'apparaît du côté droit de l'équation.* Ainsi, le Lemme F.3 permet une simplification dans le calcul du spectre de la matrice de monodromie: comme indiqué par (F.13), la dépendance du gain par rapport à l'état ne modifie pas la matrice Jacobienne $\nabla_x \psi(k, x, K_k(x))$ aux points de l'orbite périodique.

La simplification obtenu du Lemme F.3 est utilisée dans le Théorème F.4 pour définir la condition suffisante de stabilité d'une orbite périodique de (F.11).

Théorème F.4 (se reporter au *Theorem* 3.16)**.** *On suppose que la matrice Jacobienne $\nabla_x \psi(k, x, K_k(x_k^*))\big|_{x=x_k^*}$ du système* (F.11) *est nulle sur au moins un point de l'orbite périodique x_k^*. Alors, l'orbite périodique x^* est localement exponentiellement stable.* □

Grâce au Théorème F.4, on peut par exemple réduire le problème de la stabilisation des orbites périodiques des systèmes dynamiques en temps discret contrôlées par le PBC à la question de rendre tous les éléments de la matrice Jacobienne de l'orbite égale à zéro en un point de l'orbite (en utilisant la simplification proposée en Lemme F.3). L'étape suivante consiste à définir une matrice de gain $K_k(x_k)$ qui conduit au résultat désiré.

Lois de contrôle. Seront présentés ici des lois de contrôle pour stabiliser les UPOs, utilisant le PBC proposé pour les systèmes dynamiques en temps discret dont la matrice d'entrée est inversible.

Théorème F.5 (se reporter au *Theorem* 3.17)**.** *Si $\nabla_u f(k,x,u)$ est une matrice inversible et l'application linéaire qui décrit l'évolution d'une perturbation dans le voisinage d'une trajectoire du système* (F.11) *pour $u_k(x_k) = 0$ est hyperbolique, alors il existe un gain $K_k(x_k)$ satisfaisant le Théorème F.4.* □

Du Lemme F.3, la condition

$$\nabla_x \psi(k,x,K_k(x))|_{x=x_k^*} = 0_n$$

est équivalente à

$$\nabla_x f(k,x,u_k(x_k^*))|_{x=x_k^*} + [\nabla_u f(k,x,u) K_k(x) (\nabla_x \varphi(k+p,k,x,0) - I_n)]_{x=x_k^*} = 0_n. \quad \text{(F.14)}$$

Si $\nabla_u f(k,x,u)$ et $(\nabla_x \varphi(k+p,k,x,0) - I_n)$ sont inversibles, $K_k(x_k)$ peut être isolé sur le côté droit de l'équation (F.14). C'est le cas si $\nabla_x \varphi(k+p,k,x,0)$ est hyperbolique (se reporter à l'Annexe A).

Les valeurs $K_k(x_k)$ choisies par la suite satisfont le Théorème F.5.

• **Loi de contrôle LC 1.** *$K(x_0^*)$ une matrice constante définie par:*

$$K(x_0^*) = -(\nabla_u f(0,x_0^*,u)|_{u=u_0(x_0^*)})^{-1} \nabla_x f(0,x,u_0(x_0^*))|_{x=x_0^*} (\nabla_x \varphi(p,0,x,0) - I_n)^{-1}\big|_{x=x_0^*}. \quad \text{(F.15)}$$

Ce gain résulte d'une loi de contrôle linéaire invariant dans le temps dont la détermination dépend de la connaissance de l'UPO à stabiliser.

• **Loi de contrôle LC 2.** *$K_k(x_k^*)$ est une matrice variable dans le temps $k \in \mathbb{Z}$ définie par:*

$$K_k(x_k^*) = \\ -\left(\nabla_u f(k, x_k^*, u)|_{u=u_k(x_k^*)}\right)^{-1} \nabla_x f(k, x, u_k(x_k^*))|_{x=x_k^*} \left(\nabla_x \varphi(k+p, k, x, 0) - I_n\right)^{-1}\big|_{x=x_k^*}, \tag{F.16}$$

Ce gain se traduit par une loi de contrôle périodique linéaire dont la détermination dépend aussi de la connaissance de l'UPO à stabiliser.

• **Loi de contrôle LC 3.** *$K_k(x_k)$ est donné par*

$$K_k(x_k) = \\ -\left(\nabla_u f(k, x_k, u)|_{u=u_k(x_k)}\right)^{-1} \nabla_x f(k, x, u_k(x_k))|_{x=x_k} \left(\nabla_x \varphi(k+p, k, x, 0) - I_n\right)^{-1}\big|_{x=x_k}. \tag{F.17}$$

Contrairement à LC 1 et LC 2, le choix de LC 3 ne nécessite aucune connaissance préalable de l'UPO (à l'exception de la période p). Le calcul de $K_k(x_k)$ ne dépend que de l'état actuel de la trajectoire.

Un avantage de LC 3 est qu'il n'est pas nécessaire de trouver l'UPO avant de le stabiliser. Un autre avantage est que, lors de la conception du gain du contrôleur pour LC 1 ou LC 2 (ou toute autre méthode de contrôle qui dépend de la position de l'UPO), les erreurs d'approximation de l'UPO conduisent à des gains du contrôleur moins précis. Le PBC avec LC 3 peut être appliqué pour trouver (ou pour affiner des approximations inexactes) des UPOs lors de l'utilisation d'autres méthodes de contrôle.

F.2.3 Autres résultats

D'autres résultats et une revue de la littérature se trouvent dans la partie *Part* I du texte. On peut en particulier noter la proposition d'une loi de contrôle dans le cas d'un système avec matrice d'entrée non inversible (*Section* 3.4.3) et des résultats numériques (*Chapter* 4).

Dans les résultats numériques une comparaison a été faite entre les lois de contrôle dans le cas d'une matrice d'entrée inversible; une comparaison entre le PBC avec LC 3 et DFC; une brève analyse de la robustesse aux incertitudes paramétriques comparant PBC avec LC 3 et DFC; ainsi qu'une application du PBC dans le cas où le système ne possède pas une matrice d'entrée inversible.

F.2.4 Conclusions

Les résultats présentés dans la *Part* I (*Chapter* 5) ont été obtenus à partir des résultats numériques et sont résumés ci-dessous:

- Le LC 3 peut être appliqué pour trouver les UPOs et pour définir le gain pour LC 1 et 2;
- Si les trois lois de contrôle stabilisent une UPO, le LC 3 est celui qui a la plus grande vitesse de convergence des trajectoires à proximité de l'orbite et le plus petit bassin d'attraction;
- En comparant le PBC avec LC 3 et DFC, il semble que le premier ait une convergence plus rapide des trajectoires à proximité de l'orbite stabilisée, le plus grand bassin d'attraction et la capacité de stabiliser des orbites non stabilisables par DFC;
- Il a été constaté que le PBC est plus robuste que le DFC, en utilisant comme critère de comparaison la marge d'erreur paramétrique (l'erreur sur la valeur du paramètre utilisé pour concevoir des contrôleurs) pour lequel une orbite stable est obtenu. Cependant, il est moins robuste en utilisant comme critère de comparaison, la variation du multiplicateur de Floquet de plus grande magnitude et l'effort de contrôle

en régime permanent, en fonction de l'intervalle d'erreur paramétrique préservant la stabilisation;

- Il a été constaté que le taux de convergence des trajectoires vers l'orbite stabilisée pour la loi de contrôle proposée par PBC au cas de la matrice d'entrée non inversible est proche de celle obtenue en utilisant la LC 3.

F.3 Systèmes en temps continu

On considère le système dynamique en temps continu suivant:

$$\dot{x}(t) = f(t, x(t), u(t)), \qquad x(0) \text{ donné} \tag{F.18}$$

où $t \in \mathbb{R}^+$, $x : \mathbb{R}^+ \to \mathbb{R}^n$, $u : \mathbb{R}^+ \to \mathbb{R}^m$, $n, m \in \mathbb{N}$ et $f : \mathbb{R}^+ \times \mathbb{R}^n \times \mathbb{R}^m \to \mathbb{R}^n$ est une fonction T-périodique en temps, c'est-à-dire, par définition

$$\forall t \in \mathbb{R}^+,\ \forall x \in \mathbb{R}^n,\ \forall u \in \mathbb{R}^m, \qquad f(t+T, x, u) = f(t, x, u). \tag{F.19}$$

On suppose l'existence d'une solution T-périodique de la réponse libre du système (F.18), obtenu pour $u(t) = 0$, $t \geq 0$. En d'autres termes,

$$\forall t \in \mathbb{R}^+, \quad x^*(t+T) = x^*(t) \tag{F.20}$$

et

$$\forall t \in \mathbb{R}, \quad \dot{x}^*(t) = f(t, x^*(t), 0_m). \tag{F.21}$$

On suppose que cette solution périodique est instable. L'objectif principal ici est de concevoir des lois de rétroaction de contrôle périodique $u(t, x(t))$ qui stabilisent cette orbite, c'est-à-dire telles que

$$\forall t \in \mathbb{R}^+,\ \forall x \in \mathbb{R}^n, \quad u(t+T, x) = u(t, x)$$

et que x^* soit une solution stable du système en boucle fermée

$$\dot{x}(t) = f(t, x(t), u(t, x(t)) \tag{F.22}$$

avec $u : \mathbb{R}^+ \times \mathbb{R}^n \to \mathbb{R}^m$ définie dans les sections suivantes. Il est aussi intéressant de stabiliser par des moyens simples une orbite proche de l'UPO x^* de (F.18).

Le signal de contrôle u utilisé dans ce travail devrait idéalement vérifier,

$$u(t, x^*(t)) = 0 \qquad t \geq 0. \tag{F.23}$$

La condition (F.23) assure un effort de contrôle nul lorsque la trajectoire est sur la solution périodique instable x^* de la réponse libre du système. Dans le cas de la stabilisation sur une orbite dans le voisinage de l'orbite initiale x^* cette condition n'est pas satisfaite. Cependant, l'effort de contrôle restera faible au voisinage de ce nouvel attracteur.

La Section F.3.1 est dédiée à l'analyse de la stabilité des orbites périodiques en utilisant la théorie de Floquet. La Section F.3.2 est consacrée aux méthodes de contrôle DFC et PBC et aux principales contributions de ce travail à des systèmes en temps continu.

F.3.1 Théorie de la stabilité de Floquet

Cette section présente les concepts de stabilité des systèmes dynamiques linéaires périodiques en temps continu, basés sur la théorie de Floquet et ces résultats sont appliqués à l'analyse de la stabilité locale des orbites périodiques de systèmes dynamiques non linéaires à temps continu.

Systèmes linéaires

On considère un système dynamique linéaire décrit par l'équation différentielle en temps continu

$$\frac{dx(t)}{dt} = A(t)x(t), \tag{F.24}$$

où $t \in \mathbb{R}^+$, $x : \mathbb{R}^+ \to \mathbb{R}^n$ est un vecteur colonne et $A : \mathbb{R}^+ \to \mathbb{R}^{n\times n}$. On suppose que $A(t)$ est une matrice d'état périodique de période $T > 0$, qui satisfait donc

$$A(t) = A(t+T), \qquad \forall t. \tag{F.25}$$

La stabilité des systèmes périodiques linéaires selon la théorie de Floquet dépend des valeurs propres de la *matrice de monodromie* (détails dans l'Annexe A), appelées *multiplicateurs caractéristiques de Floquet* $\mu_i \in \mathbb{C}$, $i = 1, \ldots, n$:

Proposition F.6 (voir la *Proposition* 7.1)**.** (*i*) *Le système* (F.24) *est asymptotiquement stable si et seulement si les multiplicateurs caractéristiques de* $A(t)$ *ont un valeur absolue inférieure à* 1. (*ii*) *Le système* (F.24) *est stable si et seulement si les multiplicateurs caractéristiques de* $A(t)$ *ont une valeur absolue inférieure ou égale à* 1 *et si les multiplicateurs caractéristique avec une valeur absolue égale à* 1 *sont des racines simples du polynôme minimal de la matrice de monodromie* $\Psi(t)$. □

Se reporter à l'Annexe B pour la définition de la stabilité.

La matrice de transition d'état $\Phi(t, t_0)$, $t, t_0 \in \mathbb{R}$ de (F.24) est calculée comme suit: (Se reporter à l'Annexe A)

$$\begin{aligned} \frac{d\Phi(t,t_0)}{dt} &= A(t)\Phi(t,t_0) \\ \Phi(t_0,t_0) &= I_n. \end{aligned} \tag{F.26}$$

La *matrice de monodromie* $\Psi(t)$ est définie comme suit

$$\Psi(t) = \Phi(t+T, t). \tag{F.27}$$

La théorie de Floquet peut être utilisée pour analyser la stabilité des orbites périodiques de systèmes non linéaires par l'étude de la convergence / divergence d'une perturbation, régie par le système linéaire, aux alentours de l'orbite périodique [3, 40].

Application aux systèmes non linéaires

On considère le système dynamique non linéaire à temps continu décrit par l'équation différentielle (F.22) avec une solution périodique $x^*(t)$ de période T par $u(t, x(t)) = 0$ indiquée en (F.19). On étudie ici le comportement d'une trajectoire aux alentours de $x^*(t)$.

Proposition F.7 (Stabilité des orbites périodiques de systèmes en temps continu - se reporter à la *Proposition* 7.2)**.** *Une orbite périodique $x^*(t)$ d'un système dynamique à temps continu* (F.22) *est localement asymptotiquement stable si le système dynamique linéaire qui décrit l'évolution d'une trajectoire perturbée dans le voisinage de $x^*(t)$ est asymptotiquement stable.* □

F.3.2 Méthodes de contrôle des orbites périodiques

Seront décrites ici les principales contributions au DFC et au PBC, en particulier la proposition de commande basée sur une prédiction approchée *approximate prediction-based control* (aPBC). La PFC est utilisée comme comparaison, mais n'est pas décrite dans le présent résumé.

Delayed feedback control (DFC)

Cette méthode utilise comme référence l'état du système retardé de la période T de l'UPO. Le signal de contrôle pour le DFC est alors défini comme suit

$$u(t, x(t)) = K(t, x(t)) \left(x(t - T) - x(t)\right) \tag{F.28}$$

et satisfait la condition (F.23). $K(t, x(t)) \in \mathbb{R}^+ \times \mathbb{R}^n \to \mathbb{R}^{n \times n}$ est le gain du contrôleur. Le terme retardé dans le signal de contrôle fait de (F.22) une équation différentielle avec retard de dimension infinie [36].

L'application de la commande DFC ne nécessite que le stockage des valeurs passées des variables d'état sur une période T de l'UPO objectif. Cette caractéristique rend la méthode facile à appliquer.

Une des contributions contenues dans cette thèse est l'application de la méthode proposée en [10, 23, 51] pour la conception numérique d'un gain constant pour le DFC. Le principal avantage de la méthode est de réduire le problème du calcul de la matrice de monodromie d'une orbite contrôlée en utilisant DFC à un problème d'algèbre matriciel. En conséquence, on a observé une réduction du temps de calcul des multiplicateurs de Floquet pour le système en boucle fermée.

La réduction du temps de calcul induite par la méthode permet le calcul d'un gain constant pour le DFC en utilisant une méthode d'optimisation. La fonction-coût utilisée est le multiplicateur de Floquet de plus grande magnitude de l'orbite à stabiliser en fonction du gain du DFC.

Les résultats sur la commande DFC sont publiés en [14].

Approximation de la matrice de monodromie d'une orbite du système contrôlé en utilisant la DFC. Dans ce résumé seront présentées les étapes nécessaires à l'obtention de la matrice de monodromie en utilisant la méthode proposée. Les détails et les justifications sont disponibles dans la section 7.4.2.

La matrice de monodromie $\Psi_X(t) \in \mathbb{R}^{nN \times nN}$ est approchée en utilisant F.29:

$$\Psi_X(t) = (M_D - M_A + M_K)^{-1} M_K. \tag{F.29}$$

où $n \in \mathbb{N}$ est la dimension du système à contrôler et $N \in \mathbb{N}$ est le nombre de points de discrétisation s_i, avec $s_1 = 0$, $s_i < s_{i+1}$, $i = 1, 2, \ldots, N$, et $s_N = 1$, utilisé pour estimer les états retardé $x(t - s_i T)$. La matrice de monodromie est calculée pour un nouveau système dont l'état est donné par (détail dans la Section 7.4.2):

$$X(t) = \begin{bmatrix} x(t - s_1 T) \\ x(t - s_2 T) \\ \vdots \\ x(t - s_N T) \end{bmatrix}, \tag{F.30}$$

Considérons le système linéaire qui décrit l'évolution d'une trajectoire perturbée $\delta X(t)$ dans le voisinage de $X^*(t)$ (orbite périodique décrite en utilisant (F.30)):

$$\frac{d\delta X(t)}{dt} = \nabla_X F(t, X, U(t, X^*(t)))|_{X=X^*(t)}\, \delta X(t) + \nabla_U F(t, X^*(t), U)|_{U=U(t,X^*(t))}\, (I_N \otimes K)\, (\delta X(t-T) - \delta X(t)), \quad \text{(F.31)}$$

avec

$$F(t, X(t), U(t, X(t))) = \begin{bmatrix} f(t - s_1 T, x(t - s_1 T), K(x(t - (1 + s_1)T) - x(t - s_1 T)) \\ f(t - s_2 T, x(t - s_2 T), K(x(t - (1 + s_2)T) - x(t - s_2 T)) \\ \vdots \\ f(t - s_N T, x(t - s_N T), K(x(t - (1 + s_N)T) - x(t - s_N T)) \end{bmatrix}.$$

On adopte une approximation numérique de $d\delta X(t)/dt$ sous la forme

$$\frac{d\delta X(t)}{dt} \approx (D \otimes I_n)\delta X(t), \quad \text{(F.32)}$$

où $D \in \mathbb{R}^{N \times N}$ est une matrice de différenciation à coefficients constants qui peut être obtenue en utilisant des différences finies [9, 21, 86, 88], des méthodes spectrales [9, 23, 51] ou la méthode de collocation avec différents types de polynômes [10, 51].

En remplaçant (F.32) dans (F.31), nous avons:

$$M_D \delta X(t) = M_A \delta X(t) + M_K(\delta X(t-T) - \delta X(t)), \quad \text{(F.33)}$$

où

$$M_D = \begin{bmatrix} D_{ij} \otimes I_n \\ \mathbf{0}_{n \times nN} \quad I_n \end{bmatrix},$$

$$M_A = \begin{bmatrix} A(t-s_1T) & \mathbf{0}_{n\times n} & \cdots & \mathbf{0}_{n\times n} & \mathbf{0}_{n\times n} \\ \mathbf{0}_{n\times n} & A(t-s_2T) & \cdots & \mathbf{0}_{n\times n} & \mathbf{0}_{n\times n} \\ \vdots & \vdots & \ddots & \vdots & \vdots \\ \mathbf{0}_{n\times n} & \mathbf{0}_{n\times n} & \cdots & A(t-s_{N-1}T) & \mathbf{0}_{n\times n} \\ I_n & \mathbf{0}_{n\times n} & \cdots & \mathbf{0}_{n\times n} & \mathbf{0}_{n\times n} \end{bmatrix},$$

$$M_K = \begin{bmatrix} B(t-s_1T)K & \mathbf{0}_{n\times n} & \cdots & \mathbf{0}_{n\times n} & \mathbf{0}_{n\times n} \\ \mathbf{0}_{n\times n} & B(t-s_2T)K & \cdots & \mathbf{0}_{n\times n} & \mathbf{0}_{n\times n} \\ \vdots & \vdots & \ddots & \vdots & \vdots \\ \mathbf{0}_{n\times n} & \mathbf{0}_{n\times n} & \cdots & B(t-s_{N-1}T)K & \mathbf{0}_{n\times n} \\ I_n & \mathbf{0}_{n\times n} & \cdots & \mathbf{0}_{n\times n} & \mathbf{0}_{n\times n} \end{bmatrix},$$

avec $i = 1, \ldots, N-1$, $j = 1, \ldots, N$, $A(t-s_iT) = \nabla_x f(t-s_iT, x, u)|_{x=x^*(t-s_iT)}$ e $B(t-s_iT) = \nabla_u f(t-s_iT, x, u)|_{u=u^*(t-s_iT, x^*(t-s_iT))}$. Les dernières lignes des matrices assurent la périodicité [51].

La matrice de monodromie en boucle fermée $\Psi_X(t)$ est définie comme étant la matrice de transition d'état en $X^*(t)$, de $\delta X(t-T)$ à $\delta X(t)$, donnée par:

$$\delta X(t) = \Psi_X(t)\delta X(t-T), \tag{F.35}$$

où $\Psi_X(t) \in \mathbb{R}^{nN\times nN}$.

L'équation (F.29) est obtenue à partir de (F.33) et (F.35).

Prediction-based control (PBC)

La commande PBC est basée sur la prédiction *de l'état du système une période en avance, le long des trajectoires de la réponse libre du système.* Le signal de contrôle pour le PBC à temps continu est défini comme

$$u(t, x(t)) = K(t, x(t)) \left(\varphi(t+T, t, x(t), 0) - x(t)\right), \tag{F.36}$$

où $\varphi(t_1, t_0, x, 0)$ est la valeur au temps t_1 de l'état de (F.22) avec $x(t_0) = x$ et $u(t) = 0$, $t_0 \leq t \leq t_1$. $K(t, x(t))$ est le gain du contrôleur.

La solution du système (F.22) avec le signal de contrôle (F.36) est la solution de l'EDP

$$\frac{\partial X(t,0)}{\partial t} = f(t, X(t,0), K(t, X(t,0))\,(X(t,T) - X(t,0))\,, \qquad t \geq 0 \tag{F.37a}$$

$$\frac{\partial X(t,Ts)}{\partial s} = Tf(t + Ts, X(t,Ts), 0), \qquad t \geq 0, \qquad s \in [0,1] \tag{F.37b}$$

$$X(0,0) = x(0).$$

La fonction $X : \mathbb{R}^+ \times [0,T] \to \mathbb{R}^n$ est telle que $X(t,0) = x(t)$ et $X(t,T) = \varphi(t + T, t, x(t), 0)$.

La possibilité effective d'appliquer cette structure de contrôle en temps réel dépend de la possibilité de calculer $\varphi(t + T, t, x(t), 0)$.

Les résultats sur la commande PBC sont publiés en [13].

Principes de la commande *approximate prediction-based control* (aPBC)

Calculer l'état futur $\varphi(t+T, t, x(t), 0)$ exige de calculer à chaque instant t la réponse libre de l'EDO du système (F.22), du temps t au $t + T$. Cela ne peut être fait exactement en temps réel et une approximation de cette valeur est donc introduite. Nous proposons ici une nouvelle méthode de contrôle de rétroaction basée sur la différence entre l'état à l'instant courant et une approximation de l'état prédit, méthode que nous appelons *approximate prediction-based control* (aPBC).

En raison de l'approximation utilisée, on prévoit, pat application du aPBC, la stabilisation d'une nouvelle orbite du système contrôlé, proche de l'UPO du système non contrôlé.

étape 1: Approximation du terme prédit. La première étape consiste à approcher la solution de (F.37b). Ceci est fait ici par une méthode d'intégration de Runge-Kutta implicite de EDOs [35], afin d'estimer le terme prédit, c'est-à-dire, la valeur finale

$$X(t,T) = x + T\int_0^1 f\left(t+Ts, X(t,Ts), 0\right) ds, \qquad x \text{ donné.} \tag{F.38}$$

Pour approcher $X(t,T)$ défini par (F.38), $\varphi(t_2,t_1,x,0)$ est d'abord approximé par l'opérateur $\mathbf{y}$ défini par

$$\mathbf{y}(t+T,t,x) = x + T\sum_{i=1}^{N} c_i l_i(t) \tag{F.39a}$$

$$l_i(t) = f\left(t+Ts_i, x+T\sum_{j=1}^{N} a_{ij} l_j(t), 0\right), \tag{F.39b}$$

où $i = 1,\ldots,N$, $l_j : \mathbb{R}\times\mathbb{R}^n \to \mathbb{R}^n$ e $a_{ij}, c_i \in \mathbb{R}$ sont les coefficients de pondération choisis selon la méthode implicite utilisée [35]. L'approximation $\mathbf{y}(t+T,t,x(t))$ de $X(t,Ts)$, $s\in[0,1]$, est calculée aux points de discrétisation $s = s_i$, $i = 1,\ldots,N$.

Pour simplifier, (F.39b) est écrit sous forme vectorielle (F.40).

$$L(t) = F_T(t,x,L(t)), \tag{F.40}$$

où

$$\forall t \geq 0, \quad L(t) = \begin{bmatrix} l_1(t) \\ \vdots \\ l_N(t) \end{bmatrix} \in \mathbb{R}^{nN},$$

et $F_T : \mathbb{R}\times\mathbb{R}^n\times\mathbb{R}^{nN} \to \mathbb{R}^{nN}$ est défini par:

$$F_T(t,x,L) = \begin{bmatrix} f(t+Ts_1, x+\sum_{j=1}^{N} a_{1j} l_j, 0) \\ \vdots \\ f(t+Ts_N, x+\sum_{j=1}^{N} a_{Nj} l_j, 0), \end{bmatrix}, \qquad \forall x\in\mathbb{R}^n, \quad \forall L\in\mathbb{R}^{nN}.$$

Pour calculer $\mathbf{y}(t+T,t,x)$ avec (F.39a), il est nécessaire de résoudre le système d'équations algébriques (F.39b) en l'inconnue $L(t) \in \mathbb{R}^N$. En écrivant

$$C = \begin{bmatrix} c_1 & \dots & c_N \end{bmatrix}$$

et en fermant la boucle (F.22) par

$$u(t,x(t)) = K(t,x(t))(\mathbf{y}(t+T,t,x(t)) - x(t)) = TK(t,x(t))CL(t)$$

on obtient l'équation différentielle algébrique (EDA),

$$\dot{x}(t) = f(t,x(t),TK(t,x(t))CL(t)), \qquad x(0) = x_0 \tag{F.41a}$$

$$L(t) = F_T(t,x(t),L(t)). \tag{F.41b}$$

La solution en temps réel de l'EDA (F.41) exige que $L(t)$, sa partie algébrique, soit calculée à chaque instant t. De façon alternative, il est proposé par la suite d'introduire un observateur pour transformer le système contrôlé en un système d'EDOs.

étape 2: Approximation du terme de prédiction. On approche maintenant (F.41b) par la résolution de l'EDO de dimension nN (F.42) dont la solution $\hat{L}(t)$ est une estimation de $L(t)$. La valeur initiale de $\hat{L}(0)$ doit être préalablement (et précisément) calculée pour permettre un suivi du $L(t)$ de bonne qualité.

$$\frac{d}{dt}\left(\hat{L}(t) - F_T(t,x(t),\hat{L}(t))\right) + k_o\left(\hat{L}(t) - F_T(t,x(t),\hat{L}(t))\right) = 0, \qquad \hat{L}(0) \text{ donné.} \tag{F.42}$$

Le gain scalaire k_o est choisi positif, de telle sorte que la solution $\hat{L}(t)$ de (F.42) tende asymptotiquement vers la solution $L(t)$ de (F.41b) quand $t \to +\infty$, et typiquement de sorte que la dynamique du estimateur soit plus rapide que la dynamique du système contrôlé. Si effectivement l'évolution de $\hat{L}(t)$ est choisie de façon à satisfaire (F.42), la convergence sera obtenue.

De (F.42) on obtient:

$$\dot{\hat{L}}(t) = \left[I_{nN} - T\partial_3 F_T(t, x(t), \hat{L}(t))(A \otimes I_n)\right]^{-1}$$
$$\left[\partial_1 F_T(t, x(t), \hat{L}(t)) + \partial_2 F_T(t, x(t), \hat{L}(t))(\mathbf{1}_N \otimes f(t, x(t), 0)) - k_o\left(\hat{L}(t) - F_T(t, x(t), \hat{L}(t))\right)\right]. \tag{F.43}$$

où $A = (a_{ij})$ et ∂_i est la dérivée partielle par rapport à la i-ème variable. I_n est la matrice d'identité $n \times n$ et $\mathbf{1}_N$ est le vecteur colonne de dimension N avec tous les éléments égaux à 1. $\otimes$ est le produit de Kronecker.

L'obtention de (F.43) à partir de (F.42) exige l'inversibilité du premier facteur.

$G_T : \mathbb{R}^n \times \mathbb{R}^n \times \mathbb{R}^{nN} \to \mathbb{R}^{nN}$ est défini comme,

$$G_T(t, x, \hat{L}) = \left[I_{nN} - T\partial_3 F_T(t, x, \hat{L})(A \otimes I_n)\right]^{-1}$$
$$\left[\partial_1 F_T(t, x, \hat{L}) + \partial_2 F_T(t, x, \hat{L})(\mathbf{1}_N \otimes f(t, x, 0)) - k_o\left(\hat{L} - F_T(t, x, \hat{L})\right)\right]. \tag{F.44}$$

De (F.41), (F.42), (F.44) et dénotant $\hat{l}_i(t)$ les composantes de $\hat{L}(t)$, la loi de contrôle proposée se traduit par le système d'EDOs suivant en boucle fermée:

$$\begin{bmatrix}\dot{x}(t)\\ \dot{\hat{L}}(t)\end{bmatrix} = \begin{bmatrix} f\left(t, x(t), K(t, x(t))TC\hat{L}(t)\right)\\ G_T\left(t, x(t), \hat{L}(t)\right)\end{bmatrix} \qquad x(0) = x_0, \quad \hat{L}(0) = L(0). \tag{F.45}$$

La solution de (F.45) est une approximation de la solution de l'EDP donnée dans (F.37).

F.3.3 Conclusions

Les conclusions présentées pour la *Part* II (*Chapter* 9) ont été obtenues à partir des résultats numériques comparant les commandes PFC, DFC et PBC/aAPBC et sont résumées ci-dessous:

- En considérant les multiplicateurs de Floquet et les caractéristiques de performance qui leur sont associées (stabilité et vitesse de convergence des trajectoires vers la

solution stabilisée), les meilleurs résultats ont été obtenus pour la commande PFC, aPBC présentant des résultats intermédiaires et DFC les pires résultats;

- En considérant l'erreur et l'effort de contrôle en régime, les résultats obtenus avec la commande aPBC sont significativement plus faibles qu'avec d'autres méthodes;
- La commande DFC est la méthode qui a montré une meilleure robustesse aux erreurs paramétriques entre les méthodes testés;
- Il n'y a pas de limite théorique au PFC et au PBC/aPBC, contrairement au DFC qui a des limites décrites dans la littérature;
- Une limite pratique au aPBC a été identifiée. Pour le système en boucle fermée, en raison de la nécessité d'étendre l'état concernant l'état du système sans contrôle, prédire l'état futur pour les orbites de longue période nécessite un effort de calcul élevé;
- Si la commande DFC stabilise l'orbite et répond aux spécifications de performance, c'est la meilleure méthode pour une application en raison de sa simplicité. S'il est nécessaire d'utiliser une autre méthode de contrôle, la commande aPBC est la plus appropriée car elle utilise un modèle de système pour estimer l'état futur et calculer le signal de commande. Ceci est considéré comme un avantage par rapport à la nécessité pour la commande PFC de connaître intégralement l'orbite.

Bibliography

[1] K. T. Alligood, T. D. Sauer, and J. A. Yorke, *Chaos an introduction to dynamical systems*. New York: Springer-Verlag, 1996.

[2] P. J. Antsaklis and A. N. Michel, *Linear systems*. Birkhäuser, 2006.

[3] V. I. Arnol'd, *Geometrical Methods In The Theory Of Ordinary Differential Equations*, ser. Grundlehren Der Mathematischen Wissenschaften, M. Levi, Ed. Springer-Verlag, 1988.

[4] F. Asenjo, B. A. Toledo, V. Muñoz, J. Rogan, and J. A. Valdivia, "Optimal control in a noisy system," *Chaos*, vol. 18, p. 033106, Jul 2008.

[5] S. Bittanti and P. Colaneri, *Periodic Systems: Filtering and Control*. London: Springer Verlag, 2009.

[6] A. Boukabou, A. Chebbah, and N. Mansouri, "Predictive control of continuous chaotic systems," *International Journal of Bifurcation and Chaos*, vol. 18, no. 2, pp. 587–592, Feb 2008.

[7] A. Boukabou and N. Mansouri, "Fuzzy predictive controller for unknown discrete chaotic systems," *International Journal of Bifurcation and Chaos*, vol. 17, no. 6, pp. 2141–2148, Jun 2007.

[8] E. A. Butcher and S. C. Sinha, "Symbolic computation of local stability and bifurcation surfaces for nonlinear time-periodic systems," *Nonlinear Dynamics*, vol. 17, pp. 1–21, 1998, 10.1023/A:1008284325276.

[9] E. A. Butcher and O. A. Bobrenkov, "On the chebyshev spectral continuous time approximation for constant and periodic delay differential equations," *Comunications in Nonlinear Science and Numerical Simulation*, vol. 16, no. 3, pp. 1541–1554, Mar 2011.

[10] E. A. Butcher, O. A. Bobrenkov, E. Bueler, and P. Nindujarla, "Analysis of milling stability by the chebyshev collocation method: Algorithm and optimal stable immersion levels," *Journal of Computational and Nonlinear Dynamics*, vol. 4, no. 3, Jul 2009.

[11] T. P. Chagas, P.-A. Bliman, and K. H. Kienitz, "Estabilização de órbitas periódicas: comparação entre realimentação de estados atrasados e uma nova lei utilizando estados preditos," in *XVIII Congresso Brasileiro de Automática*, Bonito, Brazil, Sep. 2010.

[12] ——, "New feedback laws for stabilization of unstable periodic orbits," in *8th IFAC Symposium on Nonlinear Control Systems*, Bologna, Italy, Set. 2010.

[13] ——, "A new method for stabilizing unstable periodic orbits of continuous-time systems. application to control of chaos," in *51st IEEE Conference on Decision and Control*, Maui, USA, Dec. 2012.

[14] T. P. Chagas, B. A. Toledo, E. L. Rempel, A. C.-L. Chian, and J. A. Valdivia, "Optimal feedback control of the forced van der pol system," *Chaos, Solitons & Fractals*, vol. 45, no. 9-10, pp. 1147 – 1156, 2012.

[15] J.-H. Chen, "Controlling chaos and chaotification in the chen-lee system by multiple time delays," *Chaos, Solitons and Fractals*, vol. 36, pp. 843–852, Oct 2008.

[16] A. C.-L. Chian, F. A. Borotto, E. L. Rempel, and C. Rogers, "Attractor merging crisis in chaotic business cycles," *Chaos, Solitons and Fractals*, vol. 24, pp. 869–875, 2005.

[17] A. C.-L. Chian, E. L. Rempel, and C. Rogers, "Complex economic dynamics: Chaotic saddle, crisis and intermittency," *Chaos, Solitons and Fractals*, vol. 29, pp. 1194–1218, 2006.

[18] P. Colaneri, "Zero-error regulation of discrete-time linear periodic-systems," *Systems & Control Letters*, vol. 15, no. 2, pp. 161–167, Aug 1990.

[19] ——, "Output stabilization via pole placement of discrete-time linear periodic-systems," *IEEE Transactions on Automatic Control*, vol. 36, no. 6, pp. 739–742, Jun 1991.

[20] P. Cvitanović, "Invariant measurement of strange sets in terms of cycles," *Physical Review Letters*, vol. 61, pp. 2729–2732, Dec 1988.

[21] A. S. de Paula and A. M. Savi, "Controlling chaos in a nonlinear pendulum using an extended time-delayed feedback control method," *Chaos, Solitons and Fractals*, vol. 42, pp. 2981–2988, Apr 2009.

[22] V. S. Deshmukh and S. C. Sinha, "Control of dynamic systems with time-periodic coefficients via the lyapunov-floquet transformation and backstepping technique," *Journal of Vibration and Control*, vol. 10, no. 10, pp. 1517–1533, Oct 2004.

[23] V. Deshmukh, E. A. Butcher, and E. Bueler, "Dimensional reduction of nonlinear delay differential equations with periodic coefficients using chebyshev spectral collocation," *Nonlinear Dynamics*, vol. 52, no. 1-2, pp. 137–149, Apr 2008.

[24] R. L. Devaney, *A first course in chaotic dynamical systems: theory and experiment*. New York: Addison-Wesley, 1992.

[25] P. Faurre and M. Robin, *Éléments d'automatique*, ser. Dunod technique. Dunod, 1984.

[26] B. Fiedler, V. Flunkert, M. Georgi, P. Hövel, and E. Schöll, "Refuting the odd-number limitation of time-delayed feedback control," *Physical Review Letters*, vol. 16, p. 114101, Mar 2007.

[27] B. Fiedler, V. Flunkert, P. Hoevel, and E. Schoell, "Beyond the odd number limitation of time-delayed feedback control of periodic orbits," *European Physical Journal - Special Topics*, vol. 191, no. 1, pp. 53–70, Dec 2010.

[28] A. B. Finlayson, *The Method of Weighted Residuals and Variational Principles*. London: Academic Press, 1972.

[29] V. Franceschini, C. Giberti, and Z. Zheng, "Characterization of the lorentz attractor by unstable periodic orbits," *Nonlinearity*, vol. 6, pp. 251–258, Mar 1993.

[30] Y. C. Fung, *Theory of Aeroelasticity*, ser. Phoenix Edition Series. Dover Publications, Incorporated, 2002.

[31] P. E. Gill, W. Murray, and M. H. Wright, *Practical optimization*. Academic Press, 1981.

[32] O. M. Grasselli and F. Lampariello, "Dead-beat control of linear periodic discrete-time systems," *International Journal of Control*, vol. 33, no. 6, pp. 1091–1106, 1981.

[33] M. S. Grewal and A. P. Andrews, *Kalman Filtering: Theory and Practice Using Matlab*. Wiley, 2008.

[34] A. Guillou and J. L. Soulé, "La résolution numérique des problèmes différentiels aux conditions initiales par des méthodes de collocation," *R.I.R.O*, no. R-3, pp. 17–44, 1969.

[35] E. Hairer, S. P. Norsett, and G. Wanner, *Solving Ordinary Differential Equation I: Nonstiff Problems*. Berlin: Springer Verlag, 2008.

[36] J. K. Hale and S. M. V. Lunel, *Introduction to functional differential equations*. New York: Springer-Verlag, 1993.

[37] S. P. Han, "A globally convergent method for nonlinear programming," *Journal of Optimization Theory and Applications*, vol. 22, pp. 297–309, 1977, 10.1007/BF00932858.

[38] I. Harrington and J. E. S. Socolar, "Design and robustness of delayed feedback controllers for discrete systems," *Physical Review E*, vol. 69, no. 5, Part 2, May 2004.

[39] G. Herrmann, "A robust delay adaptation scheme for pyragas' chaos control method," *Physics Letters A*, vol. 287, pp. 245–256, Aug 2001.

[40] T. Hino, S. Yamamoto, and T. Ushio, "Stabilization of unstable periodic orbits of chaotic discrete-time systems using prediction-based feedback control," *International Journal of Bifurcation and Chaos*, vol. 12, no. 2, pp. 439–446, Feb 2002.

[41] D. Hinrichsen and A. J. Pritchard, *Mathematical Systems Theory I: Modelling, State Space Analysis, Stability and Robustness*, ser. Texts in Applied Mathematics. Springer, 2010, no. v. 1.

[42] E. W. Hooton and A. Amann, "Analytical limitation for time-delayed feedback control in autonomous systems," *Phys. Rev. Lett.*, vol. 109, p. 154101, Oct 2012.

[43] G.-H. Hsu, E. Ott, and C. Grebogi, "Strange saddles and the dimensions of their invariant manifolds," *Physics Letters A*, vol. 127, pp. 199–204, Feb 1988.

[44] H. Huijberts, W. Michiels, and H. Nijmeijer, "Stabilizability via time-delayed feedback: An eigenvalue optimization approach," *SIAM Journal on Applied Dynamical Systems*, vol. 8, no. 1, pp. 1–20, 2009.

[45] W. Just, T. Bernard, M. Ostheimer, E. Reibold, and H. Benner, "Mechanism of time-delayed feedback control," *Physical Review Letters*, vol. 78, no. 2, pp. 203–206, Jan 1997.

[46] W. Just, B. Fiedler, M. Georgi, V. Flunkert, P. Hoevel, and E. Schoell, "Beyond the odd number limitation: A bifurcation analysis of time-delayed feedback control," *Physical Review E*, vol. 76, no. 2, Aug 2007.

[47] P. T. Kabamba, "Monodromy eigenvalue assignment in linear periodic-systems," *IEEE Transactions on Automatic Control*, vol. 31, no. 10, pp. 950–952, Oct 1986.

[48] H. Kantz and P. Grassberger, "Repellers, semi-attractors, and long-lived chaotic transients," *Physica D Nonlinear Phenomena*, vol. 17, pp. 75–86, Aug 1985.

[49] W. Kaplan, *Advanced Calculus*, 5th ed. Reading: Addison-Wesley, 2003.

[50] A. Katok and B. Hasselblatt, *Introduction to the Modern Theory of Dynamical Systems*, ser. Encyclopedia of Mathematics and its Applications. Cambridge: Cambridge University Press, 1995, no. 54.

[51] F. A. Khasawneh, B. P. Mann, and E. A. Butcher, "Comparison between collocation methods and spectral element approach for the stability of periodic delay systems," in *9th IFAC Workshop on Time Delay Systems*, vol. 9, no. 1. Prague, Czech Republic: IFAC, June 2010.

[52] A. Kittel, J. Parisi, and K. Pyragas, "Delayed feedback-control of chaos by self-adapted delay-time," *Physics Letters A*, vol. 198, no. 5-6, pp. 433–436, Mar 1995.

[53] K. Konishi, M. Ishii, and H. Kokame, "Stability of extended delayed-feedback control for discrete-time chaotic systems," *IEEE Transactions on Circuits and Systems I - Fundamental Theory and Applications*, vol. 46, no. 10, pp. 1285–1288, Oct 1999.

[54] B. C. Kuo, *Automatic Control Systems*, 6th ed. New Jersey: Prentice-Hall, 1991.

[55] J. C. Lagarias, J. A. Reeds, M. H. Wright, and P. E. Wright, "Convergence properties of the nelder-med simplex method in low dimensions," *SIAM Journal of Optimization*, vol. 9, no. 1, pp. 112–147, 1998.

[56] D. P. Lathrop and E. J. Kostelich, "Characterization of an experimental strange attractor by periodic-orbits," *Physical Review A*, vol. 40, no. 7, pp. 4028–4031, Oct 1989.

[57] W. Lin, H. Ma, J. Feng, and G. Chen, "Locating unstable periodic orbits: When adaptation integrates into delayed feedback control," *Physical Review E*, vol. 82, no. 4, Part 2, Oct 2010.

[58] O. L. Mangasarian, R. R. Meyer, S. M. Robinson, and A. for Computing Machinery., *Nonlinear programming 3: proceedings of the Special Interest Group on Mathematical Programming symposium.* Academic Press, 1978, no. v. 3.

[59] P. Montagnier and R. J. Spiteri, "A gramian-based controller for linear periodic systems," *IEEE Transactions on Automatic Control*, vol. 49, no. 8, pp. 1380–1385, Aug 2004.

[60] P. Montagnier, R. J. Spiteri, and J. Angeles, "The control of linear time-periodic systems using floquet-lyapunov theory," *International Journal of Control*, vol. 77, no. 5, pp. 472–490, Mar 2004.

[61] Ö. Morgül, "On the stability of delayed feedback controllers for discrete time systems," *Physics Letters A*, vol. 335, no. 1, pp. 31–42, Jan 2005.

[62] ——, "On the stabilization of periodic orbits for discrete time chaotic systems," *Physics Letters A*, vol. 335, no. 2-3, pp. 127–138, Feb 2005.

[63] ——, "A new generalization of delayed feedback control," *International Journal of Bifurcation and Chaos*, vol. 19, no. 1, pp. 365–377, Jan 2009.

[64] H. Nakajima, "On analytical properties of delayed feedback control of chaos," *Physics Letters A*, vol. 232, pp. 207–210, Jul 1997.

[65] ——, "On the stability of delayed feedback control of chaos," in *36th IEEE Conference on Decision and Control.* St. Petersburg, Russia: IEEE, Dec. 1997, pp. 411–414.

[66] H. E. Nusse and J. A. Yorke, "A procedure for finding numerical trajectories on chaotic saddles," *Physica D*, vol. 36, no. 1-2, pp. 137–156, Jun 1989.

[67] E. Ott, C. Grebogi, and J. A. Yorke, "Controlling chaos," *Physical Review Letters*, vol. 64, pp. 1196–1199, Mar 1990.

[68] T. S. Parker and L. O. Chua, *Practical Numerical Algorithms for Chaotic Systems.* New York: Springer-Verlag, 1989.

[69] M. Powell, "A fast algorithm for nonlinearly constrained optimization calculations," in *Numerical Analysis*, ser. Lecture Notes in Mathematics, G. Watson, Ed. Springer Berlin / Heidelberg, 1978, vol. 630, pp. 144–157, 10.1007/BFb0067703.

[70] K. Pyragas, "Continuous control of chaos by self-controlling feedback," *Physics Letters A*, vol. 170, pp. 421–428, Nov 1992.

[71] ——, "Control of chaos via extended delay feedback," *Physics Letters A*, vol. 206, pp. 323–330, Feb 1995.

[72] ——, "Control of chaos via an unstable delayed feedback controller," *Physical Review Letters*, vol. 86, no. 11, pp. 2265–2268, Mar 2001.

[73] ——, "Delayed feedback control of chaos," *Royal Society of London Philosophical Transactions Series A*, vol. 364, pp. 2309–2334, Sep 2006.

[74] K. Pyragas and A. Tamaševičius, "Experimental control of chaos by delayed self-controlling feedback," *Physics Letters A*, vol. 180, pp. 99–102, Aug 1993.

[75] V. Pyragas and K. Pyragas, "Adaptive modification of the delayed feedback control algorithm with a continuously varying time delay," *Physics Letters A*, vol. 375, no. 44, pp. 3866–3871, Oct 2011.

[76] E. L. Rempel, A. C.-L. Chian, E. E. N. Macau, and R. R. Rosa, "Analysis of chaotic saddles in low-dimensional dynamical systems: the derivative nonlinear schrödinger equation," *Physica D Nonlinear Phenomena*, vol. 199, pp. 407–424, Dec 2004.

[77] J. A. Richards, *Analysis of Periodically Time-Varying Systems*, ser. Communications and Control Engineering Series, A. Fettweis, J. L. Massey, and M. Thoma, Eds. Berlin: Springer-Verlag, 1983.

[78] A. Saito and K. Konishi, "Dynamical singularities in adaptive delayed-feedback control," *Physical Review E*, vol. 84, no. 3, Part 1, Sep 2011.

[79] M. A. F. Sanjuán and C. Grebogi, *Recent Progress in Controlling Chaos*, ser. Series on stability, vibration, and control of systems. World Scientific, 2010.

[80] E. Schöll and H. G. Schuster, *Handbook of Chaos Control*. John Wiley & Sons, 2008.

[81] H. G. Schuster and M. B. Stemmler, "Control of chaos by oscillating feedback," *Physical Review E*, vol. 56, no. 6, pp. 6410–6417, Dec 1997.

[82] L. Shen, M. Wang, W. Liu, and G. Sun, "Prediction based chaos control via a new neural network," *Physics Letters A*, vol. 372, no. 46, pp. 6916–6921, Nov 2008.

[83] P. So, E. Ott, S. J. Schiff, D. T. Kaplan, T. Sauer, and C. Grebogi, "Detecting unstable periodic orbits in chaotic experimental data," *Physical Review Letters*, vol. 76, no. 25, pp. 4705–4708, Jun 1996.

[84] J. E. S. Socolar, D. W. Sukow, and D. J. Gauthier, "Stabilizing unstable periodic-orbits in fast dynamical-systems," *Physical Review E*, vol. 50, no. 4, pp. 3245–3248, Oct 1994.

[85] E. D. Sontag, *Mathematical Control Theory: Deterministic Finite Dimensional Systems*, ser. Texts in Applied Mathematics. Springer, 1998.

[86] J. C. Sprott, "Simple models of complex chaotic systems," *American Journal of Physics*, vol. 76, no. 4, pp. 474–480, 2008.

[87] J. Sreedhar and P. V. Dooren, "Pole placement via the periodic schur decomposition," in *In Proceedings American Control Conference*, 1993, pp. 1563–1567.

[88] J.-Q. Sun, "A method of continuous time approximation of delayed dynamical systems," *Communications in Nonlinear Science and Numerical Simulation*, vol. 14, pp. 998–1007, Mar 2009.

[89] Y. P. Tian and J. D. Zhu, "Full characterization on limitation of generalized delayed feedback control for discrete-time systems," *Physica D*, vol. 198, no. 3-4, pp. 248–257, Nov 2004.

[90] T. Ushio, "Limitation of delayed feedback control in nonlinear discrete-time systems," *IEEE Transactions on Circuits and Systems I - Regular Papers*, vol. 43, no. 9, pp. 815–816, Sep 1996.

[91] T. Ushio and S. Yamamoto, "Prediction-based control of chaos," *Physics Letters A*, vol. 264, pp. 30–35, Dec 1999.

[92] L. Viganò, M. Bergamasco, M. Lovera, and A. Varga, "Optmal periodic output feedback control: a continuous-time approach and case study," *International Journal of Control*, vol. 83, no. 5, pp. 897–914, 2010.

[93] J. Viladsen and M. L. Michelsen, *Solution of Differential Equation Models by Polynomial Approximation*. Englewood Cliffs: Prentice-Hall, 1978.

[94] Z. Vukić, L. Kuljaca, D. Donlagic, and S. Tesaknjak, *Nonlinear Control Systems*, ser. Control Engineering Series. Marcel Dekker Incorporated, 2003.

[95] A. Wolf, J. B. Swift, H. L. Swinney, and J. A. Vastano, "Determining lyapunov exponents from a time series," *Physica D*, vol. 16, pp. 285–317, 1985.

[96] K. Wright, "Some relationships between implicit runge-kutta collocation and lancos τ methods, and their stability properties," *BIT*, vol. 10, pp. 217–227, 1970.

[97] K. Yagasaki and M. Kumagai, "External feedback control of chaos using approximate periodic orbits," *Physical Review E*, vol. 65, no. 2, Part 2, Feb 2002.

[98] V. A. Yakubovich and V. M. Starzhinskii, *Linear differential equations with periodic coefficients*, ser. Linear Differential Equations with Periodic Coefficients. Wiley, 1975, no. v. 1.

[99] S. Yamamoto, T. Hino, and T. Ushio, "Dynamic delayed feedback controllers for chaotic discrete-time systems," *IEEE Transactions on Circuits and Systems I - Regular Papers*, vol. 48, no. 6, pp. 785–789, Jun 2001.

[100] ——, "Delayed feedback control with a minimal-order observer for stabilization of chaotic discrete-time systems," *International Journal of Bifurcation and Chaos*, vol. 12, no. 5, pp. 1047–1055, May 2002.

[101] C. Yang and C. Q. Wu, "A robust method on estimation of lyapunov exponents from a noisy time series," *Nonlinear Dynamics*, vol. 64, no. 3, pp. 279–292, May 2011.

[102] B. Zhou and G.-R. Duan, "Periodic lyapunov equation based approaches to the stabilization of continuous-time periodic linear systems," *IEEE Transactions on Automatic Control*, vol. 57, no. 8, pp. 2139–2146, Aug 2012.

[103] H. D. Zhu and Y. P. Tian, "Necessary and sufficient conditions for stabilizability of discrete-time systems via delayed feedback control," *Physics Letters A*, vol. 343, no. 1-3, pp. 95–107, Aug 2005.

[104] J. Zhu and Y.-P. Tian, "Stabilizability of uncontrollable systems via generalized delayed feedback control," *Physica D*, vol. 237, no. 19, pp. 2436–2443, Oct 2008.

[105] V. P. Zhuravlev and D. M. Klimov, "Theory of the shimmy phenomenon," *Mechanics of Solids*, vol. 45, no. 3, pp. 324–330, 2010.